SSN 0021-9673

VOL. 332 SEPTEMBER 20, 1985
COMPLETE IN ONE ISSUE

Int. Symp. on HPLC and Annual Meeting on HPLC Kyoto, Jan. 28–Feb. 1. 1985

RNAL OF HROMATOGRAPHY

RNATIONAL JOURNAL ON CHROMATOGRAPHY, ELECTROPHORESIS AND RELATED METHO

SYMPOSIUM VOLUMES

ELSEVIER

JOURNAL OF CHROMATOGRAPHY

Scope. The *Journal of Chromatography* publishes papers on all aspects of chromatography, electrophoresis and related methods. Contributions consist mainly of research papers dealing with chromatographic theory, instrumental development and their applications. The section *Biomedical Applications,* which is under separate editorship, deals with the following aspects: developments in and applications of chromatographic and electrophoretic techniques related to clinical diagnosis (including the publication of normal values); screening and profiling procedures with special reference to metabolic disorders; results from basic medical research with direct consequences in clinical practice; combinations of chromatographic and electrophoretic methods with other physicochemical techniques such as mass spectrometry. In *Chromatographic Reviews,* reviews on all aspects of chromatography, electrophoresis and related methods are published.

Submission of Papers. Papers in English, French and German may be submitted, in three copies. Manuscripts should be submitted to: The Editor of *Journal of Chromatography,* P.O. Box 681, 1000 AR Amsterdam, The Netherlands, or to: The Editor of *Journal of Chromatography, Biomedical Applications,* P.O. Box 681, 1000 AR Amsterdam, The Netherlands. Review articles are invited or proposed by letter to the Editors and will appear in *Chromatographic Reviews* or *Biomedical Applications.* An outline of the proposed review should first be forwarded to the Editors for preliminary discussion prior to preparation. Submission of an article is understood to imply that the article is original and unpublished and is not being considered for publication elsewhere. For copyright regulations, see below.

Subscription Orders. Subscription orders should be sent to: Elsevier Science Publishers B.V., P.O. Box 211, 1000 AE Amsterdam, The Netherlands. The *Journal of Chromatography* and the *Biomedical Applications* section can be subscribed to separately.

Publication. The *Journal of Chromatography* (incl. *Biomedical Applications, Chromatographic Reviews* and *Cumulative Author and Subject Indexes, Vols. 301–325*) has 34 volumes in 1985. The subscription prices for 1985 are:

J. Chromatogr. (incl. *Chromatogr. Rev.* and *Cum. Indexes, Vols. 301–325*) + *Biomed. Appl.* (Vols. 312–345):
Dfl. 5440.00 plus Dfl. 748.00 (postage) (total *ca.* US$ 2291.75)

J. Chromatogr. (incl. *Chromatogr. Rev.* and *Cum. Indexes, Vols. 301–325*) only (Vols. 312–335):
Dfl. 4320.00 plus Dfl. 582.00 (postage) (total *ca.* US$ 1795.50)

Biomed. Appl. only (Vols. 336–345):
Dfl. 1750.00 plus Dfl. 220.00 (postage) (total *ca.* US$ 729.75).

Journals are automatically sent by airmail at no extra costs to Australia, Brasil, Canada, China, Hong Kong, India, Israel, Japan, Malaysia, New Zealand, Pakistan, Singapore, South Africa, South Korea, Taiwan and the U.S.A. Back volumes of the *Journal of Chromatography* (Vols. 1 through 311) are available at Dfl. 219.00 (plus postage). Claims for issues not received should be made within three months of publication of the issue. If not, they cannot be honoured free of charge. Customers in the U.S.A. and Canada wishing information on this and other Elsevier journals, please contact Journal Information Center, Elsevier Science Publishing Co. Inc., 52 Vanderbilt Avenue, New York, NY 10017. Tel. (212) 916-1250.

Abstracts/Contents Lists published in Analytical Abstracts, Biochemical Abstracts, Biological Abstracts, Chemical Abstracts, Chemical Titles, Current Contents/Physical, Chemical & Earth Sciences, Current Contents/Life Sciences, Deep-Sea Research/Part B: Oceanographic Literature Review, Index Medicus, Mass Spectrometry Bulletin, PASCAL-CNRS, Referativnyi Zhurnal and Science Citation Index.

See page 3 of cover for Publication Schedule, Information for Authors and information on Advertisements.

0021-9673/85/$03.30

Printed in The Netherlands

For contents see p. VII

FIRST ANNOUNCEMENT

International Symposium on Coal Characterisation for Conversion Processes
Rolduc, The Netherlands, 28th April - 1st May 1986

Scope
The past decade has been characterized by a renewed interest in coal as an energy source and as a basic material for the chemical industry. This has induced a revival in coal research activities both from a fundamental and an applied point of view. Due to changing economics, however, the large scale introduction of new coal conversion processes has been postponed and, as a consequence, more time is available for research to gain fundamental insights into coal structure and to obtain a better understanding of its impact on conversion processes. In view of this, the initiative has been taken to organize the international "**Rolduc Symposia on Coal Science**". These are intended to fill the need for small-scale working symposia on specific subjects and with a limited number of participants (about 150), as a supplement to the large-scale Coal Science Conferences. The opportunity for in-depth discussions and maximum profit from exchange of knowledge and ideas can thereby be assured.

The first symposium of the series will be devoted to "Coal Characterisation for Conversion Processes". Its aim is to build a bridge between the techniques and methods nowadays available for coal characterisation and the need for relevant parameters to operate and design coal conversion processes.

Scientific Program
The scientific program will cover Coal Characterisation in relation to Gasification, Combustion, Pyrolysis, and Liquefaction. A full symposium day will be devoted to each of the four processes and each day's session will commence with a plenary lecture by an invited expert:
Gasification: **K.H. van Heek** (Bergbau-Forschung GmbH, Germany)
Combustion: **P.A. Roberts** (Int. Flame Research Foundation, The Netherlands)
Pyrolysis: **R. Cyprès** (Free University Brussels, Belgium)
Liquefaction: **C. Snape** (British Gas, U.K.)
Poster sessions and discussions on selected topics will be organized. There are no parallel sessions. The congress language will be English.

Proceedings
The participants will receive a hard-bound edition of the proceedings. This will be a reprint of a special issue of the journal *Fuel Processing Technology*, published by Elsevier.

Fee
A special symposium package, including registration, accommodation for four nights, all meals, and a copy of the proceedings will be available at approximately Dfl. 1050 per participant (about US $ 350).

Further Information
Further information can be obtained from
F. Kapteijn,
Secretary First International Rolduc Symposium on Coal Science,
Institute for Chemical Technology of the University of Amsterdam,
Nieuwe Achtergracht 166,
1018 WV Amsterdam,
The Netherlands.
Telephone 31 - (0) 20-522 3490/2265.
Telex FACWN 16460.

Do you know me ?

"Shodex" is the brand name of one of the most reliable equipments in the HPLC field. Shodex technology is ready to serve you in a variety of applications ranging from microanalysis to industrial purification of any kinds of substance.
Please contact us. We are prepared to help you at any time with plenty of technical data and application sheets.

- **Shodex** detectors and HPLC devices
  - Refractive Index Detector : Shodex RI SE-51 (Anal.), SE-52 (Prep.)
  - Ion Chromatography Kit : Shodex IC (Conductivity Detector & Columns)
  - Eluent Degassing Device : Shodex DEGAS KT-11, KT-21, KT-31
- **Shodex** Packed Columns for HPLC
  - For GPC : GPC KF-800 (THF), GPC AT-80M/S (High temp.)
  - For GFC : OHpak Q-800, OHpak B-800
  - For protein separation : PROTEIN WS-800
  - For sugar separation : SUGAR series, Ionpak KS-800
  - For organic acids separation : Ionpak KC-811
  - For adsorption/partition separation : RSpak D series
    (Porous polymer columns that replace silica columns)
- **Shodex** STANDARD (Aqueous & organic standards for SEC)

Monosaccharides
Shodex SUGAR SP-1010

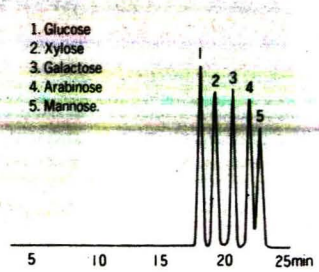

Proteins
Shodex PROTEIN WS-803F

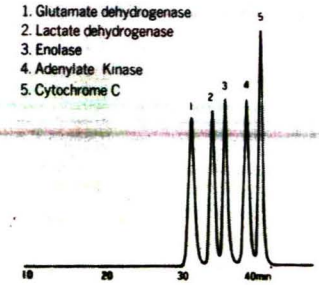

Food additives
Shodex RSpak DS-613

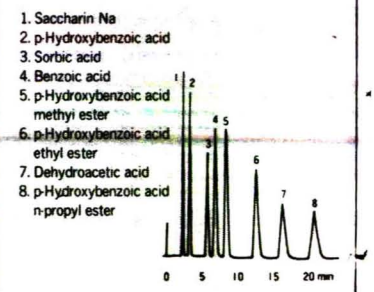

Shodex DEGAS KT-31
Eluent Degassing Device

Anions
Shodex IC I-524A

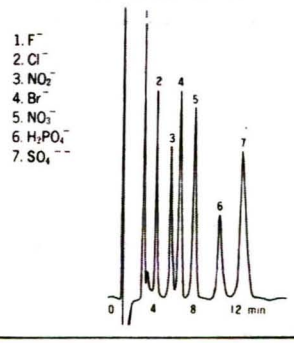

Shodex RI SE-51
Refractive Index Detector

SHOWA DENKO K.K
SPECIALTY CHEMICALS DIVISION
Shodex (Separation & HPLC) Group
13-9, Shiba Dainon 1-chome, Minato-ku
Tokyo, 105 Japan
Telephone: 03(432) 5111, Telex: J26232

SHOWA DENKO AMERICA, INC.
280 Park Avenue
West Building, 27 th Floor
New York, N.Y. 10017, U.S.A.
Telephone: 212-687-0773
Telex: 23423898

SHOWA DENKO (EUROPE) GmbH
Niederkasseler Lohweg 8
4000 Duesseldorf 11
WEST GERMANY
Telephone: 0211-5961098, Telex: 8587649

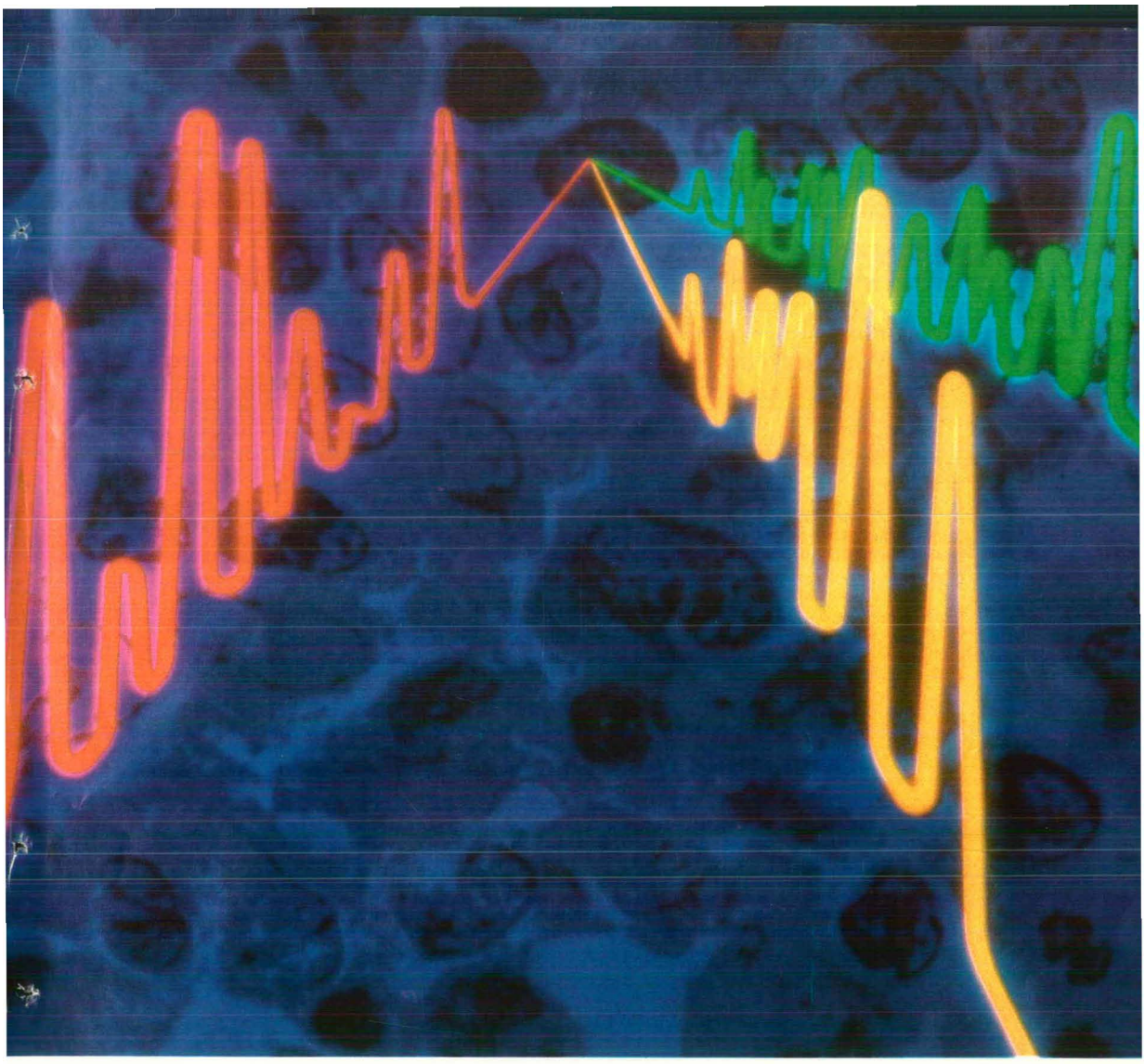

ZORBAX® Bio Series columns lift your biological separations to new peaks!

Du Pont's new Zorbax® Bio Series—a growing family of high-resolution HPLC columns to meet specific separation needs.

Separate proteins by size, from 4,000 to 900,000 daltons, with the Zorbax® Bio Series GF-250 and GF-450 alkali-stable (up to pH 8.5) silica gel filtration columns.

Isocratic analysis of PTH amino acids with excellent results using the Zorbax® Bio Series PTH Amino Acid column. Isocratic analysis maximizes reproducibility, simplifies separation adjustment, and provides long column life.

Separate peptides and proteins with the reversed phase Zorbax® Bio Series PEP-RP1 column. Optimized large-pore packing for higher resolution and excellent loading capacity.

Large-scale chromatography—Zorbax® Bio Series preparative columns and packings allow direct scale-up from analytical with no need for additional method development.

Du Pont manufactures Zorbax® Chromatography Packings in plant-scale facilities, thereby assuring long-term supplies of reproducible products.

For more information and free literature on the growing Bio Series family, **call 1-800-237-8400,** or write: DuPont, Biotechnology Systems, Leadtrack, 595 Colonial Park Drive, Room 250, Roswell, GA 30075.

Biotechnology Systems

DUPONT

REG. U.S. PAT. & TM. OFF.

Reader service coupon

JOURNAL OF

CHROMATOGRAPHY

INTERNATIONAL JOURNAL ON CHROMATOGRAPHY, ELECTROPHORESIS AND RELATED METHODS

Use this coupon (or xerox copy) for free information on the advertised products. Just quote ad no.

I would like to receive, without any obligation, further information on the following advertisement numbers:

I am especially interested in the fields indicated below:

- ☐ 6040 Analytical Chemistry
- ☐ 6042 Laboratory Instrumentation
- ☐ 6050 Chromatography
- ☐ 6140 Spectroscopy
- ☐ 6150 Mass Spectrometry
- ☐ 6240 Pharmaceutical Chemistry
- ☐ 6241 Medicinal Chemistry
- ☐ 6242 Clinical Chemistry
- ☐ 6260 Environmental Chemistry
- ☐ 16290 Scientific Software

Name: _____

Position: _____

Address: _____

_____

please use envelope; mail as printed matter

ELSEVIER SCIENCE PUBLISHERS

Advertising department

P.O. BOX 211,

1000 AE AMSTERDAM – THE NETHERLANDS

please use envelope; mail as printed matter

ELSEVIER SCIENCE PUBLISHERS

Advertising department

P.O. BOX 211,

1000 AE AMSTERDAM – THE NETHERLANDS

Reader service coupon

JOURNAL OF CHROMATOGRAPHY

INTERNATIONAL JOURNAL OF CHROMATOGRAPHY, ELECTROPHORESIS AND RELATED METHODS

Use this coupon (or photo copy) for free information on the advertised products. Just quote ad no.

I would like to receive, without any obligation, further information on the following advertisement numbers:

I am especially interested in the fields indicated below:

- ☐ 6040 Analytical Chemistry
- ☐ 6042 Laboratory Instrumentation
- ☐ 6050 Chromatography
- ☐ 6140 Spectroscopy
- ☐ 6150 Mass Spectrometry
- ☐ 6240 Pharmaceutical Chemistry
- ☐ 6241 Medicinal Chemistry
- ☐ 6242 Clinical Chemistry
- ☐ 6260 Environmental Chemistry
- ☐ 16290 Scientific Software

Name: _____

Position: _____

Address: _____

_____

New Gilson auto-sampling injector for HPLC.

NOW THE MOST BORING PROCEDURES ARE AUTOMATIC.

Gilson introduces Model 231-401, a new robotic unit with advanced capabilities for HPLC sample preparation and injection:

Automatic sample preparation.
Speeds-up routine procedures including on-line pre-column derivatizations. Adds internal standards. Performs sequential dilutions for calibration plots.

Automatic sample injection.
Loads contamination-free with minimal loss. Handles up to 120 analytes. Injects variable volumes with unlimited replicates. Automatically dilutes samples generating over-scaled peaks.

Fast, reliable, automatic. The 231-401 takes the tedium out of HPLC.

GILSON
INTERNATIONAL

France : Gilson Medical Electronics (France) S.A., B.P. 45, F - 95400 Villiers-le-Bel, France, Tél. (1) 39.90.54.41 - Télex : 696682.

United States : Gilson Medical Electronics, Inc., Box 27, 3000 W. Beltline, Middleton, WI 53562 U.S.A., Tel. 608/836-1551, Telex : 265478. MTWI.

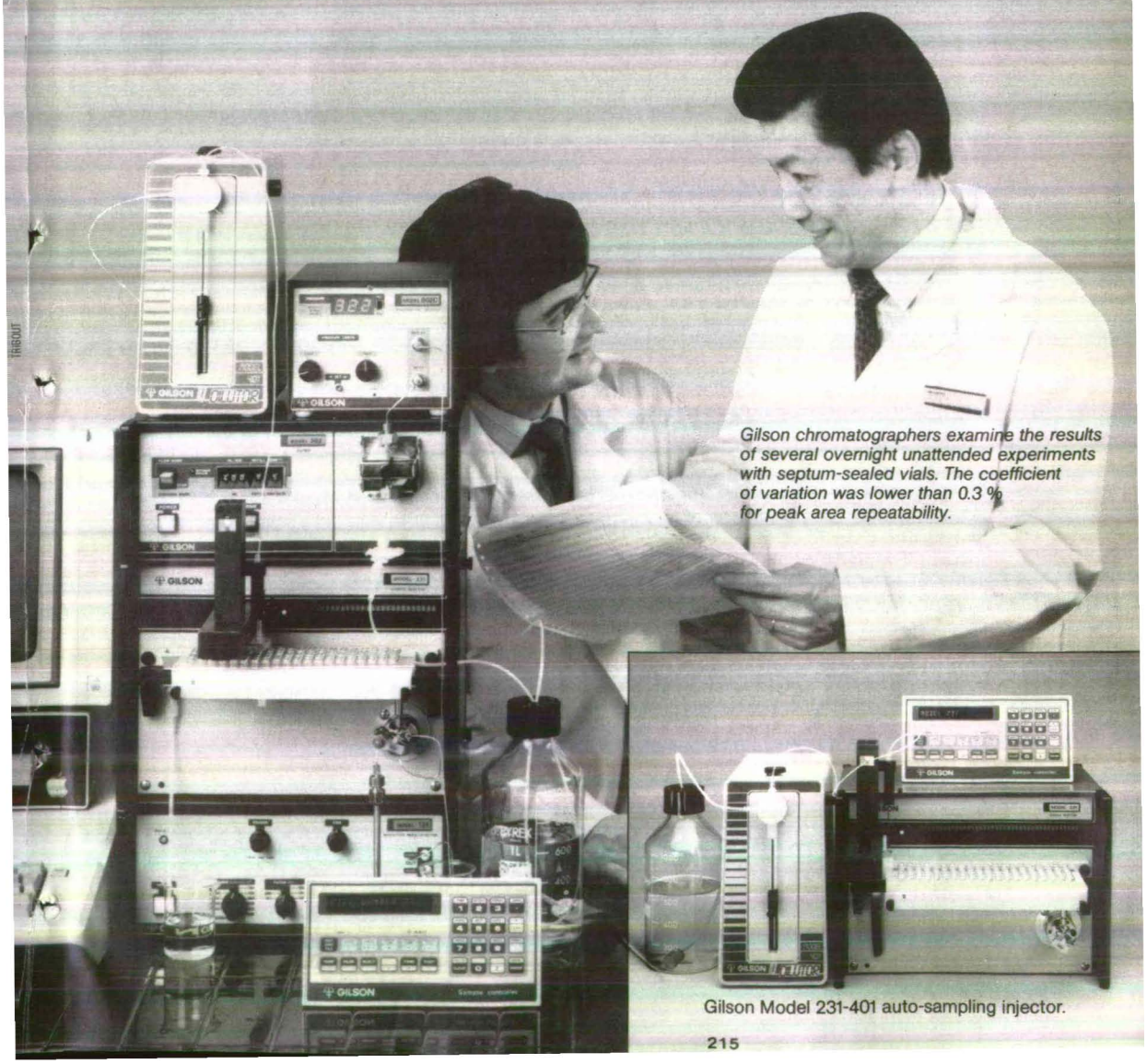

Gilson chromatographers examine the results of several overnight unattended experiments with septum-sealed vials. The coefficient of variation was lower than 0.3 % for peak area repeatability.

Gilson Model 231-401 auto-sampling injector.

If you have to say FPLC you are half way there ...

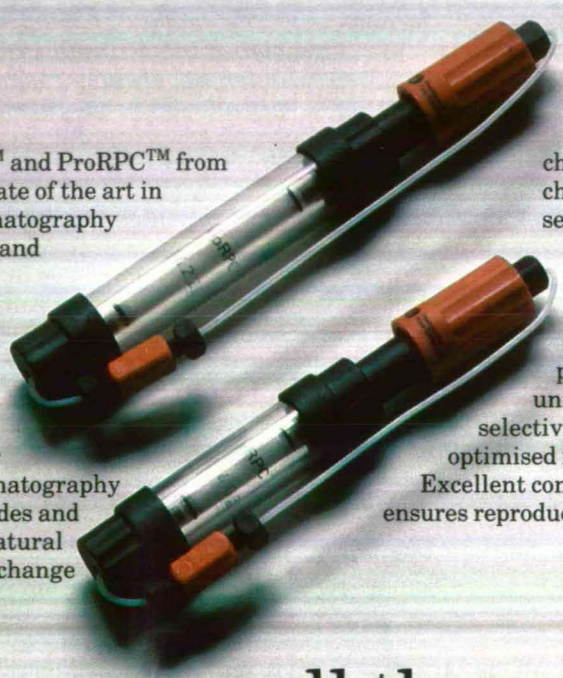

... because PepRPC™ and ProRPC™ from Pharmacia are the state of the art in reversed phase chromatography media for separating and recovering biological molecules.

Pharmacia reversed phase chromatography columns have been specially designed for high resolution chromatography of peptides, polypeptides and proteins, forming a natural complement to ion exchange chromatography and chromatofocusing when separating biomolecules using the Pharmacia FPLC System.

Pharmacia media PepRPC and ProRPC provide you with new and unique reversed phase selectivities (C_2/C_{18} and C_1/C_8) optimised for peptides and proteins. Excellent control over the new synthesis ensures reproducibility from batch to batch.

... so go all the way.

The Pharmacia RPC media are prepacked in boro-silicate glass columns with optimised lengths to utilize a range of reversed phase separation techniques for high resolution and high recoveries of both large and small polypeptides.

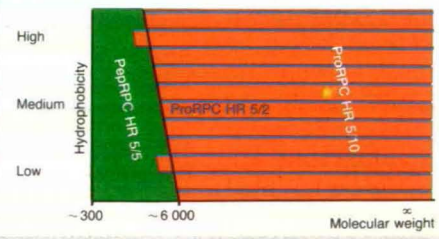

- Controlled synthesis for batch to batch reproducibility
- High recoveries of peptides and polypeptides
- High resolution of hydrophobic fragments
- Optimised bonded phase composition

FPLC from Pharmacia goes beyond HPLC with biocompatibility,

Pharmacia Fine Chemicals AB
Box 175
S-751 04 Uppsala 1
Sweden

Pharmacia Fine Chemicals

Completely Revised

Instrumental Liquid Chromatography

A Practical Manual on High-Performance Liquid Chromatography Methods

Second, completely revised edition

by **N.A. PARRIS**, E.I. du Pont de Nemours & Company, Biomedical Products Department, Research and Development Division, Experimental Station Laboratory Wilmington, DE, USA

Journal of Chromatography Library 27

This extensively revised and up-to-date book is an essential tool for the HPLC user in the laboratory. It first appeared in 1976, was twice reprinted and was described in Laboratory Practice as "one of the more useful and successful texts on HPLC . . . a most readable book packed with valuable information and advice . . . strongly recommended."

Practically orientated, it is an easy-to-follow guide containing the minimum essential theoretical background. The majority of the material is based on practical experience and highlights details which may have important operational value for laboratory workers. It helps the HPLC user to select the most appropriate instrumentation, injectors, columns etc.

Applications of liquid chromatography are described with reference to the potential of the technique for qualitative, quantitative and trace analysis as well as for the preparative application. Numerous applications from the literature are tabulated and cross-referenced to sections concerned with the optimization procedures of the particular methods. The format of the original edition proved so successful that it has remained unchanged, but some 45% of the material is either new or completely revised in order to bring the column technology and applications data up-to-date.

"The style . . . is clear. The subject is placed in perspective by comparisons with other separation techniques and should provide a good reference book for all involved in practical LC," (Laboratory Practice).

"Overall the book is well written, and, because of its practical emphasis, it is highly recommended for both the aspiring and experienced chromatographer," (J. Am. Chem. Soc.).

1984 xiv + 432 pages. Price: US $ 83.25 / Dfl. 225.00 (including postage).
ISBN 0-444-42061-4

ELSEVIER SCIENCE PUBLISHERS

P.O. Box 211, 1000 AE Amsterdam, The Netherlands
P.O. Box 1663, Grand Central Station, New York, NY 10163, USA

7331

JOURNAL OF CHROMATOGRAPHY

VOL. 332 (1985)

JOURNAL *of* CHROMATOGRAPHY

INTERNATIONAL JOURNAL OF CHROMATOGRAPHY, ELECTROPHORESIS AND RELATED METHODS

SYMPOSIUM VOLUMES

ELSEVIER
AMSTERDAM — OXFORD — NEW YORK — TOKYO

Part of "Rakuchu Rakugai Zu" (Picture of the Sights in and around Kyoto), early 17th Century, Kozu Kobunka Museum. (Reproduced with permission of the owner, Mr. Kozu Yoshiyuki.)

0021-9673/85/$03.30

Printed in The Netherlands

SYMPOSIUM VOLUME

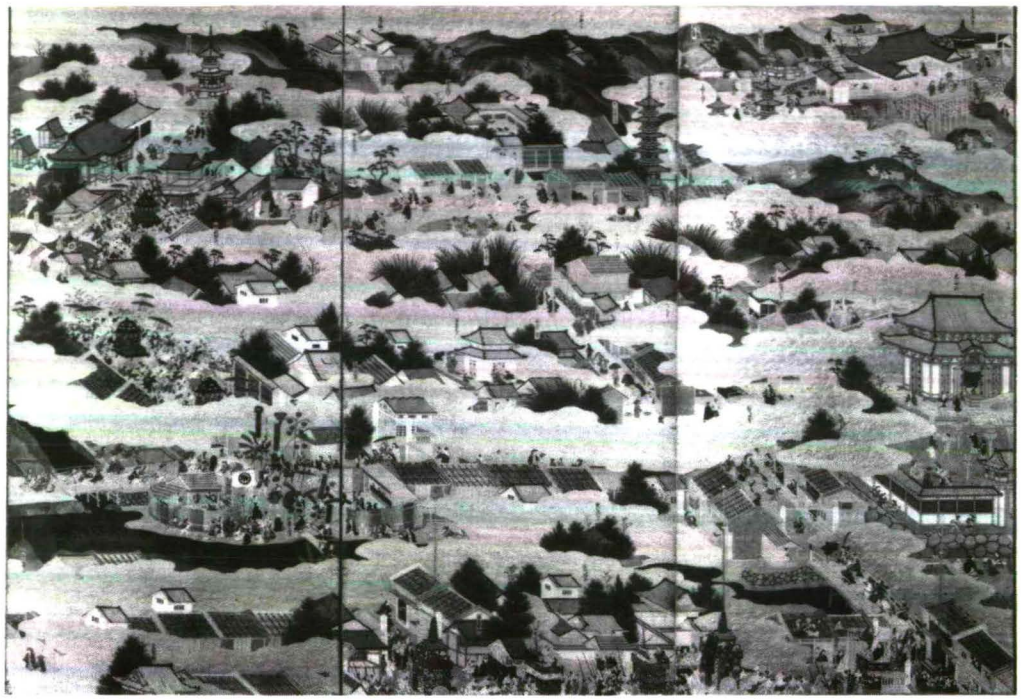

INTERNATIONAL SYMPOSIUM ON HIGH-PERFORMANCE LIQUID CHROMATOGRAPHY

Kyoto (Japan), January 28–30, 1985

and

ANNUAL MEETING ON HIGH-PERFORMANCE LIQUID CHROMATOGRAPHY OF THE JAPANESE RESEARCH GROUP ON AUTOMATIC LIQUID CHROMATOGRAPHY

Kyoto (Japan), January 31–February 1, 1985

Guest Editor

H. HATANO
(Kyoto, Japan)

CONTENTS

INTERNATIONAL SYMPOSIUM ON HIGH-PERFORMANCE LIQUID CHROMATOGRAPHY AND ANNUAL MEETING ON HIGH-PERFORMANCE LIQUID CHROMATOGRAPHY, KYOTO, JANUARY 28–FEBRUARY 1, 1985

Journal of Chromatography, 332 (1985) 1
Elsevier Science Publishers B.V., Amsterdam — Printed in The Netherlands

FOREWORD

The interesting and rapid development of high-performance liquid chromatography in the course of the last ten years suggested that an international meeting of those working in this field in Japan would be valuable, and the response to our invitations to participate in such a meeting confirmed this view. The *First International Symposium on High-Performance Liquid Chromatography* was therefore held from 28 to 30 January, 1985, in Kyoto. It was organized with the help of the Japan Society for Promotion of Science and of the Research Group on Automatic Liquid Chromatography in Japan. The Symposium was also supported by The Science Council of Japan, The Promotion Bureau, Data Committee, Science & Technology Agency, and the Nissan and Inoue Science Foundations.

The scientific contributions and discussions are collected in this volume and include invited papers giving the technical and analytical chemical background of the technique. The papers give what we believe to be an overview of recent progress in this area in Japan.

We are greatly indebted to all contributors for supplying manuscripts on time, and we are grateful to the Chemical Society of Japan, the Japan Society for Analytical Chemistry, the Biochemical Society of Japan, the Agricultural Chemistry Society of Japan and the Japan Analytical Instrument Manufacturer's Association for their co-sponsorship. We also express our sincere thanks to contributing companies for their strong financial support, and to Elsevier Science Publishers B.V. for their co-operation in publishing this volume so rapidly.

Kyoto (Japan)
April, 1985

H. HATANO

Journal of Chromatography, 332 (1985) 3–8
Elsevier Science Publishers B.V., Amsterdam — Printed in The Netherlands

CHROMSYMP. 614

ADVANCED MICROCOLUMN TECHNIQUES IN LIQUID CHROMATOGRAPHY

USE OF GLASS-LINED STAINLESS-STEEL TUBING COLUMNS

D. ISHII*, K. WATANABE, H. ASAI, Y. HASHIMOTO and T. TAKEUCHI
Department of Applied Chemistry, Faculty of Engineering, Nagoya University, Chikusa-ku, Nagoya-shi, 464 (Japan)
(Received March 18th, 1985)

SUMMARY

Micro packed columns made of glass-lined stainless-steel tubing were prepared and their chromatographic performance was examined. The use of glass-lined stainless-steel tubing of 1/16 in. O.D. facilitated operation under high pressures. The system using such columns was applicable to chromatography with carbon dioxide as the mobile phase.

INTRODUCTION

The effect of column materials on the column efficiency in micro high-performance liquid chromatography (micro HPLC) is greater than in conventional HPLC[1]. One of the reasons lies in the difficulty of polishing the inner wall of small-bore tubes. Glass[2,3] and fused-silica tubing of 0.1–0.35 mm I.D.[1,4,5] have consequently been employed as the column material in micro HPLC, as they give reasonable column efficiencies owing to their smooth and inert surface. The latter material was very convenient for long columns owing to its flexibility and good mechanical strength.

Glass-lined stainless-steel tubing of 1/16 in. O.D. with different inner diameters is commercially available. It is expected that this tubing will have a smooth surface like glass tubing and be capable of withstanding high pressures like stainless-steel tubing. Hence micro packed columns made of glass-lined stainless-steel tubing might make it possible to attain high efficiency and withstand high pressures. In addition, glass-lined stainless-steel tubing of 1/16 in. O.D. facilitates the coupling of micro columns with commercially available chromatographs.

This paper describes the performance of glass-lined stainless-steel tubing micro columns and reports some applications.

0021-9673/85/$03.30

EXPERIMENTAL

Column preparation

Glass-lined stainless-steel tubing of 30 cm × 0.3–0.5 mm I.D. was obtained from Gaskuro Kogyo (Tokyo, Japan) and a suitable length was prepared by cutting the tubing followed by grinding both ends with an Electromotive Baby Cutter (Gasukuro Kogyo). Stainless-steel unions and ferrules were attached to both ends. A 1/16 in. zero dead volume union (Valco, Houston, TX, U.S.A.) was attached to the inlet and a 1/16 × 1/32 in. zero dead volume reducing union (Valco) was attached to the outlet. Octadecylsilane (ODS) packing was slurried in acetonitrile containing 2–4% (v/v) of polyoxyethylene dodecyl ether or in tetrachloromethane containing the same nonionic detergent and packed at 300–350 bar by using a Familic-300S pump [Jasco (Japan Spectroscopoic Co.), Tokyo, Japan]. A mixture of acetonitrile and distilled water was selected as the packing solution in the former instance and methanol in the latter. The slurry solution was sucked into the stainless-steel tubing of 1.6 m × 0.8 mm I.D. The packing materials were prevented from leaking out of the column by using 1/16 in. home-made stainless-steel frits (2 μm). Develosil ODS (Nomurachemical, Seto-shi, Japan) and ODS-Hypersil (Shandon, Cheshire, U.K.) were employed as the packing materials in this work.

Apparatus

The liquid chromatograph consisted of a pump, a micro valve injector, a separation column and a detector. A Familic-300S pump, an LKB 2150 HPLC pump (LKB, Bromma, Sweden) and a microMetric metering pump (LDC/Milton Roy, Riviera Beach, FL, U.S.A.) were employed. A 20-nl volume of sample solution was injected with an ML-422 micro valve injector (Jasco). The connecting tubing between the injector and the column was prepared in the laboratory, and consisted of stainless-steel tubing of 0.2 mm O.D. × 0.08 mm I.D. soldered into stainless-steel tubing of 1/16 in. O.D. × 0.25 mm I.D. with silver solder. This led to decreased extra-column band broadening. The connecting tubing between the column and the detector consisted of fused-silica tubing of 0.24 mm O.D. × 0.055 mm I.D. The upstream end of the tubing was fixed into stainless-steel tubing of 0.8 mm O.D. × 0.25 mm I.D., which allowed the tubing to be connected with the 1/16 × 1/32 in. reducing union attached to the outlet of the column. Uvidec-100 and 100II (Jasco) UV spectrophotometers were employed as detectors. The flow cell was modified in the laboratory and the structure of the flow cell was nearly the same as that in previous work[6]. The cell volume was *ca.* 0.05 μl. The time constant of the detector was modified to *ca.* 0.05 sec for rapid separation.

Reagents

Reagents were supplied by Wako (Osaka, Japan) and employed without any treatment, unless indicated otherwise. Sodium 1-hexanesulphonate was supplied by Tokyo Chemical Industry (Tokyo, Japan).

RESULTS AND DISCUSSION

The performance of the column is strongly affected by the chemical and physical properties of the column tubing. Fused-silica and glass tubing columns give higher

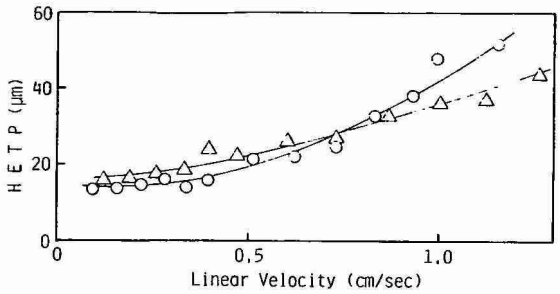

Fig. 1. HETP *versus* linear velocity. Columns: Develosil ODS-5 (5 μm); ○, fused silica, 150 × 0.34 mm I.D.; △, glass-lined stainless-steel, 141 × 0.3 mm I.D. Mobile phase: acetonitrile–water (7:3). Sample: pyrene.

efficiencies in micro HPLC, owing to their smooth surface. The performance of the glass-lined stainless-steel tubing column was compared with that of the fused-silica tubing column using 5-μm ODS particles. Fig. 1 illustrates the relationships between the theoretical plate height (HETP) and the linear velocity of the mobile phase. No difference in the efficiency of the columns is observed at lower linear velocities, whereas smaller HETP values are attained by the glass-lined stainless-steel tubing column at higher linear velocities. This result may be caused by expansion of the fused-silica tubing at higher pressures, which lead to poorer efficiency of the fused-silica tubing column at higher linear velocities compared with the glass-lined stainless-steel tubing column. The pressure drop across the fused-silica tubing column at a linear velocity of 1 cm/sec was *ca.* 180 bar under the conditions shown in Fig. 1, whereas that of the glass-lined stainless-steel tubing column was *ca.* 140 bar.

Fig. 2 shows the separation of polynuclear aromatic hydrocarbons (PAHs) on a glass-lined stainless-steel tubing column of 141 × 0.3 mm I.D. The reproducibility

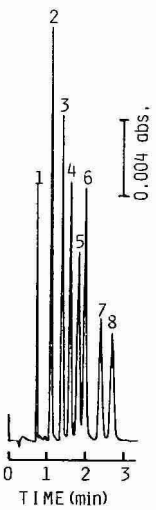

Fig. 2. Separation of PAHs. Column: Develosil ODS-5, 141 × 0.3 mm I.D. Mobile phase: acetonitrile–water (7:3). Flow-rate: 20 μl/min. Peaks: 1 = benzene; 2 = naphthalene; 3 = biphenyl; 4 = fluorene; 5 = phenanthrene; 6 = anthracene; 7 = fluoranthene; 8 = pyrene. Wavelength of UV detection: 254 nm.

of the retention time and the peak height was examined using an LKB-2150 HPLC pump. The relative standard deviations of both parameters for ten measurements were less than 1%.

Fig. 3 shows the rapid separation of an artificial mixture of L-ascorbic acid, theophylline and caffeine, and indicates that high-speed micro HPLC will be useful in routine analysis.

Fig. 4 demonstrates the separation of components in a commercially available cold medicine. One capsule of the cold medicine was extracted with 10 ml of methanol under ultrasonic vibration, the supernatant solution was filtered with a membrane filter (0.45 μm) and 20 nl of the prepared solution were injected. Acetaminophen, caffeine and methylephedrine were separated.

Fig. 3. Rapid separation of an artificial mixture. Column: ODS-Hypersil-3 (3 μm), 49 × 0.3 mm I.D. Mobile phase: methanol–10 m*M* acetic acid (25:75). Flow-rate: 20 μl/min. Peaks: 1 = L-ascorbic acid; 2 = theophylline; 3 = caffeine. Wavelength of UV detection: 265 nm.

Fig. 4. Separation of components in a cold medicine. Column: Develosil ODS-5, 150 × 0.3 mm I.D. Mobile phase: acetonitrile–0.1 *M* phosphate buffer (pH 3.0) containing 2 m*M* sodium 1-hexanesulphonate (1:9). Flow-rate: 10 μl/min. Peaks: 1 = acetaminophen; 2 = caffeine; 3 = methylephedrine. Wavelength of UV detection: 210 nm.

Glass-lined stainless-steel tubing columns facilitate operation at high pressures. The system allowed carbon dioxide to be employed as the mobile phase by keeping the pressure of the whole chromatographic system higher than the vapour pressure of carbon dioxide. The system was nearly the same as that in previous work[6] except for the separation column. A Familic-300S pump was employed in the constant-pressure mode. Fig. 5 demonstrates the rapid separation of PAHs on the ODS column. The mobile phase is liquid as the column temperature is kept lower than the critical temperature of carbon dioxide. Liquid or supercritical carbon dioxide has

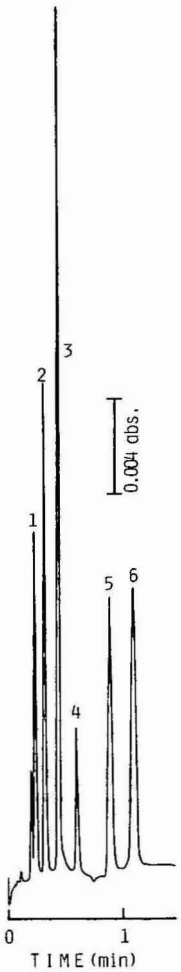

Fig. 5. Rapid separation of PAHs using liquid carbon dioxide as the mobile phase. Column: Develosil ODS-5, 141 × 0.3 mm I.D. Inlet pressure: 150 kg/cm². Temperature: 22.5°C. Wavelength of UV detection: 250 nm. Peaks: 1 = toluene; 2 = naphthalene; 3 = fluorene; 4 = anthracene; 5 = fluoranthene; 6 = pyrene.

lower a viscosity than common mobile phases in HPLC, which facilitates rapid separations. The system will be applicable to supercritical fluid chromatography with carbon dioxide as the mobile phase.

CONCLUSION

Micro packed columns made of glass-lined stainless-steel tubing give reasonable efficiencies, comparable or slightly superior to those of fused-silica tubing columns at higher linear velocities. They facilitate operation at high pressures and are applicable to liquid chromatography with carbon dioxide as the mobile phase.

REFERENCES

1 T. Takeuchi and D. Ishii, *J. Chromatogr.*, 213 (1981) 25.
2 T. Takeuchi and D. Ishii, *J. Chromatogr.*, 190 (1980) 150.
3 Y. Hirata and K. Jinno, *J. High Resolut. Chromatogr. Chromatogr. Commun.*, 6 (1983) 196.
4 F. J. Yang, *J. Chromatogr.*, 236 (1982) 265.
5 T. Takeuchi and D. Ishii, *J. Chromatogr.*, 238 (1982) 409.
6 T. Takeuchi, D. Ishii, M. Saito and K. Hibi, *J. Chromatogr.*, 295 (1984) 323.

Journal of Chromatography, 332 (1985) 9–13
Elsevier Science Publishers B.V., Amsterdam — Printed in The Netherlands

CHROMSYMP. 632

ESTIMATION OF CATECHOLAMINES BY ION-EXCHANGE CHROMATOGRAPHY ON ASAHIPAK ES-502C, USING GLYCYLGLYCINE AS THE POST-DERIVATIZING AGENT

TOKUICHIRO SEKI* and YOSHIHISA YAMAGUCHI
College of Bio-Medical Technology, Osaka University, 1-1, Machikaneyama-cho, Toyonaka, Osaka 560 (Japan)
and
KOHJI NOGUCHI and YUZO YANAGIHARA
Asahi Chemical Ind. Co., Ltd. 1-3-2, Yakoo, Kawasaki-ku, Kawasaki-shi 210 (Japan)
(First received March 27th, 1985; revised manuscript received May 15th, 1985)

SUMMARY

The estimation of catecholamines in human urine was carried out by ion-exchange chromatography on a column of a weakly acidic ion exchanger with an hydrophilic matrix. The catecholamines were first adsorbed onto Amberlite CG-50 (buffered at pH 6.5 with 0.4 *M* phosphate buffer) and selectively eluted by 0.66 *M* boric acid solution. They were then separated from impurities that responded to fluorometric detection by isocratic elution from a column of Asahipak ES-502C, a cross-linked vinyl alcohol copolymer with carboxymethyl groups, at 60°C. The mobile phase was 0.05 *M* sodium succinate buffer pH 5.25 containing 0.015 *M* borate and 0.5 m*M* ethylenediaminetetraacetate. Isoproterenol was used as the internal standard; epinephrine, norepinephrine, isoproterenol and dopamine were eluted in this order. One sample could be analyzed every 35 min. The detection limits were 0.2 ng for epinephrine and norepinephrine, 0.6 ng for dopamine. The elution pattern was quite reproducible; the elution volumes of the catecholamines had not changed after 500 determinations.

INTRODUCTION

The separation of catecholamines has been performed by ion-exchange[1–6] or ion-pair chromatography[7–10]. Reversed-phase chromatography was particularly suitable for the separation of fluorescent derivatives of catecholamines[11–14]. Eluents containing crown ethers have also been used[15]. However, when these chromatographic methods were used for the separation of urinary catecholamines, impurities to which the electrochemical detector responded or whose fluorescence was excited by the light used for fluorometric estimatioin sometimes overlapped with the peaks of catecholamines.

0021-9673/85/$03.30

Since hydrophobic interaction of the impurities with the stationary phase may be the main cause of this interference, we used a cation exchanger with an hydrophilic matrix for the separation of catecholamines in human urine. Complete separation of catecholamines from impurities that respond to the fluorometric estimation was achieved.

EXPERIMENTAL

Reagents

Epinephrine bitartrate, norepinephrine bitartrate, dopamine hydrochloride, isoproterenol hydrochloride and glycylglycine were purchased from Sigma (St. Louis, MO, U.S.A.). Other chemicals were of analytical grade and obtained from Yashima Pharmaceutical Co. (Osaka, Japan). Stock solutions of catecholamines (1 mg/ml) were prepared in 0.01 *M* hydrochloric acid, and they were diluted in a 0.027 *M* succinate–0.42 *M* borate buffer (pH 5.25), containing 3 m*M* ethylenediaminetetraacetate and β-thiodiglycol (0.1%, w/v) to give a standard solution containing 50 ng of epinephrine, 50 ng of norepinephrine, 125 ng of dopamine and 100 ng of isoproterenol per ml.

Equipment

A constant-flow pump (Jasco, Model Trirotar III) was used to pump buffer through the chromatographic column. A dual-head pump (Jasco, Model SP-024-2) was used to pump reagents and mix them with the eluate. A fluorometer (Jasco, Model FP-115), equipped with a flow cell (volume, 7 μl), was used to measure fluorescence. Samples were injected by an automatic injector (Kyowa Seimitsu, Model KSST-60J).

Preparation of Amberlite CG-50 column

Amberlite CG-50 (Type 2) was graded according to size and washed, as described previously[3]. The sodium ion form of the resin (particle size 100–140 μm) was transferred with three volumes of water into a beaker, and the suspension was adjusted to pH 6.7 with a solution of 0.4 *M* sodium dihydrogen phosphate. Then the suspension was poured into a sintered glass filter and washed with a 0.4 *M* phosphate buffer pH 6.5 until the pH of the washings was 6.5. The buffered resin was poured into a tube (10 × 0.5 cm I.D. with a 5-ml reservoir) with 0.4 *M* phosphate buffer pH 6.5 and allowed to settle under gravity to form a resin bed, 1.0 ml in volume. The column was washed with 1 ml of deionized water before use.

Separation of catecholamine fraction from humnan urine

A 1.0-ml portion of filtered urine was mixed with 0.2 ml of a 5% solution of disodium ethylenediaminetetraacetate, 0.2 ml of 1% solution of ascorbic acid and 200 ng of isoproterenol in 1.0 ml of 0.01 *M* hydrochloric acid, and the mixture was adjusted to pH 6.2–6.3 with 1 *M* sodium hydrogen carbonate solution. The mixture was then applied to an Amberlite CG-50 column, which was washed with 3 ml of deionized water and then with 0.8 ml of 2/3 *M* boric acid solution. A further 1.25 ml of boric acid solution were used to elute catecholamines from the column, the eluate being collected in a test-tube containing 0.70 ml of 0.08 *M* succinic acid and 0.05 ml each of 5% disodium ethylenediaminetetraacetate solution and 5% β-thiodiglycol solution. The catecholamine fraction was stored in a refrigerator.

Chromatographic separation and fluorometric determination

A 0.2-ml of aliquot of the sample solution was injected into a 10 × 0.76 cm I.D. column packed with Asahipak ES-502C, (a cross-linked vinyl alcohol copolymer with carboxymethyl groups, column temperature kept at 60°C). The mobile phase (pH 5.25, 0.05 *M* succinate–0.015 *M* borate–0.5 m*M* ethylenediaminetetraacetate) was pumped at a rate of 1.0 ml/min and the eluate was mixed with reagents A and B. Reagent A was a solution of 0.1 *M* glycylglycine pH 6.5 containing 0.05 *M* boric acid, 3 m*M* zinc sulphate and 0.2 *M* tartaric acid; reagent B was a 0.25 *M* potassium borate buffer pH 9.2 containing hexacyanoferrate(III) (0.01%, w/v). Each reagent was pumped at a flow-rate of 0.35 ml/min with a dual-head pump and mixed by using a T-shaped connector. The mixture of reagents and the eluate from the column was heated at 90°C in a PTFE tube (30 m × 0.5 mm I.D., 1.5 mm O.D.), immersed in a water-bath. The fluorescence was measured with a fluorometer (Jasco, Model FP-115).

RESULTS AND DISCUSSION

The elution patterns of standards and of a urine sample are shown in Fig. 1. The pH of the mobile phase was 5.25 and was optimal for the separation of four catecholamines eluted in the order: epinephrine (E), norepinephrine (N), isoproterenol (I) and dopamine (D). The use of an eluent with higher pH shifted the position of the peak of I between those of E and N, and a higher concentration of borate in the eluent reduced the elution volumes of the peaks of these catecholamines and also reduced the separation of the peaks of E, N and I. The urine sample contains a higher concentration of borate (0.42 *M*) than that in the mobile phase (0.015 *M*), but the higher concentration did not have an adverse effect on the elution pattern of catecholamines because the sodium ion concentration of the sample (0.04 *M*) is lower than that of the mobile phase (0.075 *M*). Although the resolution of the peaks of these catecholamines was better at 50°C, separation at 60°C was necessary for analysis of some samples.

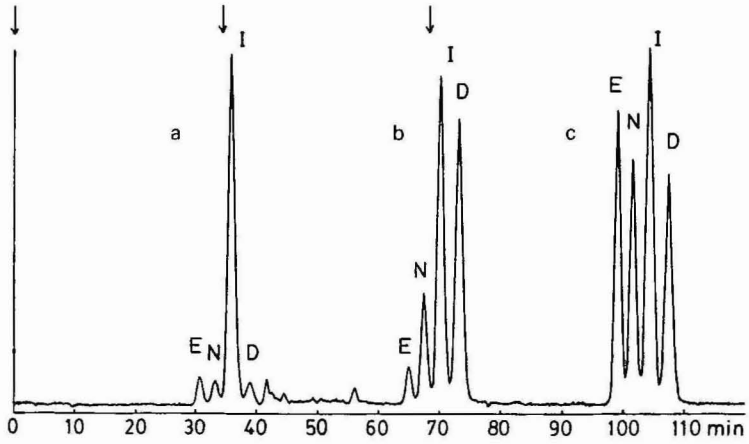

Fig. 1. Elution pattern of catecholamines. The arrows indicate the time of injection. a, 1 ng of E and N, 20 ng of I and 2.5 ng of D; b, catecholamine fraction of human urine; c, 10 ng of E and N, 20 ng of I and 25 ng of D.

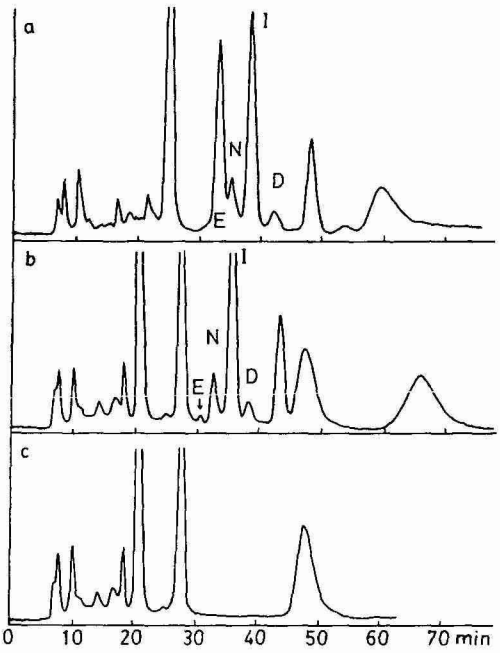

Fig. 2. Elution patterns of catecholamines in a urine sample. a, Separation at 50°C. Peak of E overlapped with the large unidentified peak just ahead of the peak of N. b, Separation at 60°C. E was eluted as the small peak between the large unidentified peak and the peak of N. c, Separation at 60°C, with water instead of reagent A. Note that the peaks of the catecholamines have disappeared.

As is shown in Fig. 2a, at 50°C the peaks of E and N overlapped with those of impurities, but the impurities were eluted before E at 60°C (Fig. 2b). When water was used instead of reagent A, the peaks due to the catecholamines disappeared completely (Fig. 2c). Therefore, the selectivity of the glycylglycine method was confirmed. The presence of zinc sulphate in reagent A, as described previously[5], increased the fluorescence intensity of the products derived from dopamine, and a further increase in intensity was observed upon addition of 0.2 *M* tartrate to reagent A.

A linear relationship between the peak height and the amount of the amines added to the column was obtained over the range 0.5–100 ng for epinephrine and norepinephrine and 1.5–150 ng for dopamine. Samples could be analyzed every 35 min, and even after 500 determinations the elution pattern was quite reproducible. Based on seven determinations of 1.0-ml aliquots of the same urine sample, the mean amounts of E, N and D per millilitre of urine were calculated to be 13.6 ± 0.34 (S.D.), 46.2 ± 1.12 and 316 ± 9.23 ng respectively. When 100 ng each of E and N and 250 ng of D were added to a urine sample and the procedure described above was carried out, the recoveries were 97.7 ± 2.66 (S.D.), 96.5 ± 3.43 and 97.0 ± 2.03% respectively (six determinations).

The results indicate that Asahipak ES-502C, a cross-linked vinyl alcohol copolymer, is suitable for the estimation of catecholamines in human urine.

REFERENCES

1 K. Mori, *J. Chromatogr.*, 218 (1981) 631.
2 E. Ueda, N. Yoshida, K. Nishimura, T. Joh, S. Antoku, K. Tsukada, S. Ganno and T. Kokubu, *Clin. Chim. Acta*, 80 (1977) 447.
3 T. Seki, *J. Chromatogr.*, 155 (1978) 415.
4 M. Hamaji and T. Seki, *J. Chromatogr.*, 163 (1979) 329.
5 T. Seki and Y. Yamaguchi, *J. Chromatogr.*, 287 (1984) 407.
6 A. Yamatodani and H. Wada, *Clin. Chem.*, 27 (1981) 1983.
7 R. M. Riggin and P. T. Kissinger, *Anal. Chem.*, 49 (1977) 2107.
8 J. Wagner, M. Palfreyman and M. Zraika, *J. Chromatogr.*, 164 (1979) 41.
9 D. S. Goldstein, R. Stull, R. Zimlichman, P. D. Levinson, H. Smith and H. R. Keiser, *Clin. Chem.*, 30 (1984) 815.
10 G. C. Davis and P. T. Kissinger, *Anal. Chem.*, 53 (1981) 156.
11 K. Imai, M. Tsukamoto and Z. Tamura, *J. Chromatogr.*, 137 (1977) 357.
12 T. P. Davis, C. W. Gehrke, C. W. Gehrke, Jr., T. D. Cunningham, K. C. Kuo, O. Gerhardt, H. D. Johnson and C. H. Williams, *Clin. Chem.*, 24 (1978) 1317.
13 G. Schwedt and H. H. Bussemas, *Fresenius' Z. Anal. Chem.*, 283 (1977) 23.
14 H. Noda, A. Mitsui and H. Ohkura, *Bunseki Kagaku*, 33 (1984) 263.
15 T. Nakagawa, *J. Chromatogr.*, 254 (1983) 27.

Journal of Chromatography, 332 (1985) 15–18
Elsevier Science Publishers B.V., Amsterdam — Printed in The Netherlands

CHROMSYMP. 633

Note

Polyallylamine-coated silica gel microbore column for liquid chromatography

SOUJI ROKUSHIKA*, DE YING HUANG*, ZONG YIN QIU** and HIROYUKI HATANO
Department of Chemistry, Faculty of Science, Kyoto University, Sakyo-ku, Kyoto 606 (Japan)
(First received April 1st, 1985; revised manuscript received May 20th, 1985)

Pellicular-type packing materials for liquid chromatography have been prepared by coating and cross-linking the amine or imine compounds on the surface of silica gel beads. Columns coated with polyamide[1] and polyvinylpyrrolidone[2] were applied to the separation of aromatic acids and phenols. Poly(ethyleneimine) (PEI)-coated and cross-linked silica gel columns have been developed and applied to the liquid chromatography of proteins[3] and oligonucleotides with up to 35 bases[4].

In previous papers[5,6], PEI-coated microbore columns have been used for the separation of isomeric derivatives of aromatic acids and phenols. Polyallylamine (PAA) is a recently commercialized compound with amino group side-chains. This paper describes the use of PAA, coated on silica gel columns.

MATERIALS AND METHODS

Chromatography was carried out with a Shimadzu LC-5A pump (Shimadzu, Kyoto, Japan) and a UV detector (a Shimadzu SPD-2AM or a JASCO UVIDEC II, Japan Spectroscopic, Tokyo, Japan). The sample injector was a Rheodyne micro injector 7410 (0.5-μl loop) or a JASCO micro loop injector (0.05 μl).

A solution of PAA hydrochloride was mixed with sodium hydroxide solution to neutralize the hydrochloric acid. To coat the silica gel beads, they were suspended in a sodium hydroxide solution of PAA hydrochloride (35 mg/ml) and dispersed with a sonicator. After leaving for 1 h, the slurry was packed into 0.8 mm I.D. or 0.33 mm I.D. stainless-steel tubes, using a JASCO FLC 700 syringe-type pump under a pressure of 250–400 kg/cm^2. After washing with water until the eluate pH decreased to 7, the column was equilibrated with the eluent. These columns have a porous Teflon frit at the end of the tubes.

PAA hydrochloride (mol.wt. 8500–11 000) was obtained from Nitto Boseki (Osaka, Japan), and spherical silica gel beads (Develosil 10, particle diameter 10 μm, and Develosil 3, 3 μm) were from Nomura Chemicals (Seto, Japan). Other chemicals were purchased from Nakarai Chemicals (Kyoto, Japan).

* Present address: Department of Chemistry, South Central Institute for National Minorities, Wuhan, China.
** Present address: Chongqing Medical College, Chongqing, Sichuan, China.

0021-9673/85/$03.30

RESULTS AND DISCUSSION

PAA could not be coated on to the silica gel surface from an aqueous solution of PAA hydrochloride. Therefore, base was added to the solution to neutralize the hydrochloric acid.

The optimum amount of alkaline reagent for the column preparation was examined. The retention of nitrophenols was used to estimate the column capacity and selectivity. Retention increased with the ratio of sodium hydroxide added and stabilized at a constant value above the equimolar ratio of base to hydrochloric acid in the PAA hydrochloride solution. Therefore, an equimolar amount of base was added to the PAA hydrochloride as a coating solution.

The retention of *p*-hydroxybenzoates is plotted in Fig. 1A as a function of PAA concentration. The retention of methyl and ethyl esters of *p*-hydroxybenzoate increased with the concentration of PAA. On the other hand, the retention of propyl and butyl esters and *o*-phenylphenol was at a maximum at 1% PAA concentration, and decreased as the PAA concentration increased. Above 10% PAA all compounds acquired constant capacity factors (k').

The plots of the k' values of mono- and dinitrophenols against PAA concentration are shown in Fig. 1B. The retention of dinitrophenols were affected more strongly than that of mononitrophenols, and maximum k' values were again attained with 10% PAA solution.

The carbon contents of the PAA-coated Develosil 3 prepared from 1% to 10% PAA concentrations increased from 3.2% to 9.6%; above 10% PAA, the carbon content became constant.

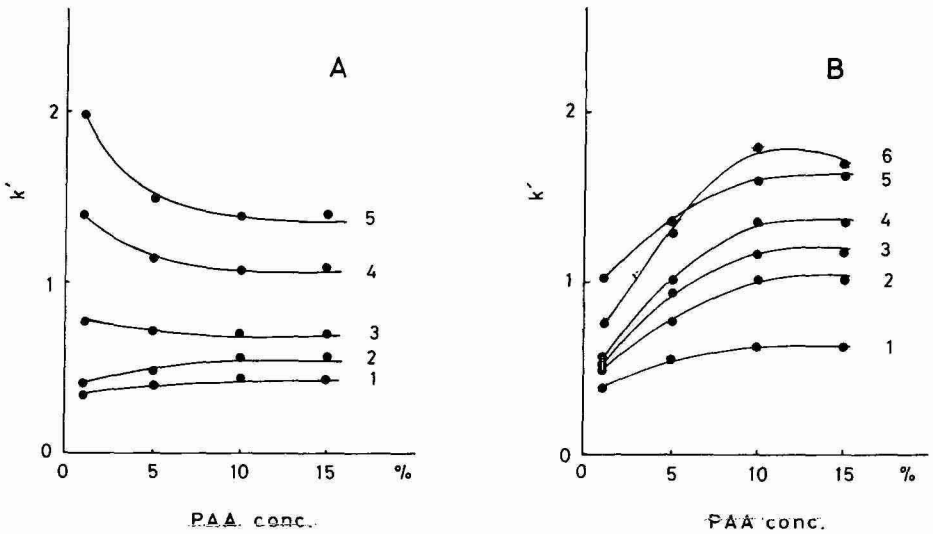

Fig. 1. Retention on a PAA column as a function of PAA concentration in the coating solutions. (A) *p*-Hydroxybenzoate esters and *o*-phenylphenol. Curves: 1 = methyl *p*-hydroxybenzoate; 2 = ethyl *p*-hydroxybenzoate; 3 = *n*-propyl *p*-hydroxybenzoate; 4 = *o*-phenylphenol; 5 = *n*-butyl *p*-hydroxybenzoate. (B) Nitrophenols. Curves: 1 = *m*-nitrophenol; 2 = *p*-nitrophenol; 3 = 2,5-dinitrophenol; 4 = 2,4-dinitrophenol; 5 = *o*-nitrophenol; 6 = 2,6-dinitrophenol. Temperature, ambient; eluent, 5 m*M* sodium hydrogen carbonate.

Silanol groups on the silica gel surface, which carry a negative charge, form ion pairs with the free amino groups in PAA, so that PAA molecules will cover the surface of silica gel. At lower concentrations, PAA molecules can spread completely over the silica surface, and most of the amino groups pair with silanol groups with the hydrocarbon chain on the outside. In this manner, the silica gel is covered by a monolayer of PAA and behaves as a reversed-phase stationary matrix. Therefore, *p*-hydroxybenzoates with large hydrocarbon groups, such as propyl and butyl esters and *o*-phenylphenol, are more strongly retained. As the concentration of PAA increases, some of the amino groups in PAA cannot form ion pairs with silanol groups. Hence the PAA molecule attaches itself partially to the silica gel surface with the remaining amino groups free in solution. The polarity of the stationary phase then increases as the PAA concentration increases. The retention of propyl and butyl esters and *o*-phenylphenol decreased with increasing PAA concentration in the coating solution, whereas more polar compounds, such as methyl and ethyl esters, were oppositely affected. Nitrophenols may be adsorbed by hydrogen bonding and/or charge-transfer interaction at the hydroxyl and nitro groups in the solute molecules on the amino groups of the stationary PAA molecule.

A chromatogram for hydroxybenzoic acid isomers obtained with a 170 × 0.8 mm I.D. column and a 5 m*M* sodium hydrogen carbonate eluent is shown in Fig. 2A. Mono-, di- and trinitrophenols were separated under the same conditions. Retention of nitrophenols increased with the number of nitro groups in the solute molecules (Fig. 2B).

PAA-coated silica gel beads with a particle diameter of 3 μm was packed into a 50 × 0.33 mm I.D. column. The separations of dinitrophenols and nitrophenols are depicted in Figs. 3A and B, respectively.

The PAA column retained phenol isomers such as nitrophenols, chlorophenols and *p*-hydroxybenzoate esters and showed excellent selectivity. However, the column showed very weak interaction with benzoic acids over an eluent pH range from 4 to 9. These results may indicate that the major interaction forces between the phenolic

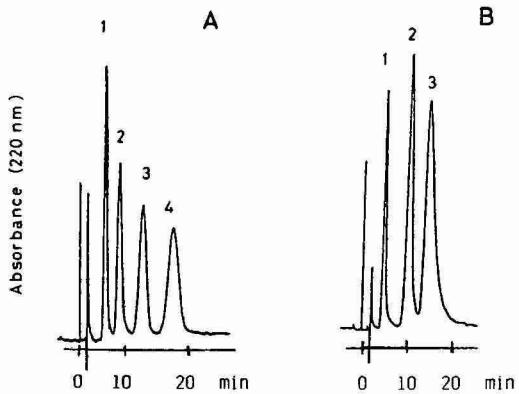

Fig. 2. Chromatograms of hydroxybenzoic acids and nitrophenols. (A) Hydroxybenzoic acid isomers. Peaks: 1 = benzoic acid; 2 = *o*-hydroxybenzoic acid; 3 = *m*-hydroxybenzoic acid; 4 = *p*-hydroxybenzoic acid. (B) Nitrophenols. Peaks: 1 = *m*-nitrophenol; 2 = 2,4-dinitrophenol; 3 = 2,4,6-trinitrophenol. Column, polyallylamine-coated Develosil 10, 170 × 0.8 mm I.D.; eluent, 5 m*M* sodium hydrogen carbonate; flow-rate, 50 μl/min; temperature, ambient; sample volume, 0.5 μl; detection wavelength, 220 nm.

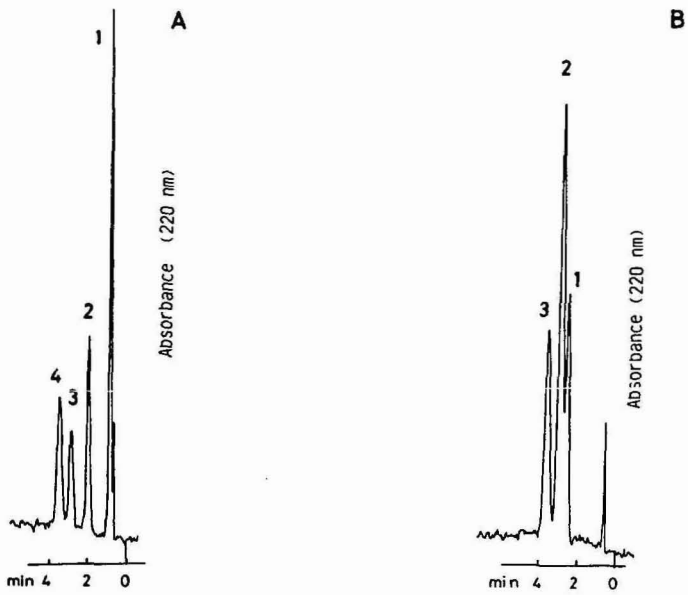

Fig. 3. Chromatograms of nitrophenols and dinitrophenols. (A) Nitrophenol isomers. Peaks: 1 = phenol; 2 = *m*-nitrophenol; 3 = *p*-nitrophenol; 4 = *o*-nitropenol. (B) Dinitrophenol isomers. Peaks: 1 = 2,5-dinitrophenol; 2 = 2,4-dinitrophenol; 3 = 2,6-dinitrophenol. Column, polyallylamine-coated Develosil 3, 50 × 0.33 mm I.D.; PAA hydrochloride concentration in coating solution, 10%; eluent, 5 m*M* sodium hydrogen carbonate (pH 8); flow-rate, 8 μl/min; pressure, 40 kg/cm²; temperature, 40°C; detection wavelength, 220 nm; sample volume, 0.05 μl.

compounds and the PAA column are hydrogen bonding and charge-transfer interaction which cooperate with hydrophobic interactions. On the other hand, ion-exchange interaction does not take part in the retention mechanisms of these compounds.

The PAA-coated pellicular-type column was easy to prepare and will be useful for the separation of isomeric phenolic compounds. The columns were stable for more than three weeks with carbonate eluents.

REFERENCES

1 L. Olsson and O. Samuelson, *J. Chromatogr.*, 106 (1975) 139.
2 L. Olsson, N. Renne and O. Samuelson, *J. Chromatogr.*, 123 (1976) 355.
3 A. J. Alpert and F. E. Regnier, *J. Chromatogr.*, 185 (1979) 375.
4 J. D. Pearson and F. E. Regnier, *J. Chromatogr.*, 255 (1983) 137.
5 Z. Y. Qiu, D. Y. Huang, S. Rokushika and H. Hatano, *Bunseki Kagaku (Jap. Anal.)*, 33 (1984) 481.
6 S. Rokushika, Z. Y. Qiu, D. Y. Huang and H. Hatano, *Anal. Lett.*, 17 (1984) 945.

Journal of Chromatography, 332 (1985) 19–27
Elsevier Science Publishers B.V., Amsterdam — Printed in The Netherlands

CHROMSYMP. 636

HIGH-PERFORMANCE LIQUID CHROMATOGRAPHIC STUDIES ON NON-MERCAPT ⇄ MERCAPT CONVERSION OF HUMAN SERUM ALBUMIN. II*

MASARU SOGAMI*, SEIICHI ERA, SHUNJI NAGAOKA, KAZUO KUWATA, KIMIHIRO KIDA and JUN SHIGEMI
Department of Physiology, Gifu University, Gifu (Japan)
KIYOSHI MIURA and EIJI SUZUKI
3rd Department of Internal Medicine, Gifu University, Gifu (Japan)
YASUTOSHI MUTO and EIICHI TOMITA
1st Department of Internal Medicine, Gifu University, Gifu (Japan)
SHIGEO HAYANO
Hayatoku Hospital, Gifu (Japan)
SHIGEKI SAWADA
Sawada Hospital, Gifu (Japan)
KOHJI NOGUCHI
Technical Development Laboratory, Asahi Chemical Industry Co. Ltd., Kawasaki (Japan)
and
SEIJI MIYATA
MB Development Department, Asahi Medical Co. Ltd., Tokyo (Japan)
(First received March 28th, 1985; revised manuscript received May 28th, 1985)

SUMMARY

High-performance liquid chromatographic (HPLC) analysis of human serum albumin (HSA) on a GS-520 column with 0.03 *M* sodium phosphate buffer–0.15 *M* sodium sulphate (pH 6.87) showed three peaks, the principal component corresponding to human mercaptalbumin (HMA) and the secondary and tertiary components to nonmercaptalbumin (HNA). Using HPLC analysis, the nonmercapt → mercapt conversion of HSA during haemodialysis and the mercapt → nonmercapt conversion after haemodialysis in chronic renal failure were re-confirmed, indicating that HMA is a covalent carrier protein for sulphur-containing amino acids. Fractions of HMA in various liver diseases were significantly lower than those of healthy male adults.

INTRODUCTION

Plasma albumin is a mixture of mercaptalbumin and non-mercaptalbumin[1–6]. Mercaptalbumin is prepared by using mercuric dimer of mercaptalbumin[1,2,4,7,8],

* For Part I, see ref. 6.

0021-9673/85/$03.30

DEAE-cellulose or DEAE-Sephadex[9–11], SE-Sephadex[12–15] or activated thiol-Sepharose[16]. In these methods, it is necessary to fractionate mercaptalbumin starting at least from Fraction V (*ca.* 95% plasma albumin) and it is therefore difficult to determine the fraction of mercaptalbumin from a small volume of serum or plasma (5–20 μl) by chromatography. While conducting high-performance liquid chromatographic (HPLC) studies on human serum albumin (HSA), we found a convenient HPLC column for the analysis of fractions of human mercaptalbumin (HMA), non-mercaptalbumin (HNA) and iodoacetamide-blocked mercaptalbumin at neutral pH, without using any pH or salt concentration gradients[5,6]. HNA is composed of at least two kinds of mixed disulphide compounds[5,6,17–19], one with cysteine [HNA(Cys)] and the other with glutathione [HNA(Glut)]. During HPLC of HSA with various buffer solutions, we found a convenient buffer for the resolution of HNA into HNA(Cys) and HNA(Glut). Using a convenient HPLC column[5,6] and buffer solution, the non-mercapt $\rightleftharpoons$ mercapt (HNA $\rightleftharpoons$ HMA) conversion of HSA[6] was re-examined in haemodialysis patients with chronic renal failure and analysed HSA in various liver diseases.

EXPERIMENTAL

Materials

HSA preparations were obtained from Calbiochem Behring (La Jolla, CA, U.S.A.) (Lot 101150), Nippon Seiyaku (Tokyo, Japan) (Lot N471) and Hyland (Glendale, CA, U.S.A.) (Lot 0625M, 127AA). HNA(Cys) and HNA(Glut) were prepared by the intermolecular sulphydryl–disulphide exchange reaction, as described previously[5,6]. Synthesized HNA(Cys) and HNA(Glut) were extensively dialysed against distilled water. Circular dichroism-resolved secondary structures[5,20], that is, values of f_α (fraction of α-helix) and f_β (fraction of β-structure) of HSA and HNA were approximately 0.72 and 0.12, respectively. The major fraction of synthesized HNA(Cys) contained a mixed disulphide with cysteine. Synthesized HNA(Glut) was composed of two kinds of mixed disulphide compounds, one with cysteine and the other with glutathione, HNA(Cys) content being high (*ca.* 40%) in a starting HSA preparation.

Plasma or serum of haemodialysis patients with chronic renal failure before and after haemodialysis were kindly supplied by Hayatoku Hospital (Gifu, Japan) and Sawada Hospital (Gifu, Japan). The haemodialysis of patients was carried out for 5 h with a hollow-fibre haemodialyser as previously described[6] under the following operating conditions: circulation speed of blood, 120–200 ml/min; flow-rate of dialysis fluid, 500 ml/min; dialysis fluid, 132 m*M* Na^+, 2 m*M* K^+, 1.25 m*M* Ca^{2+}, 0.75 m*M* Mg^{2+}, 105 m*M* Cl^-, 33 m*M* CH_3COO^-, 11.1 m*M* glucose. Plasma of healthy male adults and patients with various liver diseases was obtained after overnight fasting.

Chromatography

HPLC analyses of 10 μl of serum or plasma, HSA and HNA were carried out with a Plasmagraph (Asahi Medical, Tokyo, Japan), assembled as follows: a Degasser Model ERC-3110 (Ermer Optical Works, Tokyo, Japan); a Jasco Twincle pump (Japan Spectroscopic, Tokyo, Japan); eight columns of Asahipak GS-520H (Asahi Chemical Industry, Kawasaki, Japan) (25 × 0.75 cm I.D.; 28 ± 1°C); a Jasco Uvidec 100 IV UV monitor; and an autosampler (Model AS-48, Toyo Soda, Tokyo, Japan;

Model 638-08, Hitachi, Tokyo, Japan; or Model 710B, Japan Waters Assoc., Osaka, Japan). Eluent buffer solutions were 0.03 *M* sodium phosphate buffer–0.15 *M* sodium sulphate (pH 6.87) (sulphate buffer) and 0.10 *M* sodium phosphate buffer–0.30 *M* sodium chloride (pH 6.86) (chloride buffer). They were filtered through a Millipore Sterivex-GS filter unit (0.22 μm) or a Triton X-100-free Millipore membrane (0.45 μm) (Millipore, Bedford, MA, U.S.A.). The flow-rates of the sulphate and chloride buffer solutions were 0.80 and 0.50 ml/min, respectively, and the sample size was 10 μl. Fractions of HMA (f_{HMA}) and HNA (f_{HNA}) were obtained by HPLC on eight GS-520H columns (25 × 0.75 cm I.D.)[5,6]. The value of f_{HMA} was calculated by dividing the area under the peak corresponding to HMA by the total HSA area. To obtain these respective areas, a graphical method of symmetrical resolution was employed[6].

RESULTS AND DISCUSSION

Effect of buffer salts on the resolution of HSA into HMA, HNA(Cys) and HNA(Glut)

HPLC profiles of HSA in sulphate buffer showed two major peaks, one corresponding to HMA and the other to HNA (the lower profile in Fig. 1, f_{HMA} = 0.63)[5,6]. Mild reduction of a mixed disulphide bond by glutathione (GSH) [HSA:GSH = 1:5; 0.03 *M* sodium phosphate buffer–0.15 *M* sodium chloride (pH 7.09)] for 4.5 h at 25°C increased the principal peak in the HPLC profile, indicating the principal peak to be HMA (the upper profile in Fig. 1), as previously reported[5]*.

HNA is composed of at least two kinds of mixed disulphide compounds[5,6,15,17–19], one with cysteine [HNA(Cys)] and the other with glutathione [HNA(Glut)]. During HPLC experiments with Asahipak GS-520H, we found that retention time of HNA(Glut) is longer than that of HNA(Cys) in sulphate buffer, resulting in splitting of the HNA into two components, one corresponding to HNA(Cys) and the other to HNA(Glut), as shown in Fig. 2. The major fraction of synthesized HNA(Cys) contained a mixed disulphide with cysteine. Synthesized HNA(Glut) was composed of two kinds of mixed disulphide compounds, one with cysteine and the other with glutathione, the HNA(Cys) content being high (*ca.* 40%) in the starting HSA preparation. Thus, HPLC profiles of synthesized HNA(Glut) showed two peaks in sulphate buffer, one corresponding to HNA(Cys) and the other to HNA(Glut), as shown in Figs. 2 and 4. However, in chloride buffer, synthesized HNA(Glut), showed a broad peak, as shown in the left upper part of Fig. 2.

The lower three examples of HPLC profiles in Fig. 2 also clearly indicate that the resolution of HSA into HMA, HNA(Cys) and HNA(Glut) is far better in sulphate buffer than in chloride buffer. We analysed approximately 150 sera and/or plasma (f_{HMA} = 0.2–0.8) using both buffer solutions and found a good linear correlation between f_{HMA} values with sulphate buffer and those with chloride buffer (data

---

* Although evidence is indirect, the HMA subfraction prepared by SP-Toyopearl chromatography (Toyo Soda) at pH 4.30 and 3°C corresponded exactly to the HMA peak in Figs. 1–5 (sulphate buffer). As previously reported by us[5], synthesized HNA(Cys) monomer, prepared by Toyopearl HW-55 chromatography (chloride buffer), also corresponded exactly to the HNA peak (chloride buffer) and synthesized glucosylated HSA mainly showed the principal peak, indicated as HMA in the figures, because of reduction of a mixed disulphide bond of HNA by glucose. However, carbamylated HSA and the γ-glutamylcysteine derivative of HNA were not analysed with a GS-520H column. HPLC profiles of HSA were not affected by bound impurities, such as fatty acids[5].

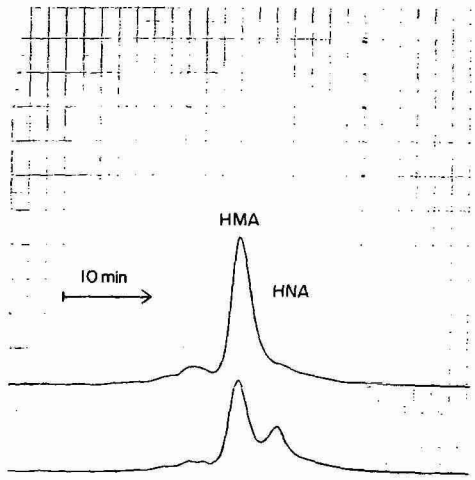

Fig. 1. The lower and upper HPLC profiles (280 nm) show HSA (f_{HMA} = 0.63) and glutathione-treated HSA (HSA:GSH = 1:5, mild reduction of a mixed disulphide bond for 4.5 h at 25°C in 0.03 *M* sodium phosphate buffer–0.15 *M* sodium chloride, pH 7.09), respectively. Flow-rate, 0.80 ml/min. Sample, 10 μl. Eluent, 0.03 *M* sodium phosphate buffer–0.15 *M* sodium sulphate, pH 6.87 (sulphate buffer). Column temperature, 28 ± 1°C. HMA and HNA indicate human mercaptalbumin and non-mercaptalbumin, respectively.

not shown). Unless stated otherwise, only results with sulphate buffer are given here. As shown in Table I, the mean value of f_{HMA} ± standard deviation (S.D.) for 28 healthy male adults of 0.75 ± 0.028 was similar to the 0.76 ± 0.025 (chloride buffer) previously reported by us[6].

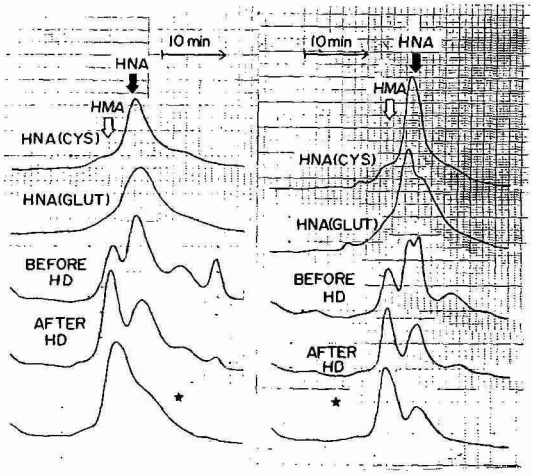

Fig. 2. HPLC profiles of synthesized HNA(Cys), synthesized HNA(Glut), plasma before and after haemodialysis (HD) and a rare example of HSA (★), which did not show a clear resolution into HMA and HNA with chloride buffer. See text on synthesized HNA. The primary and secondary peaks in HNA (sulphate buffer) might correspond to HNA(Cys) and HNA(Glut), respectively. Left (0.10 *M* sodium phosphate buffer–0.30 *M* sodium chloride, pH 6.86): sample, 10 μl; flow-rate, 0.50 ml/min. Right (0.03 *M* sodium phosphate buffer–0.15 *M* sodium sulphate, pH 6.87): sample, 10 μl; flow-rate, 0.80 ml/min.

TABLE I

f_{HMA} VALUES IN PATIENTS WITH VARIOUS LIVER DISEASES*

Parameter	*Control*	*CH*	*LC(c)*	*LC(d)*	*LC(c) and HCC*	*AH*	*FHF*
f_{HMA}	0.75 ± 0.028	0.64 ± 0.053	0.64 ± 0.050	0.49 ± 0.076	0.52 ± 0.073	0.64 ± 0.046	0.33
n	28	23	9	9	10	5	2

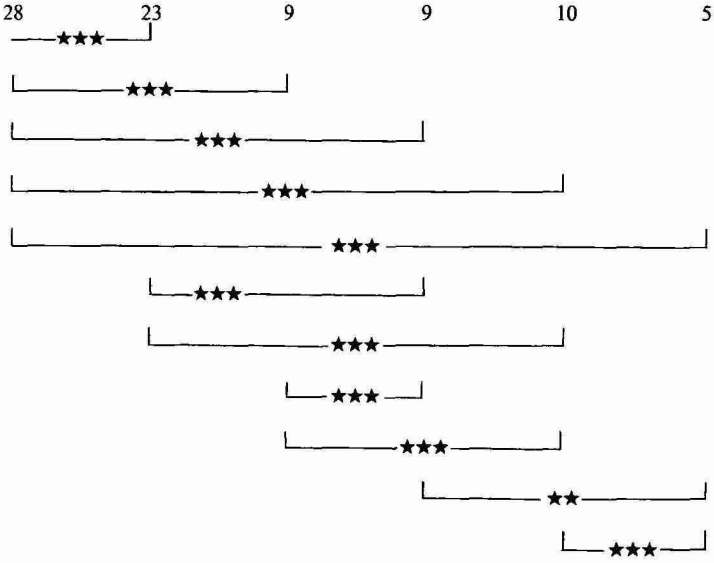

* CH = chronic hepatitis; LC(c) = liver cirrhosis (compensated); LC(d) = liver cirrhosis (decompensated); HCC = hepatocellular carcinoma; AH = acute hepatitis; FHF = fulminant hepatic failure.

** $P<0.01$.

*** $P<0.001$.

Non-mercapt ⇌ mercapt conversion of HSA in haemodialysis patients

Robins *et al.*[21] and Wilcken *et al.*[22] reported that cystine and homocysteine–cysteine mixed disulphide were significantly increased in patients with chronic renal failure and were decreased by haemodialysis for several hours. Isles and Jocelyn[23] and Sogami and co-workers[5,6] also reported that mercaptalbumin is easily converted into non-mercaptalbumin after incubation with cystine at neutral pH. We therefore analysed sera* of chronic renal failure patients by HPLC on Asahipak GS-520H. The mean value of f_{HMA} ± S.D. for 28 patients with chronic renal failure was 0.51 ± 0.096, indicating a significant increase in HNA content**. The present results support those of Isles and Jocelyn[23] as well as our own[6].

* Kindly supplied by professor T. Koshiba (School of Medicine, Kitazato University, Sagamihara, Japan).

** We found that sera and/or plasma of chronic renal failure patients, stored at 3°C, should be analysed by HPLC within a few days or should be stored at −70 to −80°C, because the sera or plasma of the patients before haemodialysis were almost completely converted into HNA on storage at −20°C for 60 days. The major mechanism for HMA → HNA conversion on storage at −20°C might be due to the unfrozen water around the protein, as extensively studied by ^{1}H NMR spectroscopy, etc. (see ref. 24 and references cited therein).

In chronic haemodialysis patients, the HPLC profiles of HSA were completely different from those of healthy adults (Table I), as shown in Figs. 3–5. The mean values of f_{HMA} ± S.D. before haemodialysis for 293 patients (1983–84) and 122 patients (1984–85) were 0.41 ± 0.073 and 0.40 ± 0.093, respectively. These mean values were similar to the value of 0.45 ± 0.08 (n = 112) previously reported by Sogami *et al.*[6] (chloride buffer). After haemodialysis for 5 h, mean values of Δf_{HMA} ± S.D. [(f_{HMA} after haemodialysis) − (f_{HMA} before haemodialysis)] for 291 patients (1983–84) and 110 patients (1984–85) were 0.15 ± 0.086 and 0.17 ± 0.077, respectively. The Δf_{HMA} values were similar to the value of 0.16 ± 0.054 (n = 100) previously reported by Sogami *et al.*[6] (chloride buffer).

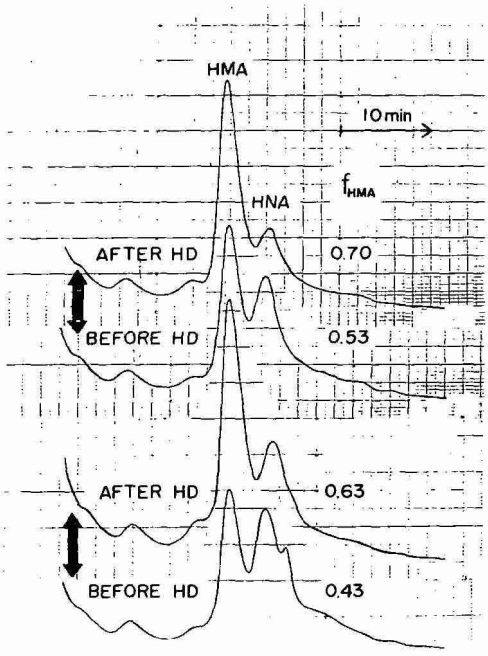

Fig. 3. Two examples (HPLC profiles) of non-mercapt → mercapt conversion (HNA → HMA) of HSA by haemodialysis for 5 h in haemodialysis patients. The double arrow indicates data on the same patient before and after haemodialysis (HD) for 5 h. Eluent, sulphate buffer; sample, 10 μl; flow-rate, 0.80 ml/min.

Two examples of HPLC profiles of HSA in chronic renal failure before and after haemodialysis are shown in Fig. 3 and an example of the time course of HNA → HMA conversion of HSA during haemodialysis for 300 min is shown in Fig. 4.

As we have previously reported[5,6], the HPLC profiles of HSA, eluted from a GS-520H column, were not affected by tightly bound lipid impurities, such as fatty acids, and the retention time of HSA disulphide dimer was very different from those indicated as HMA and HNA. Mild reduction of HSA preparations [plasma before haemodialysis, such as the samples in Fig. 3 (f_{HMA} = 0.43) and Fig. 4 (f_{HMA} = 0.32)] by glutathione (HSA:GSH ≈ 1:5, 0.15 M sodium chloride, pH 7.09) for 100 min at 25°C increased the f_{HMA} values, indicating the principal peak of HSA to be HMA

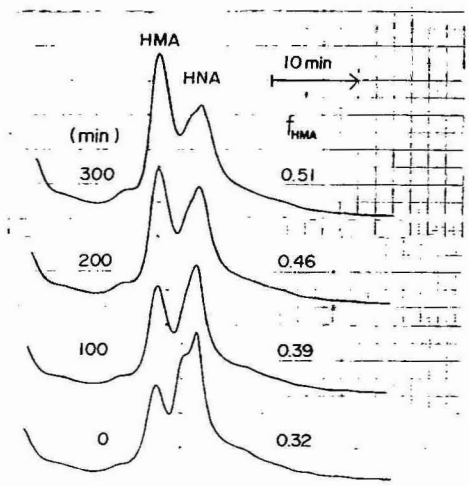

Fig. 4. Time course of non-mercapt → mercapt conversion of HSA in a haemodialysis patient during haemodialysis for 5 h. Eluent, sulphate buffer; sample, 10 μl; flow-rate, 0.80 ml/min.

(data not shown). The results in Figs. 3 and 4 suggested the conversion of HNA to HMA during haemodialysis, that is, non-mercapt → mercapt conversion (HNA → HMA) of HSA, as previously reported by Sogami *et al.*[6].

Sogami *et al.*[6] reported that no HNA → HMA conversion of HSA solution (f_{HMA} = 0.30) was observed on dialysis at 37°C when a haemodialyser was used under the same operating conditions. In order to study the HNA → HMA conversion mechanism, we carried out HPLC analyses of the inlet and outlet blood plasma of

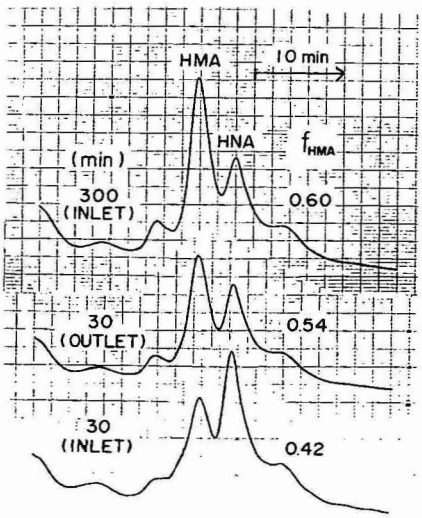

Fig. 5. Time course of non-mercapt → mercapt conversion of HSA in a haemodialysis patient during haemodialysis for 5 h. The lower and middle HPLC profiles are those for HSA of the inlet and outlet blood plasma of a hollow-fibre dialyser *ca.* 30 min after the start of haemodialysis, respectively. Eluent, sulphate buffer; sample, 10 μl; flow-rate, 0.80 ml/min.

the hollow-fibre dialyser *ca.* 30 min after the start of haemodialysis. The mean value of [(f_{HMA} of outlet plasma) − (f_{HMA} of inlet plasma)] ± S.D. for 122 haemodialysis patients was 0.092 ± 0.053, indicating the HNA → HMA conversion to be statistically significant ($P < 0.001$), as shown in Fig. 5. These results suggest some contribution of blood cells to HNA → HMA conversion of HSA during haemodialysis.

The concentration of cystine is extremely high in haemodialysis patients and is decreased by haemodialysis[21,22]. With decreasing cystine concentration on haemodialysis, HNA might be converted into HMA by certain cells, such as blood cells. With increasing cystine concentration in plasma after haemodialysis, the HMA → HNA conversion might be accelerated, as reported by Isles and Jocelyn[23] and Sogami *et al.*[6], according to

$$\text{HMA} + \text{cystine} \rightleftharpoons \text{HNA} + \text{cysteine} \quad (1)$$

and the cysteine produced might be rapidly reoxidized to cystine for re-utilization[6,23]. The present results confirm our reported conclusion that HMA might be the important covalent carrier protein for sulphur-containing amino acids in haemodialysis patients, resulting in decreases of free concentrations of cystine, glutathione disulphide and mixed disulphide compounds, such as homocysteine–cysteine and cysteine–glutathione[6].

HPLC analyses of HSA in various liver diseases

Luetscher[25,26] studied HSA in chronic renal failure, nephrotic syndrome and liver cirrhosis by moving-boundary electrophoresis in acidic medium (pH range of the N–F transition[3]) and found significant differences in the N–F transition between HSA of normal healthy adults and those of the pathological states. We therefore re-examined HSA in various liver diseases, such as chronic hepatitis, liver cirrhosis, by HPLC analyses with a GS-520H column (sulphate buffer). The HPLC profiles of HSA in various liver diseases were completely different from those of normal healthy adults (HPLC profiles not shown). As shown in Table I, f_{HMA} values in various liver diseases were significantly lower than those of healthy male adults*.

ACKNOWLEDGEMENTS

We are grateful to Professor T. Koshiba (School of Medicine, Kitazato University, Sagamihara, Japan) for discussions and supplying plasma samples of chronic renal failure patients, Asahi Medical (Tokyo, Japan) for HPLC equipment and Asahi Chemical Industry (Kawasaki, Japan) for supplies of Asahipak GS-520H HPLC columns. We also thank Asahi Keiki Kogyo (Nagoya, Japan), Japan Waters Assoc. (Osaka, Japan) and Asahi medical for loans of autosamplers. We thank Drs. H. Inouye, J. Sugihara, Y. Yanagihara and T. Hamaguchi and Miss M. Yanagihara for their help with the HPLC analyses.

* Final manuscript now in preparation by Profcssor Y. Muto's group (1st Department of Internal Medicine, School of Medicine, Gifu University) and M. Sogami's group.

REFERENCES

1 H. M. Dintzis, *Ph.D. Thesis,* Harvard University, Cambridge, MA (1952).
2 W. L. Hughes and H. M. Dintzis, *J. Biol. Chem.,* 239 (1964) 845.
3 J. F. Foster, in F. W. Putnam (Editor), *The Plasma Proteins,* Vol. 1, Academic press, New York, 1972, Ch. 6, p. 179.
4 W. L. Hughes, in H. Neurath and K. Bailey (Editors), *The Proteins,* Vol. 2B, Academic Press, New York, 1954, Ch. 21, p. 677.
5 M. Sogami, S. Nagaoka, S. Era, M. Honda and K. Noguchi, *Int. J. Pept. Protein Res.,* 24 (1984) 96.
6 M. Sogami, S. Era, S. Nagaoka, K. Kuwata, K. Kida, K. Miura, H. Inoye, E. Suzuki, S. Hayano and S. Sawada, *Int. J. Pept. Protein Res.,* 25 (1985) 398.
7 P. Clark, M. R. Rachinsky and J. F. Foster, *J. Biol. Chem.,* 237 (1962) 2509.
8 M. Sogami and J. F. Foster, *J. Biol. Chem.,* 237 (1962) 2514.
9 R. W. Hartley, Jr., E. A. Peterson and H. A. Sober, *Biochemistry,* 1 (1962) 60.
10 J. Janatova, J. K. Fuller and M. J. Hunter, *J. Biol. Chem.,* 243 (1968) 3612.
11 J. K. F. Noel and M. J. Hunter, *J. Biol. Chem.,* 247 (1972) 7391.
12 R. D. Hagenmaier and J. F. Foster, *Biochemistry,* 10 (1971) 637.
13 H. J. Nikkel and J. F. Foster, *Biochemistry,* 10 (1971) 4479.
14 S. D. Stroupe and J. F. Foster, *Biochemistry,* 12 (1973) 3824.
15 S. Era, S. Nagaoka, M. Sogami, H. Watari and K. Akasaka, *Int. J. Pept. Protein Res.,* 25 (1985) in press.
16 J. Carlsson and A. Svenson, *FEBS Lett.,* 42 (1974) 183.
17 L. Andersson, *Biochim. Biophys. Acta,* 117 (1966) 115.
18 T. P. King, *J. Biol. Chem.,* 236 (1961) PC5.
19 E. M. Spencer and T. P. King, *J. Biol. Chem.,* 246 (1971) 201.
20 S. Era, H. Ashida, S. Nagaoka, H. Inouye and M. Sogami, *Int. J. Pept. Protein Res.* 22 (1983) 333.
21 A. J. Robins, B. K. Milewezyk, E. M. Booth and N. P. Mallick, *Clin. Chim. Acta,* 42 (1972) 215.
22 D. E. L. Wilcken, V. J. Gupta and S. G. Reddy, *Clin. Sci.,* 58 (1980) 427.
23 T. E. Isles and P. C. Jocelyn, *Biochem. J.,* 88 (1963) 84.
24 I. D. Kuntz, Jr. and W. Kauzmann, *Advan. Protein Chem.,* 28 (1974) 239.
25 J. A. Luetscher, Jr., *J. Amer Chem. Soc.,* 61 (1939) 2880.
26 J. A. Luetscher, Jr., *J. Clin. Invest.,* 19 (1940) 313.

Journal of Chromatography, 332 (1985) 29–37
Elsevier Science Publishers B.V., Amsterdam — Printed in The Netherlands

CHROMSYMP. 637

ION-EXCHANGE HIGH-PERFORMANCE LIQUID CHROMATOGRAPHIC STUDIES ON SULPHYDRYL-CATALYSED STRUCTURAL ALTERATIONS OF BOVINE MERCAPTALBUMIN

KAZUO KUWATA, SEIICHI ERA, HIROSHI INOUYE* and MASARU SOGAMI*
Department of Physiology, School of Medicine, Gifu University, Gifu (Japan)
and
HIROO SASAKI
Scientific Instrument Division, Toyo Soda Manufacturing Co., Ltd., Shin-Nanyo-shi, Yamaguchi-ken (Japan)

(First received April 6th, 1985; revised manuscript received May 28th, 1985)

SUMMARY

The N–A isomerization (the intramolecular SH/S–S exchange reaction) of bovine mercaptalbumin (BMA) in alkaline medium was studied by using ion-exchange high-performance liquid chromatography (HPLC) and moving-boundary electrophoresis. Results obtained by ion-exchange HPLC on the N–A isomerization of BMA were consistent with those by moving-boundary electrophoresis and showed at least two kinds of the A-form, A_1 and A_2, indicating that the N–A isomerization is a multi-step reaction. The rate of the N–A isomerization was strongly suppressed in [^{2}H]water solution. The suppresion by [^{2}H]water might support the current view that intra- and intermolecular hydrophobic and/or hydrogen bonds are strengthened in [^{2}H]water.

INTRODUCTION

At alkaline pH, bovine mercaptalbumin (BMA) isomerizes to the aged form (A-form) by the intramolecular SH/S–S exchange reaction shown in the following equation

$$N \rightleftharpoons A_1 + mH^+ \rightleftharpoons A_2 + nH^+ \rightleftharpoons \cdots \quad (1)$$

where N and A_i are the N- and A-forms, respectively, as reported by Sogami *et al.*[1], Nikkel and Foster[2], Stroupe and Foster[3], Wallevik[4,5] and Inouye *et al.*[6] The N–A isomerization has been studied by using the pH–solubility profile[1,2,7,8], reversible-boundary spreading[9,10], moving-boundary electrophoresis[2,6,10], gel electrophoresis[3], isoelectric focusing[4,5] and ion-exchange chromatography[2]. However, these methods

* Present address: Department of Internal Medicine, School of Medicine, Gifu University, Gifu, Japan.

0021-9673/85/$03.30

are complicated and time consuming compared with ion-exchange high-performance liquid chromatography (HPLC). Ion-exchange HPLC is a convenient technique for assaying the A-form in order to study the kinetics and equilibria of the N–A isomerization in more detail. We have compared data obtained by ion-exchange HPLC with those obtained by other methods[2–6] and studied the suppressing effect of [^{2}H]water on the N–A isomerization.

EXPERIMENTAL

Materials

Crystallized bovine plasma albumin (BPA, Lot N 72905) and Fraction V of BPA (Lot V 75208) were purchased from Armour Pharmaceutical (Chicago, IL, U.S.A.) and were defatted by the modified Chen method[11,12]. Defatted BPA was filtered through a Triton X-100-free Millipore membrane (0.45 μm) (Millipore, Bedford, MA, U.S.A.). Prior to use, defatted BPA was dialysed against appropriate salt solutions or deionized, distilled water, using pre-treated Cellophane tubing[12]. Defatted bovine mercaptalbumin (BMA) was prepared from defatted Fraction V of BPA, using SE-Sephadex C-50 according to the Hagenmaier and Foster method[10]. The SH content of BMA before freeze-drying was 1.00 ± 0.02 mol/mol BMA by the modified Ellman method[6,13,14] at pH 8.02 (0.10 Γ/2 Tris buffer). In the circular dichroism-resolved secondary structure of BMA, the fractions of α-helix, β-structure and unordered form determined by Chen's method[15,16], were 0.68, 0.13 and 0.19, respectively. BPA dimer was prepared as the S–S dimer in 0.10 *M* potassium chloride at pH 3.3, *i.e.*, the mid-point of the acid-induced expansion, in the presence of a catalytic concentration of Cu^{2+} [17,18], as previously described[19]. The degrees of dimerization and polymerization were determined by HPLC on TSK G 3000SW (Toyo Soda, Tokyo, Japan) with 0.10 *M* sodium phosphate buffer–0.30 *M* sodium chloride (pH 6.86) as eluent. SH-blocked BMA or BPA was prepared as previously described by using iodoacetamide (Nakarai Chemicals, Kyoto, Japan, Lot V2H 9676)[6,12,19]. All of the protein solutions were filtered through a Millex HA (0.45 μm) filter (Millipore) before HPLC analysis[19].

In the preparations of aged BPA, a solution of charcoal-defatted BPA was exhaustively dialysed against several changes of deionized, distilled water in a cold-room. Dialyse BPA was deionized by passing it through a Dintzis column[1,6,12]. The pH of the defatted, deionized BPA solution was then raised to the desired value below pH 8.7 by adding 0.30 *M* tris(hydroxymethyl)aminomethane (Tris) and above pH 8.7 by adding 0.30 *M* Tris and 0.10 *M* potassium hydroxide[6]. The solution was then filtered through a Millex HA (0.45 μm) filter into sterilized glassware with a silicone-rubber stopper. Ageing pH values given in the text are the average of pH value before and after ageing[6]. After ageing for the appropriate time at the appropriate pH and temperature, the pH and sodium acetate concentration were adjusted to 4.82 and 0.03 *M* respectively, by adding 1/50 volumes of concentrated sodium acetate buffer. In the preparations of aged BMA, BMA was dissolved in deionized, distilled water. Aged BMA was prepared as described in the aged BPA preparation. In the ageing experiments with BMA in water–[^{2}H]water, the pL was adjusted to the appropriate value by adding 0.30 *M* Tris (water or [^{2}H]water) according to the following equation:

$$pL = (\text{meter reading}) + 0.3314\,n + 0.0766\,n^2$$

where n is the deuterium atom fraction and pL is the generalized equivalent of pH (ref. 20). After adjusting the pH to 4.82 and the sodium acetate concentration to 0.03 *M*, BPA and BMA, aged in water or water–[^{2}H]water, were dialysed against 0.03 *M* sodium acetate buffer at 3°C for at least 1 day and were analysed by moving-boundary electrophoresis and/or ion-exchange HPLC. Some HPLC experiments was carried out without dialysis. Dialysed, aged BMA and BPA were filtered through a Millex HA filter before HPLC analysis.

Methods

Moving-boundary electrophoresis was carried out on a Hitachi HTD-1 Tiselius type instrument (Hitachi, Tokyo, Japan) with a microcell (1.00 ml, 0.180 cm^2 cross-section). The electrophoresis of a dialysed 0.5% solution was conducted at 2.5°C for 1.5–2 h. The buffer was 0.03 *M* sodium acetate buffer (pH 4.82). The results obtained were analysed as previously reported[6]. The conductivities of a dialysed protein solution and buffer were measured with a Yanagimoto Model MY-7 conductometer (Yanagimoto, Osaka, Japan) at 2.5°C.

The two kinds of HPLC system used in these experiments were as follows: (A) an Erma Degasser ERC-3110 (Erma Optical Works, Tokyo, Japan); Toyo Soda HLC-803A HPLC system with a 500 μl sample loop; TSK G 3000SW column (60 × 0.75 cm I.S.); Toyo Soda LS-8 low-angle laser light scattering photometer (632.8 nm); and Jasco Uvidec 100-IV UV monitor (Japan Spectroscopic, Tokyo, Japan); (B) Toyo Soda Gradientor (HLC-803D with a 100-μl sample loop and GE-4); TSK SP-5PW column (7 × 0.75 cm I.D.); and Jasco Uvidec 100-IV UV monitor. System A with the TSK G 3000SW column was used for the determination of monomer, dimer and oligomer contents with 0.10 *M* sodium phosphate buffer–0.30 *M* sodium chloride (pH 6.86) at a flow-rate of 0.50 ml/min and 23 ± 1°C. The weight-average molecular weight was obtained using UV and low-angle laser light scattering profiles, as described previously[19]. System B with the TSK SP-5PW column was used for the determination of the fraction of the A-form. Almost all of the ion-exchange HPLC experiments were carried out on BMA. The N- and A-forms of aged BMA were separated by a 30-min linear gradient elution with increasing sodium chloride concentration from 0.085 to 1.50 *M* in 0.02 *M* sodium acetate buffer (pH 5.00) at a flow-rate of 1.00 ml/min at 23°C. The TSK SP-5PW column was equilibrated with 0.02 *M* sodium acetate buffer (pH 5.00), containing 0.085 *M* sodium chloride, at 23°C. The pH of the 0.02 *M* sodium acetate buffer, containing 1.5 *M* sodium chloride, was adjusted to exactly 5.00 because the pH value of the eluent is important for the separation of the N- and A-forms on the TSK SP-5PW column. Deaeration of buffer solutions was carried out by bubbling helium (initial flow-rate, 1 l/min for 10–20 min; flow-rate during operation, 10–30 ml/min).

The concentrations of BPA and BMA were determined with a Hitachi 320 spectrophotometer, assuming $A_1^{1\%}{}_{cm}$ at 279 nm to be 6.67. The pH measurements were made with a Hitachi–Horiba F-7SS instrument, equipped with an expanded scale, using a Radiometer GK-2401C combined electrode. Deionized, distilled water was prepared by passing glass-distilled water (reflux column height, 1.4 m; specific resistance, $0.9 \cdot 10^6$ Ω cm) through a mixed-bed column and had a specific resistance

far greater than $5 \cdot 10^6$ cm. For HPLC experiments, glass-distilled water was used as a solvent, because it was practically free of dust and was suitable for the low-angle laser light scattering photometer. However, in order to remove dust from buffer salts, buffer solutions were filtered through a Triton X-100-free Millipore membrane (0.45 μm) or a Millipore Sterivex-GS filter (0.22 μm). Cellophane tubing (Visking) was pre-treated by boiling in 50% saturated $NaHCO_3$ (half-saturation at 25°C) and by exhaustive washing with deionized, distilled water[12]. Pre-treated cellophane tubing was stored in a cold-room at 3°C in deionized, distilled water.

All chemicals employed were of analytical-reagent grade. [^{2}H]water (degree of deuteration 99.75%) and [^{2}H]hydrochloric acid and [^{2}H]hydroxide solutions were purchased from Merck (Darmstadt, F.R.G.).

RESULTS AND DISCUSSION

Ion-exchange HPLC of dimerized BPA

As previously described[18,19], Cu^{2+}-catalysed dimerization was found to arise from the intermolecular disulphide formation of BMA. Thus, the monomer in dimerized BPA might be mainly BPA, devoid of SH groups, *i.e.*, bovine nonmercaptalbumin (BNA). The HPLC profile of dimerized BPA, eluted from TSK G 3000SW with 0.10 *M* sodium phosphate buffer–0.30 *M* sodium chloride (pH 6.86) at 23°C, showed at least four components corresponding to monomer, dimer, oligomer, etc. The weight-average molecular weight (M_w) of each component was obtained according to the following equation, assuming the M_w of BMA monomer to be 66000:

$$h(\mathrm{LS})/h(\mathrm{UV}) = L_0 M_w \qquad (2)$$

where h(LS) and h(UV) are the peak heights of the light-scattering intensity at 632.8 nm and the absorbance at 279 nm, respectively, and L_0 is a constant, as described previously[19,21–23]. The values of M_w, corresponding to monomer, dimer and trimer were estimated to be 68100, 132000 and 183000, respectively. Fractions of monomer, dimer and oligomers were 0.37, 0.54 and 0.09, respectively. The ion-exchange HPLC profile of Cu^{2+}-catalysed dimerized BPA, eluted from TSK SP-5PW, showed several peaks, corresponding to monomer, dimer and oligomers. The elution volume of a major peak (the secondary peak), corresponding to dimer, was almost equal to that of the A-form, indicated as A_1 in Fig. 1. Hence small peaks in the HPLC profile of non-aged BMA, eluted from TSK SP-5PW, might be dimer and oligomers, as indicated in Fig. 1. Sogami *et al.*[1] and Inouye *et al.*[6] reported that no formation of intermolecular disulphide bonds with resultant formation of dimeric and oligomeric species during the ageing reaction was observed in ultracentrifugal and HPLC (TSK G 3000SW) analyses. Therefore, assuming the small peaks in the HPLC profile of non-aged BMA, eluted from TSK SP-5PW (left upper HPLC profile in Fig. 1), to be dimer and oligomers, the fraction of the A-form was calculated as shown in Figs. 2–4.

Ion-exchange HPLC on TSK SP-5PW

HPLC profiles of BMA, aged at pH 8.6 without added salt at 25°C for 0 min, 80 min and 26 h, are shown on the left side of Fig. 1. The schlieren patterns of BMA,

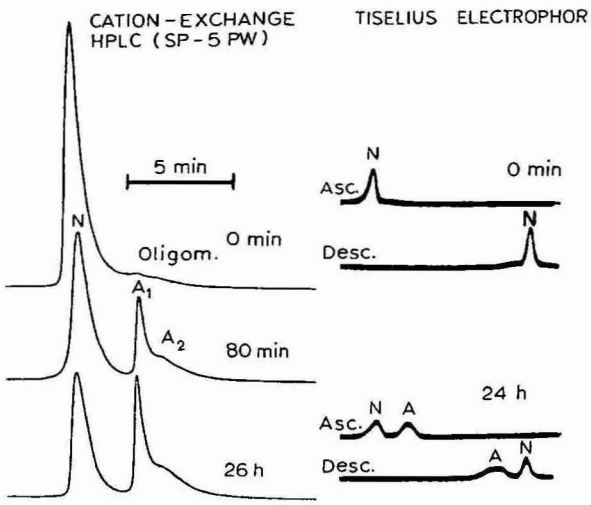

Fig. 1. Moving-boundary electrophoresis (right side, 0.03 *M* sodium acetate buffer, pH 4.82, 2.5°C) and ion-exchange HPLC (left side) of BMA, aged at pH 8.6 with no added salt at 25°C for 0 min, 80 min, 24 h and 26 h. Ion-exchange HPLC on TSK SP-5PW (7 × 0.75 cm I.D.) was carried out by 30-min linear gradient elution with increasing sodium chloride concentrations from 0.085 to 1.50 *M* in 0.02 *M* sodium acetate buffer (pH 5.00) at a flow-rate of 1.00 ml/min at 23°C. N and A (A_1, A_2) indicate the N- and A-forms, respectively. The secondary and tertiary small peaks in the ion-exchange HPLC profile of non-aged BMA might be the dimer, and oligomer, respectively. TISELIUS ELECTROPHOR indicates moving-boundary electrophoresis by a Tiselius type instrument. Asc. and Desc. indicate ascending and descending schlieren patterns, respectively.

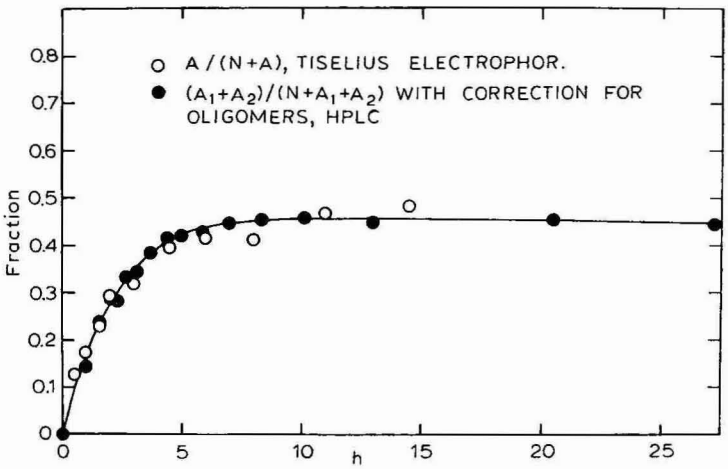

Fig. 2. Fraction of the A-form of aged BMA, $(A_1 + A_2)/(N + A_1 + A_2)$ (●), obtained by ion-exchange HPLC as a function of the time of ageing at pH 8.6 with no added salt at 25°C. Data obtained by moving-boundary electrophoresis [$A/(N + A)$, ○] were taken from ref. 6. Electrophoresis: $K_{app} = 0.95$; $k_{+1} = 4.1 \cdot 10^{-5}$ sec^{-1}; $k_{-1} = 4.3 \cdot 10^{-5}$ sec^{-1}. HPLC: $K_{app} = 0.89$; $k_{+1} = 5.7 \cdot 10^{-5}$ sec^{-1}; $k_{-1} = 6.4 \cdot 10^{-5}$ sec^{-1}. See the text for definitions of K_{app}, k_{+1} and k_{-1}.

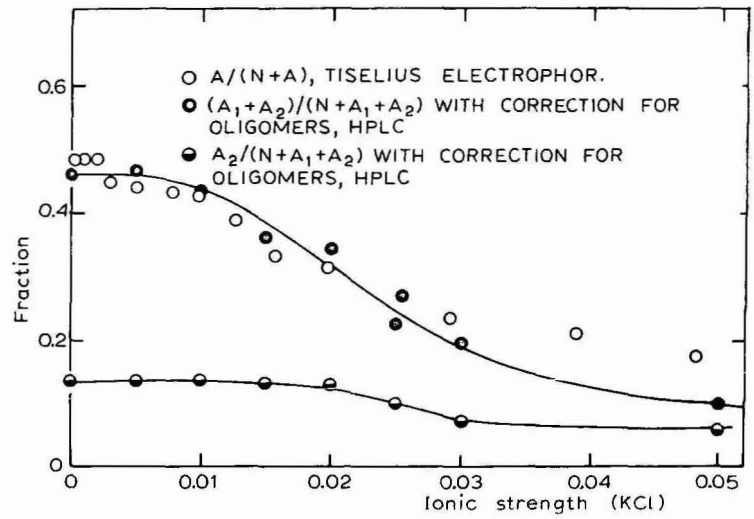

Fig. 3. Fractions of the A-form [$(A_1 + A_2)/(N + A_1 + A_2)$, ●] and the A_2-form [$A_2/(N + A_1 + A_2)$, ◒] of aged BMA, obtained by ion-exchange HPLC, as a function of the ionic strength (potassium chloride for aging at pH 8.6 at 25°C for 15 h. Data obtained by moving-boundary electrophoresis [$A/(N + A)$, O] were taken from ref. 6. A_1 and A_2 indicate two kinds of the A-form (see A_1 and A_2 in Fig. 1).

aged at pH 8.6 for 0 min and 24 h under the same ageing conditions as for HPLC experiments, are shown on the right side of Fig. 1. The schlieren patterns of the aged BMA were similar to those given by Nikkel and Foster[2] and Inouye *et al.*[6]. As reported by Nikkel and Foster[2], the A-form is more positive than the N-form below pH 5.3 and more negative above pH 5.3. Therefore, HPLC on TSK SP-5PW at pH 5.00 and moving-boundary electrophoresis at pH 4.82 could resolve the N- and A-forms, as shown in Fig. 1. The principal, secondary and tertiary (broad) peaks in the

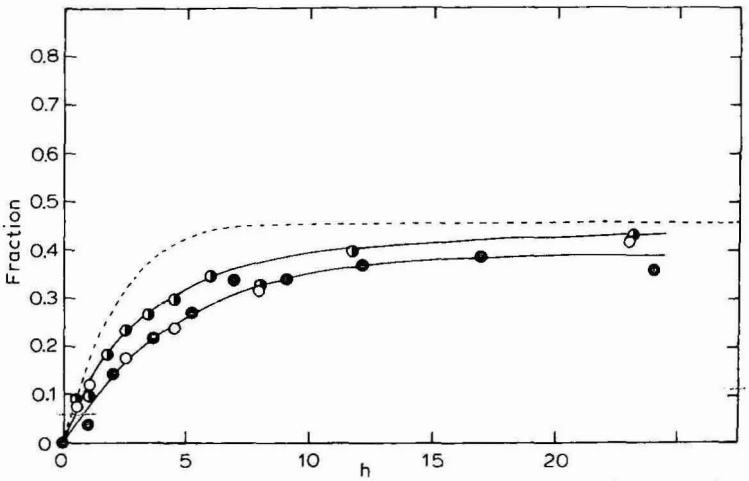

Fig. 4. Fractions of the A-form, $(A_1 + A_2)/(N + A_1 + A_2)$, of aged BMA, obtained by ion-exchange HPLC as function of [^{2}H]water volume fraction and the time of ageing at pL 8.6 with no added salt at 25°C. ----, Deuterium atom fraction, $n = 0$; ◑, $n = 0.494$; O, $n = 0.897$; ●, $n = 0.996$. pL is the generalized equivalent of pH in water–[^{2}H]water[20].

HPLC profiles on TSK SP-5PW might correspond to the N-, A_1- and A_2-forms, respectively, as indicated in eqn. 1.

The HPLC of aged BMA, eluted from TSK SP-5PW, was similar to that obtained by SE-Sephadex C-50 chromatography with 0.02 *M* sodium acetate buffer (pH 4.70) at 4°C and a linear salt gradient of 0.1–0.7 *M* sodium chloride[2]. In our HPLC experiments, we found it difficult to elute the A-form completely from TSK SP-5PW under the conditions given by Nikkel and Foster[2], *i.e.*, a linear salt gradient of 0.10–1.0 *M* sodium chloride in 0.02 *M* sodium acetate buffer (pH 4.85). Under these conditions, although the HPLC profile of the A-form, eluted from TSK SP-5PW, showed at least three components, the HPLC profile of the N-form was less symmetrical. We therefore used 0.02 *M* sodium acetate buffer (pH 5.00) and a 30-min linear gradient from 0.085 to 1.50 *M* at a flow-rate of 1.00 ml/min. Under these conditions, the N- and A-forms were almost completely separated with a nearly symmetrical principal peak, corresponding to the N-form.

Comparison of HPLC data with those obtained by moving-boundary electrophoresis

The kinetics of the N–A isomerization reaction of BMA at pH 8.6 without added salt at 25°C was studied by ion-exchange HPLC. Assuming the fraction of the A-form of the aged BMA obtained by ion-exchange HPLC to be $(A_1 + A_2)/(N + A_1 + A_2)$, the time course of the ageing reaction of BMA, obtained by ion-exchange HPLC, was in good agreement with that by the moving-boundary electrophoresis of Inouye *et al.*[6]. The solid curve in Fig. 2 was calculated from the equation for a reversible first-order reaction of the type $N \rightleftharpoons A$, as reported by Stroupe and Foster[3], using ion-exchange HPLC data:

$$[K_{app}/(1 + K_{app})] \ln(A_\infty - A_t)/A = -k_{+1}t \quad (3)$$

where $K_{app} = k_{+1}/k_{-1}$ is the apparent equilibrium constant and A_t and A_∞ are the amounts of A, *i.e.*, $(A_1 + A_2)$ at time t and infinite time, respectively. The solid curve in Fig. 2 corresponds to $k_{+1} = 5.7 \cdot 10^{-5}$ sec^{-1}, $k_{-1} = 6.4 \cdot 10^{-5}$ sec^{-1} and $K_{app} = 0.89$. These values were comparable to $k_{+1} = 4.1 \cdot 10^{-5}$ sec^{-1}, $k_{-1} = 4.3 \cdot 10^{-5}$ sec^{-1} and $K_{app} = 0.95$ obtained by Inouye *et al.*[6] by moving-boundary electrophoresis.

It has been reported by several workers[1–3,6,10] that the ageing reaction is suppressed by increasing the ionic strength. As shown in Fig. 3, the $(A_1 + A_2)/(N + A_1 + A_2)$ profile of the aged BMA, obtained by ion-exchange HPLC, was in agreement with that by the moving-boundary electrophoresis [A/(N + A)] of Inouye *et al.*[6]. Fig. 3 also shows a fraction of the A_2-form, $A_2/(N + A_1 + A_2)$. The pH profile of the ageing reaction of BMA, obtained by ion-exchange HPLC, was also in agreement with that obtained by the moving-boundary electrophoresis by Inouye *et al.*[6] (data not shown).

From the experimental evidence in Figs. 1, 2 and 3, it is possible to say that chromatography on TSK SP-5PW can resolve the aged BMA into the N- and A-forms, as in the case of moving-boundary electrophoresis. Ion-exchange HPLC appears to be a convenient method of assaying for the A-form and for studying the kinetics and equilibria of the N–A isomerization in more detail, because the amount of sample is small (less than 1 mg) and the method is less time consuming.

Effect of [²H]water on the ageing reaction

It was reported by several workers[24–26] that [²H]water might strengthen the intra- and intermolecular hydrophobic and/or hydrogen bonds. We therefore studied the effect of water–[²H]water solvents on the ageing reaction of BMA and used ion-exchange HPLC on TSK SP-5PW for analysis. The ageing reaction of BMA was carried out at pL 8.6 without added salt at 25°C. The H–²H exchange reaction (exchange-in) of BMA (*ca.* 12%) was carried out at pD 4.02 for 10 days at 3°C. The deuterated BMA was diluted 50-fold, using water–[²H]water solvents, and the pL was adjusted to 8.6 by adding 0.30 *M* Tris in [²H]water. In these experiments, the final salt concentrations were approximately 3 m*M*, and the deuterium atom fractions of the ageing solutions were 0.996 (⊖ in Fig. 4), 0.897 (○) and 0.494 (◑). Although 3 m*M* sodium chloride or potassium chloride had no stabilizing effect on the ageing reaction of BMA in water[6], as shown in Fig. 3, rates of the ageing reaction were strongly suppressed in 50% (deuterium atom fraction 0.494), 90% (0.897) and 100% (0.996) [²H]water solutions, as shown in Fig. 4. The suppression of the ageing reaction might be due to the strengthening of intramolecular hydrophobic and/or hydrogen bonds of BMA, resulting in the suppression of the intramolecular sulphydryl–disulphide exchange reaction.

There are several reports on H–²H exchange (exchange-in) and ²H–H exchange (exchange-out) of BPA and human serum albumin[27–30]. For the H–²H exchange reaction of proteins, Hvid and Nielsen[27] proposed the following exchange scheme:

$$\mathrm{M} \underset{k_2}{\overset{k_1}{\rightleftharpoons}} \mathrm{I} \xrightarrow{k_3} \text{exchange} \qquad (4)$$

in which the hydrogen in the shielded conformation, M, is not accessible to exchange with bulk solvent, and in the open conformation, I, is accessible. Benson and Hallaway[29] suggested that BPA is highly "motile", *i.e.*, it fluctuates rapidly at pH 7 and above between the M and I states. Benson and Hallaway[29] also studied the effect of ionic strength on the ²H–H exchange reaction of BPA at pH 7.7 at 0°C and found a suppression of exchange rates on increasing the ionic strength from 0 to 0.20 *M* potassium chloride, indicating that the equilibrium between M and I is shifted to the M state. However, even in 0.20 *M* potassium chloride at pH 7.7 and 0°C, significant amounts of hydrogen were exchanged[29,30]. On the other hand, the N–A isomerization, *i.e.*, the ageing reaction of BMA, was almost completely suppressed on increasing the ionic strength to 0.20 *M* potassium chloride (Fig. 3 and ref. 6). In the H–²H exchange reaction, the restricted *local* motilities might be sufficient. However, the *global* structural fluctuations of helical segments or subdomains[31] might be necessary for the ageing reaction of BMA (the intramolecular sulphydryl–disulphide exchange reaction). In the motile state above pH 7 without added salt, the restricted *local* motions might be superimposed on the *global* structural motions of helical segments or subdomains of BMA, like a librational motion[32], which is important for the intramolecular sulphydryl–disulphide exchange reaction.

ACKNOWLEDGEMENTS

We thank Professor K. Takeo (Department of Biochemistry, School of Med-

icine, Yamaguchi University, Ube, Japan) for arrangements for carrying out moving-boundary electrophoresis and to Asahi-Keiki Kogyo (Nagoya, Japan) for carrying out ion-exchange HPLC with a Gradientor (Toyo Soda HLC-803D and GE-4). We are also grateful to Systemic Instruments Engineering Laboratory, Asahi Chemical Industry (Fuji, Shizuoka-ken, Japan) for supplying the Jasco Uvidec 100-IV UV monitor and to Toyo Soda (Shin-Nanyo, Yamaguchi-ken, Japan) for supplies of TSK SP-5PW HPLC columns. We also thank Dr. S. Nagaoka and Miss M. Yanagihara for their help with the HPLC analysis.

REFERENCES

1 M. Sogami, H. A. Petersen and J. F. Foster, *Biochemistry*, 8 (1969) 49.
2 H. J. Nikkel and J. F. Foster, *Biochemistry*, 10 (1971) 4479.
3 S. D. Stroupe and J. F. Foster, *Biochemistry*, 12 (1973) 3824.
4 K. Wallevik, *Biochim. Biophys. Acta*, 420 (1976) 42.
5 K. Wallevik, *J. Clin. Invest.*, 57 (1976) 398.
6 H. Inouye, S. Era, S. Sakata, K. Kuwata and M. Sogami, *Int. J. Pept. Protein Res.*, 24 (1984) 337.
7 K. P. Wong and J. F. Foster, *Biochemistry*, 8 (1969) 4096.
8 K. P. Wong and J. F. Foster, *Biochemistry*, 8 (1969) 4104.
9 H. N. Bhargava and J. F. Foster, *Biochemistry*, 9 (1970) 1977.
10 R. D. Hagenmaier and J. F. Foster, *Biochemistry*, 10 (1971) 637.
11 R. F. Chen, *J. Biol. Chem.*, 242 (1967) 173.
12 M. Sogami and J. F. Foster, *Biochemistry*, 7 (1968) 2172.
13 M. Telegdi and F. B. Straub, *Biochim. Biophys. Acta*, 321 (1973) 210.
14 G. L. Ellman, *Arch. Biochem. Biophys.*, 82 (1959) 70.
15 Y. H. Chen, J. T. Yang and H. M. Martinez, *Biochemistry*, 11 (1972) 4120.
16 S. Era, H. Ashida, S. Nagaoka, H. Inouye and M. Sogami, *Int. J. Pept. Protein Res.*, 22 (1983) 333.
17 W. W. Everett, *J. Biol. Chem.*, 238 (1963) 2676.
18 M. Sogami, S. Ogura, K. B. Itoh, S. Sakata and S. Nagaoka, *Biochim. Biophys. Acta*, 278 (1972) 501.
19 M. Sogami, S. Nagaoka, S. Era, M. Honda and K. Noguchi, *Int. J. Pept. Protein Res.*, 24 (1984) 96.
20 P. Salomaa, L. L. Schaleger and F. A. Long, *J. Amer Chem. Soc.*, 86 (1964) 1.
21 T. Takagi, J. Miyake and T. Nashima, *Biochim. Biophys. Acta*, 626 (1980) 5.
22 K. Kameyama, T. Nakae and T. Takagi, *Biochim. Biophys. Acta*, 706 (1982) 19.
23 T. T. Herskovitts, R. C. S. Geroge and L. J. Erhumwunsee, *Biochemistry*, 20 (1981) 2580.
24 G. C. Kresheck, H. Schneider and H. A. Scheraga, *J. Phys. Chem.*, 69 (1965) 3132.
25 P. A. Baghust, L. W. Nichol and W. H. Sawyear, *J. Biol. Chem.*, 247 (1972) 3198.
26 T. J. Itoh and H. Sato, *Biochim. Biophys. Acta*, 800 (1984) 21.
27 A. Hvid and S. O. Nielsen, *Advan. Protein Chem.*, 21 (1966) 287.
28 E. S. Benson, B. E. Hallaway and R. W. Lumry, *J. Biol. Chem.*, 239 (1964) 122.
29 E. S. Benson and B. E. Hallaway, *J. Biol. Chem.*, 245 (1970) 4144.
30 A. Hvid and K. Wallevik, *J. Biol. Chem.*, 247 (1972) 1530.
31 J. R. Brown, in V. M. Rosenoer, M. Oratz and M. A. Rothschild (Editors), *Albumin Structure, Function and Uses*, Pergamon Press, Oxford, 1977, Ch. 2, p. 27.
32 M. E. Johnson, *Biochemistry*, 17 (1978) 1223.

Journal of Chromatography, 332 (1985) 39–46
Elsevier Science Publishers B.V., Amsterdam — Printed in The Netherlands

CHROMSYMP. 611

NEW GEL PERMEATION COLUMN FOR THE SEPARATION OF WATER-SOLUBLE POLYMERS

YOSHIO KATO*, TAKAO MATSUDA and TSUTOMU HASHIMOTO
Central Research Laboratory, Toyo Soda Mfg. Co., Ltd., Tonda, Shinnanyo, Yamaguchi (Japan)
(First received March 8th, 1985; revised manuscript received April 22nd, 1985)

SUMMARY

A new column, TSK gel GMPW, has been evaluated for use in gel permeation chromatography of water-soluble polymers. It has a wide separation range, and the molecular weight calibration curve for polyethylene glycol is almost linear over the range 10^2–10^6. A variety of water-soluble polymers have been fractionated according to molecular size, with no evidence of adsorption providing an appropriate eluent was employed. Therefore, GMPW should be very useful in the determination of molecular weight distributions of water-soluble polymers.

INTRODUCTION

Gel permeation chromatography (GPC) has been widely used for determining molecular weight distributions and average molecular weights of polymers, owing to its rapidity, ease of operation and good reproducibility. GPC in organic solvent systems has developed rapidly since its introduction by Moore in 1964[1], and the use of high-performance GPC columns, packed with very small particles, was introduced in advance of other modes of liquid chromatography[2,3]. Columns packed with a mixture of sorbents differing in pore size were also developed at an early stage[2]. Such columns have wide separation ranges and hence are very versatile. Their benefits have been discussed in detail[4,5].

On the other hand, high-performance mixed-bed columns, suitable for aqueous GPC, were not available until very recently. For this purpose, we have prepared columns packed with a mixture of TSK gels G2500PW, G3000PW and G6000PW, which have different pore sizes. Recently, these columns have become commercially available under the trade-name of TSK gel GMPW (Toyo Soda, Tokyo, Japan). In this report, the results of an evaluation of the separation range, resolution and applications of these columns are presented.

EXPERIMENTAL

GPC was performed with a Toyo Soda HLC-803D liquid chromatograph, equipped with a differential refractometer RI-8, at 25°C and a flow-rate of 1 ml/min. The GMPW columns were packed with sorbents of particle diameter *ca.* 17 μm.

0021-9673/85/$03.30

The molecular weight calibration curves were determined with polyethylene glycols of narrow molecular weight distribution in distilled water. A 0.5-ml aliquot of a 0.02–0.05% solution of each sample was injected.

The theoretical plate numbers of the columns were determined by injecting 20 μl of 1% ethylene glycol in distilled water.

The twenty-four water-soluble polymers listed below were separated on two 600 × 7.5 mm I.D. GMPW columns, connected in series, with distilled water, aqueous sodium nitrate, mixtures of aqueous sodium nitrate and acetonitrile or aqueous acetic acid containing sodium sulphate as eluents. The injection volume was 0.5 ml and the sample concentrations were 0.05–0.1%. Non-ionic polymers were: dextran, pullulan, soluble starch, methyl-cellulose, hydroxyethyl-cellulose, polyethylene glycol, polyvinyl alcohol, polyacrylamide and polyvinylpyrrolidone. Anionic polymers were: chondroitinsulphate sodium salt, alginic acid sodium salt, hyaluronic acid sodium salt, carboxymethyl-cellulose, polyacrylic acid sodium salt, sulphonated lignin sodium salt and sodium polystyrenesulphonate. Cationic polymers were: glycol chitosan, diethylaminoethyl (DEAE) dextran, poly(trimethylammonioethyl methacrylate) iodide salt, poly(N-methyl-2-vinylpyridinium) iodide salt and poly(4-vinylbenzyltrimethylammonium chloride). Amphoteric polymers were: Blue dextran, collagen and gelatin.

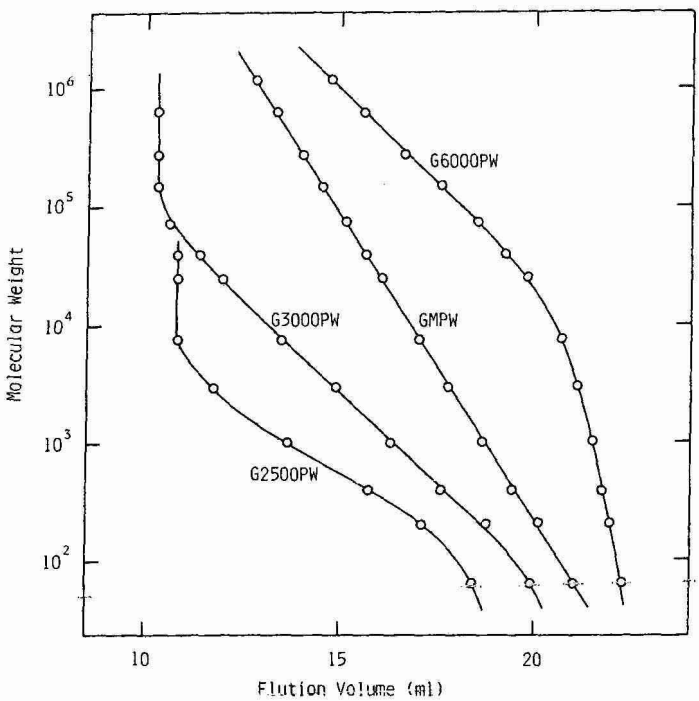

Fig. 1. Molecular-weight calibration curves of TSK gel GMPW, G2500PW, G3000PW and G6000PW columns (600 × 7.5 mm I.D.) for polyethylene glycol in distilled water.

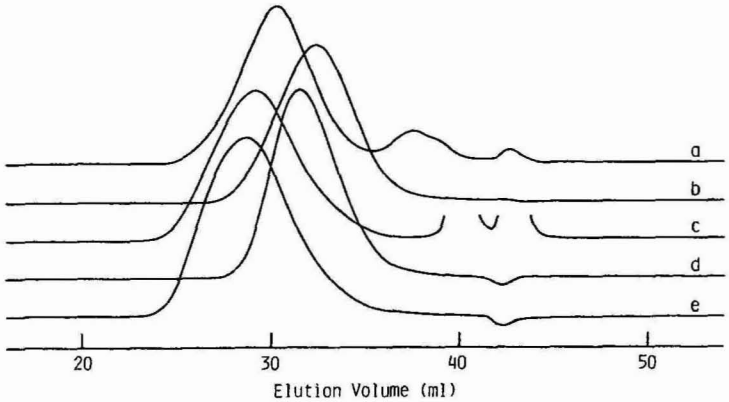

Fig. 2. Chromatograms of pullulan (a), methyl-cellulose (b), hydroxyethyl-cellulose (c), polyvinyl alcohol (d) and polyacrylamide (e) obtained with 0.1 *M* sodium nitrate.

RESULTS AND DISCUSSION

The molecular weight calibration curves of GMPW, G2500PW, G3000PW and G6000PW for polyethylene glycol are shown in Fig. 1. The separation range of GMPW is very wide, extending over a molecular weight range from less than 100 to several millions for this polymer. In addition, the calibration curve of GMPW is almost linear over this molecular weight range. This facilitates the accurate conversion of GPC chromatograms into molecular weight distribution curves[4–7]. Consequently, GMPW should be very useful in the separation of water-soluble polymers over a wide range of molecular weight.

The theoretical plate numbers of several GMPW columns (600 × 7.5 mm I.D.), as determined with ethylene glycol, ranged between 15 000 and 20 000 plates per m, which means that these columns give fairly high resolution.

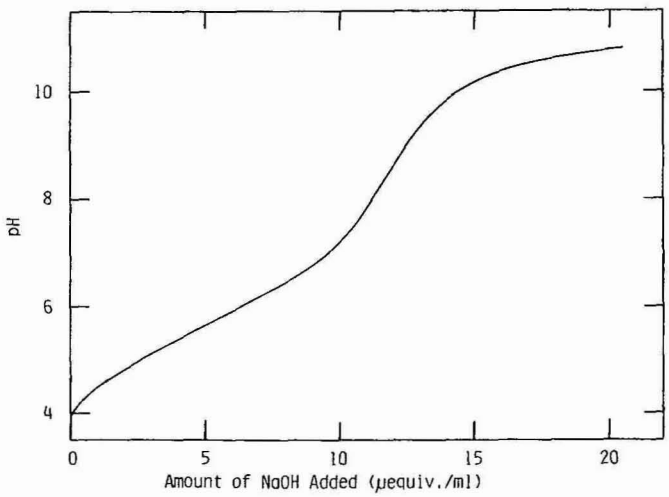

Fig. 3. Titration curve of GMPW. The sorbent was titrated in 0.5 *M* sodium chloride with 0.5 *M* sodium hydroxide.

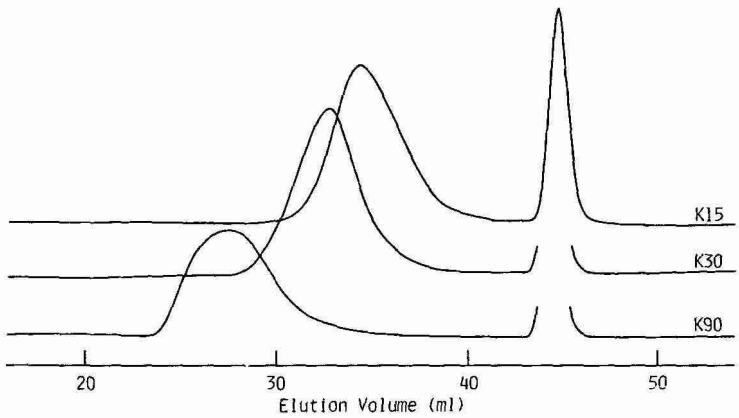

Fig. 4. Chromatograms of polyvinylpyrrolidones obtained in 0.1 *M* sodium nitrate–acetonitrile (80:20, v/v). Molecular weights: K15, 10 000; K30, 40 000; K90, 360 000.

All of the non-ionic polymers except polyvinylpyrrolidone were successfully fractionated in 0.1 *M* sodium nitrate. Under these conditions, there was no sign of adsorption (sharp leading edge followed by tailing of the peak, small peak area, retardation of elution and lack of reproducibility) nor of ionic repulsion (early elution near void volume). Fig. 2 shows some examples of the chromatograms obtained. In distilled water, however, normal chromatograms were obtained only with polyethylene glycols and dextran of low molecular weight. For the polymers in water, either minor peaks appeared near the void volume in addition to the main peaks, or chromatograms of abnormal shapes were observed. This is probably because charged components in the samples interact with the negative charges carried by GMPW. According to titration (see Fig. 3), GMPW contains *ca.* 12 μequiv. of negative charges per ml; these are believed to reside on carboxyl groups. In the fractionation of polyvinylpyrrolidone in 0.1 *M* sodium nitrate, a slightly sharp start-up was observed, suggesting weak adsorption of the sample on the sorbent. However, normal chromatograms were obtained reproducibly by use of 0.1 *M* sodium nitrate–acetonitrile

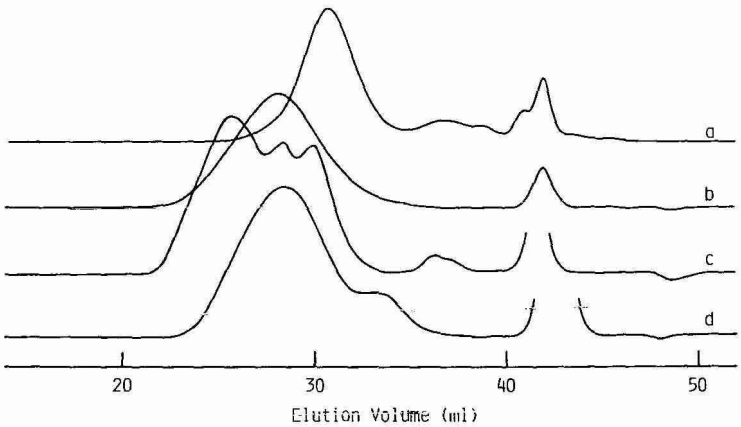

Fig. 5. Chromatograms of chondroitinsulphate sodium salt (a), alginic acid sodium salt (b), hyaluronic acid sodium salt (c) and carboxymethyl-cellulose sodium salt (d), obtained with 0.1 *M* sodium nitrate.

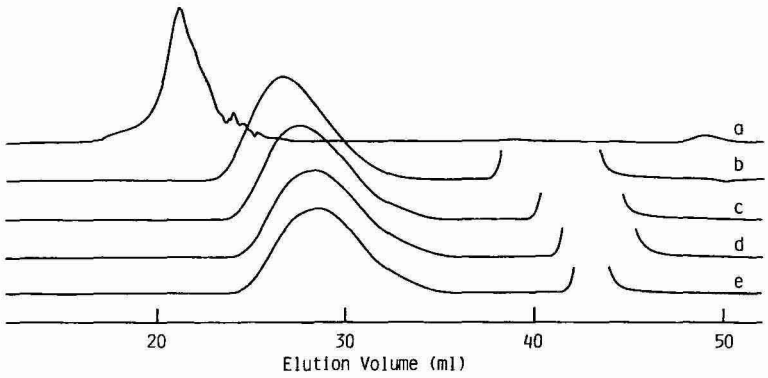

Fig. 6. Effect of eluent ionic strength on the separation of anionic polymers (polyacrylic acid sodium salt) in aqueous sodium nitrate solution. Sodium nitrate concentrations: a, 0; b, 0.01 *M*; c, 0.025 *M*; d, 0.05 *M*; e, 0.1 *M*.

(80:20, v/v), as shown in Fig. 4. It is likely that polyvinylpyrrolidone was retained by hydrophobic interaction with the sorbent in 0.1 *M* sodium nitrate and the hydrophobic interaction was eliminated by the addition of acetonitrile.

Most of the anionic polymers examined were also fractionated in 0.1 *M* sodium nitrate without interaction with the sorbent, as exemplified in Fig. 5. When the anionic polymers were fractionated in distilled water, they were eluted very early, near the void volume, owing to ionic repulsion between the samples and the sorbent. However, as shown in Fig. 6, the addition of sodium nitrate, even at a concentration of only 0.01 *M*, resulted in normal elution and peak shape. Although the peaks shifted slightly toward higher elution volumes with increasing sodium nitrate concentration, they had the same shape at sodium nitrate concentrations above 0.1 *M*. Therefore, an ionic strength of 0.1 seems to be sufficient to suppress ionic interactions between anionic polymers and GMPW. The hydrophobic anionic polymers, sulphonated lignin sodium salt and sodium polystyrenesulphonate, were not eluted by 0.1 *M* sodium nitrate. However, they were successfully fractionated after the addition of the organic solvent acetonitrile to the eluent (Fig. 7).

All the cationic polymers examined were fractionated, with no evidence of

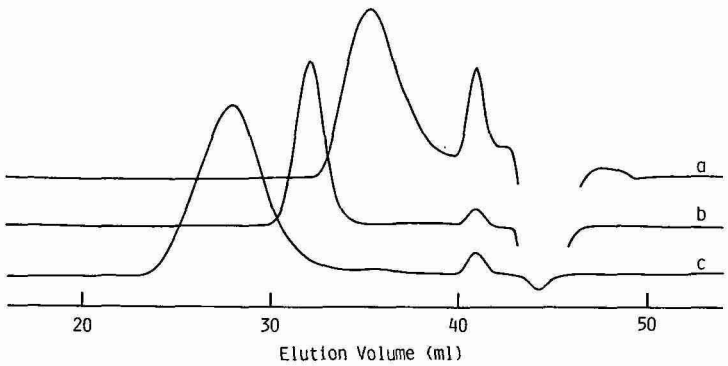

Fig. 7. Chromatograms of sulphonated lignin sodium salt (a) and sodium polystyrenesulphonate (b, 90% sulphonation; c, 100% sulphonation) obtained with 0.1 *M* sodium nitrate–acetonitrile (80:20, v/v).

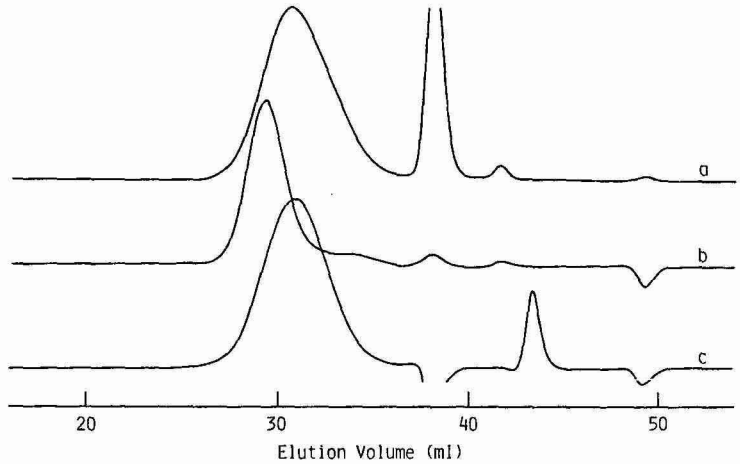

Fig. 8. Chromatograms of glycol chitosan (a), poly(N-methyl-2-vinylpyridinium) iodide salt (b) and poly(4-vinylbenzyltrimethylammonium chloride) (c), obtained with 0.5 *M* acetic acid containing 0.3 *M* sodium sulphate.

interactions with the sorbent, in 0.5 *M* acetic acid containing 0.3 *M* sodium sulphate. Fig. 8 shows examples of the chromatograms. When the sodium sulphate concentration was reduced to 0.1 *M*, the peak area became rather small and the results were not reproducible. The hydrophilic cationic polymers, glycol chitosan, DEAE-dextran and poly(trimethylammonioethyl methacrylate) iodide salt, were successfully fractionated also in 0.8 *M* sodium nitrate, as shown in Fig. 9. However, sodium nitrate concentrations below 0.4 *M* were not sufficient to prevent adsorption (see Fig. 10). On the other hand, the hydrophobic cationic polymers, poly(4-vinylbenzyltrimethylammonium chloride) and poly(N-methyl-2-vinylpyridinium) iodide salt, were not eluted from the column even in 0.8 *M* sodium nitrate, and in this case the addition of 20% acetonitrile was not effective in eliminating the adsorption.

Three amphoteric polymers were successfully fractionated in 0.1 *M* sodium nitrate–acetonitrile (80:20, v/v), as shown in Fig. 11. When acetonitrile was not included in the eluent, the peak areas were small and the results were not reproducible.

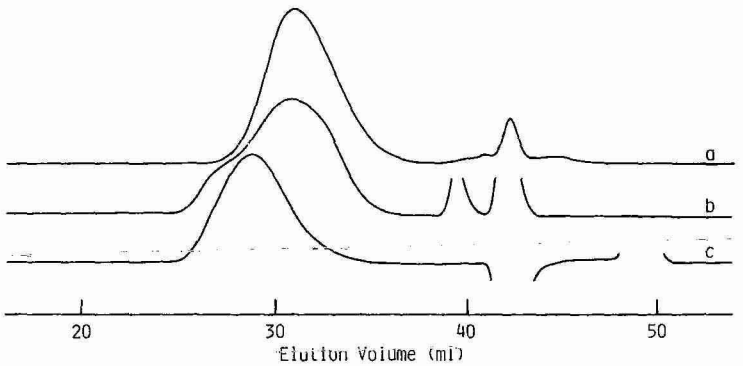

Fig. 9. Chromatograms of glycol chitosan (a), DEAE-dextrans (b) and poly(trimethylammonioethyl methacrylate) iodide salt (c), obtained with 0.8 *M* sodium nitrate.

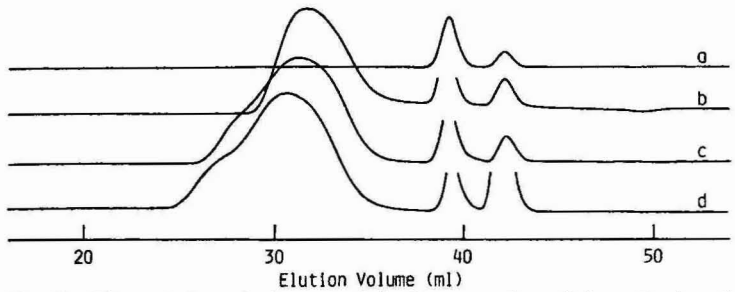

Fig. 10. Effect of eluent ionic strength in the separation of the cationic polymer DEAE-dextran with aqueous sodium nitrate solution. Sodium nitrate concentrations: a, 0.1 *M*; b, 0.2 *M*; c, 0.4 *M*; d, 0.8 *M*.

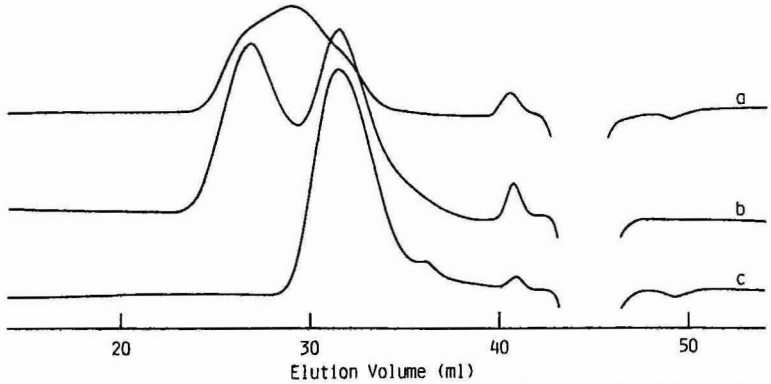

Fig. 11. Chromatograms of Blue dextran(a), collagen(b) and gelatin(c), obtained with 0.1 *M* sodium nitrate–acetonitrile (80:20, v/v).

This is probably because these amphoteric polymers contain aromatic rings and hence they tend to be adsorbed on the sorbent by hydrophobic interaction.

As shown above, twenty-four water-soluble polymers with various properties have been fractionated on TSK gel GMPW, with little or no interaction with the sorbent in an appropriate eluent. Suitable eluents are summarized in Table I.

TABLE I

SUITABLE ELUENTS FOR VARIOUS TYPES OF WATER-SOLUBLE POLYMERS

Type of polymer	*Suitable eluent*
Non-ionic hydrophilic polymer	Salt solution, *e.g.*, 0.1 *M* sodium nitrate (Distilled water)
Non-ionic hydrophobic polymer	Salt solution containing organic solvent, *e.g.*, 0.1 *M* sodium nitrate–acetonitrile (80:20, v/v)
Anionic hydrophilic polymer	Salt solution, *e.g.*, 0.1 *M* sodium nitrate
Anionic hydrophobic polymer	Salt solution containing organic solvent, *e.g.*, 0.1 *M* sodium nitrate–acetonitrile (80:20, v/v)
Cationic hydrophilic polymer	Salt solution, *e.g.*, 0.8 *M* sodium nitrate
Cationic hydrophobic polymer	Acetic acid solution containing salt, *e.g.*, 0.5 *M* acetic acid containing 0.3 *M* sodium sulphate
Amphoteric hydrophilic polymer	Salt solution, *e.g.*, 0.1 *M* sodium nitrate
Amphoteric hydrophobic polymer	Salt solution containing organic solvent, *e.g.*, 0.1 *M* sodium nitrate–acetonitrile (80:20, v/v)

REFERENCES

1 J. C. Moore, *J. Polym. Sci., Part A*, 2 (1964) 835.
2 Y. Kato, S. Kido and T. Hashimoto, *J. Polym. Sci., Polym. Phys. Ed.*, 11 (1973) 2329.
3 Y. Kato, S. Kito, M. Yamamoto and T. Hashimoto, *J. Polym. Sci., Polym. Phys. Ed.*, 12 (1974) 1339.
4 W. W. Yau, C. R. Ginnard and J. J. Kirkland, *J. Chromatogr.*, 149 (1978) 465.
5 W. W. Yau, J. J. Kirkland and D. D. Bly, *Modern Size-Exclusion Liquid Chromatography*, Wiley, New York, 1979.
6 H. E. Pickett, H. J. R. Cantow and J. F. Johnson, *J. Appl. Polym. Sci.*, 10 (1966) 917.
7 W. W. Yau and S. W. Fleming, *J. Appl. Polym. Sci.*, 12 (1968) 2111.

Journal of Chromatography, 332 (1985) 47–56
Elsevier Science Publishers B.V., Amsterdam — Printed in The Netherlands

CHROMSYMP. 625

SUPERCRITICAL FLUID CHROMATOGRAPHY–INFRARED SPECTROSCOPY OF OLIGOMERS: USE OF BUFFER-MEMORY TECHNIQUE

CHUZO FUJIMOTO, YUKIO HIRATA and KIYOKATSU JINNO*
School of Materials Science, Toyohashi University of Technology, Toyohashi 440 (Japan)
(First received March 28th, 1985; revised manuscript received May 13th, 1985)

SUMMARY

The feasibility of using the buffer-memory technique for supercritical fluid chromatography–infrared spectroscopy (SFC–IR) is demonstrated. The effluent from a microtubular packed SFC column was deposited onto a crystal (or crystals) of potassium bromide as a continuous, narrow band (width about 1 mm) with instantaneous elimination of the mobile phase. This technique is compatible with IR detection of medium polarity oligomers, separated by SFC with 10% ethanol in hexane as the mobile phase. Chromatographic resolution is maintained, even for closely separated peaks, and identifiable spectra of the peaks can be obtained from the plate.

INTRODUCTION

Although supercritical fluid chromatography (SFC) was described as early as 1962 by Klesper *et al.*[1], it has experienced rather slow growth and limited acceptance as an analytical tool because of the technological difficulties in handling supercritical fluids in chromatographic systems. Recently, interest in SFC has revived. The previous technical limitations have been overcome through the availability of high-pressure instrumentation (solvent pumps and sample injection systems) developed for high-performance liquid chromatography (HPLC). Further, encouraging results have been obtained by the use of open microtubular columns[2,3] and microtubular columns packed with microparticles[4–7].

SFC has several advantages compared to gas chromatography (GC) and HPLC. As is well known, the properties of a supercritical fluid are intermediate between those of gases and liquids. Solute diffusivities are about 100 times higher in a supercritical fluid than in the corresponding liquid phase and viscosities are similar to those in the gas phase. Furthermore, the greater density of supercritical fluids compared with gases imbues the mobile phase with solvating powers, which can readily be controlled by application of pressure. As a result, these properties should enable greatly enhanced chromatographic efficiency compared to HPLC (although not as high as in GC), shorter analysis times than in HPLC and the possibility of separating high-molecular-weight and thermally labile compounds that cannot be separated by GC. Comprehensive reviews have been published[8–17].

0021-9673/85/$03.30

However, as in the case of HPLC, detection is currently the weakpoint of SFC. Most GC and HPLC detectors have been used with SFC, including flame ionization[10,12,18–22], thermal conductivity[21], UV-absorption[11–15], fluorescence[3,23] and refractive index[24] detectors, but a means of identifying the eluted components still exists. The ideal detector for SFC (and perhaps for all chromatographic separation techniques) is a mass spectrometer, because of its higher sensitivity compared with other detectors and its specificity in identifying unknown compounds or for confirming the presence of suspected compounds. However, the combination of SFC and mass spectrometry (MS) is in a relatively early stage of development[25–33].

An alternative possibility is infrared (IR) spectroscopy. This enables certain functional groups in the compounds to be analyzed. Besides, except for optical isomers, no two compounds having different structures have the same IR spectra. The sensitivity provided by IR instruments is poorer than that achieved by MS, yet as regards the available information, IR spectroscopy is more often complementary to mass spectrometry than competitive. Shafer and Griffiths[34] reported the first results of Fourier transform infrared (FTIR) spectroscopic detection in SFC, using a high-pressure resistant flow-cell and a mobile phase of carbon dioxide. More recently, a detailed discussion of this approach was provided by Novotny and co-workers[35], who had previously predicted the importance of SFC–FTIR[2]. However, as far as the flow-cell technique is concerned, the situation resembles that in HPLC. Measurements made by use of a flow-cell show severe spectroscopic interference from the intense absorption bands of the mobile phase. Moreover, when pressure programming (which is equivalent to temperature programming in GC or gradient elution in HPLC) is performed in order to vary the solvent strength, solvent compensation is essentially impossible since the absorptivities of the bands in the spectrum of a supercritical fluid increase with pressure. Shafer and Griffiths[34] and Novotny and coworkers[35] have found that carbon dioxide shows a few transparent regions just above the critical pressure, but some band intensities dramatically increase as the pressure is increased.

A solution to this problem is to eliminate the mobile phase, leaving the separated components for IR analysis. For HPLC–FTIR, at least two solvent-elimination techniques have been proposed, involving heating of an effluent containing the separated components and deposition of the concentrated sample onto a potassium bromide plate for absorption spectroscopy[36–39], or onto a potassium chloride powder for measurements by diffuse reflectance infrared Fourier transform spectroscopy (DRIFT)[40,41]. Preliminary results using SFC–DRIFT have recently been published[42].

This report describes the first practical demonstration of SFC combined with IR spectroscopy, using the buffer-memory technique, for the analysis of oligomers. In the present work, a ratio-recording IR spectrophotometer is used and the components are separated on a packed microcapillary column with a hexane-based solvent. An FTIR spectrophotometer is desirable because it has several distinct advantages over conventional dispersive instruments[43], but its use is often prohibited in many laboratories because of the high cost. The performance of the spectrometer used is essentially comparable to that of FTIR spectrophotometers except for the longer scan time required.

EXPERIMENTAL

Apparatus

The SFC–IR system used is shown schematically in Fig. 1. It includes a LC-840 pump (pump A) (Du Pont, Wilmington, DE, U.S.A.), a Twincle pump (pump B) (JASCO, Tokyo, Japan), a 7410 loop injector (volume 1.0 μl) (Rheodyne, Berkeley, CA, U.S.A.) a GC oven (Shimadzu, Kyoto, Japan) and a JASCO Uvidec 100-III UV detector. The mobile phase, *n*-hexane modified by ethanol, was delivered at room temperature into a fused-silica capillary column (100 cm × 0.5 mm I.D.) packed with Develosil ODS-10 (Nomura Chemical Co., Seto, Japan) which was placed in the oven. Constant-pressure operation was carried out solely by using pump A, which contained a stainless-steel coil partially filled with the mobile phase. The pressure programming was achieved by delivering the mobile phase of pump B to pump A at a constant flow-rate (about 1 ml/min), after setting the pressure of pump A and closing the valve located between a nitrogen cylinder and pump A, so that the pressure at the column inlet was allowed to increase with time. The flow-rate of the mobile phase fed into the column was varied between 7 and 10 μl/min. The programming rate can be determined by the preset pressure of pump B or the amount of mobile phase stored in pump A. The effluent from the column was transferred through a fused-silica capillary column, packed with Develosil ODS-5 (75 × 0.2 mm I.D.), onto a potassium bromide plate. This short column served as a pressure restrictor.

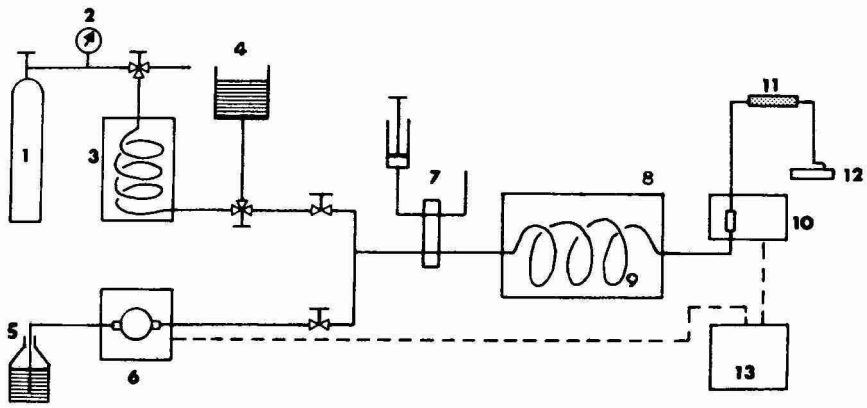

Fig. 1. Schematic diagram of the buffer-memory technique for SFC–IR. 1 = Nitrogen cylinder; 2 = pressure gauge; 3 = pump A; 4 and 5 = solvent reservoirs; 6 = pump B; 7 = sample injector; 8 = GC oven; 9 = packed capillary column (Develosil ODS-10, 100 cm × 0.5 mm I.D.); 10 = UV detector; 11 = restrictor (75 × 0.2 mm I.D. capillary column, packed with Develosil ODS-5); 12 = potassium bromide plate, mounted on the interface; 13 = recorder.

The design and construction of the interfacing device used in this work is the same as one used previously in the HPLC–IR interface[37]. The species eluted from the SFC column were deposited onto a continuously moving potassium bromide plate. The mobile phase was evaporated on contact with the plate, leaving a permanent record of the solutes on the plate. When the chromatogram was complete, the plate was simply transferred to an IR spectrophotometer and the IR chromatogram recorded by monitoring the absorption at a preset wavenumber.

The chromatograms and spectra were obtained on a JASCO Model 810, double-beam ratio-recording IR spectrophotometer. It was fitted with a 3X beam condenser and a 4 × 1.7 mm aperture. The spectrum of each chromatographic peak recorded on the plate was obtained as follows. A reference spectrum was obtained from ten scans of a pure potassium bromide crystal and then stored in the data system. At each peak maximum on the IR chromatogram the plate was stopped and the IR spectrum was scanned ten times. The spectra of both sample and reference were measured with slit program W (spectral resolution: 5.4 cm^{-1} at 1000 cm^{-1}), and corrected for the absorption bands due to moisture on the beam condenser.

Chemicals

The styrene oligomer A-500 (nominal molecular weight 500) and the methylphenylsiloxane DC-710 (50% phenyl, nominal molecular weight 2600) were purchased from Toyo Soda Manufacturing Co. (Tokyo, Japan) and Gasukuro Kogyo Inc. (Tokyo, Japan), respectively. *n*-Hexane and ethanol were of reagent grade and based as the mobile phase without further purification. Potassium bromide crystals (40 × 10 × 3 mm) were obtained from JASCO.

RESULTS AND DISCUSSION

The previous studies of SFC–IR employed pure carbon dioxide[34,35] or carbon dioxide modified by methanol[42] as the mobile phase; carbon dioxide is the most convenient fluid for SFC, mainly because of its low critical temperature (T_c = 31.3°C). Throughout this work, *n*-hexane modified by 10% ethanol was used as the mobile phase. The critical temperature is 241.5°C, as found on linear interpolation[44] with T_c (*n*-hexane) = 234.2°C and T_c (ethanol) = 243.4°C. This mobile phase was chosen for several reasons. First, it is able to dissolve many oligomers even at room temperature, which enables the sample injection as well as the UV flow-cell detection to be performed at that temperature. Consequently, the chromatographic instrumentation is simplified. Secondly, because it is a liquid at room temperature, the deposition of the effluent onto a potassium bromide plate is easily accomplished. Thirdly, because it has a high vapour pressure under atmospheric conditions, the evaporation of the mobile phase is very easy. Finally, the utilization of the mobile phase prevents the generation of bubbles at the column exit; this is not the case when *n*-pentane modified by 10% ethanol is used. There may be a difference in selectivity between carbon dioxide and *n*-hexane, but we have no data which support this.

Before applying the buffer-memory technique to oligomers, it must be determined whether the separation efficiency achieved originally by the SFC column is decreased while the sample components are travelling through the connecting tube between the UV detector and the deposition point (see Fig. 1). In order to explore this problem, another UV detector was connected to the exit of the connecting tube, *i.e.*, at the position of the potassium bromide plate in Fig. 1. Fig. 2 illustrates the broadening due to the connecting tube. An oligostyrene sample, A-500, was used as a test solute; oligostyrenes have become almost "standard" samples for examining the quality of chromatographic systems. The sample (total amount 30 μg) was introduced as a solution in the mobile phase. The separation was carried out isobarically at 60 atm. The column temperature was held well above the critical temperature of

the mobile phase in order to reduce the effect of thermal variations upon the mobile phase. In Fig. 2 the degree of oligomerization is tentatively assigned above each peak. Calculation of the height equivalent to a theoretical plate (HETP) for the $n = 4$ peaks in the two chromatograms showed that the values differ only by 5%. This difference is smaller than expected; this may partly be due to the fact that the effluent enters the restrictor, which comprises a short slurry-packed capillary column. A 3-μg amount of A-500 was injected into the column, and it was demonstrated that the introduction of a large sample (as large as 30 μg) affects the resolution only slightly. Based upon the increased sample capacity, it is possible to inject a larger amount of oligostyrene for SFC than for HPLC, carried out on a column of the same size.

A-500 was chromatographed under the same conditions as described in Fig. 2 and the effluent was continuously deposited onto a single potassium bromide plate until the eighth peak had been eluted. A typical IR chromatogram at 698 cm^{-1}, which was generated from the plate, is shown in Fig. 3. It is seen that the resolution is somewhat diminished between almost all neighbouring peaks, but that the "chromatogram" is clearly recorded on the plate. The IR spectrum of the $n = 4$ peak (marked with an asterisk in Fig. 3) is shown in Fig. 4. Despite the fact that the amount corresponding to this chromatographic peak is very small, as expected from the response of the UV and IR chromatograms, this technique produces a high-quality spectrum, which is ideal for identification purposes.

The value of SFC is perhaps best realized when considering its applicability to a mixture of oligomers which span a wide range of molecular weights. We applied

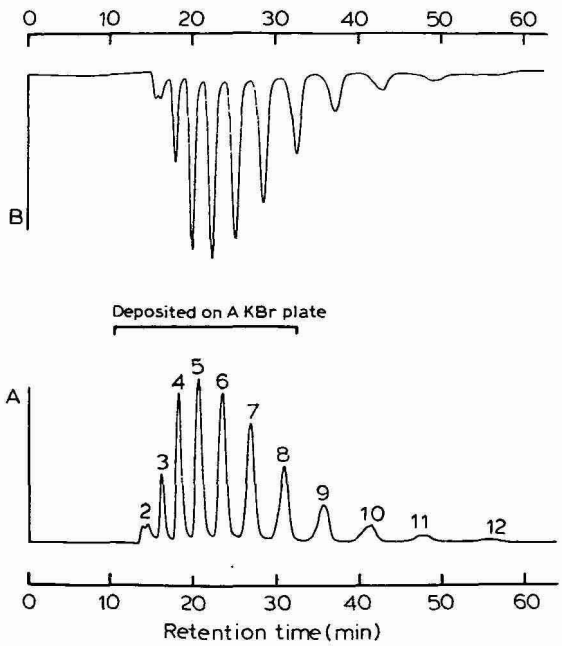

Fig. 2. Band broadening caused by the connecting tube between the column outlet and the deposition point: A, first UV detector; B, second UV detector. Column: 100 cm × 0.5 mm I.D., Develosil ODS-10. Mobile phase: 10% ethanol in *n*-hexane. Column temperature: 255°C. Column inlet pressure: 60 atm. Sample: 3% oligostyrene A-500 (1 μl). Detection: 225 nm.

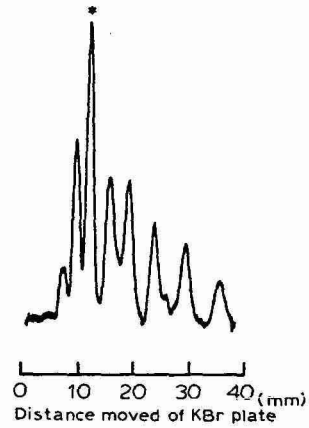

Fig. 3. IR chromatogram of oligostyrene A-500, obtained by using the buffer-memory technique. Detection wavenumber: 698 cm^{-1}.

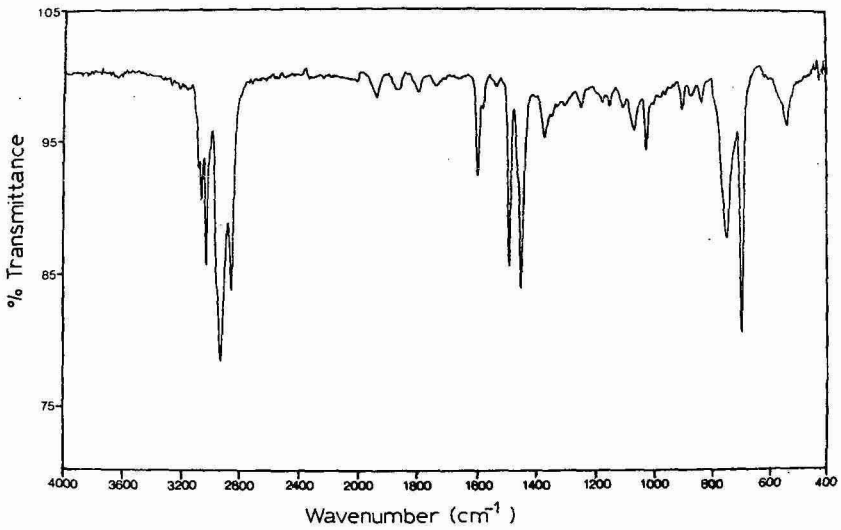

Fig. 4. IR spectrum of the peak marked by the asterisk in Fig. 3.

the buffer-memory technique to Dow-Corning (DC-710), which is one of the most widely used GC stationary phases. DC-710 can be prepared by an equilibration reaction involving clearage and reformation of the siloxane bonds

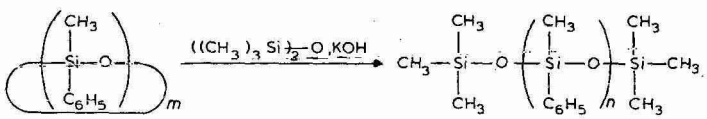

where m and n are equal to the number of difunctional units in the oligomer. Obviously, in addition to a linear polysiloxane, some cyclic oligomers result from residual starting material[45]. Nieman and Rogers[46] reported the SFC separation of DC-710 with conventional packed columns. Fig. 5 shows the UV chromatogram of DC-710 where the separation was performed using essentially the same chromatographic conditions as those used for the separation shown in Fig. 2, except for the pressure applied. The pressure was maintained isobarically at 47.5 atm for 30 min after which it was programmed at 0.17 atm/min to 73.5 atm. It is seen that oligomers up to peak 33 are resolved, after which the trace returns to the baseline. On two sections of the potassium bromide plate a limited number of oligomers, from peak 1 to peak 11, were deposited. The resulting IR chromatogram is shown in Fig. 6; the spectrophotometer was set at 1126 cm^{-1}. The appearance of the chromatogram is similar to that in Fig. 5, except that the unresolved portion of the material is decreased. The IR spectra corresponding to each peak deposited on the plate were scanned, and are shown in Fig. 7 for peaks 1–5. All of the peaks following peak 5 showed identical spectra to that of peak 5. It is interesting that for peaks 1 and 3 the intensity of the band at 1050 cm^{-1} relative to that of both the bands at 1126 and 1026 cm^{-1} is greater than in the case of peaks 2, 4 and 5. Also, the band at 842 cm^{-1} found for peaks 2, 4 and 5 is not present in the spectra of peaks 1 and 3. Therefore, peaks 2, 4 and 5 represent homologous species which are different from peaks 1 and 3.

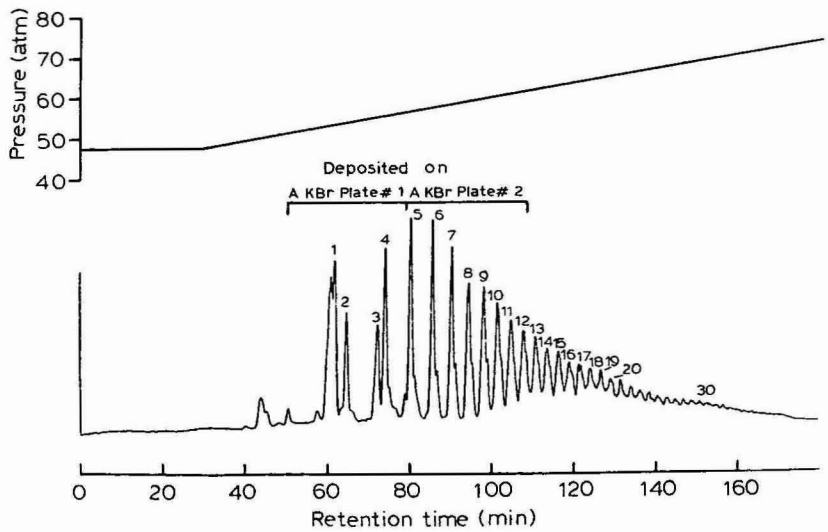

Fig. 5. UV chromatogram of methylphenylpolysiloxane DC-710. Column and mobile phase as in Fig. 2. Column temperature: 260°C. Sample load: 1 μl of 10% DC-710 in mobile phase. Detection: 254 nm.

Many reports have dealt with the spectra of polysiloxanes, but the vibrational assignments are by no means definite, even for simple oligomers such as dimethylpolysiloxanes[47]. The absorption characteristic of the phenyl group in combination with a silicon atom can be seen at 1429 and 1124 cm^{-1}. The strong bands lying in the 1087–1025 cm^{-1} region are assigned to the antisymmetric Si–O–Si stretching

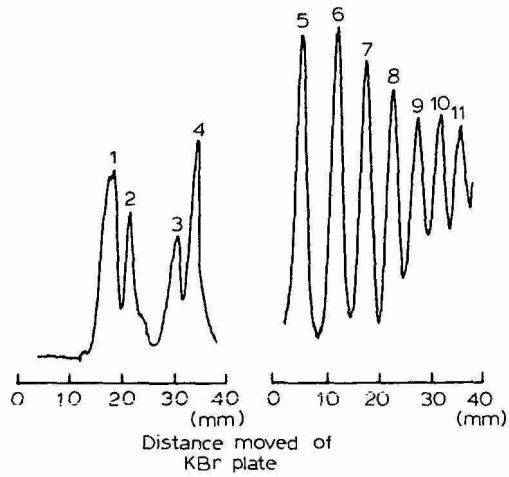

Fig. 6. IR chromatogram of DC-710, measured at 1126 cm^{-1}.

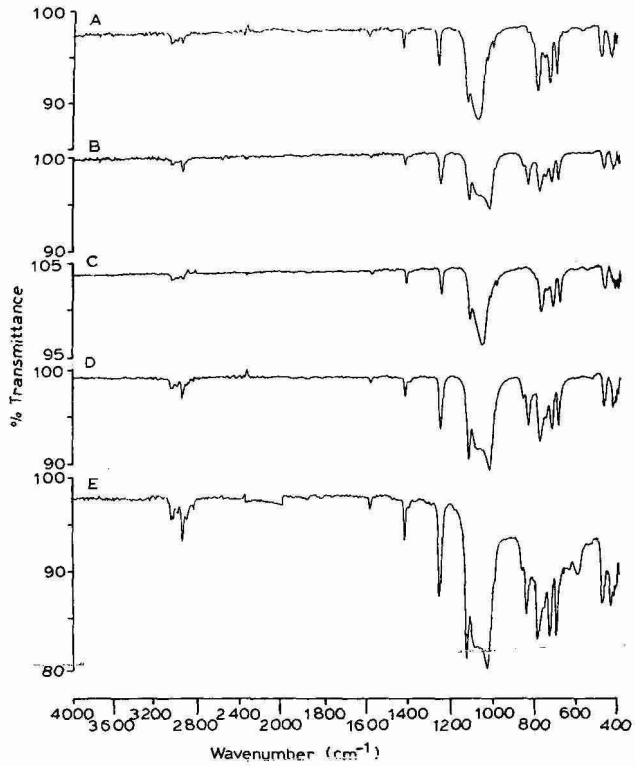

Fig. 7. IR spectra of the components of DC-710: peaks 1 (A), 2 (B), 3 (C), 4 (D) and 5 (E). See Fig. 6 for peak numbers.

mode. Less certain are the methyl rocking and Si–C stretching modes, found between 842 and 698 cm^{-1}, since there is a great possibility of mixing of the vibrations. The absorption at 1260 cm^{-1} may be due to the methyl symmetrical deformation. Taking into account the fact that the bulk of the material is a linear polysiloxane, it can be concluded that peaks 1 and 3 are due to cyclic polysiloxanes, whereas peaks 2, 4 and 5 are linear ones. Also, neither peak 1 nor 3 seems to be a six-membered methylphenylsiloxane, in that an intense band at 1020–1010 cm^{-1}, expected for the cyclic trimers of siloxane oligomers, is not found in their spectra.

It may be noted that IR spectroscopy does not give information about molecular weight, which is the most important item for identification purposes. If this need arises, the material may be scraped off the potassium bromide plate and than subjected to MS analysis[39]. In summary, the present work demonstrates that the buffer-memory technique is a powerful one for the SFC–IR analysis of oligomers. Unlike the flow-cell technique, it is compatible with a mobile phase containing a polar modifier.

ACKNOWLEDGEMENT

We gratefully acknowledge the loan of the Model 810 infrared spectrophotometer by JASCO.

REFERENCES

1 E. Klesper, A. H. Corwin and D. A. Turner, *J. Org. Chem.*, 27 (1962) 700.
2 M. Novotny, S. R. Springston, P. A. Peaden, J. C. Fjeldsted and M. L. Lee, *Anal. Chem.*, 53 (1981) 407A.
3 P. A. Peaden, J. C. Fjeldsted, M. L. Lee, S. R. Springston and M. Novotny, *Anal. Chem.*, 54 (1982) 1090.
4 Y. Hirata and F. Nakata, *J. Chromatogr.*, 295 (1984) 315.
5 Y. Hirata, *J. Chromatogr.*, 315 (1984) 31.
6 Y. Hirata, *J. Chromatogr.*, 315 (1984) 39.
7 T. Takeuchi, D. Ishii, M. Saito and K. Hibi, *J. Chromatogr.*, 295 (1984) 323.
8 L. G. Randall, in S. Ahuja (Editor), *Ultrahigh Resolution Chromatography*, American Chemical Society, Washington, DC, 1984, pp. 135–169.
9 W. P. Jackson, B. E. Richter, J. C. Fjeldsted, R. C. Kong and M. L. Lee, in S. Ahuja (Editor), *Ultrahigh Resolution Chromatography*, American Chemical Society, Washington, DC, 1984, pp. 121–133.
10 J. C. Giddings, M. N. Myers, L. McLaren and R. A. Keller, *Science (Washington, D.C.)*, 162 (1968) 67.
11 E. Klesper, *Angew. Chem., Int. Ed. Engl.*, 17 (1978) 738.
12 U. van Wasen, I. Swaid and G. M. Schreider, *Angew. Chem., Int. Ed. Engl.*, 19 (1980) 575.
13 T. H. Gouw and R. E. Jentoft, *J. Chromatogr.*, 68 (1972) 303.
14 T. H. Gouw and R. E. Jentoft, *Adv. Chromatogr.*, 13 (1975) 1.
15 P. A. Peaden and M. L. Lee, *J. Liq. Chromatogr.*, 5 (suppl.) (1982) 179.
16 L. G. Randall, *Sep. Sci. Technol.*, 17 (1982) 1.
17 E. Klemper and W. Hartmann, *Eur. Polym. J.*, 14 (1978) 77.
18 S. T. Sie, W. Van Beersum and G. W. A. Rijnders, *Sep. Sci.*, 1 (1966) 459.
19 M. N. Myers and J. C. Giddings, in E. S. Perry and C. J. Van Oss (Editors), *Progress in Separation and Purification*, Vol. 3, Wiley-Interscience, New-York, 1970, pp. 133–152.
20 D. Bartmann, *Ber. Bunsenges. Phys. Chem.*, 76 (1972) 336.
21 D. Bartmann, *Ph.D. Dissertation*, University of Bochum, 1972.
22 J. C. Fjeldsted, R. C. Kong and M. L. Lee, *J. Chromatogr.*, 279 (1983) 449.
23 J. C. Fjeldsted, B. E. Richter, W. P. Jackson and M. L. Lee, *J. Chromatogr.*, 279 (1983) 423.

24 W. Asche, *Chromatographia*, 11 (1978) 411.
25 L. G. Randall and A. L. Wahrhaftig, *Anal. Chem.*, 50 (1978) 1705.
26 L. G. Randall, *Ph.D. Dissertation*, University of Utah, 1979.
27 L. G. Randall and A. L. Wahrhaftig, *Rev. Sci. Instrum.*, 52 (1981) 1283.
28 R. D. Smith, J. C. Fjeldsted and M. L. Lee, *J. Chromatogr.*, 247 (1982) 231.
29 R. D. Smith, H. T. Kalinoski, H. R. Udseth and B. W. Wright, *Anal. Chem.*, 56 (1984) 2476.
30 R. D. Smith, H. R. Udseth and H. T. Kalinoski, *Anal. Chem.*, 56 (1984) 2971.
31 B. W. Wright, H. R. Udseth, R. D. Smith and R. N. Hazlett, *J. Chromatogr.*, 314 (1984) 253.
32 R. D. Smith, W. D. Felix, J. C. Fjeldsted and M. L. Lee, *Anal. Chem.*, 54 (1982) 1883.
33 R. D. Smith and H. R. Udseth, *Anal. Chem.*, 55 (1983) 2266.
34 K. H. Shafer and P. R. Griffiths, *Anal. Chem.*, 55 (1983) 1939.
35 S. V. Oleski, S. B. French and M. Novotny, *Chromatographia*, 18 (1984) 489.
36 K. Jinno and C. Fujimoto, *J. High Resolut. Chromatogr. Chromatogr. Commun.*, 4 (1981) 532.
37 K. Jinno, C. Fujimoto and Y. Hirata, *Appl. Spectrosc.*, 36 (1982) 67.
38 K. Jinno, C. Fujimoto and D. Ishii, *J. Chromatogr.*, 239 (1982) 625.
39 C. Fujimoto, K. Jinno and Y. Hirata, *J. Chromatogr.*, 258 (1983) 81.
40 D. Kuehl and P. R. Griffiths, *J. Chromatogr. Sci.*, 17 (1979Z) 471.
41 D. Kuehl and P. R. Griffiths, *Anal. Chem.*, 52 (1980) 1394.
42 K. H. Shafer, S. L. Pentoney, Jr. and P. R. Griffiths, *J. High Resolut. Chromatogr. Chromatogr. Commun.*, 7 (1984) 707.
43 P. R. Griffiths, *Chemical Infrared Fourier Transform Spectroscopy*, Wiley-Interscience, New York, 1975.
44 R. C. Reed and T. K. Sherwood, *The Properties of Gases and Liquids*, McGraw-Hill, New York, 2nd ed., 1966.
45 W. Noll, *Chemistry and Technology of Silicones*, Academic Press, New York, 1968.
46 J. A. Nieman and L. B. Rogers, *Separ. Sci.*, 10 (1975) 517.
47 A. L. Smith and D. R. Anderson, *Appl. Spectrosc.*, 38 (1984) 822.

Journal of Chromatography, 332 (1985) 57–69
Elsevier Science Publishers B.V., Amsterdam — Printed in The Netherlands

CHROMSYMP. 623

ON-COLUMN PREPARATION OF CHEMICALLY BONDED STATIONARY PHASE WITH MAXIMUM SURFACE COVERAGE AND HIGH REPRODUCIBILITY, AND ITS APPLICATION TO PACKED MICROCAPILLARY COLUMNS

NOBUO TANAKA*, HIROSHI KINOSHITA and MIKIO ARAKI
Faculty of Textile Science, Kyoto Institute of Technology, Matsugasaki, Sakyo-ku, Kyoto 606 (Japan)
and
TAKAO TSUDA
Laboratory of Analytical Chemistry, Nagoya Institute of Technology, Gokiso-cho, Showa-ku, Nagoya 466 (Japan)
(First received March 27th, 1985; revised manuscript received May 13th, 1985)

SUMMARY

A method for the on-column preparation of chemically bonded stationary phase with monofunctional reagents was studied in conventional stainless-steel columns and in glass capillary columns for packed microcapillary chromatography. Simple reactions of the silica surface with octadecyldimethyl-N,N-diethylaminosilane in packed columns resulted in a surface coverage of more than 3.0 μmol/m^2, comparable to the stationary phase of maximum coverage prepared in batch. The extent of surface coverage and the amount of residual silanols were carefully examined by using positively charged amines and neutral compounds. Although the results indicate a slight difference between the C_{18} phases in stainless-steel columns and in packed microcapillary columns, excellent reproducibility was found for the on-column bonding reaction, as expected for the reaction using monofunctional reagents.

INTRODUCTION

The preparation of chemically bonded stationary phase such as C_{18} or C_8 in packed columns has been attracting considerable attention. In some areas of high-performance liquid chromatography (HPLC), on-column bonding reaction is an indispensable technique.

When columns for packed microcapillary (PMC) chromatography are prepared, glass tubing packed with silica particles is drawn at high temperatures to produce narrow-bore columns of less than 50 μm I.D. and up to 100 m long. The preparation of chemically bonded stationary phases with these columns must be achieved after the preparation of packed columns. The preparation of chemically bonded stationary phases for open-tubular microcapillary (OTC) chromatography also requires similar procedures.

0021-9673/85/$03.30

Gilpin and co-workers reported the use of alkyltrichlorosilanes for on-column bonding reactions of C_{18}[1] and other phases[2] in conventional columns. Alkylsilylation in PMC and OTC columns was carried out similarly by using octadecyltrichlorosilane[3,4] and alkyltriethoxysilanes[5–9].

In reactions with these polyfunctional reagents, special care has to be taken concerning the purity of the reagents, the elimination of water from the silica surface and the water content of the solvents, as the reagents are very sensitive to the presence of moisture and may polymerize. Although the use of monofunctional reagents with OTC columns has been reported, the extent of surface coverage was not critically examined[10]. The clogging of narrow-bore columns with the use of tri- and monochlorosilanes has also been reported.

In the preparation of stationary phases for reversed-phase liquid chromatography (RPLC) in batch for conventional HPLC columns, increasing numbers of stationary phases are being prepared by using monofunctional instead of polyfunctional reagents in order to obtain high reproducibility without special precautions. The use of monofunctional reagents ensures the formation of monolayers on the silica surface, which is preferable from the chromatographic point of view[11].

In spite of their lower reactivity than polyfunctional reagents, monofunctional reagents such as octadecyldimethylchlorosilane (ODS-Cl) show excellent reproducibility and completeness of the bonding reaction when applied with suitable amines[12,13]. The use of monochlorosilane, however, has been limited in the preparation of bonded phases in PMC and OTC columns, because of the lower reactivity without amines and precipitate formation with amines under the usual reaction conditions. The potential utility of PMC and OTC chromatography is well recognized[14–17], and these chromatographic modes would be enhanced further by operating them under reversed-phase conditions using well characterized stationary phases that possess similar retention characteristics to those in conventional HPLC.

It is desirable to develop an on-column bonding procedure using monofunctional silanes that will allow maximum surface coverage such as is obtained in the reaction in batch without precipitate formation in the columns. In this paper we report the use of alkyldimethyl-N,N-dialkylaminosilanes in on-column bonding reactions and show that maximum coverages can be achieved with high reproducibility. The resulting stationary phases were equivalent to those obtained in the usual reactions in batch in terms of the surface coverage and the amount of residual silanols.

EXPERIMENTAL

Materials and columns

Preparation of octadecyldimethyl-N,N-diethylaminosilane (ODS-DEA). Diethylamine (25 ml) was added to 300 ml of an *n*-hexane solution of 21 g of ODS-Cl. The reaction mixture was kept at 50°C for 1 h with stirring and the salt formed was

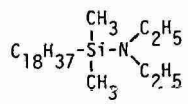

ODS-DEA

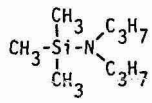

TMS-DPA

filtered off with a PTFE membrane filter. The product, ODS-DEA, was obtained directly from the reaction mixture by distillation under reduced pressure (b.p. 180°C/0.1 mmHg). Trimethyl-N,N-di-*n*-propylaminosilane (TMS-DPA) was prepared similarly from trimethylchlorosilane (TMS-Cl) and di-*n*-propylamine (b.p. 67.0°C/29 mmHg).

Silica gel particles. Develosil (10 μm, 330 m^2/g) (Nomura Chemicals, Seto, Japan) was used following acid treatment[18]. Heat treatment of the silica gel was performed in an electric furnace at 800°C for 3 h.

PMC columns. Soda-lime glass tubing (0.5 mm I.D., 6 mm O.D.) was dry-packed with the silica particles, and drawn to produce PMC columns (40–50 μm I.D., 0.5 mm O.D.) with a glass-drawing machine (GDM-1) (Shimadzu, Kyoto, Japan), as described previously[8,19].

Conventional stainless-steel columns. Silica particles or chemically bonded C_{18} phases were packed into stainless-steel columns (10 cm × 4.6 mm I.D.) using conventional slurry techniques.

OTC columns. Soda-lime glass tubing (0.4 mm I.D., 6 mm O.D.) was drawn to produce OTC columns (25 μm I.D., 0.5 mm O.D.) in a similar manner to PMC columns. The OTC columns were treated with 0.5 *N* NaOH at 50°C for 18 h prior to the bonding reaction.

Chemical bonding reaction

In batch. Octadecylsilylation of silica particles was performed as previously described[12,13], using ODS-Cl and pyridine for stationary phases A–F and ODS-DEA

TABLE I

PREPARATION METHODS OF THE VARIOUS COLUMNS

Column No.	*Column type**	*Stationary phase*	*Preparation method of bonded phase*	*Reagents*
A-1	SS	C_{18}	Batch	ODS-Cl
B-1	SS	C_{18}	Batch	ODS-Cl
C-1	SS	C_{18}	Batch	ODS-Cl
D-1	SS	C_{18}	Batch	ODS-Cl
E-1	SS	C_{18}	Batch	ODS-Cl
F-1	SS	C_{18}	Batch	ODS-Cl
G-1	SS	C_{18}	Batch	ODS-DEA
D-2	SS	C_{18} + TMS	Batch	ODS-Cl + TMS-Cl
E-2	SS	C_{18} + TMS	Batch	ODS-Cl + TMS-Cl
F-2	SS	C_{18} + TMS	Batch	ODS-Cl + TMS-Cl
G-2	SS	C_{18} + TMS	Batch	ODS-DEA + TMS-DPA
H-1	SS	C_{18}	On-column	ODS-DEA
H-2	SS	C_{18} + TMS	On-column	ODS-DEA + TMS-DPA
PMC-C_{18}-1	PMC	C_{18}	On-column	ODS-DEA
PMC-C_{18}-2	PMC	C_{18} + TMS	On-column	ODS-DEA + TMS-DPA
PMC-C_{18}-3	PMC	C_{18}	On-column	$C_{18}H_{37}Si(OC_2H_5)_3$

* SS = conventional stainless-steel columns; PMC = packed microcapillary columns.

for stationary phase G (see Table I for the identity of each stationary phase). The carbon contents of stationary phases with less than the maximum coverage were controlled by the amount of ODS-Cl in the reaction mixture. Trimethylsilylation was carried out similarly using TMS-Cl and hexamethyldisilazane for stationary phases D-2–F-2 and TMS-DPA for stationary phase G-2.

On-column. A stainless-steel column packed with silica gel was connected to an injector equipped with a 5-ml loop. The silica gel in the column was washed with 10 ml of tetrahydrofuran (THF) at room temperature and 10–20 ml of toluene at 110°C. A 5-ml volume of 20% ODS-DEA solution in toluene was introduced into the injector loop. After pumping 2–3 ml of the reagent solution through the column, which was maintained at 105–110°C, the flow was interrupted and the silica was allowed to react with the reagent. After reaction for 1 h, the flow of toluene was resumed. The column was washed with 10 ml of THF at room temperature and 10–20 ml of toluene at 110°C. The reaction with ODS-DEA and the washing with THF and toluene were repeated again. Finally, the column was washed with methanol, then with 0.02 *M* phosphate buffer (pH 3) in 50% methanol prior to use in RPLC. On-column trimethylsilylation was performed similarly using 5 ml of 35% TMS-DPA in toluene.

The on-column bonding reaction of PMC columns was carried out under a flow of a silylating reagent. A PMC column (3–4 m × 44 μm I.D.) was washed with THF for 30 min and with toluene for 1 h with a column inlet pressure of 200 kg/cm^2. The reagent solution, 0.5 ml of 20% ODS-DEA in toluene, was passed through the column with a column inlet pressure of 150 kg/cm^2 at 110°C. After reaction for 1 h, the PMC column was washed with THF and toluene as indicated above. The whole process was repeated three or four times to ensure maximum surface coverage, although the reaction was almost complete after the second run. Trimethylsilylation was carried out similarly using 0.5 ml of 35% TMS-DPA in toluene. A final wash with methanol and phosphate buffer was carried out as with conventional columns.

Equipment

The conventional HPLC system consisted of an LC-3A pump (Shimadzu, Kyoto, Japan), an M-440 UV detector (Waters Assoc., Milford, MA, U.S.A.), a 98.00 RI detector (Knauer, Berlin, F.R.G.) and a 7000A data processor (System Instrument, Tokyo, Japan). PMC chromatography was performed using a Tri Rotar-V pump and a Uvidec-100-V UV detector (both from Japan Spectroscopic, Tokyo, Japan) equipped with a home-made fused-silica capillary cell (50 μm I.D., *ca.* 10 cm from the column end to the light path). Split injection was employed for PMC chromatography, using a tee-joint with an SS22RS2 micro-metering valve (Whitey, Highland Hights, OH, U.S.A.) in the waste line. The column temperature was controlled using a water-bath for stainless-steel columns and an air-bath for PMC columns.

Chromatographic measurements

Chromatographic runs were carried out in duplicate. The elution volume of ^2H_2O was taken as t_0 for the conventional system, and that of uracil was used to determine t_0 for the PMC system using k' values of uracil on stainless-steel columns. Retention ratios were used instead of k' values for the comparison between conventional and PMC columns in order to minimize the effect of the difference between the two chromatographic systems.

RESULTS AND DISCUSSION

In the alkylsilylation of a silica surface, polyfunctional reagents are in general more reactive than monofunctional reagents, and have been used for on-column bonding reactions. Gilpin *et al.*[1] used octadecyltrichlorosilane for the preparation of chemically bonded phases in conventional columns[1]. In batch reactions using monochlorosilanes, amines such as pyridine are added to the reaction mixture to take up the HCl formed by the reaction in order to increase the reactivity in the usual chemical bonding reactions[12].

Körösi and Kováts[20] reported the alkylsilylation of a glass surface using alkyldimethyl-N,N-dimethylaminosilanes with dimethylamine as a byproduct. We have adopted this approach in order to achieve high reactivity accompanied by a liquid byproduct in *in situ* bonding reactions. Dimethylamine has a very low boiling point of 7°C and bubbles in a column under normal reaction conditions when alkyldimethyl-N,N-dimethylaminosilanes are applied to on-column reactions.

Diethylamine and di-*n*-propylamine have higher boiling points (55 and 110°C, respectively) and still give boiling points of octadecylsilanes low enough to allow easy distillation. Combinations of ODS-Cl and diethylamine and of TMS-Cl and di-*n*-propylamine were found to give amine hydrochloride precipitates that are easy to filter off during the preparation of the reagents. The reagents, ODS-DEA and TMS-DPA, are also reactive enough to yield readily maximum surface coverage in a short period of time, as shown below. The present method has the advantage that toluene can be used as received, without drying.

The *in situ* bonding reactions were carried out by simply introducing the aminosilane solutions in toluene from the injector loop into the silica packed column. The aminosilane solution was kept in contact with silica at 110°C for 1 h each time. The reaction was slower at lower temperatures. The reaction was repeated twice for regular stainless-steel columns and three or four times for PMC columns in order to attain maximum coverage. The total preparation time was about 4 h for stainless-steel columns including the wash time between the repeated reactions with THF and toluene. The final wash was carried out with methanol and an acidic buffer. With PMC columns the flow-rate of the reagent solution was maintained at 1–1.5 μl/min during the reaction.

In order to evaluate the surface coverage achieved by the on-column reaction, stationary phases having various carbon contents (A–F) were prepared in batch using ODS-Cl. Of these, F-1 was prepared under conditions that should give the maximum coverage with octadecylsilyl groups. It has been found that the preparation of stationary phases with maximum surface coverage using ODS-Cl in batch was highly reproducible[18].

The C_{18} phase H-1 prepared by the *in situ* reaction was compared with the C_{18} phase G-1 prepared in batch from the same reagent, ODS-DEA, and with other stationary phases prepared by using ODS-Cl. The results are shown in Table II. The carbon content and the surface coverage of G-1 were slightly higher than those of F-1, indicating the high reactivity of ODS-DEA, as reported[20]. Stationary phase H-1, prepared by the *in situ* reaction, showed a very similar extent of surface coverage to G-1. This indicates that the reaction in the column using ODS-DEA can afford maximum surface coverage, as in batch reactions. The extent of surface coverage

TABLE II

SURFACE COVERAGES AND HYDROPHOBIC PROPERTIES OF THE STATIONARY PHASES

Stationary phase	*Carbon content (%)*	*Surface coverage (μmol/m²)*	$\alpha_{CH_2}^{*}$ *(80% methanol)*
A-1	8.85	1.26	0.1359
B-1	11.37	1.68	0.1479
C-1	16.97	2.74	0.1727
D-1	17.82	2.92	0.1730
E-1	18.17	3.00	0.1743
F-1	19.06	3.19	0.1755
G-1	20.06	3.42	0.1767
D-2	18.13	–	0.1771
E-2	19.06	–	0.1775
F-2	19.19	–	0.1797
G-2	20.28	–	0.1780
H-1	19.71	3.34	0.1753
H-2	19.79	–	0.1775
PMC-C_{18}-1	–	–	0.1756
PMC-C_{18}-2	–	–	0.1789

* The α_{CH_2} values were obtained from the slopes of the graphs of log k' of alkylbenzenes (ethyl-, propyl-, butyl- and pentylbenzene) against the carbon number of the alkyl groups in 80% methanol at 30°C. Each regression line had a correlation coefficient of better than 0.9999.

achieved in stationary phases F, G and H agreed very well with those reported to be maximum[21].

In order to confirm the maximum surface coverages indicated by the carbon content of the bonded phases, the stationary phases were further evaluated chromatographically in terms of their hydropohobic properties and the amounts of residual silanols. The retention increment due to one methylene group in a linear alkyl chain correlates very well with the hydrophobic character of the stationary phases[22,23]. As shown in Table II, the retention increment due to one methylene group (α_{CH_2}) increases with increase in surface coverage. Stationary phases H and PMC-C_{18} showed very similar α_{CH_2} values to stationary phases F and G, having maximum surface coverage, indicating that PMC-C_{18} also has a high density of octadecylsilyl groups, probably higher than 3.0 μmol/m², on the silica surface.

In addition to their hydrophobic character, the amounts of residual silanols on each stationary phase were compared by using so-called silanophilic solutes. This was first tried in 60% methanol using benzene derivatives as solutes. The group contribution of a polar group, or the relative retention of acetophenone (AP) with respect to benzene (B), $\alpha_{AP/B}$, and that of methyl benzoate (MB) to benzene, $\alpha_{MB/B}$, show the silanol effect[13], and the group contribution of the methyl group or the relative retention of toluene (T) to benzene, $\alpha_{T/B}$, indicates the hydrophobic character of the stationary phase. The former decrease and the latter increases with increase in surface coverage by C_{18} and also by trimethylsilylation, as shown in Table III.

TABLE III

RETENTIONS (k') AND SEPARATION FACTORS (α) OF BENZENE DERIVATIVES

Mobile phase, 60% methanol; temperature, 30°C.

Stationary phase	k'_{AP} ($\alpha_{AP/B}$)	k'_{MB} ($\alpha_{MB/B}$)	k'_B	k'_T ($\alpha_{T/B}$)
A-1	0.94 (0.69)	1.54 (1.12)	1.37	2.28 (1.66)
B-1	1.20 (0.63)	2.04 (1.06)	1.92	3.35 (1.74)
C-1	1.59 (0.49)	3.08 (0.94)	3.26	6.21 (1.90)
D-1	1.61 (0.47)	3.17 (0.92)	3.46	6.61 (1.91)
E-1	1.60 (0.45)	3.19 (0.92)	3.57	6.88 (1.93)
F-1	1.55 (0.44)	3.09 (0.87)	3.55	6.84 (1.93)
G-1	1.49 (0.42)	3.00 (0.84)	3.57	6.91 (1.94)
D-2	1.48 (0.43)	2.97 (0.86)	3.45	6.68 (1.94)
E-2	1.46 (0.40)	2.98 (0.83)	3.61	7.00 (1.94)
F-2	1.38 (0.38)	2.83 (0.79)	3.60	7.02 (1.95)
G-2	1.35 (0.38)	2.77 (0.79)	3.51	6.82 (1.94)
H-1	1.49 (0.43)	2.99 (0.85)	3.50	6.73 (1.92)
H-2	1.32 (0.38)	2.71 (0.78)	3.46	6.70 (1.94)
PMC-C_{18}-1	0.76 (0.47)	1.42 (0.88)	1.61	3.09 (1.92)
PMC-C_{18}-2	0.68 (0.41)	1.34 (0.81)	1.66	3.19 (1.92)
PMC-C_{18}-3	0.56 (0.83)	0.81 (1.21)	0.67	1.11 (1.66)

The results with stationary phases H-1 and H-2 agreed very well with those with F-1 and F-2, and with those with G-1 and G-2 having maximum surface coverages prepared in batch using ODS-Cl and ODS-DEA, respectively. With these stainless-steel columns, the k' values of benzene derivatives on stationary phase H showed excellent agreement with those on F or G, indicating similar packing densities in the columns. With PMC columns, however, the k' values of the benzene derivatives were about half of those for conventional packed columns. This is primarily due to the lower packing density of silica particles in PMC columns. PMC columns are known to show much lower flow resistance than conventional columns, by a factor of 5 or more[19]. The looser packing of silica in PMC columns leads to a larger interparticle space and higher permeability. Based on k' values for non-polar solutes, benzene and toluene, the phase ratio V_s/V_m in PMC columns was estimated to be about 45% of that in conventional packed columns. This is supported by the results of studies with size exclusion chromatography using trimethylsilylated PMC columns, which showed the pore volume of the silica particles in PMC columns to be about 20% of the total column volume, compared with about 40% in conventional columns[24]. Therefore, the comparison of surface coverages among the stationary phases should be made on the basis of group contributions of polar and non-polar groups.

PMC-C_{18} showed $\alpha_{AP/B}$ and $\alpha_{MB/B}$ values very slightly larger than those of G or H with maximum surface coverage, indicating slightly lower surface coverages of PMC columns. The α values are very close to those found for stationary phases E or F, which possess 3.0–3.2 μmol/m^2 of alkylsilyl groups.

PMC-C_{18}-3 was prepared by using octadecyltriethoxysilane according to the reported procedure[8]. Although the reaction was repeated three times, the α values indicate a low surface coverage. This shows the much higher reactivity of aminosilanes compared with triethoxysilanes. The on-column bonding reaction using aminosilanes is also free from column clogging problems.

The retention of caffeine is much more sensitive to the amount of residual silanols. Caffeine is eluted later than phenol with peak tailing from stationary phases of low coverage. The stationary phases are compared on the basis of the relative retention of caffeine with respect to phenol. The results are shown in Table IV. Although H-2 gave similar results to F-2 and G-2, PMC-C_{18}-2 showed slightly larger $\alpha_{caffeine/phenol}$ values than the stationary phases with maximum surface coverage. It should be noted that the *in situ* bonding reaction employed in the preparation of stationary phase H in stainless-steel columns gave very similar surface coverages (or maximum coverage) as the conventional method in batch used to produce F or G. The same reaction conditions resulted in stationary phases with slightly more silanols for PMC-C_{18} columns, although the surface coverages of PMC-C_{18} columns seem to be close to the maximum, or about 3.0 μmol/m^2. The exact reason for this result is not clear at present, and may be related to the hysteresis of silica particles in drying and the tubing-drawing process associated with PMC columns at temperatures above 750°C. The heat treatment of silica at such temperatures may reduce the number of surface hydroxyl groups and reduce the pore size[25], leading to lower surface coverage.

TABLE IV

k' VALUES OF CAFFEINE AND AMINES AND THEIR RELATIVE RETENTION WITH RESPECT TO PHENOL ON STATIONARY PHASES WITH VARIOUS SURFACE COVERAGES AT 30°C

Stationary phase	k'_X ($\alpha_{X/phenol}$)				
	20% methanol, caffeine	*40% methanol, pH 2.9**		*40% methanol, pH 7.7**	
		PA	*NAPA*	*PA***	*NAPA***
D-1	10.32 (1.50)*	0.02 (0.01)	0.16 (0.07)	1.67 (0.73)	2.48 (1.09)
E-1	10.83 (1.56)*	0.04 (0.02)	0.18 (0.07)	1.77 (0.69)	2.63 (1.03)
F-1	10.29 (1.20)*	0.03 (0.01)	0.15 (0.06)	1.28 (0.49)	1.77 (0.67)
G-1	7.69 (0.90)	0.02 (0.01)	0.14 (0.06)	0.64 (0.24)	1.08 (0.41)
D-2	6.83 (0.85)	0.01 (0.01)	0.14 (0.06)	0.38 (0.15)	0.95 (0.37)
E-2	6.07 (0.75)	0.03 (0.01)	0.15 (0.06)	0.35 (0.14)	0.91 (0.35)
F-2	6.38 (0.73)	0.03 (0.01)	0.15 (0.06)	0.35 (0.13)	0.91 (0.34)
G-2	6.02 (0.71)	0.02 (0.01)	0.15 (0.06)	0.36 (0.14)	0.88 (0.33)
H-1	8.59 (1.01)*	0.02 (0.01)	0.15 (0.06)	1.19 (0.46)	1.46 (0.56)
H-2	5.97 (0.70)*	0.02 (0.01)	0.14 (0.05)	0.39 (0.15)	0.89 (0.34)
PMC-C_{18}-1	3.13 (0.93)*	0.09 (0.08)	0.17 (0.14)	1.15 (1.02)	1.41 (1.25)
PMC-C_{18}-2	2.58 (0.77)	0.10 (0.08)	0.20 (0.17)	0.36 (0.30)	0.59 (0.49)

* Tailed peak.

** 0.02 *M* phosphate buffer was used to maintain pH.

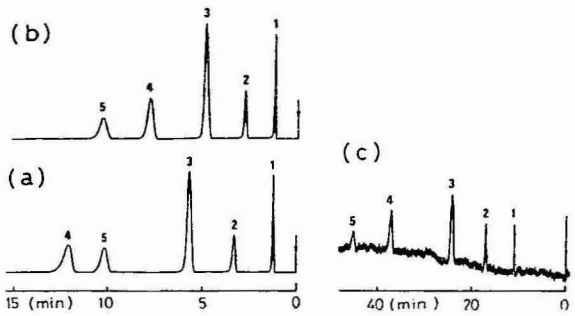

Fig. 1. Elution of uracil (1), theobromine (2), theophylline (3), caffeine (4) and phenol (5) on stationary phases F-1 (a) and F-2 (b) at a flow-rate of 1 ml/min and on PMC-C_{18}-2 (3.6 m × 44 μm I.D.) (c) with a column inlet pressure of 250 kg/cm². Mobile phase, 20% methanol; temperature, 30°C.

C_{18} stationary phase prepared in batch similarly to G-1 from silica particles treated at 800°C for 3 h showed a considerably lower carbon content (16.80%), supporting the present explanation. The bonded phase in PMC-C_{18}-2, however, apparently possesses a surface coverage of close to 3.0 μmol/m². The similar retention ratios seen with PMC-C_{18} phases as stationary phases prepared in batch imply little difference in the surface concentrations of silanols after the drawing process with PMC columns. As shown in Fig. 1, the chromatogram of xanthine derivatives on PMC-C_{18}-2 was similar to that on F-2 with maximum surface coverage prepared in batch, showing the practical utility of the present on-column reaction for the preparation of reversed-phase PMC columns.

The stationary phases prepared by on-column reaction were further examined with positively charged amines as solutes. It was shown that so-called silanol effects are the combined effects of neutral silanols and some dissociated anionic sites that are present in chemically bonded phases even at acidic pH[18]. The former is responsible for the retention of polar neutral compounds such as caffeine, and the latter, presumably related to the highly acidic silanols or metal impurities in the silica structure, is responsible for the retention of positively charged solutes. The retention of positively charged amines such as procainamide (PA) [H_2N–C_6H_4–$CONHCH_2CH_2N(C_2H_5)_2$] and N-acetylprocainamide (NAPA) [CH_3CONH–C_6H_4–$CONHCH_2CH_2N(C_2H_5)_2$] at pH below 3 indicates the presence of the ion-exchange sites at such pH values, and the retention of these compounds at pH above 7 is provided by the dissociated form of silanols and the anionic sites which contribute to the retention of amines at pH below 3.

Stationary phase H showed almost no retention of PA and NAPA at pH below 3 in 40% methanol, indicating the presence of essentially no anionic sites on the silica surface, as is the case with stationary phases prepared in batch. This is to be expected from the acid treatment of the silica gel used in the preparation of these stationary phases[18]. Stationary phase H-2 also showed a very low retention at pH 7.7, indicating that very few silanols are present as in stationary phases D-2–G-2. The results confirm the completeness of surface coverage by the *in situ* reaction under the present reaction conditions.

PMC-C_{18}-2, however, showed a slightly higher retention of PA and NAPA at pH 2.9, indicating the presence of small amount of ion-exchange sites. PMC-C_{18}-2 also showed a slight retention of PA and NAPA at pH 7.7, indicating the presence of dissociated silanols and ion-exchange sites. It has been shown that silanols in the form of SiOH are not responsible for the retention of positively charged amines, but silanols do contribute to the retention of such compounds at pH above 7 where silanols undergo dissociation[18]. If one compares the results obtained with PMC-C_{18}-2 with those for D-1, E-1 and F-1, which were not trimethylsilylated, the retention of PA on PMC-C_{18}-2 was higher than on D-1, E-1 and F-1 at pH 2.9, indicating the presence of more ion-exchange sites on PMC-C_{18}-2. At pH 7.7, k'_{PA} on PMC-C_{18}-2 was lower than the value on D-1, E-1 and F-1. These stationary phases possess more silanols than PMC-C_{18}-2, as shown in Tables III and IV. These results indicate that the retention of PA and NAPA on PMC-C_{18}-2 is mainly caused by the presence of ion-exchange sites. The possible source of such dissociated anionic sites in PMC-C_{18} phases is the glass wall of PMC columns. In addition to these ion-exchange sites, small amounts of silanols may be left unreacted owing to the modified surface structure or the reduced pore size of silica particles, as mentioned earlier. Further study is needed to explain in detail the small difference between conventional and PMC columns.

In spite of the presence of small numbers of ion-exchange sites and silanols, the performance of PMC-C_{18}-2 obtained with the present *in situ* bonding reaction for silanophilic solutes will be comparable to that of the best stationary phases commercially available, judging from the retention of PA and NAPA at pH 2.9 and 7.7[26].

The completeness of surface coverage of the on-column bonding reaction was shown above. Another important factor in the chemical bonding reaction is its re-

TABLE V

REPRODUCIBILITY OF ON-COLUMN REACTION

Mobile phase, 60% methanol.

Column type	*Run No.*	*Stationary phase*	k'_{AP} ($\alpha_{AP/B}$)	k'_{MB} ($\alpha_{MB/B}$)	k'_B	k'_T ($\alpha_{T/B}$)
Stainless-steel	1	C_{18}	1.42 (0.42)	2.83 (0.84)	3.38	6.51 (1.93)
	2	C_{18}	1.45 (0.42)	2.92 (0.84)	3.48	6.71 (1.93)
	3	C_{18}	1.50 (0.42)	3.01 (0.85)	3.55	6.85 (1.93)
	4	C_{18}	1.51 (0.43)	3.01 (0.85)	3.55	6.83 (1.92)
	5	C_{18}	1.49 (0.43)	2.99 (0.85)	3.50	6.73 (1.92)
	6	C_{18} + TMS	1.32 (0.39)	2.70 (0.79)	3.41	6.60 (1.94)
	7	C_{18} + TMS	1.32 (0.38)	2.71 (0.78)	3.46	6.70 (1.94)
PMC	1	C_{18}	0.73 (0.48)	1.35 (0.89)	1.51	2.86 (1.89)
	2	C_{18}	0.69 (0.47)	1.29 (0.88)	1.46	2.79 (1.91)
	3	C_{18}	0.76 (0.47)	1.42 (0.88)	1.61	3.09 (1.92)
	4	C_{18} + TMS	0.60 (0.39)	1.23 (0.80)	1.54	2.95 (1.92)
	5	C_{18} + TMS	0.68 (0.41)	1.34 (0.81)	1.66	3.19 (1.92)

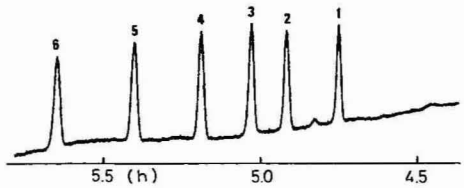

Fig. 2. Separation of benzene (1), toluene (2), ethylbenzene (3), propylbenzene (4), butylbenzene (5) and pentylbenzene (6) on a PMC-C_{18} column (16.2 m × 44 μm I.D.) with a column inlet pressure of 100 kg/cm². Mobile phase, methanol; temperature, 30°C.

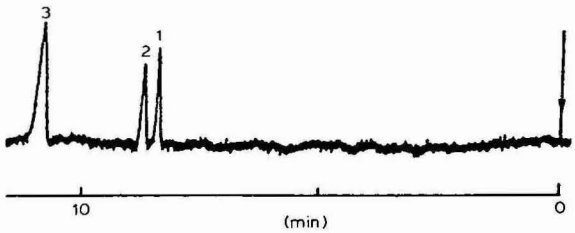

Fig. 3. Elution of uracil (1), phenol (2) and acetophenone (3) on an OTC-C_{18} column (4.5 m × 25 μm I.D.) prepared from soda-lime glass with a column inlet pressure of 20 kg/cm². Mobile phase, water; temperature, 30°C.

producibility. This can be seen in Table V. For conventional columns, excellent reproducibility was achieved with the selectivity between benzene derivatives and also with the k' values, which can be affected by the packing density of silica particles in the columns. The variation of k' with PMC columns was slightly greater than with conventional columns. This probably reflects the slight variation in the packing density of silica particles in glass capillary tubing prepared separately. The reproducibility in terms of α, however, was excellent, as is the case with stainless-steel columns.

Long reversed-phase PMC columns can now be prepared easily and reproducibly at close to maximum surface coverage. Fig. 2 shows the performance of a 16.2-m PMC-C_{18} column with alkylbenzenes. This column afforded more than $5 \cdot 10^5$ plates per column in absolute methanol at 30°C for ethylbenzene with a k' value of 0.11 at a mobile phase linear velocity of 6 cm/min. This approach to attaining a very high number of theoretical plates is very promising in comparison with conventional or micro-bore columns[27], as the PMC columns show a much lower flow resistance than the usual packed columns. A theoretical study and practical applications of these PMC columns with maximum surface coverage are currently in progress.

Apart from ODS-Cl, any type of chlorosilanes can be used for the *in situ* bonding reaction following the preparation of aminosilanes. The preparation of the reagent is facile, provided that the functional group is compatible with aminosilane functions. The present method also allows the regeneration of stationary phases in conventional reversed-phase columns when they lost some alkylsilyl groups during use.

The on-column bonding reaction is naturally applicable to OTC columns. Fig. 3 shows the chromatogram obtained with an OTC-C_{18} column (4.5 m × 25 μm I.D.) prepared under the present reaction conditions after base treatment of the soda-lime glass tubing. The extent of surface coverage is yet to be determined in this instance, but the results show the potential of the procedures reported here in the preparation of this type of reversed-phase column.

CONCLUSION

The on-column preparation of chemically bonded stationary phases was studied using the monofunctional reagents ODS-DEA and TMS-DPA. By the simple reaction of the silica surface with the aminosilanes, a monomeric C_{18} stationary phase was prepared on silica packed in columns with maximum surface coverage and high reproducibility, comparable to those for stationary phases prepared in batch using ODS-Cl or ODS-DEA. The method was also applied to the preparation of reversed-phase PMC columns. The PMC-C_{18} columns also showed near maximum surface coverage, estimated to be *ca.* 3 μmol/m^2. Although the PMC-C_{18} stationary phases were shown to possess slightly more residual silanols and anionic sites, their retention characteristics were very similar to those of stationary phases with maximum surface coverage.

The proposed method allows the reproducible preparation of very long reversed-phase PMC columns to generate large numbers of theoretical plates inexpensively. The on-column reaction also allows the preparation of reversed-phase OTC columns and the regeneration of chemically bonded stationary phases in conventional stainless-steel columns.

ACKNOWLEDGEMENT

The authors are grateful to Dr. S. Terabe of Kyoto University for his helpful suggestions.

REFERENCES

1 R. K. Gilpin, J. A. Korpi and C. A. Janicki, *Anal. Chem.*, 46 (1974) 1314.
2 R. K. Gilpin and W. R. Sisco, *Anal. Chem.*, 50 (1978) 1337.
3 T. Tsuda, K. Hibi, T. Nakanishi, T. Takeuchi and D. Ishii, *J. Chromatogr.*, 158 (1978) 227.
4 K. Hibi, D. Ishii and T. Tsuda, *J. Chromatogr.*, 189 (1980) 179.
5 Y. Hirata, M. Novotny, T. Tsuda and D. Ishii, *Anal. Chem.*, 51 (1979) 1807.
6 D. Ishii and T. Takeuchi, *J. Chromatogr.*, 218 (1981) 189.
7 T. Tsuda, K. Tsuboi and G. Nakagawa, *J. Chromatogr.*, 214 (1981) 283.
8 T. Tsuda, I. Tanaka and G. Nakagawa, *J. Chromatogr.*, 239 (1982) 507.
9 T. Takeuchi and D. Ishii, *J. Chromatogr.*, 279 (1983) 439.
10 J. W. Jorgenson and E. J. Guthrie, *J. Chromatogr.*, 255 (1983) 335.
11 B. L. Karger and R. W. Giese, *Anal. Chem.*, 50 (1978) 1048A.
12 H. Hemetsberger, M. Kellermann and H. Ricken, *Chromatographia*, 10 (1977) 726.
13 N. Tanaka, H. Goodell and B. L. Karger, *J. Chromatogr.*, 158 (1978) 233.
14 J. H. Knox, *J. Chromatogr. Sci.*, 18 (1980) 453.
15 T. Tsuda and M. Novotny, *Anal. Chem.*, 50 (1978) 271.

16 M. Novotny, *Anal. Chem.*, 53 (1981) 1294A.
17 D. Ishii and T. Takeuchi, *J. Chromatogr. Sci.*, 22 (1984) 400.
18 N. Tanaka, M. Araki, K. Kimata, K. Iwaguchi, R. Eksteen and B. L. Karger, *J. Chromatogr.*, submitted for publication.
19 T. Tsuda, I. Tanaka and G. Nakagawa, *Anal. Chem.*, 56 (1984) 1249.
20 G. Körösi and E. sz. Kováts, *Colloids Surfaces*, 2 (1981) 315.
21 G. E. Berendsen and L. de Galan, *J. Liq. Chromatogr.*, 1 (1978) 561.
22 B. L. Karger, J. R. Gant, A. Hartkopf and P. H. Weiner, *J. Chromatogr.*, 128 (1976) 65.
23 N. Tanaka and E. R. Thornton, *J. Amer. Chem. Soc.*, 99 (1977) 7300.
24 T. Tsuda, N. Tanaka, H. Kinoshita and M. Araki, unpublished results.
25 K. K. Unger, *Porous Silica*, Elsevier, Amsterdam, 1979, Ch. 1 and 2.
26 N. Tanaka, M. Araki, K. Kimata, K. Iwaguchi, R. Eksteen and B. L. Karger, *J. Chromatogr.*, submitted for publication.
27 H. G. Menet, P. C. Gareil and R. H. Rosset, *Anal. Chem.*, 56 (1984) 1770.

Journal of Chromatography, 332 (1985) 71–106
Elsevier Science Publishers B.V., Amsterdam — Printed in The Netherlands

CHROMSYMP. 612

SEPARATION OF FREE RADICALS BY HIGH-PERFORMANCE LIQUID CHROMATOGRAPHY WITH ELECTRON SPIN RESONANCE DETECTION

KEISUKE MAKINO*,*, FUMIO MORIYA** and HIROYUKI HATANO
Department of Chemistry, Faculty of Science, Kyoto University, Kitashirakawa, Sakyo-ku, Kyoto 606 (Japan)
(Received March 29th, 1985)

SUMMARY

Studies on the separation of free radicals by high-performance liquid chromatography with electron spin resonance detection (HPLC–ESR) are described. Aqueous solutions of amino acids, dipeptides and tripeptides were γ-irradiated in the presence of a spin trap, 2-methyl-2-nitrosopropane. The stable aminoxyl radicals (spin adducts) produced were isolated by HPLC on cation-exchange columns. An ESR spectrometer was utilized as a detector for monitoring the eluted radicals. Various types of spin adducts were identified and characterized by ESR spectroscopy. The individual components of several pairs of diastereomeric radicals could be separated.

INTRODUCTION

Free radicals are considered to be important intermediates of reactions occurring in living tissues[1]. The detection of radical species generated from biologically important molecules by high energy, *e.g.*, ionizing radiation, is very important in exploring the mechanisms of the induced reactions in biological systems[2,3]. However, especially in aqueous solutions, ambiguous assignments have been made, mainly because of the short life of the species.

In order to overcome this problem, the method of spin trapping was developed by several research groups[4–11] and subsequently applied in biochemistry[12,13]. In this method, short-lived free radicals are converted into relatively stable aminoxyl radicals (spin adducts) through reactions with spin traps such as nitroso or nitrone compounds. The lifetimes of spin adducts are often of the order of minutes or hours. Therefore, one can carry out electron spin resonance (ESR) measurements of the spin adducts, and by analyzing the resulting spectra, can determine the structures of the original short-lived radicals.

* Present address: Department of Polymer Science and Engineering, Faculty of Textile Science, Kyoto Institute of Technology, Matsugasaki, Sakyo-ku, Kyoto 606, Japan.
** Present address: Department of Chemistry, Kobe University of Commerce, Tarumi-ku, Kobe 655, Japan.

0021-9673/85/$03.30

The spin-trapping method can be applied to reactions of aqueous systems by use of water-soluble spin traps and, therefore, has been extensively utilized to study short-lived free radicals produced in aqueous solutions of biomolecules by ionizing radiations, photochemical reactions, etc.[14–27]. In this way, many short-lived radicals not previously detected by conventional methods were identified. However, as the number of applications increased, a problem arose. As expected, in many systems, several different types of short-lived radicals are produced and can be spin-trapped simultaneously. In such cases, it is not easy to identify each of the components because of the overlap of several different ESR spectra due to the similarity in g values of the spin adducts. Liquid chromatography has been employed together with ESR spectroscopy for the separation and detection of radical mixtures[28]. This technique has been applied to the spin adducts in γ-irradiated aqueous solutions of several nucleotides[29,30] using 2-methyl-2-nitrosopropane (MNP) as a spin trap.

In the present work, we developed this technique further by employing high-performance liquid chromatography (HPLC). Our technique, called spin-trap HPLC–ESR, was applied to γ-irradiated aqueous solutions of amino acids, dipeptides and tripeptides containing MNP. The reaction of MNP with short-lived free radicals (·R) is represented by:

$$\textit{tert.}\text{-Bu-N}=\text{O} + \cdot\text{R} \rightarrow \textit{tert.}\text{-Bu–N(O·)–R} \leftrightarrow \textit{tert.}\text{-Bu–}\dot{\text{N}}^{+}(\text{O}^{-})\text{–R} \qquad (1)$$

It is well known that γ-radiolysis of water gives rise to highly reactive species such as hydroxyl radicals (·OH), hydrated electrons (e_{aq}^{-}) and hydrogen atoms (·H)[31,32]. Spin adducts produced by the reaction of such active species with the amino acids and peptides were separated and detected. Various types of spin adducts were identified and characterized by ESR spectroscopy. Several pairs of diastereomeric radicals having mutually different hyperfine splitting constants (h.f.s.c.s) were separated.

EXPERIMENTAL

MNP was synthesized as described previously[33]. Immediately prior to use, aqueous MNP solutions (*ca.* 57 mM) were prepared with stirring at 45°C for 1 h in the dark. The samples, amino acids (0.06–1.0 M) and di- and tripeptides (0.1 M), were dissolved in the MNP solutions. The resulting solutions were irradiated in a ^{60}Co γ-cell at dose rates of 4.5–6 kGy/h and a total dose of 3 kGy (unless otherwise specified) at ice temperature. The sample solutions were not deaerated because dissolved MNP is easily lost.

Immediately after irradiation, the sample solutions (1–1.7 ml) were separated by HPLC–ESR, the flow diagram for which is shown in Fig. 1. The columns contained cation exchangers (IEX-210SC, 60 × 0.75 cm unless otherwise specified) from Toyo Soda Manufacturing Co., Tokyo. The high-performance liquid chromatograph was a Toyo Soda Model HLC-803. All the separations were performed in the dark. The ESR spectrometer (JEOL, Model PE-3X, X-band, 100-kHz field modulation) used as a detector was set up as illustrated in Fig. 1. An UV flow monitor (Schoeffel Flow Monitor SF-770 or JASCO UVIDEC 100) was tuned to 240 nm. A quartz flow cell (working part 5 cm × 0.6 mm I.D.) was placed in the cavity of the ESR detector and connected to the column exit with PTFE tubing (0.25 mm I.D.). The exit of the

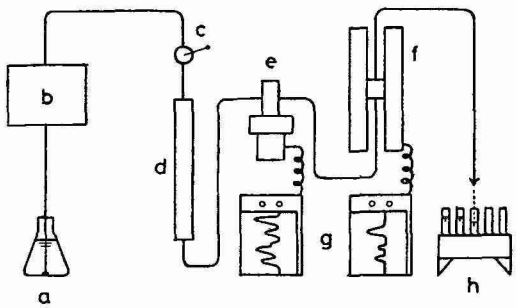

Fig. 1. Flow diagram of HPLC–ESR system. a = Eluents; b = pump; c = sample injector; d = column; e = UV detector; f = ESR detector; g = recorders; h = fraction tubes.

cell was connected to the UV monitor. In order to detect radicals passing through the ESR cavity during chromatography, the magnetic field was fixed at the position where the ESR signals were expected. For example, the fixed positions are indicated by the vertical arrows in Figs. 2, 6a, 8a–d and 12a. The amplitude of the magnetic field modulation applied was 1 mT unless specified otherwise.

The eluents used for the chromatographic separations of the spin adducts were Na_2HPO_4–NaH_2PO_4, NaOH–H_3BO_3 · NaCl and/or NaOH–Na_2HPO_4 buffers. In order to improve the retention, in some experiments, stepwise or gradient elution was applied. Other chromatographic conditions were as follows: pressure, 10–100 kg/cm^2; flow-rate, 0.1–0.3 ml/min; temperature, *ca.* 25°C.

The spin adducts isolated in the chromatographic fractions were identified by conventional ESR measurements carried out at *ca.* 25°C in the dark. Before the measurements, a gentle stream of nitrogen was passed through some of the fractions for *ca.* 1 min to remove dissolved oxygen which broadens the ESR spectral lines. The h.f.s.c.s were measured by using Mn^{2+} in MgO as a reference. To obtain accurate h.f.s.c.s, simulation of the ESR spectra was carried out by using a JEOL JEC-980A microcomputer. The line shapes adopted for the simulation were Lorentzian. The UV-VIS absorption spectra were recorded with a Cary 17 spectrophotometer (Varian, Palo Alto, CA, U.S.A.). Ninhydrin-positive fractions were analyzed by an amino acid analyzer (KLA-3B; Hitachi, Japan).

RESULTS AND DISCUSSION

Preparation of aqueous MNP solutions[34,35]

MNP is not very stable in aqueous solution. In the present investigation, the aqueous MNP solutions should not contain contaminants which may prevent adequate spin trapping, form free radicals and produce spin adducts interfering with accurate ESR analysis. Therefore, detailed studies were made of the aqueous MNP solutions.

MNP is known to exist as a dimer in the solid state and to participate in a monomer–dimer equilibrium in solution[33]:

$$\underset{\text{(monomer)}}{2\ \textit{tert.}\text{-Bu–N=O}} \rightleftarrows \underset{\text{(dimer)}}{\textit{tert.}\text{-Bu–N}^{+}(\text{O}^{-})=\text{N}^{+}(\text{O}^{-})\text{–}\textit{tert.}\text{-Bu}} \qquad (2)$$

The forward and backward reactions in aqueous solutions are slow compared to those in other solvents. For example, it takes 12 h at 30°C in aqueous solution to obtain the maximum concentration of the monomer. Since short-lived free radicals can be spin-trapped only by the monomer a sufficient concentration of the monomer is required. The concentrations of monomer and dimer in aqueous solution are determined by observing the absorbance at 662 nm (molar extinction coefficient, $\varepsilon \approx 20$ l mol^{-1} cm^{-1})[36] and 287 nm ($\varepsilon \approx 8000$ l mol^{-1} cm^{-1})[36].

Upon incubating aqueous MNP solutions at 45°C, an absorption band other than those due to the two forms of MNP was observed at 224 nm and grew with time. The relevant compound could be separated by HPLC on the cation exchanger and identified as *tert.*-butylnitrosohydroxylamine which is produced by heterolytic cleavage of the MNP dimer:

$$\textit{tert.}\text{-Bu–N}^{+}(\text{O}^{-})=\text{N}^{+}(\text{O}^{-})\text{–Bu-}\textit{tert.} \rightarrow \textit{tert.}\text{-Bu–N}^{+}(\text{O}^{-})=\text{N–O}^{-} + \underset{\text{CH}_3\text{–C}^{+}(\text{CH}_3)_2}{}$$

$$\xrightarrow{\text{H}_2\text{O}} \textit{tert.}\text{-Bu–N(OH)–N=O} + \textit{tert.}\text{-BuOH} + \text{CH}_2=\text{C(CH}_3)_2 \qquad (3)$$

The concomitant formation of *tert.*-butyl alcohol and isobutene was also confirmed by gas chromatography and NMR spectroscopy.

Since γ-radiolysis of the sample solutions in the presence of these undesirable contaminants leads to complex ESR spectra which are extremely difficult to analyze, the aqueous MNP solutions were prepared by stirring an aqueous suspension of the dimer for less than 2 h at 45°C and used immediately afterwards.

Separation of spin adducts from MNP[37,38]

In order to develop the method of HPLC separation and ESR analysis for spin adducts from biologically important molecules, the fundamental separation conditions had to be determined. When aqueous solutions, for instance, of amino acids were γ-irradiated in the presence of MNP, spin adducts were formed from the spin trap as well as from the solutes. As a preliminary, therefore, the separation of the spin adducts generated from MNP by γ-radiolysis was performed using an IEX-210SC column (60 × 0.4 cm).

When an aqueous MNP solution prepared by stirring for more than 2 h was irradiated, the ESR spectrum shown in Fig. 2 was produced. Upon loading the same sample on the column and using borax–sodium hydroxide buffer (*ca.* 60 m*M*, pH 11.5) as an eluent, five peaks (A–E) due to the MNP spin adducts appeared in the chromatogram as shown in Fig. 3. The production of negative or positive peaks was dependent both on the constant magnetic field and on the ESR signals detected in the derivative mode. Peak A, eluted near the void volume, produced an ESR spectrum comprised of 3 × 3 lines due to the aminoxyl nitrogen and two equivalent β-hydrogens. The h.f.s.c.s obtained are listed in Table I. When the pH of the solution was varied from 11.5 to 4.5, a reversible spectral change was observed. At pH 6.0, the spectrum observed corresponded to a superimposition of those at pH 11.5 and 4.5, with equal intensities. Consequently the pK_a value of the adduct could be determined to be 6.0, which corresponds to the value of *tert.*-butylnitrosohydroxylamine[34,35]. The first peak was also found to increase as a function of the time required to prepare

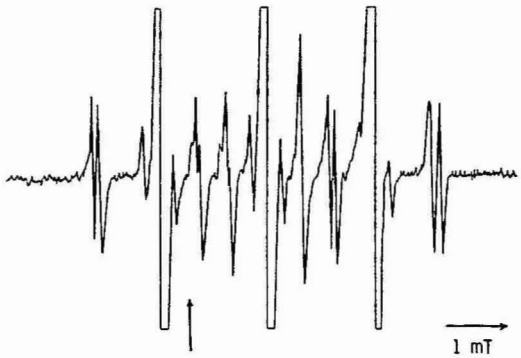

Fig. 2. ESR spectrum of a γ-irradiated aqueous MNP solution adjusted to pH 12.0 after irradiation. During chromatography, the magnetic field of the ESR detector was fixed at the position indicated by the vertical arrow.

the aqueous MNP solutions. The spectrum was assigned to the adduct from *tert.*-butylnitrosohydroxylamine:

$$tert.\text{-Bu–N(O}^{\bullet}\text{)–CH}_2\text{–C(CH}_3)_2\text{–N(OH)–N=O (at pH 4.5)} \qquad \text{I}$$

Since spin adduct I has a retention time similar to those of the adducts from the substrates studied, the proposed procedure for preparing aqueous MNP solutions is useful in reducing the generation of adduct I, which interferes with the analysis of the ESR spectra obtained. The other four spin adducts from MNP were eluted slowly, whereas the spin adducts from the amino acids and peptides investigated were eluted much more rapidly, without separation. In this work, therefore, eluents weaker than the buffer used for the MNP adducts were utilized for the separation of adducts from the amino acids and peptides. This led to significantly increased elution volumes of the MNP adducts.

Peak B gave rise to 3 × 4 lines in the ESR spectrum, due to the aminoxyl nitrogen and three equivalent β-hydrogens. The h.f.s.c.s are shown in Table I. This spectrum was assigned to the spin adduct of the methyl radical, *tert.*-Bu–N(O•)–CH_3 (II). The parent radical was produced by the C–C bond scission in MNP upon γ-radiolysis.

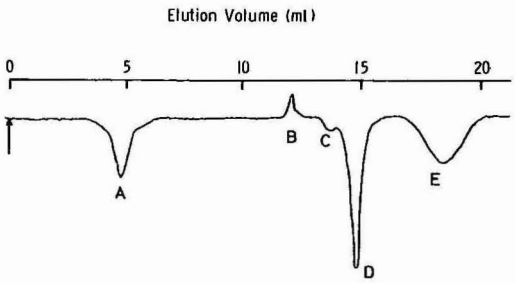

Fig. 3. Chromatogram of a γ-irradiated aqueous MNP solution. The ordinate is relative signal intensity obtained by ESR detection. The eluent was a borax–sodium hydroxide buffer (*ca.* 60 m*M*, pH 11.5).

TABLE I

H.F.S.C.S OF THE SPIN ADDUCTS FROM MNP

Spin adduct	*pH*	*h.f.s.c. (mT)*	
		a_N	$a_{\beta H}$
I	11.5	1.62	1.01 (2H)
	4.5	1.62	1.14 (2H)
II	11.5	1.73	1.42 (3H)
III	11.5	1.66	1.11 (2H)
Unidentified	11.5	1.68	
IV	11.5	1.72	

Peak C gave an ESR spectrum consisting of 3 × 3 lines attributed to the aminoxyl nitrogen and two equivalent β-hydrogens. The h.f.s.c.s obtained are shown in Table I and were found to be pH-independent. The structure tentatively assigned to the adduct is:

tert.-Bu–N(O·)–$CH_2C(CH_3)_2N=O$ (monomeric)

or III

tert.-Bu–N(O·)–$CH_2C(CH_3)_2N^+(O^-)=N^+(O^-)$–*tert.*-Bu (dimeric)

The ESR spectra of peaks D and E were simple triplets having different N-h.f.s.c.s. The value for peak D was 1.68 mT and that for E was 1.72 mT. The spin adduct of peak E was identified as di-*tert.*-butylnitroxide (DTBN), *tert.*-Bu–N(O·)–Bu-*tert.* (IV). The 1.68-mT triplet has not been identified, although the height of peak D was found to correspond to the concentration of the MNP dimer in the solution before irradiation.

Post radiolysis growth of ESR spectra[35]

It has been previously reported that the ESR signals of the spin adducts produced in aqueous thymine solutions light-irradiated in the presence of MNP was increased in intensity during storage[21,27]. A similar behaviour has been found for some aminoxyl radicals[39–41]. In the present work, the increase in the signal due to DTBN produced upon γ-irradiation of aqueous MNP solutions (initial pH 4–5) with increasing pH was observed. Spectrophotometric evidence was found for the formation of nitrous acid and it was shown that some of the spin adducts produced in the solution formed diamagnetic species and were then converted gradually into their paramagnetic form by hydrolysis. The mechanism proposed is as follows: monomeric MNP is cleaved into free radicals, ·NO and *tert.*-Bu·, upon irradiation:

$$tert.\text{-Bu–N=O} \rightarrow {}^{\cdot}NO + tert.\text{-Bu}^{\cdot} \quad (4)$$

Nitrous acid is produced from ·NO

$$^{\cdot}NO + 1/2\,O_2 \rightarrow NO_2 \quad (5)$$

$$^{\cdot}NO + NO_2 + H_2O \rightleftarrows 2\,HNO_2 \quad (6)$$

and then partially oxidized to nitric acid

$$HNO_2 \rightarrow HNO_3 \tag{7}$$

resulting in a lowering of the pH. The produced *tert.*-butyl radical is spin-trapped by MNP:

$$tert.\text{-}Bu^{\cdot} + tert.\text{-}Bu\text{–}N{=}O \rightarrow tert.\text{-}Bu\text{–}N(O^{\cdot})\text{–}tert.\text{-}Bu \tag{8}$$

Spin adducts as well as DTBN form diamagnetic intermediates (Y^{n+}) at low pH through the reaction with nitrous acid

$$\text{Spin adduct} + HNO_2 + X \xrightarrow{H^+} Y^{n+} \tag{9}$$

where X is a diamagnetic compound which could not be identified in this work. By raising the pH, the intermediates (Y^{n+}) are decomposed releasing the original spin adducts[42]:

$$Y^{n+} \xrightarrow{OH^-} \text{Spin adduct} + \cdot NO + NO_2 + X \tag{10}$$

As explained above, the increase in the signal intensity during storage is not due to the generation of new radicals but due to the release of the adducts.

Columns for separation of spin adducts from amino acids and peptides

Although aminoxyl radicals are relatively stable in solution, they are still readily decomposed on the columns. In this work, therefore, column selection was made carefully so that all the spin adducts produced from the amino acids and peptides could be detected.

Silica-based columns are used most extensively for the purification and identification of biological samples. In the separation of the spin adducts, however, such columns were found to inactivate the radicals. Only polymer-based ion-exchange columns yielded acceptable results. The eluents used for the ion exchangers were unique. Usually, with a cation exchanger, slightly acidic solutions are employed to keep the samples cationic. On the contrary, we found that neutral or basic buffers yielded better separations of the spin adducts from the amino acids and peptides studied. Also, many of the radicals were better isolated on cation exchangers than on anion-exchange columns. Consequently, the separation of the adducts was exclusively carried out by use of a cation-exchange column, IEX-210SC (Toyo Soda), containing sulphonated styrene–divinylbenzene copolymer. First, it was determined whether radicals were generated during the chromatography. Aqueous solutions containing amino acids and MNP without γ-irradiation were loaded on the column and no ESR signals were detected from the eluates. In another experiment, samples were injected which had been prepared by adding aqueous MNP solutions to γ-irradiated solutions containing only amino acids. No spin adducts were detected in the eluates. Consequently IEX-210SC columns were employed throughout this work.

Separation of spin adducts from amino acids

Free radicals generated from twelve amino acids by γ-irradiation of their aqueous solutions were investigated by spin-trap HPLC–ESR. In a preliminary experiment using the IEX-210SC column (60 × 0.75 cm unless specified otherwise), it was found that negatively charged spin adducts were eluted much more rapidly than neutral, positively charged or zwitterionic spin adducts in neutral or basic eluents. Most spin adducts produced by the self-trapping of MNP[37,38] were adsorbed on the column and were eluted very slowly with diffusion. The ESR signal intensities of these broad chromatographic peaks were so small that they were not always observable.

Glycine[43]. An aqueous solution of glycine (1.0 *M*) containing MNP was loaded on the column immediately after irradiation and subsequent addition of 2 *M* sodium phosphate buffer. A 0.2 *M* sodium phosphate buffer, pH 7.0, was used as an eluent. In the chromatogram obtained by ESR detection, three peaks appeared. Since it is well known that irradiation of water results in generation of highly reactive primary species, mainly hydrated electrons (e_{aq}^-), hydroxyl radicals ($^{\bullet}OH$) and hydrogen atoms ($^{\bullet}H$)[31,32], the reactions involving these species were considered to be responsible for the formation of the spin adducts giving rise to the peaks.

The first peak appeared close to the void volume and the fraction corresponding to it yielded an ESR spectrum comprised of a triplet arising from the aminoxyl nitrogen each line of which was further split into a 1:2:1 triplet. Since the latter triplet is due to two equivalent hydrogens, the spin adduct was identified as

tert.-Bu–N($O^{\bullet}$)–CH_2–COO^- V

which was produced by the deamination reaction caused by the attack of e_{aq}^- and subsequent spin trapping. The reaction of e_{aq}^- with amino acids leads to reductive deamination[44,45]:

$$NH_3^+–CH(R)–COO^- + e_{aq}^- \rightarrow$$
$$NH_3^+–CH(R)–{}^{\bullet}C(O^-)–O^- \rightarrow NH_3 + {}^{\bullet}CH(R)COO^- \quad (11)$$

This assignment is supported by the rapid elution of the peaks. The h.f.s.c.s obtained are listed in Table II. In neutral and alkaline solutions, the spectral pattern of adduct V was pH-independent, which implies the absence of an amino group. However, in the pH range *ca.* 2–4, reversible pH-dependent shifts of the signals were observed, and could be attributed to the acid dissociation of the carboxyl group whose pK_a value is *ca.* 3.

The second peak exhibited an ESR spectrum interpreted as a triplet further split into five lines with the intensity ratio of 1:1:2:1:1 upon raising the pH to 11.1 at which the adduct was relatively stable. The 1:1:2:1:1 splitting pattern was due to a β-hydrogen and a β-nitrogen. The h.f.s.c.s obtained by the computer simulation are shown in Table II. The spin adduct was assigned to structure VI:

tert.-Bu–N($O^{\bullet}$)–$CH(NH_2)COO^-$ VI

This adduct is derived from a short-lived radical produced by hydrogen abstraction

TABLE II

H.F.S.C.S OF THE SPIN ADDUCTS FROM GLYCINE, L-ALANINE, AND L-VALINE

Spin adduct	*pH*	*h.f.s.c. (mT)*			
		a_N	$a_{\beta H}$	$a_{\beta N}$	$a_{\gamma H}$
Glycine					
V	7.0	1.61	0.845 (2H)		
	1.4	1.58	0.86 (2H)		
VI	11.1	1.59	0.33	0.15	
L-*Alanine*					
VII	7.0	1.61	0.53		0.042 (3H)
	1.3	1.59	0.27		0.035 (3H)
VIII	7.0	1.64	1.67		0.045
			1.09		
	7.0 (80°C)	1.65	1.54		
			1.13		
	10.5	1.66	1.41		0.065
			1.09		
	1.7	1.63	1.63		0.05
			1.37		
L-*Valine*					
IX	6.5	1.57	0.38		0.03
X	6.5	1.64			
XIa	6.5	1.68	1.45		0.07
			1.05		
	11.0	1.69	1.67		0.06
			0.64		
	2.2	1.66	1.24 (2H)		0.06
XIb	6.5	1.64	1.30		0.07
			0.90		
	11.0	1.68	1.34		0.07
			0.92		
	2.2	1.65	1.28		0.07
			0.96		

from the α-carbon of glycine, by ·OH mainly. The reaction of ·OH with amino acids results in hydrogen abstraction from the saturated carbons[31,46–48]:

$$\begin{array}{c} | \\ -C-H \\ | \end{array} + \cdot OH \rightarrow \begin{array}{c} | \\ -C\cdot \\ | \end{array} + H_2O \qquad (12)$$

Unreacted glycine, detected by using an amino acid analyzer, was eluted near the third peak, for which no substantial ESR signal was observed.

L-Alanine[43]. Separation of the spin adducts produced by irradiation of an aqueous solution of L-alanine (1.0 *M*) containing MNP was performed by use of the same buffer as that used for glycine; two spin adducts originating from L-alanine could be isolated and assigned to structures VII and VIII:

tert.-Bu–N(O·)–$CH(CH_3)COO^-$ VII

tert.-Bu–N(O·)–CH_2–*$CH(NH_3^+)COO^-$ VIII

In structure VIII, the asterisk indicates an asymmetric carbon atom. The h.f.s.c.s obtained are listed in Table II.

Spin adduct VII produced through the reductive deamination of L-alanine by e_{aq}^- showed a reversible pH-dependent shift of the ESR signals. In Fig. 4, the h.f.s.c. for the β-hydrogen atom is plotted against the pH of the solution. Since the interchange between the acid form (A) and the base form (B) of the adduct is rapid, the h.f.s.c. observed in the intermediate pH region is the weighted average of the values for the two forms[49]. By taking the values, a_A and a_B, for each form (see Table II) and using eqn. 13

$$a_{\beta H} = \frac{a_A + a_B \times 10^{pH - pK_a}}{1 + 10^{pH - pK_a}} \tag{13}$$

the variation of $a_{\beta H}$ with pH can be calculated. The pK_a value of adduct VII was determined to be 3.2 by fitting eqn. 13 to the experimental points.

The ESR spectrum of spin adduct VIII consisted of six narrow and six broad lines as depicted in Fig. 5. The intensities of the two types of lines were similar. This ESR pattern is typical of an aminoxyl radical which has an α-methylene group and an asymmetric β-carbon atom, that is, *tert.*-Bu–N(O·)–CH_2–*CXYZ. The characteristic non-equivalence of the two β-hydrogens with linewidth alternation (LWA) has been interpreted by assuming, for example, insufficiently rapid interconversion between the two minimum energy rotamers having mutually different sets of β-H h.f.s.c.s[50]. For spin adduct VIII, a pH titration was carried out to obtain the $pK_{NH_3^+}$ value. The ESR signals arising from the zwitterion form and the anion form overlapped with equal intensities when the interchange between them was slow, yielding a $pK_{NH_3^+}$ value of 8.9.

L-*Valine*[51,52]. A complicated ESR spectrum (Fig. 6a) was obtained upon γ-irradiation of an aqueous 0.07 *M* L-valine solution containing MNP. The overlapping

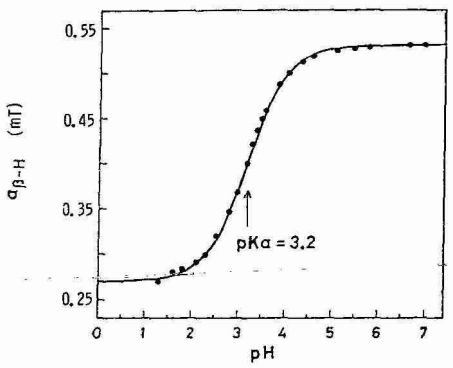

Fig. 4. The effect of pH on the β-H h.f.s.c. for spin adduct VII from L-alanine. Circles indicate experimental results. The best fit solid curve was calculated by use of eqn. 13.

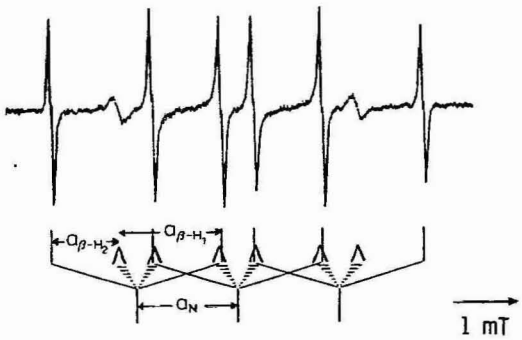

Fig. 5. ESR spectrum and stick diagram of spin adduct VIII from L-alanine (pH 7.0, *ca.* 25°C).

of ESR signals is due to the presence of several spin adducts. By use of a sodium phosphate buffer (150 m*M*, pH 6.5), the ESR and UV chromatograms shown in Fig. 6b were obtained. There are five peaks (A–E) in the ESR chromatogram. Peaks A, C, D and E exhibited ESR spectra shown in Fig. 7 a–d, respectively. The corresponding h.f.s.c.s are listed in Table II. No analyzable ESR spectrum could be obtained for peak B.

Peak A appeared near the void volume and produced an ESR spectrum consisting of 3 × 2 lines (Fig. 7a). The spin adduct was assigned to the structure IX

tert.-Bu–N(O·)–CH(COO^-)$CH(CH_3)_2$ IX

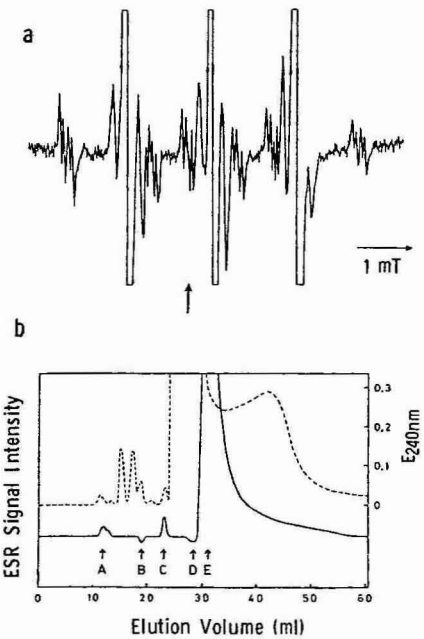

Fig. 6. (a) ESR spectrum of an aqueous solution of L-valine (0.07 *M*) containing MNP immediately after γ-irradiation. During chromatography, the magnetic field was fixed at the position indicated by the vertical arrow. (b) Chromatogram of the solution obtained by UV (broken line) and ESR (solid line) detection. Flow-rate, 0.2 ml/min. Eluent: 0.15 *M* sodium phosphate buffer, pH 6.5.

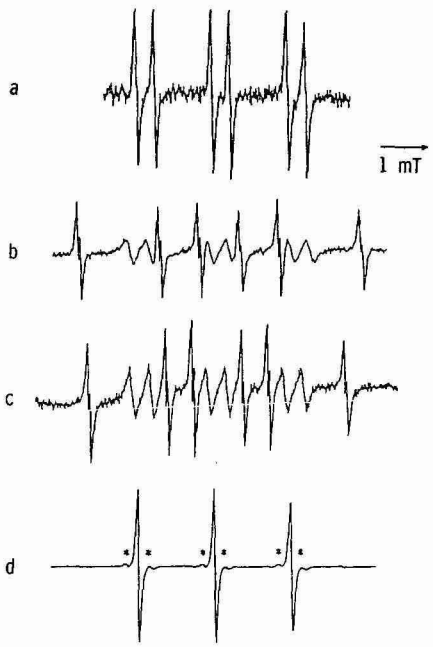

Fig. 7. ESR spectra obtained at pH 6.5 from the fractions giving peaks A (a), C (b), D (c) and E (d) in Fig. 6b. In d the satellite signals (indicated with asterisks) are due to secondary splittings (0.50 mT) caused by an α-^{13}C nucleus.

the parent radical of which was derived through the deamination by e_{aq}^-.

Peak E produced a simple triplet (Fig. 7d) whose h.f.s.c. due to the aminoxyl nitrogen (1.64 mT) is different from those for the adducts obtained by the self-trapping of MNP (1.68 and 1.72 mT). This triplet was identified as due to the adduct produced by hydrogen abstraction by ·OH:

$$\textit{tert.}\text{-Bu–N(O·)–C(CH}_3\text{)}_2\text{CH(NH}_3^+\text{)COO}^- \qquad \text{X}$$

The six ESR signals labelled with asterisks in Fig. 7d are satellites (splitting 0.50 mT) due to the presence of an α-^{13}C nucleus.

The spectra obtained from peaks C and D produced splitting patterns similar to that of spin adduct VIII from L-alanine. These patterns are characteristic of aminoxyl radicals, *tert.*-Bu–N(O·)–CH_2–C*XYZ[50]. Consequently both peaks C and D were assigned to structure XI

$$\textit{tert.}\text{-Bu–N(O·)–CH}_2\text{–C*H(CH}_3\text{)C*H(NH}_3^+\text{)COO}^- \qquad \text{XI}$$

i.e., these adducts are a pair of diastereomeric radicals, (*S,S*) and (*R,S*) forms. Isomers XIa and XIb refer to the adducts contained in peaks C and D, respectively. We could not make each isomer XIa and XIb correspond to their individual absolute configuration, the (*S,S*) and (*R,S*) forms. The scheme by which these isomers were formed is represented by:

$$(CH_3)_2CH\text{–}C^*H(NH_3^+)COO^- \xrightarrow{\cdot OH} \cdot CH_2C^*H(CH_3)\text{–}C^*H(NH_3^+)COO^-$$

$$\xrightarrow{MNP} \textit{tert.}\text{-Bu–N(O}\cdot\text{)–}CH_2C^*H(CH_3)\text{–}C^*H(NH_3^+)COO^- \quad (14)$$

(*S*,*S*) and (*R*,*S*) forms

where the diastereoisomerism results from the primary asymmetric centre of L-valine and the new asymmetric centre introduced by hydrogen abstraction from a methyl group in L-valine by ·OH.

The pH-dependent spectral changes for the isomers were observed. Isomer XIa showed a β-H LWA pattern in the form of a triplet at acidic pH, and as a quartet in basic and neutral solutions. The triplet whose central line was broadened indicates that the two β-hydrogens are still non-equivalent. On the other hand, the β-H of isomer XIb produced a four-line LWA pattern at any pH. All the h.f.s.c.s obtained are summarized in Table II. The pK_a values of the isomers could be obtained by changing the pH and simultaneously observing the spectral changes. The p$K_{NH_3^+}$ values were 8.9 and 8.4 for isomers XIa and XIb, respectively.

TABLE III

H.F.S.C.S OF THE SPIN ADDUCTS FROM L-ISOLEUCINE AND L-LEUCINE

Spin adducts	*pH*	*h.f.s.c. (mT)*			
		a_N	$a_{\beta H}$	$a_{\beta N}$	$a_{\gamma H}$
L-*Isoleucine*					
XII	6.0	1.57	0.36		
XIII	6.5	1.64		0.08	
	12.0	1.71			
XIV	6.5	1.62	0.21		
	12.0	1.66	0.31		
XV	7.0	1.69	1.19		0.07 (2H)
			0.98		
XVI	11.5	1.67	1.37		
			0.96		
	7.0	1.60	1.14 (2H)		
XVIIa	6.0	1.59			
XVIIb	6.0	1.61			
L-*Leucine*					
XVIII	6.0	1.58	0.38		0.04 (2H)
VIII	6.5	1.64	2.76* (2H)		
XIX	6.5	1.52			
XX	6.5	1.54			
XXI	10.0	1.69			
XXII	6.5	1.69	1.31		
			1.06		
	11.4	1.69	1.35		
			0.98		

* $a_{H(1)} + a_{H(2)} = 2.76$ mT.

L-*Isoleucine*[53]. The radiolytic decomposition of L-isoleucine in the presence of MNP resulted in a number of spin adducts. The previously mentioned methods of elution did not resolve the peaks in the presence of the excess of unreacted L-isoleucine and the final decomposition products. Therefore, gradient elution was applied. Since the retention volumes of the adducts were found to be highly dependent on the pH of the eluent, the separation could not be achieved by stepwise elution. A linear gradient (90 min) from 0.15 *M* sodium phosphate buffer (pH 6.0) to 0.2 *M* borax–sodium hydroxide buffer (pH 10.0) was applied. Also, isocratic elution with 0.15 *M* phosphate buffer was used in order to isolate the adducts unstable in alkaline solution. Seven different spin adducts could thus be isolated; the corresponding h.f.s.c.s are listed in Table III.

From the fractions obtained by gradient elution, five bands could be detected and 0.3 ml of each fraction was used for further analyses. As expected, from the first peak, the deamino adduct

$$\textit{tert.}\text{-Bu–N(O}^{\bullet}\text{)–CH(COO}^{-}\text{)CH(CH}_3\text{)C}_2\text{H}_5 \qquad \text{XII}$$

was obtained. This adduct was eluted much more rapidly than the other four.

An ESR spectrum obtained for the second peak consisted of a triplet further split into a triplet with lines of equal intensity. The secondary splitting is attributed to the amino nitrogen, and the adduct was assigned to:

$$\textit{tert.}\text{-Bu–N(O}^{\bullet}\text{)–C(NH}_3^{+}\text{)(COO}^{-}\text{)CH(CH}_3\text{)C}_2\text{H}_5 \qquad \text{XIII}$$

The amino β-N h.f.s.c. is fairly small compared to values corresponding to the amido nitrogens in the adducts from dipeptides (see Table VI). This type of spin adduct was not observed for the smaller amino acids such as L-alanine and L-valine, which may suggest that the lifetime of aminoxyl radicals from amino acids except glycine is dependent on the size of the adduct.

The spectrum obtained for the third fraction was assigned to the structure:

$$\textit{tert.}\text{-Bu–N(O}^{\bullet}\text{)–CH(CH}_3\text{)CH(CH}_3\text{)CH(NH}_3^{+}\text{)COO}^{-} \qquad \text{XIV}$$

The fourth fraction contained the spin adduct:

$$\textit{tert.}\text{-Bu–N(O}^{\bullet}\text{)–CH}_2\text{CH}_2\text{*CH(CH}_3\text{)CH(NH}_3^{+}\text{)COO}^{-} \qquad \text{XV}$$

The ESR spectrum of this adduct comprised a triplet with a secondary splitting into a 1:1:1:1 quartet which was further split into a 1:2:1 triplet. Although in this spin adduct there are two methylene groups between the aminoxyl nitrogen and the asymmetric carbon atom, a four-line splitting pattern due to the two non-equivalent β-hydrogens was observed. By varying the pH of the fractions, it was found that the h.f.s.c.s of adduct XIV, in which there are two carbons between the amino group and the α-carbon, are highly pH-dependent in neutral and basic solutions, while the values for adduct XV, where the α-carbon is three carbons away from the amino group, were almost unchanged. This may indicate the limit of the effect of structural changes in the amino group on the h.f.s.c.s.

The fifth peak gave an ESR spectrum comprised of three sets of four lines when the pH was 11.5, and was assigned to the structure:

tert.-Bu–N(O·)–$CH_2CH(C_2H_5)CH(NH_2)COO^-$ XVI

The four lines, however, were converted into an extremely broad triplet with an intensity ratio of 1:2:1 in neutral solution. This broadening is considered to be unique because it is introduced by the change in the pH.

By the isocratic elution, two simple triplets with the N-h.f.s.c.s different from those of the similar triplets from MNP were obtained. These adducts were characterized as a pair of diastereomers:

tert.-Bu–N(O·)–$*C(CH_3)(C_2H_5)*CH(NH_3^+)COO^-$ XVIIa and XVIIb

These adducts were highly unstable at alkaline pH.

L-*Leucine*[53]. Gradient elution analogous to that used for L-isoleucine was applied and seven different spin adducts were isolated and identified by ESR spectroscopy. All the h.f.s.c.s obtained are summarized in Table III.

The spectrum of the first fraction eluted near the void volume was assigned to the adduct formed via deamination by e_{aq}^-:

tert.-Bu–N(O·)–$CH(COO^-)CH_2CH(CH_3)_2$ XVIII

The second fraction contained the same spin adduct as that (structure VIII) generated from L-alanine. This implies the occurrence of C–C bond scission.

The spectra observed for the third, fourth and sixth fractions each comprised broad triplets, and were tentatively assigned to spin adducts XIX, XX and XXI, respectively:

tert.-Bu–N(O·)–$C(NH_3^+)(COO^-)CH_2CH(CH_3)_2$ XIX

tert.-Bu–N(O·)–$CH[CH(NH_3^+)COO^-]CH(CH_3)_2$ XX

tert.-Bu–N(O·)–$C(CH_3)_2CH_2CH(NH_2)COO^-$ XXI

The seventh fraction produced an ESR spectrum with secondary splitting to a quartet with LWA due to the two non-equivalent β-hydrogens[50]. Consequently the spectrum was assigned to the adduct:

tert.-Bu–N(O·)–$CH_2*CH(CH_3)CH_2*CH(NH_3^+)COO^-$ XXII

The adduct contained in the fifth fraction showed a similar four-line pattern. Both of the adducts in the fifth and seventh peaks showed significant spectral changes upon varying the pH. The adduct in the fifth peak was assigned as a diastereomer of the adduct in the seventh fraction.

DL-Methionine[54,55]. Spin adducts formed upon irradiation of aqueous DL-methionine solution containing MNP were found to be inactivated during the separation with a long column. Therefore, a short cation-exchange column (10 cm × 4 mm I.D., IEX-210SC) was used with 63 m*M* borax–sodium hydroxide buffer (pH 11.5) as eluent. All the h.f.s.c.s obtained from the individual spectra are listed in Table IV.

TABLE IV

H.F.S.C.S OF THE SPIN ADDUCTS FROM DL-METHIONINE, L-GLUTAMINE, L-ASPARAGINE, SODIUM L-GLUTAMATE, SODIUM L-ASPARTATE, L-SERINE, AND L-THREONINE

Spin adduct	*pH*	*h.f.s.c. (mT)*					
		a_N	$a_{\beta H}$	$a_{\beta N}$	$a_{\gamma H}$	$a_{\gamma N}$	$a_{\delta H}$
DL-*Methionine*							
XXIII	11.5	1.56	0.47		0.08 (2H)		
II	11.5	1.73	1.42 (3H)				
XXIV	11.5	1.68	1.12 (2H)		0.10 (2H)		
L-*Glutamine*							
XXV	6.8	1.56	0.47		0.055 (2H)		
XXVI	6.8	1.60		0.10	0.14		
					0.10		
					0.05 (3H, amino)		
	11.0	1.61		0.10	0.135		
					0.10		
XXVII	6.8	1.53	0.40		0.06 (2H)	0.06	0.06 (amide)
	11.0	1.55	0.34		0.07 (2H)	0.07	0.07 (amide)
L-*Asparagine*							
XXVIIIa	1.3	1.51	0.53				
	6.8	1.51	0.41		0.11		
	11.0	1.52	0.33			0.075 (amino or amide)	
							0.075 (amide)
XXVIIIb	6.8	1.51	0.36				
Sodium L-*glutamate*							
XXIX	6.8	1.56	0.45		0.055 (2H)		
XXX	1.6	1.53	0.28				
	6.8	1.57	0.48		0.055 (2H)		
	12.0	1.55	0.44		0.06 (2H)		
Sodium L-*aspartate*							
XXXI	6.8	1.57	0.58		0.06 (2H)		
XXXIIa	1.6	1.50	0.34				
	6.8	1.53	0.39				
	11.0	1.54	0.49				
XXXIIb	1.6	1.52	0.25		0.07		
	6.8	1.57	0.32		0.07		
	11.0	1.56	0.44		0.06		
L-*Serine*							
XXXIII	5.4	1.50	0.17				
XXXIV	1.6	1.54	0.26		0.03 (2H)		
	6.8	1.56	0.44		0.04 (2H)		
L-*Threonine*							
XXXV	1.5	1.53	0.27				
	6.8	1.56	0.42				
XXXVI	6.8	1.63	1.51		0.08		
			0.68				
	11.0	1.65	1.57		0.08		
			0.64				

The first peak was found to contain the deamino adduct from DL-methionine:

tert.-Bu–N(O·)–$CH(COO^-)CH_2CH_2SCH_3$ XXIII

The second fraction contained two kinds of adducts. One of the ESR spectra gave three sets of four lines with an intensity ratio of 1:3:3:1 due to adduct II. The other comprised 3 × 3 × 3 lines and was assigned to the adduct:

tert.-Bu–N(O·)–$CH_2CH_2CH(NH_3^+)COO^-$ XXIV

This assignment supports the scheme proposed previously[23]:

$$e_{aq}^- + CH_3SCH_2CH_2CH(NH_3^+)COO^- \rightarrow$$
$$CH_3S^- + {\cdot}CH_2CH_2CH(NH_3^+)COO^-$$
and (15)
$${\cdot}CH_3 + {}^-SCH_2CH_2CH(NH_3^+)COO^-$$

However, spin adducts of S-centered radicals could not be observed in the present work.

L-*Glutamine*[56]. Aqueous L-glutamine solutions irradiated in the presence of MNP produced a highly complex ESR spectrum due to the overlap of the spectra of several spin adducts. For the separation of the adducts, 0.2 *M* phosphate buffer (pH 6.8) was used and five peaks appeared in the ESR chromatogram. The elution volumes of the peaks were 9.8, 14.8, 16.8, 18.0 and 20.5 ml. Analyzable spectra were obtained from the first, third and fifth fractions. The h.f.s.c.s of the three spin adducts are summarized in Table IV.

The ESR spectrum obtained for the first rapidly eluted fraction was not changed at alkaline pH, and was assigned to the deamino adduct from L-glutamine:

tert.-Bu–N(O·)–$CH(COO^-)CH_2CH_2CONH_2$ XXV

The ESR spectrum obtained from the third peak was highly complex and consisted of three sets of eleven lines with small h.f.s.c.s. In order to analyze this spectrum, ESR measurements were carried out in water and deuterium oxide. Also the second derivatives of the spectra were obtained. The eleven lines observed in water were converted into ten lines in deuterium oxide, implying that the former spectrum involved hyperfine splittings due to at least one exchangeable hydrogen in the amino group or the amide group of the spin adduct. The spectrum observed in alkaline solutions was different from that in neutral water, revealing that the aminoxyl group is relatively close to the amino group. Based on these results, the spectrum was assigned to the structure:

tert.-Bu–N(O·)–$C(NH_3^+)(COO^-)CH_2CH_2CONH_2$ XXVI

This assignment was confirmed by computer simulation of the spectra.

The fifth peak produced an ESR spectrum comprised of a triplet further split into 2 × 6 lines in water and 2 × 5 lines in deuterium oxide. Since it is reasonable

to infer that this spectral change was caused by the change in splittings arising from one of the two exchangeable amide hydrogens, the spin adduct was assigned to the following structure:

tert.-Bu–N(O·)–CH(CONH$_2$)CH$_2$CH(NH$_3^+$)COO$^-$ XXVII

The ESR parameters used for the simulation of the spectrum in deuterium oxide were the same as those for the spectrum in water except that the h.f.s.c. for the amide hydrogen was replaced by zero.

L-*Asparagine*[56]. The same eluent as that for the L-glutamine system was used for the chromatographic separation of a γ-irradiated aqueous L-asparagine solution, which produced three peaks. The elution volumes of the peaks were 11.9, 19.6 and 27.4 ml.

From the second and third peaks the diastereomeric spin adduct XXVIII could be isolated:

tert.-Bu–N(O·)–*CH(CONH$_2$)*CH(NH$_3^+$)COO$^-$ XXVIII

The secondary splittings of the spectrum of the second fraction gave a relatively broad doublet at pH 6.8 and a doublet of quartets at pH 11.0 in water, a doublet at pH 6.8 and a doublet of triplet at pH 11.0 in deuterium oxide. All the h.f.s.c.s obtained for the isomers are summarized in Table IV.

Sodium L-*glutamate*[56]. The γ-irradiated aqueous solution of sodium L-glutamate containing MNP yielded two rapidly eluted peaks (elution volumes: 10.1 and 10.6 ml) due to the existence of two carboxyl groups in the adduct. A flow-rate of 0.1 ml/min was used for the separation.

The spectrum of the first fraction comprised of 3 × 2 × 3 lines and was assigned to the deamino adduct:

tert.-Bu–N(O·)–CH(COO$^-$)CH$_2$CH$_2$COO$^-$ XXIX

From the second fraction, a triplet of doublets was obtained. By observation of the changes in h.f.s.c.s upon varying the pH (see Table IV), this spectrum was assigned to the spin adduct:

tert.-Bu–N(O·)–CH(COO$^-$)CH$_2$CH(NH$_3^+$)COO$^-$ XXX

All the h.f.s.c.s are listed in Table IV.

Sodium L-aspartate[56]. The chromatographic conditions for the separation of the adducts from sodium L-aspartate were the same as those used for sodium L-glutamate. From the first band (elution volume: 10.9 ml), the spin adduct XXXI could be isolated:

tert.-Bu–N(O·)–CH(COO$^-$)CH$_2$COO$^-$ XXXI

The spin adducts from the second and third fractions were found to be a pair of diastereomeric radicals:

tert.-Bu–N(O·)–*CH(COO$^-$)*CH(NH_3^+)COO$^-$ XXXII

The detailed assignment of both spectra was performed by changing the solvent to deuterium oxide. The h.f.s.c.s of the three adducts are summarized in Table IV.

L-*Serine*[56]. The major component of the ESR spectrum obtained immediately after radiolysis of an aqueous L-serine solution containing MNP consisted of 3 × 2 lines and was assigned to the structure:

tert.-Bu–N(O·)–CH(OH)CH(NH_3^+)COO$^-$ XXXIII

The chromatographic separation of the sample under the same conditions as those used for the L-glutamine system yielded a species exhibiting a spectrum comprised of 3* × 2 × 3 lines which was assigned to the structure:

tert.-Bu–N(O·)–CH(COO$^-$)CH_2OH XXXIV

The h.f.s.c.s obtained are shown in Table IV.

L-*Threonine*[56]. The chromatographic analysis of an irradiated aqueous solution containing L-threonine and MNP, under the same conditions as those used for the L-glutamine system, yielded two spin adducts. The spin adduct contained in the first fraction was assigned to the structure:

tert.-Bu–N(O·)–CH(COO$^-$)CH(OH)CH_3 XXXV

From the second peak, an ESR spectrum consisting of 3 × 4 lines with LWA was obtained and assigned to the adduct:

tert.-Bu–N(O·)–CH_2*CH(OH)*CH(NH_3^+)COO$^-$ XXXVI

The h.f.s.c.s of these two adducts are listed in Table IV.

Separation of spin adducts from L-*proline and its 4-substituted derivatives*[57,58]

L-*Proline and cis-4-chloro-*L-*proline.* An aqueous solution containing L-proline (Pro) and MNP, cooled in an ice-bath, was γ-irradiated with a total dose of 3 kGy. The ESR spectrum of this solution just after γ-irradiation is shown in Fig. 8a. Chromatography of the solution with ESR detection gave six peaks (A–F) as shown in Fig. 9a. The fraction corresponding to peak A gave no ESR signals. The ESR spectrum obtained from the fraction corresponding to peak D was complex, and a satisfactory identification could not be made. Fig. 10a–d shows ESR spectra obtained from the fractions corresponding to peaks B, C, E and F, respectively. Most of the spin adducts produced by self-trapping of MNP[37,38] were adsorbed on the column and eluted very slowly.

Fig. 10a shows the ESR spectrum obtained for peak B at pH 7. At pH 11.4 the spectral pattern showed little change. The h.f.s.c.s are given in Table V. Whereas the deamino adducts originating from the attack of e_{aq}^- on amino acids are excluded when chromatographed using a cation-exchange column with neutral eluents, as described above, the spin adduct found here is not excluded under these chromato-

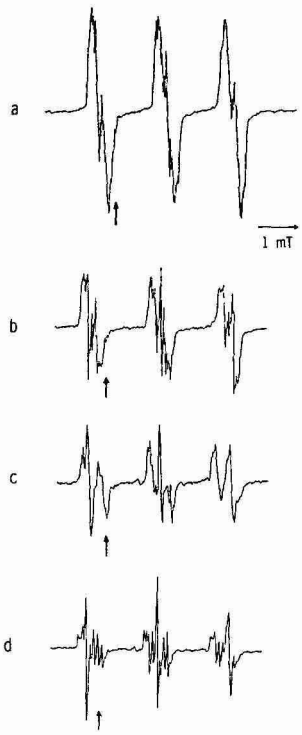

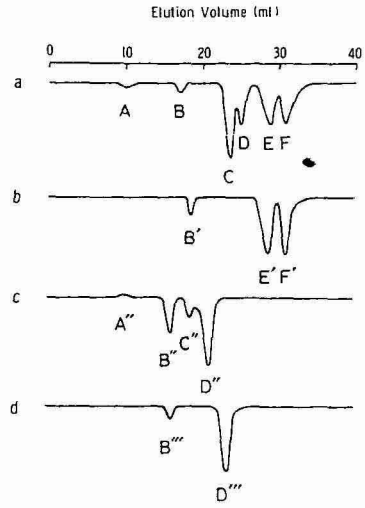

Fig. 8. ESR spectra of γ-irradiated aqueous solutions of 0.2 *M* Pro (a), 0.1 *M* Cl-Pro and 0.3 *M* sodium formate (b), 0.2 *M* *trans*-4-Hyp (c) and 0.2 *M* *cis*-4-Hyp containing 5 mg/ml MNP (d). During chromatography, the magnetic fields were fixed at the positions indicated by the vertical arrows.

Fig. 9. Chromatograms of γ-irradiated aqueous solutions containing MNP obtained by ESR detection: Pro (a); Cl-Pro with sodium formate (b); *trans*-4-Hyp (c); *cis*-4-Hyp (d). The units of the vertical axes represent relative ESR signal intensities. The chromatographic conditions were as follows: column, IEX-210SC (Toyo Soda, 60 × 0.75 cm); pressure, *ca.* 70 kg/cm^2; flow-rate, *ca.* 0.2 ml/min; temperature, *ca.* 25°C. The column was first equilibrated with 0.2 *M* sodium phosphate buffer (pH 6.8). After the sample injection, a 90-min gradient (X^4 mode, Gradient Device GE-2, Toyo Soda) was started: 0.2 *M* sodium phosphate buffer (pH 6.8) to 0.2 *M* Na_2HPO_4–NaOH buffer (pH 11.5).

graphic conditions, which suggests that the adduct is not negatively charged. Consequently, the spin adduct was assigned as the cleavage adduct from L-proline, with the structure:

$$\textit{tert.}\text{-Bu–N(O·)–CH(COO}^-\text{)CH}_2\text{CH}_2\text{CH}_2\text{NH}_3^+ \qquad \text{XXXVII}$$

Spin adduct XXXVII originates from reductive cleavage of the pyrrolidine ring induced by the addition of a hydrated electron to the carboxyl group[31,44].

Computer simulations of the ESR spectra of fraction C in water (Fig. 10b) and deuterium oxide were conducted. The parameters estimated are shown in Table V. On the basis that the adduct has observable h.f.s.c.s for a β-hydrogen and a β-nitrogen atom, it was assigned to the structure XXXVIII,

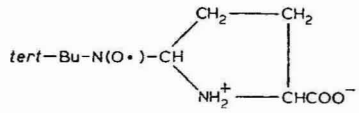

XXXVIII

which is the Pro C-5 adduct arising from hydrogen abstraction from the C-5 position by a hydroxyl radical.

Fig. 10c and d shows the ESR spectra for the fractions corresponding to peaks E and F, respectively. Computer simulations were conducted for solutions in both water and deuterium oxide, and the parameters estimated are shown in Table V.

In order to identify the spin adducts more reliably, the Pro C-4 adduct

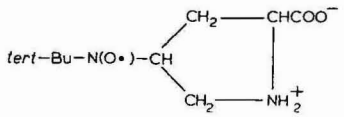

XXXIX

was produced as follows. The spin-trapping and HPLC–ESR techniques were applied to a γ-irradiated aqueous solution of *cis*-4-chloro-L-proline (Cl-Pro) contain-

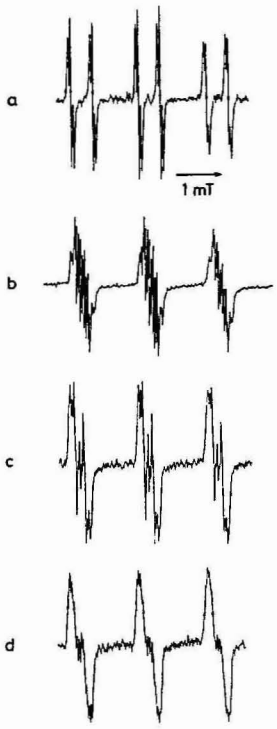

Fig. 10. ESR spectra (a–d) (pH 7, water) obtained from the fractions giving peaks B, C, E and F respectively in Fig. 9a.

TABLE V

H.F.S.C.S OF THE SPIN ADDUCTS FROM L-PROLINE AND 4-SUBSTITUTED L-PROLINE

Spin adduct	*Peak*[a]	*pH*	*h.f.s.c. (mT)*					ΔH_{pp}[b]	*Ratio*[c]
			a_N	$a_{\beta H}$	$a_{\beta N}$	$a_{\gamma H}$	$a_{\delta H}$		
XXXVII	B	7	1.56	0.50		0.05 (2H)			
		11	1.57	0.49		0.05 (2H)			
XXXVIII	C	7	1.60	0.23	0.046	0.092 (2H)			
						0.04[d]			
						(0.006)[e]		0.030	
XXXIXa[f]	E, E′	7	1.61	0.21		0.09	0.035[d]	0.031	
						0.085	(0.0055)[e]		
						0.04			
						0.03			
XXXIXb[f]	F, F′	7	1.60	0.20		0.10	0.035[d]	0.030	
						0.09	(0.0055)[e]		
						0.05	0.03		
						0.045			
XL	B′	7	1.55	0.50		0.06 (2H)			
		11	1.55	0.47		0.06 (2H)			
XLI[g]	B″	7	1.57	0.49		0.05 (2H)			
		11	1.57	0.46		0.05 (2H)			
	B‴	7	1.56	0.49		0.06 (2H)			
		11	1.57	0.45		0.06 (2H)			
XLII[h]	D″	7	1.53	0.255	0.085	0.085		0.050	
						0.03[d]			
						(0.0045)[e]			2/1[i]
			1.53	0.255	0.06	0.06		0.050	
						0.03[d]			
						(0.0045)[e]			
	D‴	7	1.56	0.255	0.085	0.085		0.035	
						0.025[d]			
						(0.004)[e]			3/1[i]
			1.56	0.255	0.10	0.10		0.035	
						0.025[d]			
						(0.004)[e]			

[a] Chromatographic peak in Fig. 9.
[b] Lorentzian peak-to-peak linewidth (mT) used for spectrum simulation.
[c] Concentration ratio for spectrum simulation: upper set/lower set.
[d] NH hydrogen convertible into ND deuterium in ^2H_2O.
[e] a_D(ND) value in ^2H_2O.
[f] XXXIXa and XXXIXb correspond to the *cis* and *trans* isomers, respectively. For further details about the isomers see the text.
[g] Each fraction giving peaks B″ and B‴ was a mixture of a pair of diastereomeric adducts. All h.f.s.c.s are the average of the values of the two diastereoisomers. Each adduct from peak B″ is the enantiomer of either adduct from peak B‴.
[h] Each fraction giving peaks D″ and D‴ was a mixture of a pair of epimeric adducts. Each adduct from peak D″ is also epimeric for either adduct from peak D‴ with respect to the C-4 position.
[i] The coexisting epimeric adducts from peaks D″ or D‴ have the same *g* values.

ing sodium formate, which reacts with $^{\cdot}OH$[59]:

$$^{\cdot}OH + HCOO^- \rightarrow H_2O + {}^{\cdot}COO^- \qquad (16)$$

Pro C-4 adducts are derived from the selective dechlorination by $\cdot COO^-$ [59]:

$$\begin{array}{c} | \\ -C-Cl \\ | \end{array} + \cdot COO^- \rightarrow \begin{array}{c} | \\ -C\cdot \\ | \end{array} + Cl^- + CO_2 \qquad (17)$$

Figs. 8b and 9b show the ESR spectrum and the chromatogram of a γ-irradiated aqueous Cl-Pro solution containing sodium formate and MNP. The ESR chromatogram gave three peaks (B′, E′ and F′) as shown in Fig. 9b. In the absence of sodium formate, peaks E′ and F′ were not observed. Typical ESR spectra for the fractions corresponding to peaks B′, E′ and F′ are depicted in Fig. 11a–c.

The spin adduct of peak B′, which produces the ESR spectrum shown in Fig. 11a, was assigned to the structure

tert.-Bu–N(O·)–*CH(COO^-)–CH_2–*CHCl–$CH_2NH_3^+$ XL

the cleavage adduct from Cl-Pro, on the basis that its hyperfine structure (h.f.s.) and elution position are very similar to those of adduct XXXVII from L-proline. It is concluded that peak B′ comprises a mixture of the diastereomers XL having very similar ESR parameters[60].

Fig. 11b and c shows the ESR spectra for the fractions corresponding to peaks

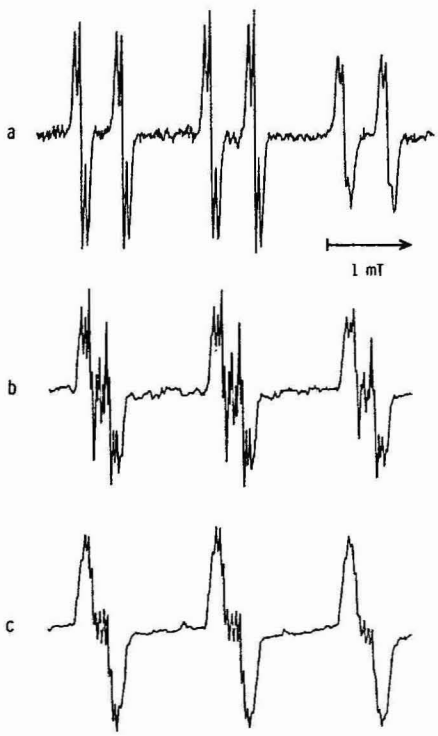

Fig. 11. ESR spectra (a–c) (pH 7, water) obtained from the fractions giving peaks B′, E′ and F′ respectively in Fig. 9b.

E′ and F′, respectively. Their retention times and spectral patterns are virtually identical with those of peaks E and F of the Pro system (Fig. 9a). Since sodium formate was essential for the observation of peaks E′ and F′, as stated above, both spin adducts were assigned the structure XXXIX, *i.e.*, a pair of the diastereomeric Pro C-4 adducts, which originate from the dechlorination of the C-4 position in Cl-Pro by $\cdot COO^-$ (eqn. 17)[59]. The two possible absolute configurations of spin adducts XXXIX are the *cis*- and *trans*-isomers

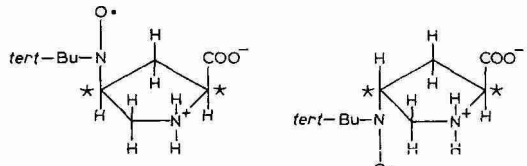

XXXIX a XXXIX b

with respect to the carboxyl and the *tert.*-butyl aminoxyl groups in the pyrrolidine rings. The absolute configurations of the isomers from peaks E and E′ and from F and F′ were examined. The so-called "W-plan" (2 V) for spin transmission through σ bonds is the most important empirical concept used for explaining the stereoselectivity of long-range h.f.s.c.s[61]. The relationship between the δ-H h.f.s.c.s given in Table V and the minimum energy conformations for the *cis*- and *trans*-isomers was considered in terms of the extended W-plan (2.5 V, *i.e.* \\\ ) arrangement. Consequently, it is suggested that the diastereomer from peaks E and E′ corresponds to configuration XXXIXa (*cis*) and that from F and F′ to XXXIXb (*trans*).

*trans- and cis-4-Hydroxy-*L*-proline.* Figs. 8c and 9c show the ESR spectrum and the chromatogram of a γ-irradiated aqueous solution of *trans*-4-hydroxy-L-proline (*trans*-4-Hyp) containing MNP. The ESR chromatogram contained four peaks (A″–D″) as shown in Fig. 9c. The fraction corresponding to peak A″ did not give any signals, and peak C″ did not contain a sufficient amount of the spin adduct for analysis.

Figs. 8d and 9d show the ESR spectrum and the chromatogram of the *cis*-4-hydroxy-L-proline (*cis*-4-Hyp) system. The chromatogram exhibited two peaks (B‴ and D‴) as shown in Fig. 9d.

The retention time and ESR spectrum of peak B″ are virtually identical with those of peak B‴. These peaks were thus assigned to the cleavage adduct from *trans*- and *cis*-4-Hyp, respectively:

tert.-Bu–N(O·)–*CH(COO$^-$)–CH_2–*CH(OH)–$CH_2NH_3^+$ XLI

The partial distortion found in the ESR spectrum of peak B″ suggests the coexistence of a pair of diastereomeric adducts, *R,R* and *S,R* forms, whose enantiomers (*S,S* and *R,S* forms, respectively) were obtained from peak B‴. The average h.f.s.c.s at pH 7 and 11 are summarized in Table V.

The ESR spectrum corresponding to peak D″ resembles that for peak D‴. Computer simulations of the spectra were conducted by assuming that each of the fractions is a mixture of two kinds of radicals having slightly different ESR parameters. The ESR parameters estimated from the simulations are summarized in Table V. All of these four spin adducts were assigned the structure:

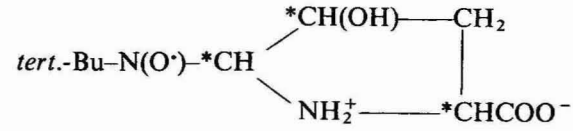

XLII

The two adducts in peak D″ were regarded as a pair of diastereomeric C-5 adducts from *trans*-4-Hyp arising from hydrogen abstractions from the C-5 positions by hydroxyl radicals[31]. The two adducts mixed in peak D‴ were regarded as a pair of epimeric C-5 adducts from *cis*-4-Hyp, each of which is also epimeric for either of the C-5 adducts from *trans*-4-Hyp as regards the C-4 positions whose asymmetric centres are different from each other.

The h.f.s.c.s of the spin adducts formed upon γ-irradiation of aqueous solutions of L-proline and its 4-substituted derivatives containing MNP are summarized in Table V. The spin adducts XXXVII, XL and XLI (cleavage adducts) are derived from reductive cleavages of the pyrrolidine rings induced by the addition of hydrated electrons to the carboxyl groups[31,44]:

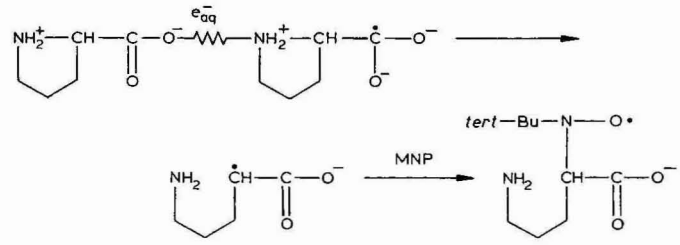

(18)

The C-4 (XXXIX) and C-5 (XXXVIII and XLII) adducts are derived from short-lived radicals produced by hydrogen abstraction from the carbons of the saturated alkyl groups by hydroxyl radicals.

Separation of spin adducts from dipeptides[62,63]

Aqueous solutions of four dipeptides, glycylglycine (Gly-Gly), glycyl-L-alanine (Gly-L-Ala), L-alanylglycine (L-Ala-Gly) and L-alanyl-L-alanine (L-Ala-L-Ala), were γ-irradiated at a dose rate of 0.1 kGy/min with a total dose of 3 kGy in the presence of 5 mg/ml MNP. The concentration of the dipeptides was 0.1 *M*. The irradiated solutions were chromatographed by stepwise elution with two buffers.

Glycylglycine[62]. A 0.25 *M* sodium phosphate buffer, pH 6.0, and 0.2 *M* Na_2HPO_4–NaOH, pH 11.5, were used as the first and the second eluents, respectively, and were switched at the elution volume of *ca.* 30 ml. In the ESR chromatogram of the γ-irradiated Gly-Gly solution, two peaks were eluted at 12.4 and 17.6 ml, and the corresponding fractions gave characteristic ESR spectral patterns.

The spin adduct in the first peak was assigned to the deamino adduct from Gly-Gly:

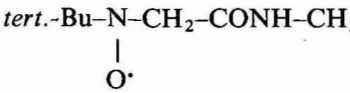

XLIII

The ESR pattern at pH 6.0 obtained for the second peak suggests the formation of a spin adduct having a component *tert.*-Bu–N(O·)–CH–N<:

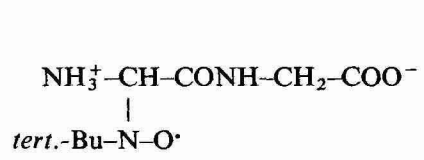

XLIV

or

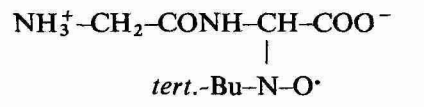

XLV

Whereas in neutral and alkaline solutions the ESR pattern was independent of pH, in the acidic pH range the signals due to the spin adduct exhibited reversible pH-dependent shifts. These changes are mainly due to an increase in the β-h.f.s.c. differences. From the observation of such reversible pH effects, the spin adduct was assigned not to structure XLIV but to XLV, that is, the C-terminal backbone adduct from Gly-Gly. The h.f.s.c.s are given in Table VI. The pK_{COOH} value has been determined to be 2.0 from a plot of the pH dependence of Δa_β ($= a_{\beta N} - a_{\beta H}$)

$$\Delta a_\beta = \frac{\Delta a_\beta^A + \Delta a_\beta^B \times 10^{pH-pK_a}}{1 + 10^{pH-pK_a}} \tag{19}$$

where $\Delta a_\beta^A = 0.11$ mT and $\Delta a_\beta^B = 0.02$ mT for the acid form and the base form, respectively.

Glycyl-L-alanine[62] A 0.1 *M* sodium phosphate buffer, pH 6.0, and 0.2 *M* Na_2HPO_4–NaOH buffer, pH 11.5, were used as the first and the second eluents, respectively, and were switched at the elution volume of *ca.* 24 ml. In the ESR chromatogram of a γ-irradiated Gly-L-Ala solution containing MNP, three peaks were eluted at 11.4, 14.4 and 25.6 ml. The spin adducts of the first, second and third peaks were assigned to the deamino adduct (structure XLVI), the C-terminal backbone adduct (XLVII) and the side-chain adduct (XLVIII) from Gly-L-Ala, respectively:

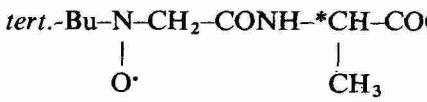

XLVI

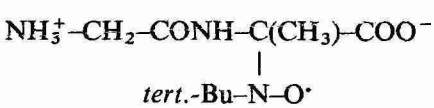

XLVII

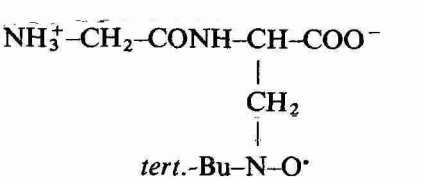

XLVIII

TABLE VI

H.F.S.C.S OF THE SPIN ADDUCTS FROM DIPEPTIDES

Spin adduct	*pH*	*h.f.s.c. (mT)*				
		a_N	$a_{\beta H}$	$a_{\beta N}$	$a_{\gamma H}$	$a_{\gamma N}$
Gly-Gly						
XLIII	6.0	1.59	0.91 (2H)			
XLV	1.0	1.52	0.16	0.26		
	6.0	1.56	0.22	0.24		
Gly-L-Ala						
XLVI	6.0	1.60	1.00			
			0.82			
XLVII	6.0	1.52		0.34	0.03 (13H)	
XLVIII	2.0	1.64	1.37 (2H)		0.07	
	6.0	1.64	1.46		0.07	
			0.97			
	8.4	1.64	1.42		0.07	
			0.99			
	12.2	1.64	1.39		0.07	
			1.01			
L-Ala-Gly						
XLIX	6.0	1.58	0.33		0.047 (3H)	0.047
La	0.8	1.52	0.160	0.260		
	6.0	1.55	0.233	0.233		
	11.2	1.57	0.215	0.235		
Lb	0.8	1.53	0.150	0.270		
	6.0	1.56	0.193	0.258		
	11.3	1.58	0.205	0.245		
LI	2.0	1.62	1.53		0.05	
			1.18			
	5.9	1.62	*		0.05	
	8.0	1.65	1.26 (2H)		0.07	
L-Ala-L-Ala						
LIIa	6.0	1.575	0.385		0.045 (3H)	0.045
LIIb	6.0	1.580	0.365		0.050 (3H)	0.050
LIIIa	6.0	1.53		0.339	0.034 (10H)	
LIIIb	6.0	1.52		0.350	0.032 (13H)	
LIV	1.0	1.65	1.39 (2H)		0.07	
	6.1	1.64	1.43		0.07	
			0.99			
	7.9	1.64	1.40		0.07	
			1.01			
	12.4	1.63	1.36		0.07	
			1.05			
LV	7.9	1.65	1.28 (2H)		0.07	

* The two β-hydrogens were presumably non-equivalent ($\Sigma a_{\beta H} = 2.63$ mT).

Their h.f.s.c.s are given in Table VI.

It was found that spin adduct XLVI exhibits ESR spectra with unequal splittings for the two β hydrogens, while spin adduct XLIII does not. It has already been

known that in the aminoxyl radical *tert.*-Bu–N(O·)–CH_2–*CXYZ the asymmetry of the β-carbon causes unequal splittings for the two β-hydrogens[50]. In the present case the spectrum of spin adduct XLVI revealed that in the aminoxyl radical *tert.*-Bu–N(O·)–CH_2–CONH–*CXYZ even the assymetry of the δ-carbon causes unequal splittings for the two β-hydrogens through the peptide bond. The ESR spectra of spin adduct XLVIII changed remarkably with pH through the acid-dissociation equilibria of the carboxyl or amino group. The pK_a value for the carboxyl group of adduct XLVIII has been determined to be 3.0.

L-*Alanylglycine*[63]. A 0.15 *M* sodium phosphate buffer, pH 6.0, and 0.2 *M* Na_2HPO_4–NaOH, pH 11.5, were used as the first and the second eluents, respectively, and were switched at the elution volume of *ca.* 31 ml. The ESR chromatogram of a γ-irradiated aqueous L-Ala-Gly solution containing MNP exhibited four peaks, eluted at 11.5, 17.0, 19.5 and 33.0 ml. The spin adducts of the first, second, third and fourth peaks were assigned to the deamino adduct (XLIX), the C-terminal backbone adducts (La and Lb) and the side-chain adduct (LI) from L-Ala-Gly, respectively:

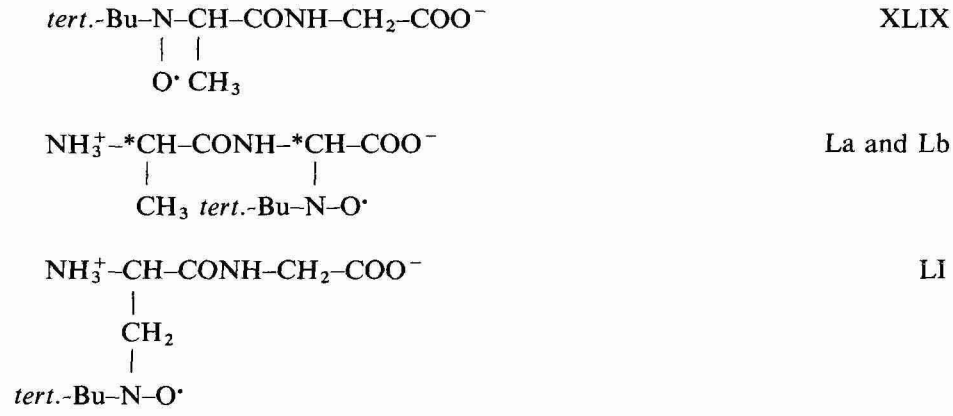

Spin adducts La and Lb are interpreted as a pair of diastereomeric radicals, *S,S* and *S,R* forms, involving the primary asymmetric centre of the L-alanine residue and a new asymmetric centre formed by the addition of MNP to the short-lived radical. Upon separation the individual diastereomeric radicals revealed mutually different h.f.s.c.s (Table VI). Their ESR spectra changed remarkably with pH through the acid-dissociation equilibria of the carboxyl groups. By the use of eqn. 19, the pK_a values have been determined to be 1.8 and 1.6 for the carboxyl groups of adduct La and Lb, respectively.

L-*Alanyl*-L-*alanine*[63]. When a 0.15 *M* sodium phosphate buffer, pH 6.0, and the 0.2 *M* H_3BO_3 · NaCl–NaOH buffer, pH 9.0, were used as the first and the second eluents, respectively, and were switched at *ca.* 33 ml, four peaks were eluted at 11.5, 15.3, 16.8 and 37.0 ml in the ESR chromatogram of a γ-irradiated aqueous L-Ala-L-Ala solution containing MNP.

By computer simulation of the ESR spectrum, the first peak fraction was interpreted to be a (1:1) mixture of a pair of diastereomeric deamino adducts (LIIa and LIIb), *S,S* and *R,S* forms:

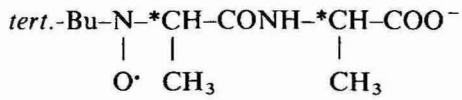

LIIa andLIIb

The spin adducts of the second, third and fourth peaks were assigned to a pair of diastereomeric C-terminal backbone adducts (LIIIa and LIIIb), and the C-terminal side-chain adduct (LIV) from L-Ala-L-Ala, respectively:

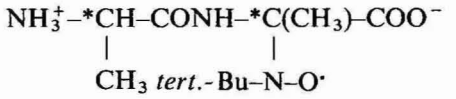

LIIIa and LIIIb

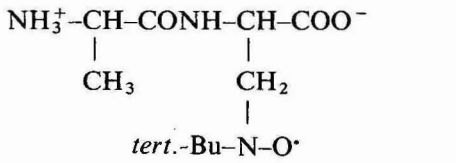

LIV

When sodium phosphate buffers of 0.05 *M*, pH 6.0, and 0.1 *M*, pH 8.0, were used as the first and second eluents, respectively, the N-terminal side-chain adduct

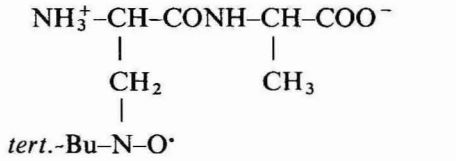

LV

from L-Ala-L-Ala was found in the fraction of pH 7.9.

The h.f.s.c.s of the spin adducts formed upon γ-irradiation of aqueous solutions of Gly-Gly, Gly-L-Ala, L-Ala-Gly and L-Ala-L-Ala containing MNP are summarized in Table VI. The observed γ-h.f.s. for the spin adducts XLVII, LIIIa and LIIIb contained the nine γ-hydrogens in the *tert.*-butyl group arising from MNP. The γ-H hyperfine splittings due to the *tert.*-butyl group are rarely observable. The pH-dependent spectral changes for the side-chain adducts from the dipeptides (XLVIII, LI, LIV and LV) suggest that, in an aqueous solution of *tert.*-Bu–N(O·)–CH_2–*CXYZ, the function of the β asymmetric centre which makes the methylene hydrogens non-equivalent[50] is enhanced by electric charges in proximity to it. It appears from the electron-withdrawing character of the aminoxyl group that the determined pK_{COOH} values of spin adducts VII, XLV, La and Lb are lower than those of the compounds in which the *tert.*-butyl aminoxyl groups of the adducts are substituted by hydrogens.

Separation of spin adducts from tripeptides[64]

Aqueous solutions of four tripeptides (0.1 *M*), Gly-Gly-Gly, Gly-Gly-L-Ala, Gly-L-Ala-Gly and L-Ala-Gly-Gly, were γ-irradiated at a dose rate of *ca.* 75 Gy/min with a total dose of 3 kGy in the presence of 5 mg/ml MNP.

Glycylglycylglycine. A 0.25 *M* sodium phosphate buffer, pH 6.0, and 0.2 *M*

Na_2HPO_4–NaOH buffer, pH 11.5, were used as the first and the second eluents, respectively, and were switched at the elution volume of *ca.* 31 ml. In the ESR chromatogram of the irradiated Gly-Gly-Gly solution, three peaks were eluted at 11.9, 18.1 and 20.0 ml. The spin adducts of the first, second and third peaks were assigned to the deamino adduct (structure LVI), the C-terminal backbone adduct (LVII) and the internal backbone adduct (LVIII) from Gly-Gly-Gly, respectively:

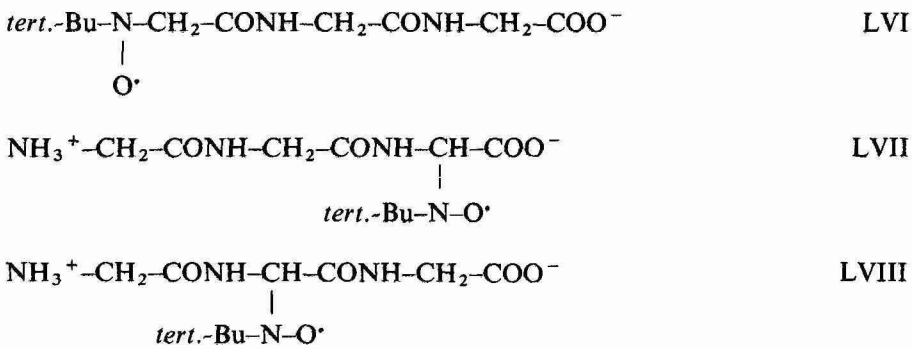

Glycylglycyl-L-alanine. Fig. 12 shows the ESR spectrum and chromatogram of a γ-irradiated aqueous Gly-Gly-L-Ala solution containing MNP. The ESR chromatogram exhibited four peaks (A–D) as shown by the solid line in Fig. 12b. Typical

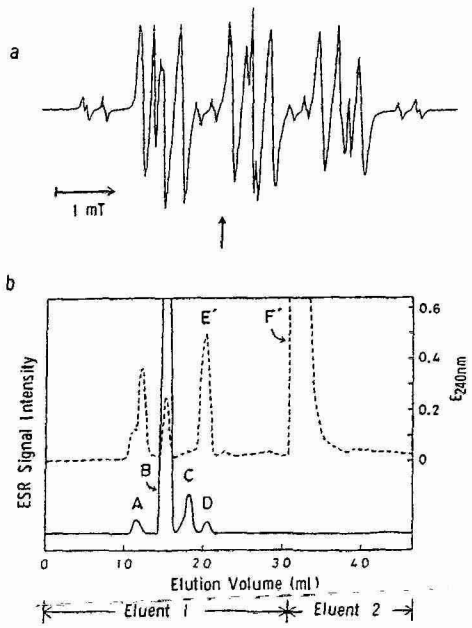

Fig. 12. (a) ESR spectrum of an aqueous solution of Gly-Gly-L-Ala containing MNP observed immediately after γ-irradiation (at pH 5.7). During chromatography, the magnetic field was fixed at the position indicated by the vertical arrow. (b) Chromatogram of the solution obtained by UV (broken line) and ESR (solid line) detection. Flow-rate: *ca.* 0.2 ml/min. Eluents: 1, 0.25 *M* sodium phosphate buffer, pH 6.0; 2, 0.2 *M* Na_2HPO_4–NaOH buffer, pH 11.5.

ESR spectra for the fractions corresponding to peaks A–D are depicted in Fig. 13a–d. Most spin adducts produced by the self-trapping of MNP[37,38] were adsorbed on the column and eluted very slowly with diffusion. In the UV chromatogram shown as the broken line in Fig. 12b, peak E′ is due to unreacted Gly-Gly-L-Ala, detected by using an amino acid analyzer, and peak F′ mainly due to *tert.*-butylnitrosohydroxylamine, *tert.*-BuN(OH)N=O, characterized by the pH dependence of the UV spectra[34,35].

Fig. 13a shows the ESR spectrum (modulation amplitude 0.05 mT) obtained for peak A, and the h.f.s.c.s are given in Table VII. The spin adduct was assigned the structure

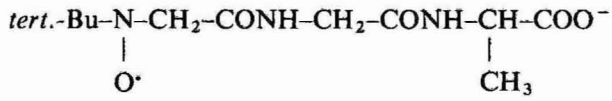

LIX

the deamino adduct from Gly-Gly-L-Ala.

Fig. 13b shows the ESR spectrum for peak B, which is apparently a major component of the ESR spectrum in Fig. 12a. This ESR pattern was assigned the structure

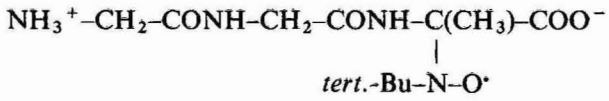

LX

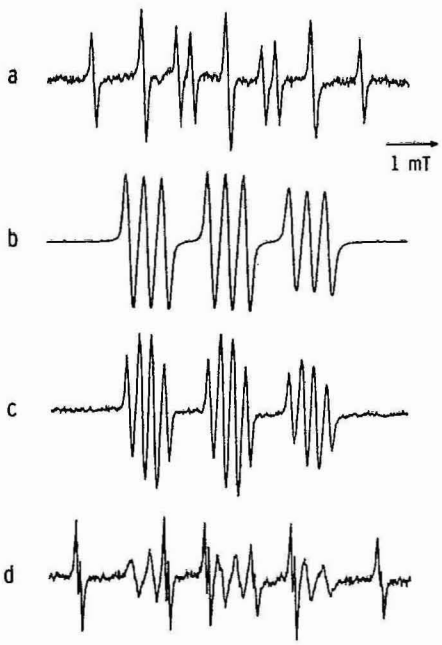

Fig. 13. ESR spectra (a–d) obtained from the fractions giving peaks A–D respectively in Fig. 12b. pH 5.9 (a and d); 6.0 (b and c).

TABLE VII

H.F.S.C.S OF THE SPIN ADDUCTS FROM TRIPEPTIDES

Spin adduct	*pH*	*h.f.s.c. (mT)*				
		a_N	$a_{\beta H}$	$a_{\beta N}$	$a_{\gamma H}$	$a_{\gamma N}$
Gly-Gly-Gly						
LVI	6.0	1.58	0.92 (2H)			0.03
LVII	0.6	1.52	0.16	0.255		
	6.0	1.56	0.20	0.24		
	11.1	1.59	0.20	0.26		
LVIII	0.7	1.50	0.21	0.235		
	6.3	1.51	0.20	0.24		
	11.2	1.53	0.20	0.23		
Gly-Gly-L-Ala						
LIX	5.9	1.59	0.92 (2H)			0.03
LX	6.0	1.52		0.33		
LXI*	1.0	1.51	0.27	0.22		
	6.0	1.51	0.25	0.22		
	12.0	1.53	0.25	0.22		
LXII	5.9	1.63	1.36		0.07	
			1.02			
Gly-L-Ala-Gly						
LXIII	6.0	1.59	0.95			0.03
			0.89			
LXIVa**	0.6	1.52	0.16	0.265		
	6.0	1.54	0.20	0.24		
	11.3	1.56	0.21	0.245		
LXIVb**	0.6	1.52	0.155	0.255		
	6.0	1.55	0.20	0.24		
	11.1	1.56	0.21	0.24		
LXV	0.4	1.46		0.31		
LXVI	6.1	***	***		0.06	
L-Ala-Gly-Gly						
LXVII	5.7	1.56	0.33		0.045 (3H)	0.045
LXVIII*	0.4	1.52	0.15	0.255		
	6.0	1.55	0.21	0.24		
	11.5	1.56	0.205	0.245		
LXIX*	0.5	1.50	0.22	0.24		
	6.0	1.51	0.19	0.24		
	11.7	1.52	0.20	0.23		
LXX	6.6	1.64	1.33§		0.06	

* All h.f.s.c.s are the average values of two diastereoisomers.

** LXIVa and LXIVb are a pair of diastereomeric adducts which were separated.

*** $2a_N + a_{\beta H1} + a_{\beta H2} = 5.78$ mT.

§ Average value for two hydrogens.

the C-terminal backbone adduct from Gly-Gly-L-Ala.

Fig. 13c shows the ESR spectrum for peak C. The spectral pattern was almost pH-independent. The spin adduct was assigned the structure

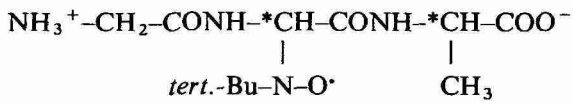

LXI

the internal backbone adduct from Gly-Gly-L-Ala.

Fig. 13d shows the ESR spectrum for peak D, which apparently exhibited a mixture of six narrow and six broad lines. Such a spectrum is typical of an aminoxyl radical, *tert.*-BuN(O·)–CH_2–*CXYZ[50]. The spin adduct was assigned the structure

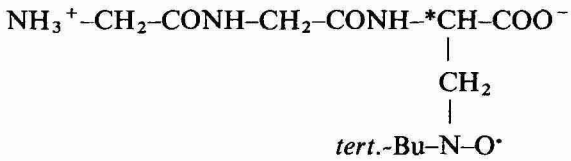

LXII

the side-chain adduct from Gly-Gly-L-Ala.

Glycyl-L-alanylglycine and L-alanylglycylglycine. γ-Irradiated aqueous solutions of Gly-L-Ala-Gly and L-Ala-Gly-Gly were also analyzed under analogous conditions by the HPLC–ESR method. From the irradiated Gly-L-Ala-Gly solution, the deamino adduct (structure LXIII), the C-terminal backbone adducts (LXIVa and LXIVb), the internal backbone adduct (LXV) and the side-chain adduct (LXVI) were identified:

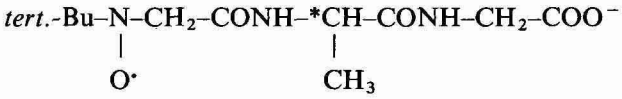

LXIII

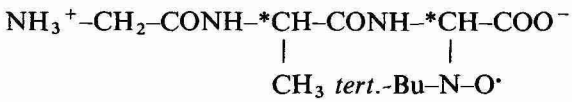

LXIVa and LXIVb

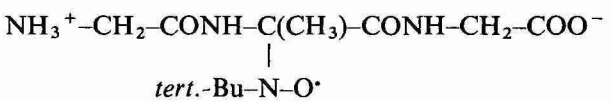

LXV

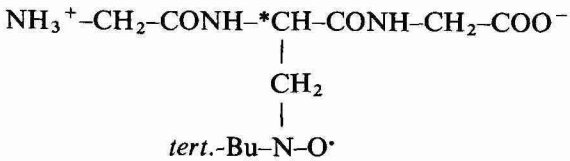

LXVI

The pair of diastereomeric adducts, LXIVa and LXIVb, were separated from each other. From the irradiated L-Ala-Gly-Gly solutions, four spin adducts were identified:

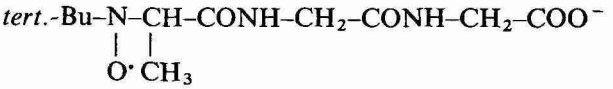

LXVII

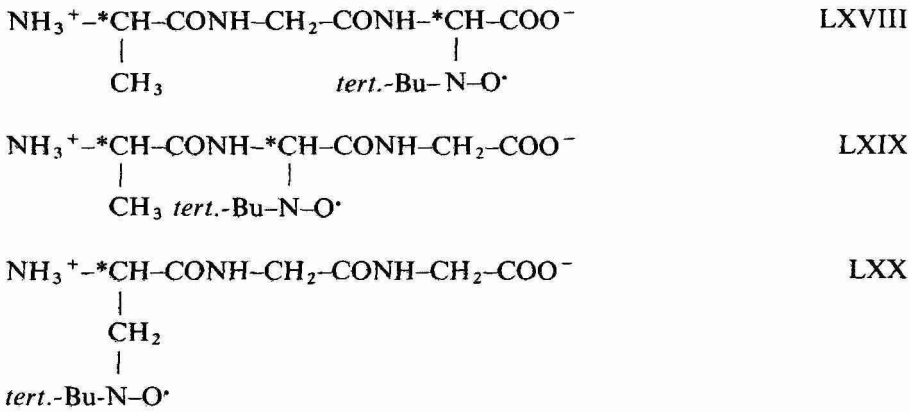

LXVIII

LXIX

LXX

Spin-trapping of polyglycine radical. An aqueous solution of polyglycine (*ca.* 1 m*M*, approximate molecular weight 6000) containing 5 mg/ml MNP was cooled by ice and γ-irradiated at a dose rate of *ca.* 75 Gy/min with a total dose of 0.2 kGy, without deaeration. ESR measurements of the irradiated solution revealed a spin adduct which was assigned the structure

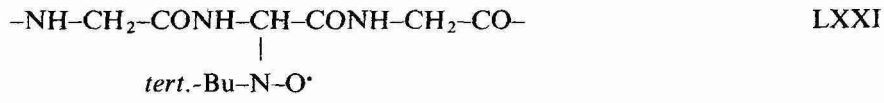

LXXI

the internal backbone adduct from polyglycine. Its h.f.s.c.s at pH 4.7 are a_N = 1.50 mT, $a_{\beta H}$ = 0.25 mT and $a_{\beta N}$ = 0.27 mT. The backbone adduct from polyalanine was reported previously[24].

The spin adducts from dipeptides and tripeptides, whose h.f.s.c.s are summarized in Tables VI and VII, respectively, can be grouped into four general types, as follows: (a) deamino adducts derived from short-lived radicals produced by reductive deaminations upon addition of hydrated electrons to the N-terminal peptide carbonyl groups; (b) C-terminal backbone adducts; (c) internal backbone adducts and (d) side-chain adducts derived from short-lived radicals produced by hydrogen abstractions mainly by hydroxyl radicals, from α-carbon atoms in the C-terminal and internal main chains and a carbon in an aliphatic side-chain, respectively. The detection of the internal backbone adducts from the tripeptides and polypeptides suggest that, in general, short-lived backbone radicals, –CONH–ĊR–CONH–, are produced in γ-irradiated aqueous solutions by hydrogen abstraction from an internal α-carbon atom in the main chains of proteins, mainly by ·OH:

(20)

CONCLUSIONS

The HPLC–ESR method described is expected to be widely applicable for studies on the structures and properties of free radicals, as shown in the present work

by the separation of diastereomeric radicals, the differentiation of their absolute configurations, the determination of pK_a values, the magnetic non-equivalence of the β-H h.f.s.c.s caused by the asymmetry of the δ-carbon atom, etc.

ACKNOWLEDGEMENTS

The authors express their sincere gratitude to Dr. Souji Rokushika, Mr. Nobuhiro Suzuki and Mr. Naohisa Iguchi, Kyoto University, for their invaluable contributions.

REFERENCES

1 W. A. Pryor (Editor), *Free Radicals in Biology*, Vols. 1–5 (1976–1982), Academic Press, New York, and references therein.
2 H. Dertinger and H. Jung, *Molecular Radiation Biology*, Springer, Berlin, 1st ed., 1970, and references therein.
3 T. Henriksen, T. B. Melø and G. Saxebøl, in W. A. Pryor (Editor), *Free Radicals in Biology*, Vol. 2, Academic Press, New York, 1976, Ch. 8, and references therein.
4 E. G. Janzen and B. J. Blackburn, *J. Am. Chem. Soc.*, 90 (1968) 5909.
5 E. G. Janzen, *Acc. Chem. Res.*, 4 (1971) 31, and references therein.
6 C. Lagercrantz and S. Forshult, *Nature (London)*, 218 (1968) 1247.
7 C. Lagercrantz, *J. Phys. Chem.*, 75 (1971) 3466, and references therein.
8 G. R. Chalfont and M. J. Perkins, *J. Am. Chem. Soc.*, 89 (1967) 3054.
9 M. J. Perkins, *Adv. Phys. Org. Chem.*, 17 (1980) 1, and references therein.
10 S. Terabe and R. Konaka, *J. Am. Chem. Soc.*, 91 (1969) 5655.
11 I. H. Leaver and G. C. Ramsey, *Tetrahedron*, 25 (1969) 5669.
12 E. G. Janzen, in W. A. Pryor (Editor), *Free Radicals in Biology*, Vol. 4, Academic Press, New York, 1980, Ch. 4, and references therein.
13 P. B. McCay, T. Noguchi, K.-L. Fong, E. K. Lai and J. L. Poyer, in W. A. Pryor (Editor), *Free Radicals in Biology*, Vol. 4, Academic Press, New York, 1980, Ch. 5, and references therein.
14 C. Lagercrantz, *J. Am. Chem. Soc.*, 95 (1973) 220.
15 H. Taniguchi and H. Hatano, *Chem. Lett.*, (1974) 531.
16 H. Taniguchi and H. Hatano, *Chem. Lett.*, (1975) 9.
17 K. N. Jobin, A. W. Johnson, M. F. Lappert and B. K. Nicholson, *J. Chem. Soc., Chem. Commun.*, (1975) 441.
18 A. Joshi, S. Rustgi and P. Riesz, *Int. J. Radiat. Biol. Relat. Stud. Phys. Chem. Med.*, 30 (1976) 151.
19 S. Rustgi and P. Riesz, *Int. J. Radiat. Biol. Relat. Stud. Phys. Chem. Med.*, 33 (1978) 21.
20 S. Rustgi and P. Riesz, *Radiat. Res.*, 75 (1978) 1.
21 A. Joshi, H. Moss and P. Riesz, *Int. J. Radiat. Biol. Relat. Stud. Phys. Chem. Med.*, 34 (1978) 165.
22 S. Rustgi, A. Joshi, H. Moss and P. Riesz, *Int. J. Radiat. Biol. Relat. Stud. Phys. Chem. Med.*, 31 (1977) 415.
23 S. Rustgi, A. Joshi, P. Riesz and F. Friedberg, *Int. J. Radiat. Biol. Relat. Stud. Phys. Chem. Med.*, 32 (1977) 533.
24 A. Joshi, S. Rustgi, H. Moss and P. Riesz, *Int. J. Radiat. Biol. Relat. Stud. Phys. Chem. Med.*, 33 (1978) 205.
25 S. Rustgi and P. Riesz, *Int. J. Radiat. Biol. Relat. Stud. Phys. Chem. Med.*, 34 (1978) 127.
26 S. Rustgi and P. Riesz, *Int. J. Radiat. Biol. Relat. Stud. Phys. Chem. Med.*, 34 (1978) 449.
27 P. Riesz and S. Rustgi, *Radiat. Phys. Chem.*, 13 (1979) 21.
28 S. Rokushika, H. Taniguchi and H. Hatano, *Anal. Lett.*, 8 (1975) 205.
29 S. Kominami, S. Rokushika and H. Hatano, *Int. J. Radiat. Biol. Relat. Stud. Phys. Chem. Med.*, 30 (1976) 525.
30 S. Kominami, S. Rokushika and H. Hatano, *Radiat. Res.*, 72 (1977) 89.
31 M. H. Klapper and M. Faraggi, *Quart. Rev. Biophys.*, 12 (1979) 465, and references therein.
32 B. H. J. Bielski and J. M. Gebicki, in W. A. Pryor (Editor), *Free Radicals in Biology*, Vol. 3, Academic Press, New York, 1977, Ch. 1, and references therein.

33 J. C. Stowell, *J. Org. Chem.*, 36 (1971) 3055.
34 K. Makino, N. Suzuki, F. Moriya, S. Rokushika and H. Hatano, *Anal. Lett.*, 13 (1980) 311.
35 K. Makino, N. Suzuki, F. Moriya, S. Rokushika and H. Hatano, *Radiat. Res.*, 86 (1981) 294.
36 C. N. R. Rao and K. R. Bhaskar, in H. Feuer (Editor), *The Chemistry of the Nitro and Nitroso Group*, Part 1, Interscience, New York, 1969, Ch. 3, and references therein.
37 K. Makino, N. Suzuki, F. Moriya, S. Rokushika and H. Hatano, *Chem. Lett.*, (1979) 675.
38 K. Makino, *J. Phys. Chem.*, 84 (1980) 1012.
39 U. Deffner and W. Schimmack, *Int. J. Radiat. Biol. Relat. Stud. Phys. Chem. Med.*, 29 (1976) 71.
40 D. F. Bowman, T. Gillan and K. U. Ingold, *J. Am. Chem. Soc.*, 93 (1971) 6555.
41 W. Brackman and C. J. Gaasbeek, *Rec. Trav. Chim. Pays-Bas*, 85 (1966) 221.
42 K. Makino, M. M. Massoba and P. Riesz, *Radiat. Res.*, 95 (1983) 519.
43 F. Moriya, K. Makino, N. Suzuki, S. Rokushika and H. Hatano, *J. Phys. Chem.*, 84 (1980) 3085.
44 W. M. Garrison, *Radiat. Res. Rev.*, 3 (1972) 305, and references therein.
45 M. D. Sevilla, *J. Phys. Chem.*, 74 (1970) 2096.
46 H. Taniguchi, K. Fukui, S. Ohnishi, H. Hatano, H. Hasegawa and T. Maruyama, *J. Phys. Chem.*, 72 (1968) 1926.
47 P. Neta, M. Simic and E. Hayon, *J. Am. Chem. Soc.*, 74 (1970) 4763.
48 P. Neta, M. Simic and E. Hayon, *J. Phys. Chem.*, 75 (1971) 738.
49 Y. Kirino, *J. Phys. Chem.*, 79 (1975) 1296.
50 B. C. Gilbert and M. Trenwith, *J. Chem. Soc., Perkin Trans. 2*, (1973) 1834.
51 K. Makino, N. Suzuki, F. Moriya, S. Rokushika and H. Hatano, *Anal. Lett.*, 13 (1980) 301.
52 K. Makino, *J. Phys. Chem.*, 84 (1980) 1016.
53 K. Makino, *J. Phys. Chem.*, 84 (1980) 1968.
54 K. Makino and H. Hatano, *Chem. Lett.*, (1979) 119.
55 K. Makino, *J. Phys. Chem.*, 83 (1979) 2520.
56 N. Iguchi, F. Moriya, K. Makino, S. Rokushika and H. Hatano, *Can. J. Chem.*, 62 (1984) 1722.
57 N. Suzuki, K. Makino, F. Moriya, S. Rokushika and H. Hatano, *J. Phys. Chem.*, 85 (1981) 263.
58 F. Moriya, K. Makino, N. Iguchi, N. Suzuki, S. Rokushika and H. Hatano, *J. Phys. Chem.*, 88 (1984) 2373.
59 A. L. J. Beckwith and R. O. C. Norman, *J. Chem. Soc. B*, (1969) 400, and references therein.
60 L. Jonkman, H. Muller and J. Kommandeur, *J. Am. Chem. Soc.*, 93 (1971) 5833.
61 F. W. King, *Chem. Rev.*, 76 (1976) 157, and references therein.
62 F. Moriya, K. Makino, N. Suzuki, S. Rokushika and H. Hatano, *J. Phys. Chem.*, 84 (1980) 3614.
63 F. Moriya, K. Makino, N. Suzuki, S. Rokushika and H. Hatano, *J. Am. Chem. Soc.*, 104 (1982) 830.
64 F. Moriya, N. Iguchi, K. Makino, S. Rokushika and H. Hatano, *Can. J. Chem.*, 62 (1984) 2206.

Journal of Chromatography, 332 (1985) 107–116
Elsevier Science Publishers B.V., Amsterdam — Printed in The Netherlands

CHROMSYMP. 622

NEW DOUBLE-STAGE SEPARATION ANALYSIS METHOD

DIRECTLY COUPLED LABORATORY-SCALE SUPERCRITICAL FLUID EXTRACTION–SUPERCRITICAL FLUID CHROMATOGRAPHY, MONITORED WITH A MULTIWAVELENGTH ULTRAVIOLET DETECTOR

K. SUGIYAMA
Research Institute, Morinaga & Co., Ltd., 2-1-1 Shimosueyoshi, Tsurumi-ku, Yokohama 230 (Japan)
and
M. SAITO*, T. HONDO and M. SENDA
JASCO, Japan Spectroscopic Co., Ltd, No. 2967-5 Ishikawa-cho, Hachioji City, Tokyo 192 (Japan)
(First received March 30th, 1985; revised manuscript received May 2nd, 1985)

SUMMARY

Instrumentation and applications of a new double-stage separation analysis method are described. The new method incorporates supercritical fluid extraction as the first separation step and supercritical fluid chromatography as the second separation step. The extraction section of the instrument was tested by caffeine extraction from roasted coffee beans with carbon dioxide, and the effects of extraction parameters on the extracted amounts of caffeine were examined by high-performance liquid chromatography. Then, directly coupled supercritical fluid extraction–supercritical fluid chromatography, monitored with a highly sensitive multiwavelength detector, was performed on the powdered coffee beans, and separation was successfully carried out without any special pretreatment. The obtained data were graphically presented by a data processor, as three-dimensional plots of supercritical fluid chromatograms, at 250 and 270 nm, and a spectrum at 9.60 min, which showed clear characteristics of the caffeine spectrum.

INTRODUCTION

Although the fundamental principles have been known for more than 100 years, supercritical fluid extraction (SFE) was introduced by Zosel *et al.*[1] only about two decades ago. Since then, the method seems to have developed mainly as an industrial-scale extraction technique[2–12], independently of the development of high-performance liquid chromatography (HPLC), which is a separation analysis method not only contemporary with SFE, but also with a similar history of development. In addition to their use in separation, these two techniques have many things in common from the instrumentation aspect. Both use high-pressure pumps, sample introduction devices, packed or hollow separation columns, etc. Since the late 1960s, numerous

0021-9673/85/$03.30

reports on HPLC and SFE have been published. However, they have little to do with each other. Stahl and Schiltz developed an extraction system which was combined with thin-layer chromatography[13,14]. Nieass *et al.* examined the solubility of organic substances in liquefied carbon dioxide by using a high-pressure cylinder, connected to an HPLC system[15,16]. Recently, Unger and Roumeliotis reported a coupling device that allows on-line HPLC analysis of extracts[17]. They aimed primarily to investigate optimal conditions for SFE.

Supercritical fluid chromatography (SFC), which uses supercritical fluid as the mobile phase, also originated, in the 1960s, from high-pressure gas chromatography. It was developed by several research groups[18–27]. In the early 1980s, advances in micro HPLC renewed the interests in SFC. Rapid mass transfer in supercritical mobile phases attracted researchers as it offers high speed separation with high resolution on an open tubular capillary column and also on a packed capillary column. The low consumption of the fluid encouraged chromatographers to use flammable and even toxic fluids under high pressures and at high temperatures. Thus, extensive research has been performed by a number of groups[28–37]. In addition to an HPLC UV detector with a high-pressure cell, other detectors have been used in SFC: mass spectrometry[38–40], Fourier transform infrared spectroscopy[41–43], flame ionization detection[44–46]. Sophisticated SFC systems have also reported by Gere *et al.*[47], and Greibrokk *et al.*[48].

Although SFC seems to be closer to SFE than other types of chromatography, they have little in common[49] and direct coupling of SFE with SFC has not yet been attempted.

Recent advances in HPLC instrumentation technology readily permit SFE to be directly combined with an SFC system. In this paper, the instrumentation of the directly coupled SFE–SFC system and its application to caffeine extraction from roasted coffee beans are described.

INSTRUMENTATION OF THE SFE–SFC SYSTEM

We investigated the direct coupling of SFE to SFC and developed a double-stage separation analysis method[50,51], which consists of extraction with supercritical fluid followed by supercritical fluid chromatography for on-line analysis of the SFE extracts. In this new method, SFE is used as the first separation step in a similar way to a sample pretreatment in HPLC, SFC is used as the second separation step. This configuration allows an analyst to place a raw and/or solid sample in the system in order to obtain a chromatogram of the sample extract. We also used a multiwavelength UV detector, equipped with a high-pressure cell, as an extraction and/or chromatographic monitor. Three-dimensional spectrometric data, namely absorbance, wavelength and time, graphically presented in various fashions by computer-aided techniques, are very effective in the detailed examination of components in the SFE extract. Furthermore, application of peak deconvolution[52–54] allows further investigation of chromatographic peak components of the extract.

In SFE, carbon dioxide is generally the preferred supercritical extraction medium and is widely used[2,3,6–17,22,24,25,31–34,39–48], because it is non-toxic, non-flammable, non-polluting and inexpensive. In addition, it has a relatively low critical pressure, 73 bar, and a low critical temperature, 31.3°C, so that a supercritical phase

is easily obtained. Our system is also primarily designed to use carbon dioxide as both the extraction medium and the chromatographic mobile phase.

In order to operate the SFE–SFC system successfully:

(1) the volume of the extraction chamber should be appropriate for the sample size for SFC;

(2) the pressure decrease of the supercritical carbon dioxide should be kept to a minimum during the transfer of the extract from the extraction cartridge to the sample loop of the SFC system.

(3) the SFC system should be pre-pressurized and equilibrated at the SFC analysis pressure before the extract is introduced.

The hydraulics of the SFE–SFC system we designed are shown in Fig. 1. The system allows several modes of operation:

(1) directly coupled SFE–SFC, *i.e.*, batch SFE with a trap loop, which is followed by SFC analysis with direct sample introduction;

(2) continuous flow SFE with an extract trap column, which can be followed by off-line analysis by gas chromatography (GC), HPLC, etc.;

(3) continuous flow SFE with an extract trap column in a recycle operation, which can also be followed by off-line analysis, by GC, HPLC, etc.

Liquefied carbon dioxide from the cylinder (1) is fed to the pump (2) whose pump heads are cooled with dry ice at 0–5°C (TRI ROTAR-II modifed for liquefied carbon dioxide delivery; JASCO, Tokyo, Japan). An entrainer or modifier solvent is

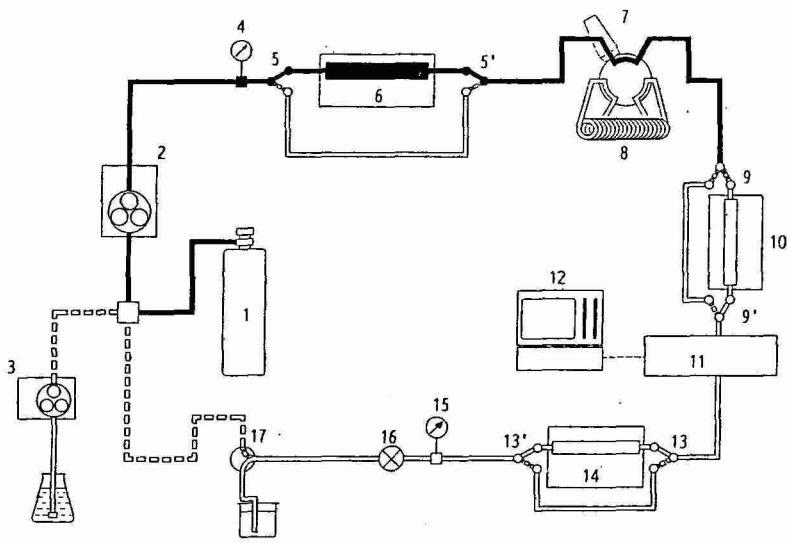

Fig. 1. Hydraulics of directly coupled SFE–SFC for extraction. Components: 1 = carbon dioxide cylinder; 2 = pump for delivering liquefied carbon dioxide; 3 = pump for delivering modifier solvent; 4 = pressure gauge; 5/5′ = six-way valve; 6 = extraction cartridge, thermostatted in oven; 7 = injector valve; 8 = extract trap loop; 9/9′ = six-way valve; 10 = chromatographic separation column in oven; 11 = highly sensitive multiwavelength UV detector; 12 = data processor for 11; 13/13′ = six-way valve; 14 = extract trap column in oven; 15 = pressure gauge for monitoring back-pressure; 16 = pressure regulator; 17 = three-way valve. After SFE, the injector (7) is switched to load the extract trap loop (8) with the extract. The injector is then switched back to by-pass the loop for pre-pressurization and equilibration of the separation column (10), while the loop holds the extract.

delivered by the pump (3) (JASCO TRI ROTAR-V) and pre-mixed with liquefied carbon dioxide before entering the pump (2). The pump (2) is operated generally in the constant-pressure mode up to 300 bar, while the pump (3) is in the constant-flow mode. The switching valves (5)/(5′), (9)/(9′), and (13)/(13′) (three JASCO HV-614 high-pressure six-way valves) are switched in accordance with the desired mode.

Hydraulics of directly coupled SFE–SFC

The flow-line for the directly coupled SFE–SFC mode is indicated by the solid line in Fig. 1. Carbon dioxide is delivered to the extraction cartridge (6), where extraction takes place, then to the injector valve (7) (JASCO VL-614) with the extract trap loop (8), which is purged with carbon dioxide gas at atmospheric pressure prior to the extraction. The valve (9)/(9′) is set in the non-connecting position to make a dead-end for the extraction line and, at the same time, the valve (9)/(9′) maintains the pressure of the column, which has been pre-pressurized and is to be equilibrated at the SFC pressure. The extraction cartridge (6), the separation column (10) and the extract trap column (14) are thermostatted in an oven (JASCO TU-300). When SFC is performed at a different temperature, a separate oven is used.

At the beginning of the extraction, the pump delivers liquefied carbon dioxide at its maximum flow-rate to pressurize the extraction cartridge (6) quickly. As the pressure approaches the preset extraction pressure, the flow-rate is gradually decreased and, finally, the flow is automatically stopped when the pressure reaches the preset value. Then, the pressure will be maintained throughout extraction period. On completion of the extraction, the injector valve (7) is switched into the position shown in Fig. 2, to load the trap loop (8) with the extract, and the pump (2) automatically starts operating to compensate for the pressure decrease caused by the transfer of carbon dioxide and the extract in the extraction cartridge (6) to the trap loop (8), which has been purged with carbon dioxide gas at atmospheric pressure. When the transfer is completed and the pressure is restored, the pump (2) is stopped. Then, the injector valve (7) is switched back to the position shown in Fig. 1, so that the loop (8) is by-passed, and the extract dissolved in the supercritical carbon dioxide is retained in the loop (8) until the injection is made. The valves (5)/(5′) and (9)/(9′) are then switched to the SFC separation line, as indicated by the solid line in Fig. 2. The system is now operated in the chromatography mode for equilibration of the separation column (10).

Finally, the injector (7) is switched to the position shown in Fig. 2, to inject the extract into the separation column (10). The chromatography mode can be easily converted from SFC to ordinary HPLC by using an ordinary solvent without any hardware modification. A highly sensitive multiwavelength UV detector (11) (JASCO MULTI-320, modified for high-pressure application) together with its dedicated data processor (12) (JASCO DS-L800) are used as an extraction and/or chromatographic monitor. The flow-cell, whose volume is 4 μl, is modified to withstand 300 bar pressure to meet pressure requirements in SFE and SFC. The flow detector cell is kept at the necessary pressure for SFE and SFC by a pressure regulator (16) (TESCOM, Minneapolis, MN, U.S.A.) where the main pressure drop takes place. The back-pressure is monitored by the pressure gauge (15), and the column effluent is vented into water through the three-way valve (17).

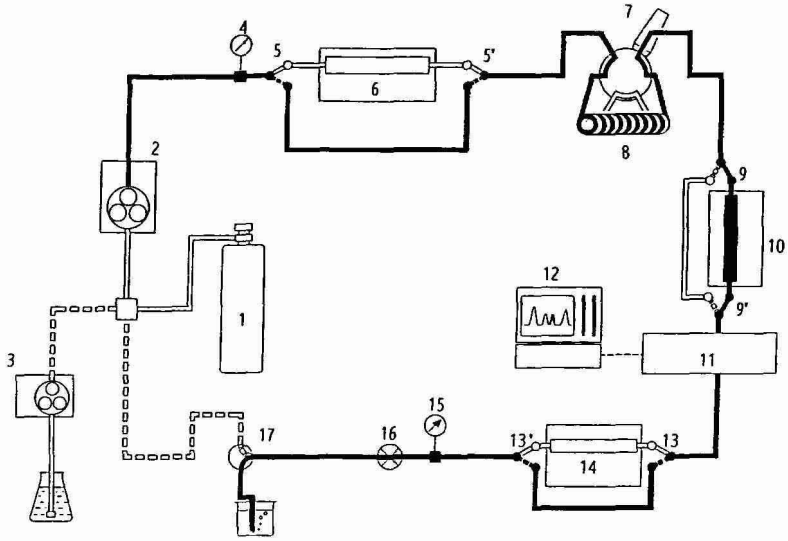

Fig. 2. Hydraulics of directly coupled SFE–SFC for chromatography. After pre-pressurization and equilibration of the separation column, the injector is switched to inject the extract held in the trap loop into the column. The injector valve in this figure is shown in the position for injection.

Hydraulics of SFE with extract trap column

In SFE in the extract trap column mode, the fluid flows through the extraction cartridge (6), the detector (11), by-passing the separation column (10), via the extract trap column (14), the pressure gauge (15), and the pressure regulator (16), and then to the waste or back to the pump (2) via the valve (17), when recycle is selected. After SFE, the extract trap column (14) is disconnected from the system, and the extract is eluted with solvent. The extract is then applied to other analytical instruments, such as GC or HPLC systems.

RESULTS AND DISCUSSION

For our preliminary work, we started with caffeine extraction from coffee beans, which is one of the classical applications of SFE, using continuous flow SFE in the extract trap column mode. The coffee extract, which was eluted from the extract trap column, has been applied to an HPLC system (off-line SFE–HPLC). SFE was performed under various conditions, and the contribution of each extraction parameter to the extracted amount of caffeine was examined.

After the extraction conditions had been examined, directly coupled SFE–SFC was performed successfully, and three-dimensional SFC data of the coffee extract were obtained by placing the coffee powder in the system. The data were represented, by the data processor, as three-dimensional plots, chromatograms at 250 and 270 nm and a spectrum at 9.60 min, which showed clear characteristics of the caffeine spectrum.

SFE–HPLC analysis of coffee beans

In the food industry, decaffeination or caffeine extraction is usually performed

on green coffee beans with a particular water content[1]. In our experiment, roasted coffee beans were used instead of green beans. Roasted coffee beans, obtained from a grocery store, were ground and sieved to 30–60 mesh. They contained 1–2% water, significantly less than in green beans. In order to vary the water content, different amounts of water were added to *ca.* 20 g of coffee powder kept in a glass vessel (100-ml capacity) with an air-tight stopper, mixed by shaking, then equilibrated for at least 24 h. Then, *ca.* 350 mg of the moistened powder were packed by tapping into an extraction cartridge (50 × 4.6 mm I.D.). Extraction was performed with continuous flow in a recycle operation with a trap column of the same dimensions, packed with activated carbon (30–60 mesh; Gasukuro Kogyo, Tokyo, Japan). After SFE, the column was disconnected from the system, and the extract was eluted with 25 ml of methanol–water (55:45). Then, 20 μl of the solution was injected into the HPLC system, consisting of a TRI ROTAR-V pump, a VL-614 injector, a Fine Pak SIL C_{18} column and UVIDEC-100-V UV detector (all from JASCO). Carbon dioxide (Toyoko Kagaku, Kawasaki, Japan) was used as the extraction medium.

Fig. 3 shows an HPLC chromatogram of the coffee extract, obtained by the procedure described above. The coffee powder contained added water (20% of the coffee weight), besides the original water content. The extraction pressure was 200 bar, the temperature was 48°C, and the time was 60 min.

Amount of caffeine extracted from coffee beans under various conditions

The amount of caffeine extracted from coffee beans was examined under var-

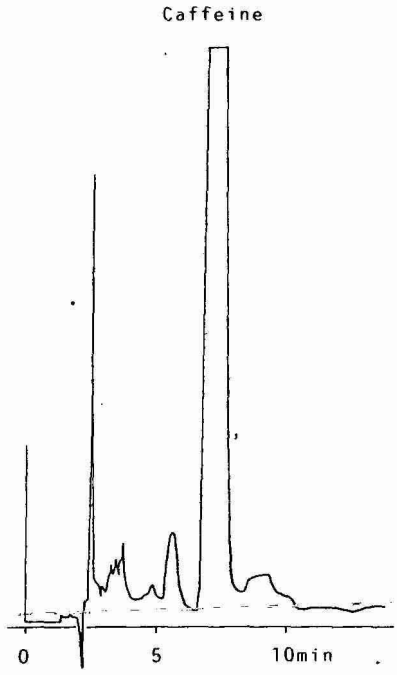

Fig. 3. HPLC chromatogram of coffee extract by SFE. SFE conditions: pressure, 200 bar; temperature, 48°C; added water, 20%; time, 60 min. HPLC conditions: column, JASCO Fine Pak SIL C_{18}; eluent, methanol–water (55:45); flow-rate, 1.2 ml/min; UV monitored at 272 nm and 0.64 a.u.f.s.

ious conditions of pressure, extraction time, added water and temperature, by the procedure described above. In Fig. 4 the amounts of caffeine extracted are represented as percentages of the amount extracted with hot water, *i.e.*, as percentages of the caffeine level in ordinary drinking coffee. The amounts increased with increasing extraction pressure and time, as shown by the heavy lines. However, the amounts rapidly decreased with increasing temperature, and above 60°C, caffeine was hardly extracted. This decrease is considered to be due to the decrease of caffeine solubility in carbon dioxide, resulting from the density reduction. As the amount of added water decreased, the amount of caffeine extracted also decreased. This suggests that the water content of coffee plays the role of an entrainer solvent in extraction. Therefore, in order to extract caffeine from the roasted coffee beans efficiently, the extraction temperature should be below 50°C and an amount, at least 15% of the coffee weight, of water should be added.

The variation of the extracted amounts of caffeine in five successive experi-

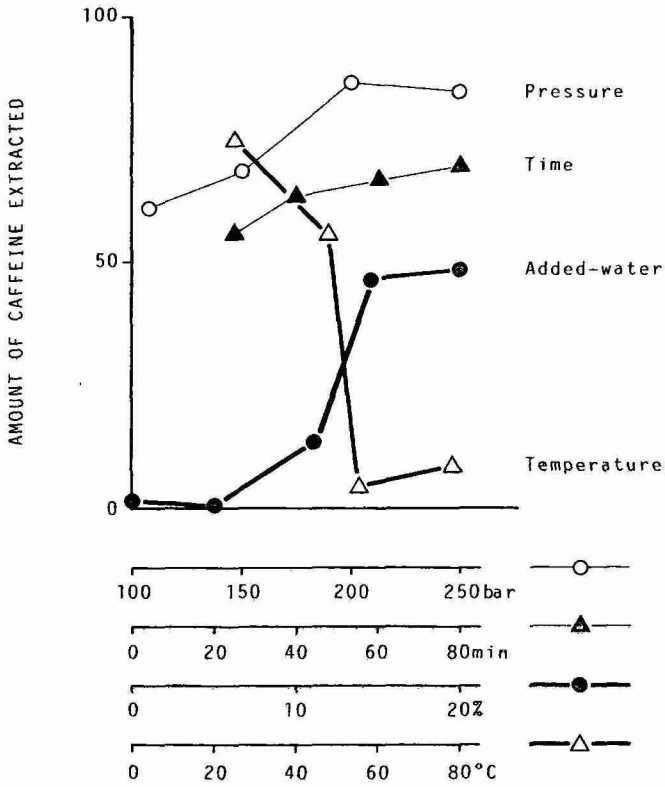

Fig. 4. Amounts (percentages) of caffeine extracted from roasted coffee beans under various conditions, with hot water. Curves: —○—, various pressures with the added water, temperature, and extraction time constant at 20%, 48°C, and 60 min, respectively; —▲—, various extraction times with other parameters constant, at 150 bar, 20% and 48°C; —●—, various amounts of water added to coffee powder with other parameters constant, at 150 bar, 48°C and 60 min; —△—, various temperatures with other parameters constant, at 150 bar, 60 min and 20%. The temperature and the amount of added water have significant effects on the extraction, as shown by heavy lines.

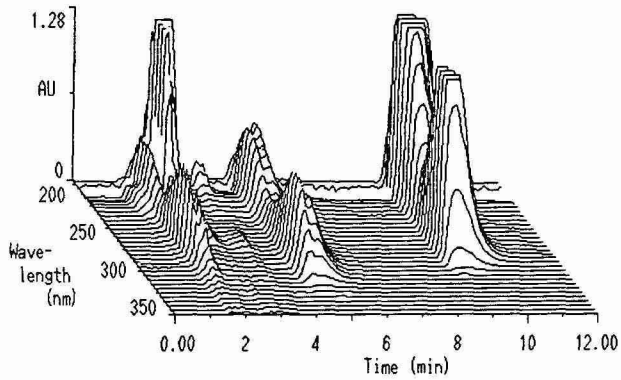

Fig. 5. Three-dimensional SFC chromatogram obtained by directly coupled SFE–SFC. SFE conditions: pressure, 200 bar; temperature, 40°C; added water, 20%; time, 15 min. SFC conditions: mobile phase, supercritical carbon dioxide–methanol (100 μl/min); total flow-rate, *ca.* 5 ml/min as liquid; pressure, 150 bar; column, JASCO Fine Pak SIL C_{18} (150 × 6 mm I.D.); temperature, 40°C.

ments was calculated to be ± 8% under the following conditions: pressure, 200 bar; temperature, 48°C;added water, 20%; time, 60 min.

Directly coupled SFE–SFC analysis of coffee beans

About 100 mg of the same coffee powder was placed in the extraction cartridge by the same procedure in SFE–HPLC. Batch SFE was then performed with a 500-μl trap loop instead of the extract trap column. After SFE, the carbon dioxide containing the extract was transferred to the trap loop, and introduced directly into the separation column by switching the injector valve, as described in *Hydraulics of directly coupled SFE–SFC.*

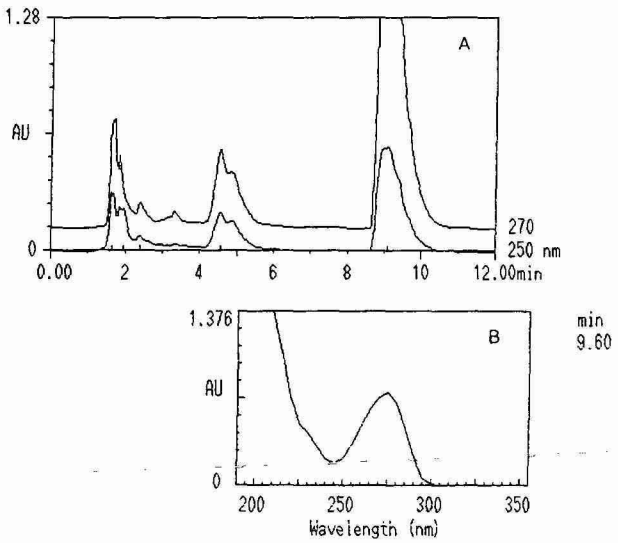

Fig. 6. (A) Chromatograms monitored at 250 and 270 nm and (B) UV spectrum taken at 9.60 min. The chromatograms were produced from the three-dimensional chromatogram shown in Fig. 5. The UV spectrum shows that the chromatographic peak eluted at 9.2 min is that of caffeine.

The three-dimensional chromatogram obtained by the SFE–SFC method is shown in Fig. 5 (the conditions are listed in the caption). A large caffeine peak is clearly seen at 9.2 min in the chromatogram. Ordinary chromatograms monitored at 250 and 270 nm are shown in Fig. 6A; these are not very informative without spectral data. In order to identify the caffeine peak chromatographically, one might subject the caffeine standard to SFC. However, the solvent in which caffeine is dissolved influences the retention behaviour significantly, resulting in identification difficulties. Therefore, spectral data are necessary for efficient identification of peak components in SFC. Fig. 6B shows the spectrum taken at 9.60 min. The curve shows the clear characteristics of the caffeine spectrum.

So far, we have discussed the directly coupled SFE–SFC method from the viewpoint of qualitative analysis. The quantitative accuracy of the method has not yet been closely examined, partly because the amount of coffee powder was so large that the chromatographic peak gave absorbances too high for quantitation, and partly because the volume of the extraction cartridge did not properly match the volume of the trap loop for quantitative analysis. A study of quantitative analysis by this method is currently underway.

CONCLUSION

We have demonstrated that the directly coupled SFE–SFC system allows the analyst to apply raw and/or solid samples to the system to obtain chromatograms of sample extracts. This could be a powerful technique for extending the application of chromatography to natural products, biological compounds, petrochemical products, etc., where extraction is necessary before analysis.

In addition, a highly sensitive multiwavelength detector permits on-line UV spectrum monitoring of the extraction process, which has not previously been possible in a large-scale extraction system. Therefore, one can easily investigate optimal extraction parameters at low cost without operating a pilot-plant extraction system, which requires large amounts of sample and extraction medium.

ACKNOWLEDGEMENT

We thank Mr. Konishi for drawing the schematics for this paper.

REFERENCES

1 G. M. Schneider, E. Stahl and G. Wilke (Editors), *Extraction with Supercritical Gases*, Verlag Chemie, Weinheim, 1980, p. 1.
2 E. Stahl and E. Schutz, *Planta Med.*, 40 (1980) 262.
3 E. Stahl, E. Schutz and H. Mangold, *J. Agr. Food Chem.*, 28 (1980) 1153.
4 D. F. Williams, *Chem. Eng. Sci.*, 36 (1981) 1769.
5 H. Coenen and P. Rinza, *Tech. Mitt. Krupp-Werksberichte*, 39 (1981) H1, Z1.
6 H. Brogle, *Chem. Ind. (London)*, 19 June 1982.
7 R. P. de Filippi, *Chem. Ind. (London)*, 19 June 1982.
8 T. R. Bott, *Chem. Ind. (London)*, 19 June 1982.
9 R. Vollbrecht, *Chem. Ind. (London)*, 19 June 1982.
10 J. P. Calame and R. Steiner, *Chem. Ind. (London)*, 19 June 1982.
11 D. S. Gardner, *Chem. Ind. (London)*, 19 June 1982.

12 G. Brunner and S. Peter, *Ger. Chem. Eng.*, 5 (1982) 181.
13 E. Stahl and W. Schiltz, *Z. Anal. Chem.*, 280 (1976) 99.
14 E. Stahl, *J. Chromatogr.*, 142 (1977) 15.
15 C. S. Nieass, M. S. Wainwright and R. P. Chaplin, *J. Chromatogr.*, 194 (1980) 335.
16 C. S. Nieass, R. P. Chaplin and M. S. Wainwright, *J. Liq. Chromatogr.*, 5 (1982) 2193.
17 K. K. Unger and P. Roumeliotis, *J. Chromatogr.*, 282 (1983) 519.
18 E. Klesper, A. H. Corwin and D. A. Turner, *J. Org. Chem.*, 27 (1962) 700.
19 N. M. Karayannis, A. H. Corwin, E. W. Baker, E. Klesper and J. A. Walter, *Anal. Chem.*, 40 (1968) 1736.
20 M. N. Myers and J. C. Giddings, *Anal. Chem.*, 38 (1966) 294.
21 M. N. Myers and J. C. Giddings, *Anal. Chem.*, 37 (1965) 1453.
22 J. C. Giddings, M. N. Myers and J. W. King, *J. Chromatogr. Sci.*, 7 (1969) 276.
23 R. E. Jentoft and T. H. Gouw, *J. Chromatogr. Sci.*, 8 (1970) 138.
24 R. E. Jentoft and T. H. Gouw, *Anal. Chem.*, 44 (1972) 681.
25 T. H. Gouw and R. E. Jentoft, *J. Chromatogr.*, 68 (1972) 303.
26 M. Novotný, W. Bertsch and A. Zlatkis, *J. Chromatogr.*, 61 (1971) 17.
27 D. Bartmann and G. M. Schneider, *J. Chromatogr.*, 83 (1973) 135.
28 M. Novotny, S. R. Springston, P. A. Peaden, J. C. Fjeldsted and M. L. Lee, *Anal. Chem.*, 53 (1981) 407A.
29 P. A. Peaden, J. C. Fjeldsted, M. L. Lee, S. R. Springston and M. Novotny, *Anal. Chem.*, 54 (1982) 1090.
30 S. R. Springston and M. Novotny, *Anal. Chem.*, 56 (1984) 1762.
31 P. A. Peaden and M. L. Lee, *J. Chromatogr.*, 259 (1983) 1.
32 P. A. Peaden and M. L. Lee, *J. Liq. Chromatogr.*, 5 (1982) 179.
33 J. C. Fjeldsted and M. L. Lee, *Anal. Chem.*, 56 (1984) 619A.
34 T. Takeuchi, D. Ishii, M. Saito and K. Hibi, *J. Chromatogr.*, 295 (1984) 323.
35 Y. Hirata and F. Nakata, *J. Chromatogr.*, 295 (1984) 315.
36 Y. Hirata, *J. Chromatogr.*, 315 (1984) 39.
37 Y. Hirata, *J. Chromatogr.*, 315 (1984) 31.
38 R. D. Smith, W. D. Felix, J. C. Fjeldsted and M. L. Lee, *Anal. Chem.*, 54 (1982) 1883.
39 R. D. Smith, H. T. Kalinoski, H. R. Udseth and B. W. Wright, *Anal. Chem.*, 56 (1984) 2476.
40 J. B. Crowther and J. D. Henion, *Pitts. Conf. Abs.*, (1985) No. 539.
41 K. H. Shafer and P. R. Griffiths, *Anal. Chem.*, 55 (1983) 1939.
42 S. V. Olesik, S. B. French and M. Novotny, *Chromatographia*, 18 (1984) 489.
43 C. C. Johnson, J. W. Jordan, R. J. Skelton and L. T. Taylor, *Pitts. Conf. Abs.*, (1985) No. 538.
44 M. G. Rawdon, *Anal. Chem.*, 56 (1984) 831.
45 T. A. Norris and M. G. Rawdon, *Anal. Chem.*, 56 (1984) 1767.
46 T. L. Chester, *J. Chromatogr.*, 299 (1984) 424.
47 D. R. Gere, R. Board and D. McManigill, *Anal. Chem.*, 54 (1982) 736.
48 T. Greibrokk, A. L. Blilie, E. J. Johansen and E. Lundanes, *Anal. Chem.*, 56 (1984) 2681.
49 L. G. Randall, *Separ. Sci. Technol.*, 17 (1982) 1.
50 K. Sugiyama, M. Saito and A. Wada, *Jap. Pat. Appl.*, 58-117773 (1983).
51 K. Sugiyama, M. Saito and A. Wada, *U.S. Pat. Appl.*, 676,200 (1984).
52 S. Tohei, S. Kohara and M. Saito, *Pitts. Conf. Abs.*, (1984) No. 179.
53 T. Hoshino, M. Senda, T. Hondo, M. Saito and S. Tohei, *J. Chromatogr.*, 316 (1984) 473.
54 K. Jinno, T. Hondo and M. Saito, *Chromatographia*, 20 (1985) in press.

Journal of Chromatography, 332 (1985) 117–125
Elsevier Science Publishers B.V., Amsterdam — Printed in The Netherlands

CHROMSYMP. 638

LOW DEAD VOLUME COULOMETRIC DETECTOR FOR LIQUID CHROMATOGRAPHY

YOSHINORI TAKATA*,* and MAMORU TAKI
Branch Laboratory at Hitachi Research Laboratory, Central Research Laboratory, Hitachi Ltd., 4026 Kuji-machi, Hitachi, Ibaraki 319-12 (Japan)
MITSUO ITO
Naka Works, Hitachi Ltd., 882 Ichige, Katsuta, Ibaraki 312 (Japan)
and
TOSHIRO MURAO
Hitachi Instrument Engineering Co. Ltd., 882 Ichige, Katsuta, Ibaraki 312 (Japan)
(First received April 5th, 1985; revised manuscript received May 24th, 1985)

SUMMARY

A low dead volume coulometric detector flow cell for liquid chromatography was designed. Its cylindrical flow cell structure is simple and the cell volume is extremely small. The working and counter electrodes are made of bundled carbon fibres, and the working and counter electrode compartments are separated by a cation-exchange tube. The detector is applicable to many types of compounds. The detection limit for catecholamines is 0.05 pmol.

INTRODUCTION

Electrochemical and electrical conductivity detectors, etc., have recently been demonstrated to be useful in high-performance liquid chromatography (HPLC) in addition to conventional spectroscopic methods, absorption and emission spectrophotometry. The electrochemical detector is unique owing to its selectivity and low detection limit[1–4]. Many biochemical compounds are electrochemically active, and their concentrations in biological systems are extremely low, so that the electrochemical detector is a powerful instrument in the analysis of biochemical samples.

Of electrochemical detectors for liquid chromatography, the amperometric detector has been used more often than the coulometric detector as its simple and small cell volume structure is suitable for use as an HPLC detector[1,4]. The electrolytic efficiency in the amperometric detector, however, is low, being about 30% or less with standard columns, and is easily affected by the environmental conditions, so that sometimes the poor reproducibility of its sensitivity is a problem. The coulo-

* Present address: Naka Works, Hitachi Ltd., 882 Ichige, Katsuta, Ibaraki 312, Japan.

0021-9673/85/$03.30

metric detector[4–7] has an electrochemical efficiency of about 100% and the reproducibility of the signal intensity is superior to that of the amperometric detector. However, this higher electrolytic efficiency dose not necessarily lead to lower detection limits, because the background current of the coulometric detector is much higher than that of the amperometric detector. Hence a small cell volume and a lower background current are required in order to achieve lower detection limits.

The coulometric detector cell first made by Takata and Muto[3,5] had a working electrode consisting of carbon cloth or metal gauze (platinum or silver) to enlarge its surface area. The reference electrode was made of silver–silver iodide wire netting and gave a uniform potential over the entire working electrode. An ion-exchange membrane tube diaphragm separated the working and reference electrode compartments. Two glassy carbon plates were used as electrodes in Lankelma and Poppe's cell[6], one being the working electrode and the other the counter electrode. The detection limit of this detector was 1 pmol for perphenazine. Recently, Hagihara *et al.*[7] reported a coulometric detector for HPLC that could detect 10 fmol of catecholamines. The working electrode was a glassy carbon plate, the counter electrode was a stainless-steel tube and the reference electrode was made of silver netting soaked in saturated potassium chloride solution. The coulometric detector flow cells proposed so far have a flat and stacked electrode structure.

We propose here a coulometric detector flow cell with a cylindrical cell structure. The cell structure is simple and the effective flow cell volume is much smaller than 1 μl. The detection limit of this coulometric detector is 0.05 pmol for catecholamines, and many types of compounds, such as phenols, organic acids and inorganic anions, are detectable.

EXPERIMENTAL

Design of the coulometric detector flow cell

The structure of the coulometric detector flow cell is shown in Fig. 1. The working electrode was made of a bundle of carbon fibres of diameter 7 μm (Torayca

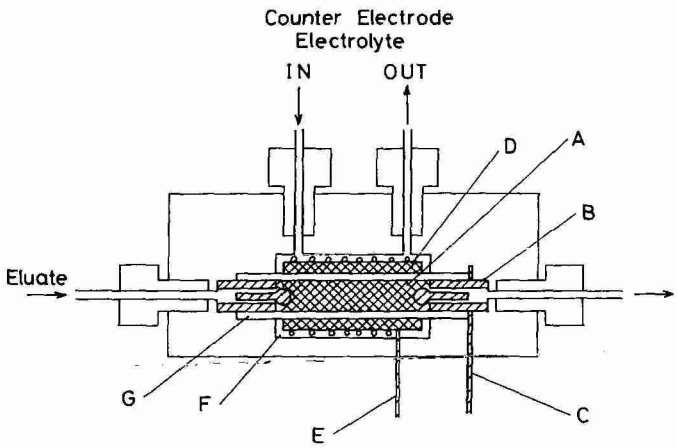

Fig. 1. Construction of the coulometric flow cell. A, Working electrode; B, platinum tube; C, working electrode lead; D, counter electrode; E, counter electrode lead; F, counter electrode compartment; G, Nafion tube.

M40; Toray, Tokyo, Japan). The electrode was constructed as follows. Pre-treatment of the carbon fibres was necessary to remove the surface coating materials. An appropriate number of carbon fibres were soaked in concentrated sulphuric acid for 10 min, washed with distilled water, neutralized with Na_2CO_3 solution until evolution of bubbles of CO_2 ceased and finally rinsed with distilled water. The pre-treated carbon fibres were soaked in distilled water. About 10000 fibres 8 mm long were used to make the working electrode. The bundle of carbon fibres was inserted into a cation-exchange tube of 0.8 mm I.D. and 1.0 mm O.D. (Nafion tube 21T20GA-11-2048; DuPont, Wilmington, DE, U.S.A.), then two platinum tubes of 0.6 mm I.D. and 0.8 mm O.D. were inserted into the Nafion tube from each end. The platinum tubes were kept in contact with the carbon fibre working electrode electrically. The counter electrode was also made of the same carbon fibres. About 20000 carbon fibres were cut to 8 mm in length. The working electrode Nafion tube described above was wrapped with the counter electrode carbon fibres and bound with 0.3 mm diameter platinum wire. The flow cell was installed in the counter electrode compartment. With this configuration, a uniform electrolytic potential was obtained. The maximum usable pressure of the flow cell was 25 kg/cm^2.

As the counter electrode electrolyte $K_3Fe(CN)_6$–$K_4Fe(CN)_6$–KNO_3–KOH solution with a concentration of 0.2 *M* of each component flowed through the counter electrode compartment. The potential of the counter electrode was maintained constant by chemical equilibrium, and then the electrolytic potential of the working electrode, determined as the sum of the counter electrode potential and the settled circuit potential, was constant.

Equipment

The chromatographic system consisted of a Hitachi HPLC pump (Models 635, 655 and 655-15, Hitachi, Tokyo, Japan), a pulse damper (Hitachi Model 655-1681 or a Model LOD-1, Gasukuro Kogyo, Tokyo, Japan) and a Rheodyne 7125 injection valve equipped with a 20- or 100-μl sample loop (Rheodyne, Berkeley, CA, U.S.A.).

Separation System

Catecholamines. The separation column was a 50 × 4 mm I.D. stainless-steel tube packed with Hitachi Gel 3013-C a –COOH-modified polystyrene–divinylbenzene (PS–DVB) cation exchanger (Hitachi). The mobile phase for catecholamine analysis was 2% CH_3COOH–2% CH_3CN–10^{-4} *M* Na_2EDTA solution, pumped at a flow-rate of (a) 1.0 ml/min and (b) 0.6 ml/min. The column was used at the room temperature. The catecholamines DOPA, noradrenaline (NA), adrenaline (A) and dopamine (DA) were purchased from Tokyo Kasei (Tokyo, Japan). The electrolytic potential for catecholamine analysis was +0.6 V *vs.* $Fe(CN)_6^{3-}$–$Fe(CN)_6^{4-}$.

Catecholamine metabolites. 3,4-Dihydroxymandelic acid (DOMA), vanillylmandelic acid (VMA), vanillyl acetic acid (VLA), homovanillic acid (HVA), 5-hydroxyindoleacetic acid (5-HIAA) and 2,5-dihydroxyphenylacetic acid were purchased from Tokyo Kasei. The separation column was Hitachi Gel 3013-O, a-OH-modified PS–DVB polymer (Hitachi)packed in a 150 × 4 mm I.D. column maintained 35°C. The mobile phase was 0.05 *M* tartaric acid–CH_3CN–1 *M* NaOH (88:12:1.5) at a flow-rate of 0.5 ml/min. The electrolytic potential for catecholamine metabolites was +0.5 V *vs.* $Fe(CN)_6^{3-}$–$Fe(CN)_6^{4-}$.

Lactic acid. A mixed sample of *d*- and *l*-lactic acids was separated with a 250 × 4 mm I.D. Chiralpak-WH column (Daicel Chemical Industries, Osaka, Japan). The mobile phase was 0.25 m*M* $CuSO_4$ solution at a flow-rate of 1.0 ml/min. The column was used at ambient temperature. The electrolytic potential for lactic acid was +1.1 V *vs.* $Fe(CN)_6^{3-}$–$Fe(CN)_6^{4-}$.

Inorganic anions. MCI-SCAO2 (Mitsubishi Chemical Industries, Tokyo, Japan) anion-exchange resin packed in a 150 × 4 mm I.D. column was used for the separation of inorganic anions. The mobile phase was 1 m*M* phthalic acid solution containing 10^{-4} *M* Na_2EDTA, the pH being adjusted to 4.0 with KOH. The pumping rate of the eluent was 1.0 ml/min. The column was used at ambient temperature. The electrolytic potential was varied from +0.8 to +1.1 V *vs.* $Fe(CN)_6^{3-}$–$Fe(CN)_6^{4-}$.

RESULTS AND DISCUSSION

Contruction of the coulometric detector cell

Number of working electrode carbon fibres. As an electrolytic efficiency of 100% is essential for a coulometric detector, we examined the effect of the number of carbon fibres used in the working electrode on the electrolytic efficiency. The number was varied from 6000 to 10000 while the length of the working electrode was fixed at 8 mm. The results are shown in Fig. 2. When the number of carbon fibres was less than 8000 the electrolytic efficiency was in the range 20–90%. On the other hand, when the number of carbon fibres was 10000, the efficiency became 90–100%. When the number of carbon fibres was less than 8000, the electrolytic efficiency was affected by the mode of insertion of the working electrode in the Nafion tube. A working electrode with a twisted bundle of carbon fibres displayed a higher efficiency than that with non-twisted fibres. When the number of carbon fibres was less than 8000, it was difficult to make a flow cell with a reproducibly high electrolytic efficiency.

Length of working electrode. The length of the working electrode carbon fibres

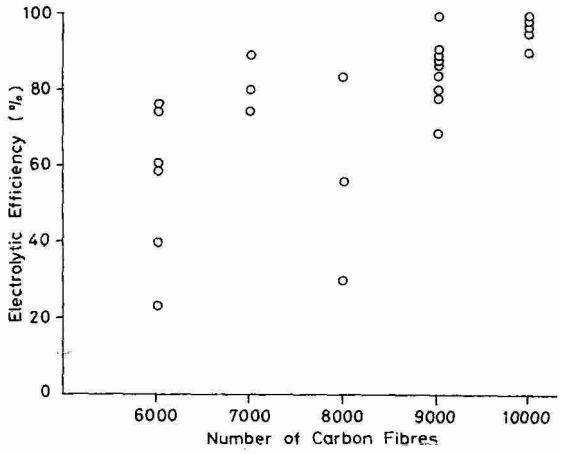

Fig. 2. Relationship between electrolytic efficiency and the number of carbon fibres. The length of the working electrode is 8 mm.

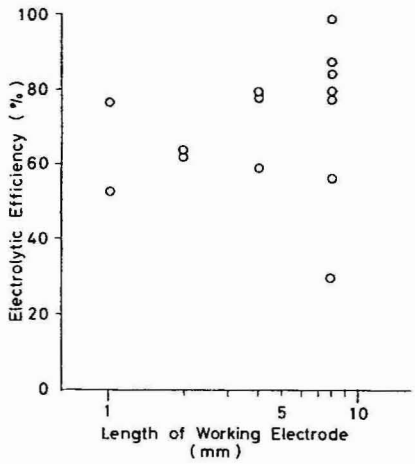

Fig. 3. Relationship between electrolytic efficiency and the length of the working electrode. The number of carbon fibres is 8000–9000.

was varied from 1 to 8 mm, keeping the number of fibres in the range 8000–9000. As shown in Fig. 3. There was a slight increase in electrolytic efficiency with increasing length of the working electrode. However, the electrolytic efficiency with a particular length of the working electrode was variable and was probably dependent on the treatment of the carbon fibres.

Electrolytic efficiency vs. electrolytic potential. Fig. 4 shows the relationship between the electrolytic potential and electrolytic efficiency. The sample was a mixture of 100 pmol each of DOPA, noradrenaline, adrenaline and dopamine with amount. When the electrolytic potential was lower than +0.3 V, the catecholamines were not oxidized. With increasing potential above +0.3 V the electrolytic efficiency increased rapidly and reached 100% at +0.5 V. Each catecholamine showed similar behaviour. On the other hand, the background current increased gradually with increase in electrolytic potential. At a potential lower than +0.3 V, the background

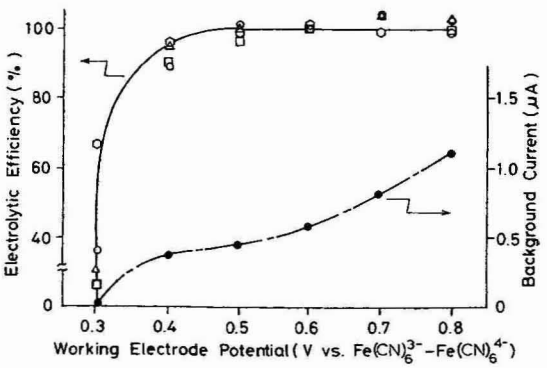

Fig. 4. Dependence of electrolytic efficiency and background current on electrolytic potential. Counter electrode electrolyte: $K_3Fe(CN)_6$–$K_4Fe(CN)_6$–KNO_3–KOH (each 0.2 *M*). ○, DOPA; △, noradrenaline; □, adrenaline; ◇, dopamine.

current was negligibly small. For the purpose of analysis, it is preferable that the electrolytic efficiency is saturated while the background current is as low as possible. It was found that the optimum potential for catecholamine analysis was in the range +0.5 to +0.6 V.

Detection limit of the coulometric detector

We compared the detection limit of the coulometric detector described above with that of a Hitachi 630 coulometric detector in which the working electrode consists of carbon fibre cloth. The sample was a mixture of the catecholamines DOPA, noradrenaline, adrenaline and dopamine. The flow cell volume of the Hitachi 630 coulometric detector is large (360 μl when the carbon fibre cloth working electrode is not installed) and the background current is large. The chromatographic peaks were broad in such a large flow cell, and hence the intensity and the resolution of the chromatogram were low. On the other hand, the coulometric detector described here had a small cell volume of 2 μl when the working electrode was not installed and the ultimate cell volume may be much smaller than 1 μl, and had a lower background current. The reduction in intensity and loss of resolution in the chromatogram was minimized by the extremely small cell volume, and the lower background current made it possible to achieve higher sensitivity. As can be seen from Fig. 5, the new coulometric detector showed a detection limit two orders of magnitude lower than the Hitachi 630 coulometric detector at an equal signal-to-noise ratio.

Good linearity was obtained between the peak height and the amount of sample injected over the range 1–100 pmol.

Applications

Catecholamines. For rapid analysis of catecholamines, we examined a packing material of smaller particle size. The column used was 50 × 4 mm I.D. packed with Hitachi Gel 3057 silica ODS (3 μm diameter particle size) (Hitachi), the mobile phase

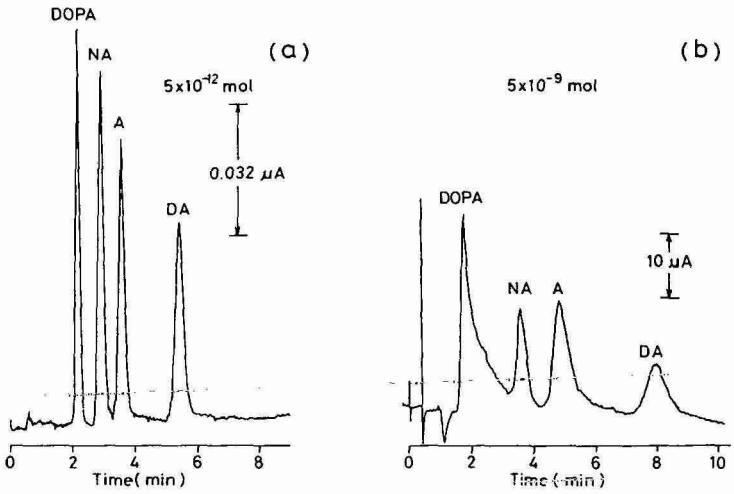

Fig. 5. Chromatogram of catecholamines. Detector: (a) coulometric detector described here; (b) Hitachi 630 coulometric detector. For conditions, see Experimental.

was an aqueous solution of 0.1 *M* $MgSO_4$–0.04 *M* KH_2PO_4–4% CH_3CN–0.1 m*M* Na_2EDTA at a flow-rate of 1.0 ml/min and the working electrode potential was +0.6 V. As shown in Fig. 6, all four catecholamines were eluted within 60 sec. Owing to the small cell volume, the dispersion in the flow cell was small. Hence the coulometric detector flow cell described above is particularly suitable for liquid chromatography with smaller particle columns. A 0.5 pmol amount of each catecholamine could easily be detected, and we conclude that the detection limit for catecholamines with this detector is 0.05 pmol.

Catecholamine metabolites. Fig. 7a shows the analysis of a mixture of the catecholamine metabolites DOMA, VMA, HVA and 5-HIAA and 2,5-dihydroxyphenylacetic acid.

The metabolism of catecholamines is affected by disease in neuroblasts, and the analysis of catecholamines and their metabolites is desirable in biochemistry and medicine. A 10-μl sample of human urine without pre-treatment was analyzed and the result is shown in Fig. 7b.

Lactic acid. Fig. 8 shows the separation of the *d*- and *l*-enantiomers of lactic acid on a Chiralpak-WH column with 0.25 m*M* $CuSO_4$ solution as the mobile phase and an electrolytic potential of +1.1 V. However, the separating conditions were not suitable for the detector system. Cu^{2+} ion in the eluent penetrates the cation-exchange tube and forms insoluble $Cu_2Fe(CN)_6$ on the surfaces of the Nafion tube and the counter electrode, with a reduction in electrolytic efficiency. A different counter electrode solution must be used that does not form a complex or insoluble compound with the mobile phase, *e.g.*, hydroquinone–benzoquinone.

Inorganic anions. Inorganic ions are usually detected with a conductivity detector (ion chromatography[8–10]). Other detectors with a selective sensitivity are needed, because the universality of the sensitivity of the conductivity detector sometimes makes it difficult to detect a specific ion of interest.

Some kinds of inorganic anions and metal cations are electrochemically active,

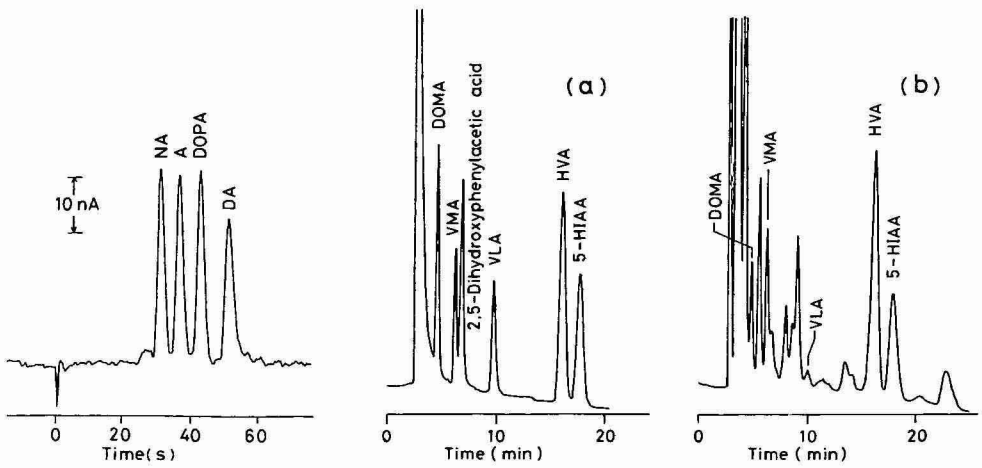

Fig. 6. Rapid separation of catecholamines. Sample amount, 0.5 pmol each. For conditions, see text.

Fig. 7. (a) Chromatogram of catecholamine metabolites. Sample amount, 20 ng. (b) 10-μl human urine sample without pre-treatment. For conditions, see Experimental.

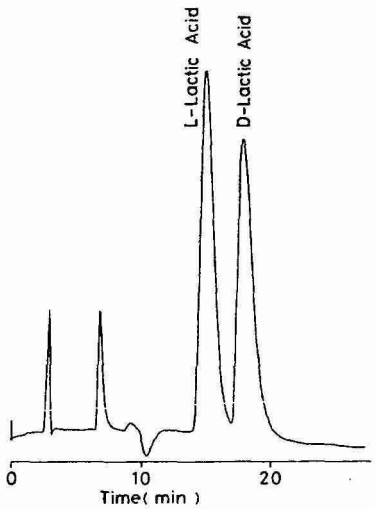

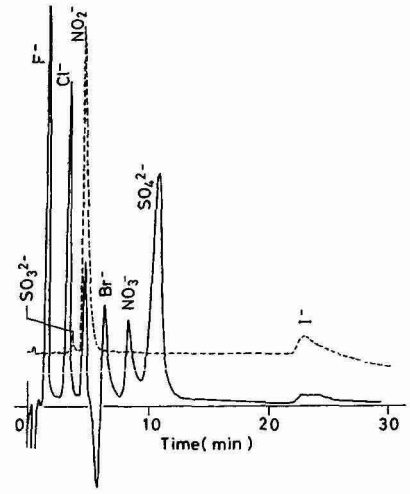

Fig. 8. Separation of lactic acid enantiomers. For conditions, see Experimental; potential, +1.1 V.

Fig. 9. Chromatogram of inorganic anions. solid line: indirect photometry at 270 nm; broken line, coulometry at +0.8 V. For conditions, see Experimental.

and an electrochemical detector is useful for such compounds owing to its unique selectivity and high sensitivity. The solid line in Fig. 9 shows inorganic anions detected by indirect photometry[11]. Each compound in the sample had a concentration of 10 ppm. The broken line shows the chromatogram of the same sample detected with the coulometric detector at a potential of +0.8 V. Of the anions F^-, Cl^-, Br^-, I^-, NO_2^-, NO_3^-, SO_3^{2-} and SO_4^{2-}, three species, SO_3^{2-}, NO_2^- and I^-, were detectable. The signal intensity of SO_3^{2-} was very low compared with the initially added sample concentration. It is expected that the SO_3^{2-} ion is readily oxidized in aqueous solution. For the SO_3^{2-} sample solution, the SO_4^{2-} signal was also observed by indirect photometry.

Two results are of interest: (1) NO_2^- was detected by our coulometric detector, whereas the detection of NO_2^- in an electrochemical detector with a silver working electrode was not reported[12]; (2) on the other hand, Br^- was not detected by the carbon fibre working electrode but it is detectable by a silver working electrode[12]. This may be explained as follows. The process $Ag + Br^- \rightarrow AgBr + e^-$ is a primary process in the detection of Br^- with a silver electrode system, whereas the corresponding process does not occur on the surface of the carbon fibre electrode.

CONCLUSION

It is easy to miniaturize a coulometric detector flow-cell by use of an ion-exchange tube as a diaphragm in such a flow cell structure as described above. In this work, we constructed a flow cell with an effective cell volume of less than 1 μl. It is expected that a coulometric flow cell with a smaller volume and a lower background current could be constructed by use of a thinner ion-exchange tube, and that this flow cell will be applicable to micro-HPLC.

ACKNOWLEDGEMENTS

We thank to Dr. S. Ganno and Mr. K. Tsukada of Naka Works, Hitachi, Ltd. for helpful discussions and advice.

REFERENCES

1 P. T. Kissinger, C. J. Refshauge, R. Dreiling, L. Blank, R. Freeman and J. Adams, *Anal. Lett.*, 6 (1973) 465.
2 D. C. Johnson and J. Larochelle, *Talanta*, 20 (1973) 959.
3 Y. Takata and G. Muto, *Bunseki Kagaku (Jap. Anal.)*, 14 (1965) 453.
4 P. T. Kissinger, *Anal. Chem.*, 49 (1977) 448A.
5 Y. Takata and G. Muto, *Anal. Chem.*, 45 (1973) 1864.
6 J. Lankelma and H. Poppe, *J. Chromatogr.*, 125 (1976) 375.
7 B. Hagihara, K. Kogoh, M. Saito, S. Shiraishi, T. Hashimoto, K. Tagawa and H. Wada, *J. Chromatogr.*, 281 (1983) 59.
8 H. Small, T. S. Stevens and W. C. Bauman, *Anal. Chem.*, 47 (1975) 1801.
9 D. T. Gjerde, J. S. Fritz and G. Schmuckler, *J. Chromatogr.*, 186 (1979) 509.
10 T. S. Stevens, J. C. Davis and H. Small, *Anal. Chem.*, 53 (1981) 1488.
11 H. Small and T. E. Miller, Jr., *Anal. Chem.*, 54 (1982) 462.
12 R. D. Rocklin and E. L. Johnson, *Anal. Chem.*, 55 (1983) 4.

Journal of Chromatography, 332 (1985) 127–137
Elsevier Science Publishers B.V., Amsterdam — Printed in The Netherlands

CHROMSYMP. 629

REVERSED-PHASE LIQUID CHROMATOGRAPHIC INVESTIGATION OF NUCLEOSIDES AND BASES IN MUCOSA AND MODIFIED NUCLEOSIDES IN URINES FROM PATIENTS WITH GASTROINTESTINAL CANCER

KATSUYUKI NAKANO*, KATSUHISA SHINDO and TOSHIO YASAKA
Perfect Liberty (PL) Medical Data Center, 1 Kamiyamacho, Tondabayashi, Osaka 584 (Japan)
and
HIDEKI YAMAMOTO
The Second Department of Surgery, Osaka University Medical School, Fukushima-ku, Osaka 553 (Japan)
(First received March 25th, 1985; revised manuscript received May 7th, 1985)

SUMMARY

Reversed-phase high-performance liquid chromatography (HPLC) has been used to determine the level of nucleic acid metabolites in perchloric acid extracts of gastrointestinal mucosa. By comparing the levels of these compounds in the normal portion with the levels in the neoplastic portion of mucosa resected from patients with malignant cancer, it was found that uracil was significantly elevated in the neoplastic colorectal mucosa (adenocarcinoma) of eight patients with colorectal cancer ($P < 0.01$, statistically significant with the paired t test). The mean level of uracil in neoplastic colorectal mucosa was 2.7-fold higher than that in normal mucosa. However, in neoplastic gastric mucosa, only one out of four patients with gastric cancer showed elevated uracil. In neoplastic mucosa, the levels of hypoxanthine and uridine for colorectal cancer, and inosine for gastric cancer, were also significantly higher than those in normal mucosa ($P < 0.05$, with the paired t test). The urinary modified nucleosides were prefractionated with a boronate affinity gel column, and their levels determined by the same HPLC method. No significant differences in the concentrations of pseudouridine, 1-methylguanosine, N^2-methylguanosine or N^2,N^2-dimethylguanosine were observed in pre- and post-operative urines from patients with colorectal cancer and normal urines.

INTRODUCTION

Nucleotides in biological samples have been studied using several modes of high-performance liquid chromatography (HPLC) in order to examine normal metabolic and disease processes[1–3] in the liver[4–7], heart[8–11], brain[12], granulation tissue[13], Hela cells[14] and tissue perfusates[15,16]. Less information is available on the level of nucleosides and bases in tissue, because the major metabolites of nucleic acid catabolism in tissues such as the liver and heart, or blood cells, examined so far were nucleotides and coenzymes. Until now, the endogenous compounds in acid extracts

0021-9673/85/$03.30

of gastrointestinal (GI) mucosa have not been studied by the HPLC method. The investigation of mucosal compounds is of primary importance because most GI adenocarcinomas arise originally from the mucosal tissue of the stomach or intestine. Therefore, differences in the profiles of ultraviolet (UV)-absorbing compounds in normal and neoplastic mucosa could provide important information on the nucleic acid metabolism in mucosa of patients with malignant cancer.

On the other hand, the urinary modified nucleosides derived from the enzymatic degradation of transfer RNA have been investigated as biochemical markers in cancer detection[17–20]. In more recent studies, these nucleosides have been prefractionated on a boronate affinity gel column, and then determined by reversed-phase HPLC techniques[21,22].

Recently, we used reversed-phase HPLC to examine the UV-absorbing compounds in perchloric acid extracts of the normal portion and the neoplastic portion of mucosa, resected surgically from patients with GI cancer. We also studied the change in nucleoside levels in urine samples collected before and after surgical operation on the same patient with colorectal cancer. In this paper, we describe the results complementary to the accompanying paper[23].

EXPERIMENTAL

Chromatographic conditions

The UV-absorbing compounds and nucleoside fractions in perchloric acid extracts of GI mucosa, and the urinary nucleosides of patients with colorectal cancer and of normal subjects, were analyzed under the following chromatographic conditions: HPLC instrument, Hitachi 638-30 (Hitachi, Tokyo, Japan); column, Develosil ODS-5 (5 μm, 250 × 4.6 mm I.D.; Nomura Chemicals, Nagoya, Japan); pre-column, Develosil ODS (15–30 μm, 50 × 4.0 mm I.D.); elution, linear gradient from 0.02 *M* KH_2PO_4 (pH 4.53) to 40% methanol–water (3:2, v/v) in 35 min; flow-rate, 1.2 ml/min; temperature, ambient; detection, UV at 260 and 280 nm (0.16 a.u.f.s.); sample volume, 100 μl unless stated otherwise.

Boronate gel affinity chromatography

The boronate affinity gel column technique was used to isolate nucleosides in 1 ml of perchloric acid extracts of mucosa homogenate and 0.5 ml of urine samples. The isolation procedure was a slight modification of the method developed by Gehrke *et al.*[21]. The boronate gel, Affi-gel 601 (Bio-Rad Labs., Richmond, CA, U.S.A.), was packed in the plastic column (60 × 9 mm I.D.; bed volume, 0.83 ml) and equilibrated with 0.25 *M* ammonium acetate, pH 8.8. A 1-ml volume of the mucosa extracts or 0.5 ml of urine samples (samples were adjusted to pH 9.5 with 2.5 *M* ammonium acetate) was loaded on top of the column. The column was washed with 8 ml of 0.25 *M* ammonium acetate, pH 8.8. Nucleosides were eluted with 4 ml of 0.2 *M* formic acid. The eluate was evaporated under reduced pressure and redissolved in 0.5 ml of the starting buffer for HPLC analysis.

Sample collection

The normal and neoplastic portions of mucosa from the colorectum and stomach were obtained by surgical operation on eight patients with malignant colorectal

cancer and four patients with malignant gastric cancer, respectively. Resected mucosa samples were frozen immediately after the operation and kept at −70°C until used.

Urine samples one day before and one week after the surgical operations on eight patients with malignant colorectal cancer were collected in the morning after a 12-h fasting period. Urine samples from sixteen normal subjects were obtained from the PL Osaka Health Control Center.

Sample preparation

The preparation of normal and neoplastic mucosa samples was as follows. Mucosa samples (colorectum or stomach), 1.25 g wet weight, were minced with scissors to ease the following homogenization. After the addition of 3 ml of cold water, the minced mucosa samples were homogenized using a micro Waring blender. The blender vessel was washed with 1 ml of cold water, then 5 ml of cold perchloric acid (5%, w/v) were added to the homogenized mucosa. The mixture was vortexed vigorously and allowed to stand on ice for about 30 min. Then, the mixture was centrifuged at 1500 *g* for 10 min. The supernatant was neutralized with 10 *M* potassium hydroxide (to approximately pH 5). The pH-adjusted samples were centrifuged to remove precipitable perchlorate. The resulting supernatants were stored at −20°C until HPLC analysis.

Urine samples were stored at −20°C, and centrifuged at low speed to remove the precipitable compounds before use.

Peak identification

The UV-absorbing compounds in the perchloric acid extracts of GI mucosa and in prefractionated urines were identified on the basis of the retention times, simultaneous injection of standards, peak-height ratios, UV-absorption spectra of fractionated HPLC peaks and the enzymatic peak shift, as developed by Brown and co-workers[24–26]. In addition, the nucleosides were confirmed by the HPLC separation of samples prefractionated on the boronate affinity gel column.

RESULTS

Chromatograms of extracts of mucosa and muscle

The chromatograms in Fig. 1 show the UV-absorbing compounds in perchloric acid extracts of the normal and neoplastic portions of mucosa, and of normal muscle from sigmoid colon, resected surgically from a patient with sigmoid colon cancer. Fig. 1 is typical of the profiles observed for most GI mucosa and muscle. The peaks present in the majority of GI mucosa samples are numbered.

The chromatograms of standards appear in the accompanying paper[23]. The chromatographic conditions developed by Hartwick *et al.*[27] were slightly modified to improve the separation of the early part of a chromatogram of serum profile[26] for UV-absorbing compounds. Based on all the data from the identification techniques, the endogenous compounds present in GI mucosa and muscle were identified as uracil, uric acid, hypoxanthine, xanthine, uridine, inosine and guanosine. Peak 1 in Fig. 1 was confirmed as uracil from the characteristic change (bathochromic shift) of the UV-absorption spectrum at alkaline pH, as shown in Fig. 2, as well as from the retention time, simultaneous injection of the standard and the peak-height ratio.

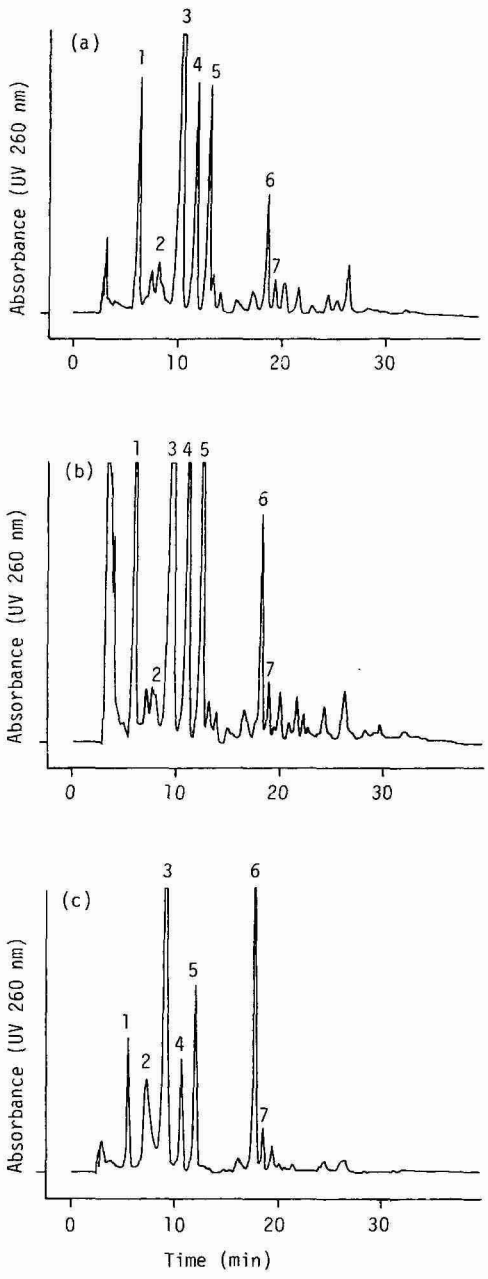

Fig. 1. Chromatograms of perchloric acid extracts of normal mucosa (a), neoplastic mucosa (b) and normal muscle (c) of the sigmoid colon from a patient with malignant sigmoid colon cancer. Injection volume: 100 μl, corresponding to 13.9 mg of wet tissue. For chromatographic conditions see text. Peaks: 1 = uracil; 2 = uric acid; 3 = hypoxanthine; 4 = xanthine; 5 = uridine; 6 = inosine; 7 = guanosine.

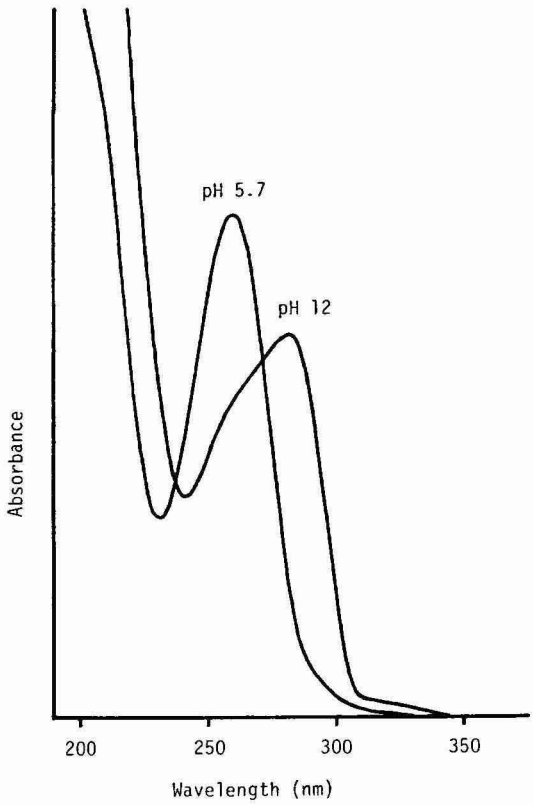

Fig. 2. UV absorption spectra of peak 1 (uracil) in Fig. 1.

The majority of these peaks corresponded to components found in serum[26] and saliva[28]. Compared with the profiles of serum and saliva, the profiles of GI mucosa and muscle showed relatively high levels of hypoxanthine, xanthine and especially uracil, and a low level of uric acid as seen in Fig. 1.

Fig. 1 also compares the chromatograms of normal mucosa with those of neoplastic mucosa and normal muscle from the same patient. A considerable increase in all the major components except uric acid was found in neoplastic mucosa.

Peak 2 in Fig. 1c represents uric acid and nucleotides. From the HPLC analysis obtained after using the boronate affinity gel column, it was found that muscle samples contained relatively large amounts of nucleotides.

Compound levels in mucosa from cancer patient

The concentrations of endogenous compounds in perchloric acid extracts of GI mucosa were determined by the HPLC method described. Fig. 3 shows the levels of these compounds in the normal and neoplastic portions of mucosa from the same patient. A significant elevation of uracil was found in neoplastic colorectal mucosa (adenocarcinoma) from eight patient with colorectal cancer ($P < 0.01$, statistically significant with the paired t test). The mean level of uracil in neoplastic colorectal mucosa was 2.7-fold higher than in normal mucosa. In the neoplastic mucosa of

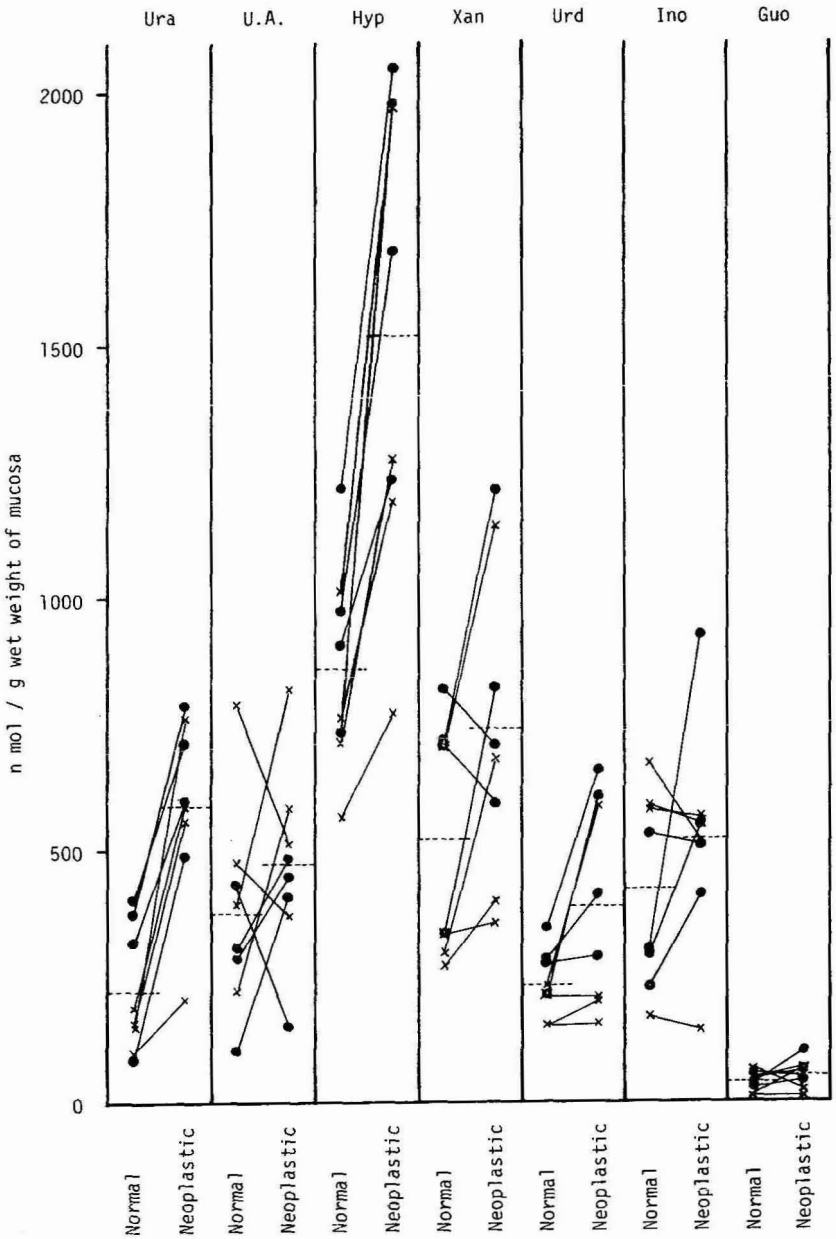

Fig. 3. The levels of compounds in perchloric acid extracts of normal and neoplastic mucosa from colorectum, resected surgically from eight patients with colorectal cancer. The broken lines are the mean levels. The dots represent males, the crosses females. Abbreviations used: Ura = uracil; U.A. = uric acid; Hyp = hypoxanthine; Xan = xanthine; Urd = uridine; Ino = inosine; Guo = guanosine.

colorectum, the levels of hypoxanthine and uridine were also significantly higher than those in normal mucosa ($P < 0.05$, with the paired t test).

However, an increase in the uracil level in neoplastic mucosa was found in only one out of four patients with gastric cancer, as shown in Fig. 4. In the neoplastic

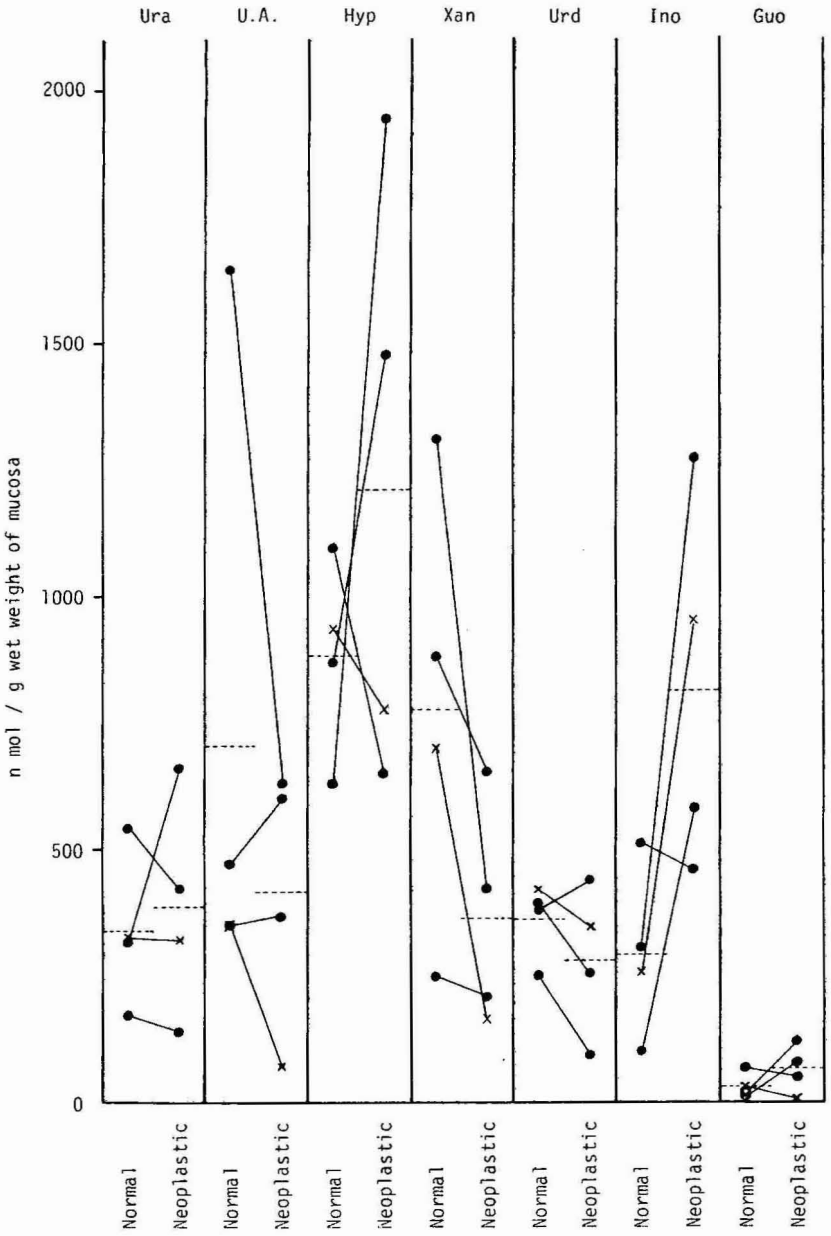

Fig. 4. The levels of compounds in perchloric acid extracts of normal and neoplastic mucosa from the stomach, resected surgically from four patients with gastric cancer. For symbols and abbreviations, see Fig. 3.

mucosa of the stomach, the level of inosine was significantly higher than that in normal mucosa according to the paired t test ($P < 0.05$).

Urinary nucleosides analysis

Urinary nucleosides were isolated by using a boronate affinity gel column. They were then separated and quantified by the HPLC procedure described. Fig. 5

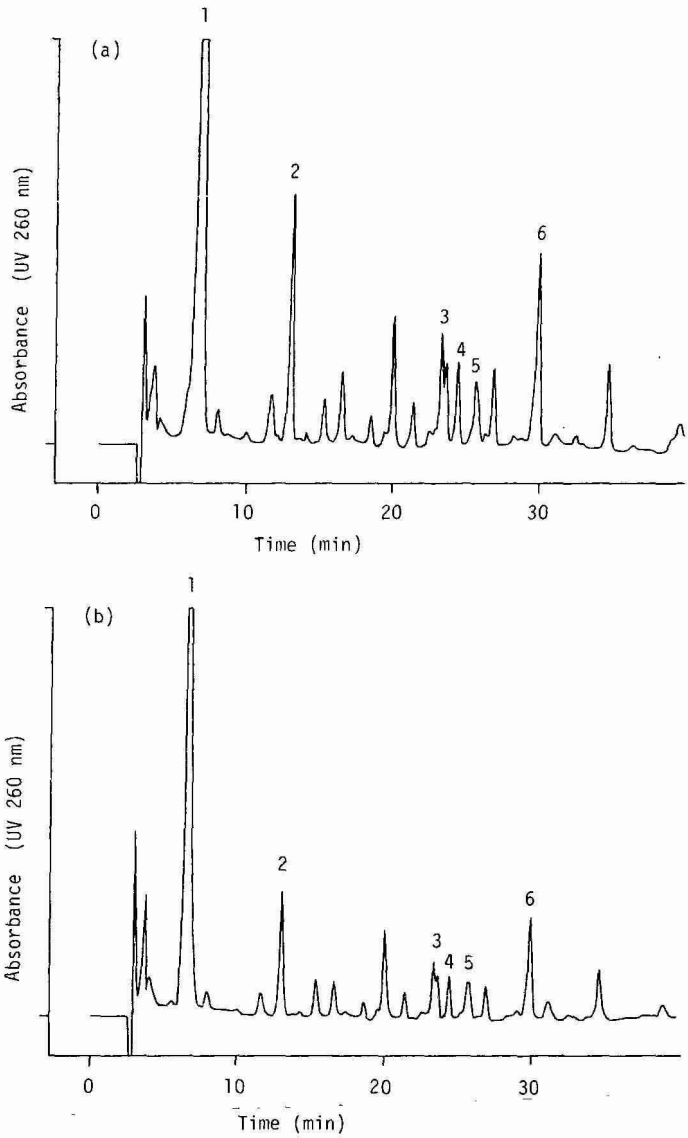

Fig. 5. Chromatograms of nucleosides in urine collected before (a) and after (b) surgical operation on a patient with malignant rectal cancer. Injection volume: 200 μl, equivalent to the same volume of urine. For chromatographic conditions see text. Peaks: 1 = pseudouridine; 2 = uridine + 1-methyladenosine; 3 = 1-methylinosine + unknown compound; 4 = 1-methylguanosine; 5 = N^2-methylguanosine; 6 = N^2,N^2-dimethylguanosine.

shows chromatograms of nucleosides in urines taken before and after a surgical operation on a patient with malignant rectal cancer.

Based on the data from the identification techniques and the results reported by Gehrke *et al.*[21,22], the nucleosides present in the majority of urine samples were identified as pseudouridine, 1-methylguanosine, N^2-methylguanosine and N^2,N^2-dimethylguanosine. The peak with the retention time of 13 min (peak 2) contained 1-methyladenosine + uridine and the peak with the retention time of 23.5 min (peak 3) was identified as 1-methylinosine together with an unknown compound.

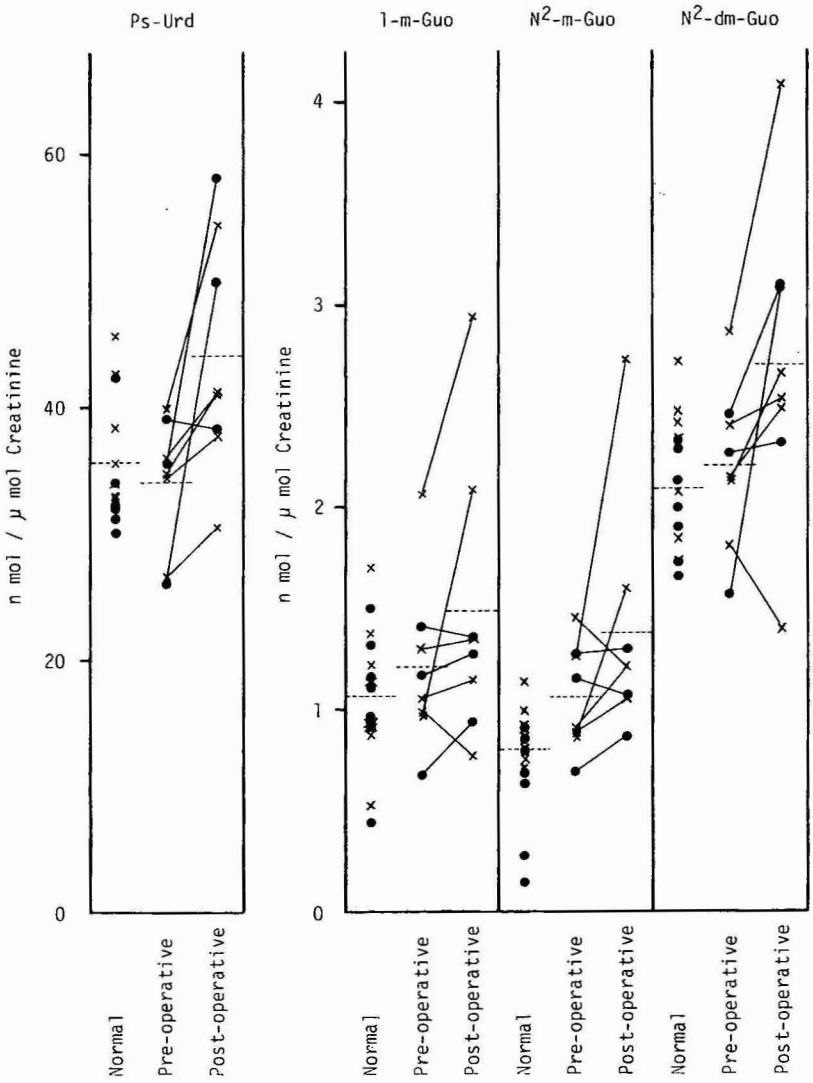

Fig. 6. The levels of urinary modified nucleosides pre- and post-operation for eight patients with colorectal cancer, and sixteen normal subjects. For symbols, see Fig. 3. Abbreviations used: Ps-Urd = pseudouridine; 1-m-Guo = 1-methylguanosine; N^2-m-Guo = N^2-methylguanosine; N^2-dm-Guo = N^2,N^2-dimethylguanosine.

Urinary nucleoside levels of cancer patients

The concentration of modified nucleosides in urine samples was determined by the HPLC method. The urinary nucleoside levels were then converted on the basis of the urinary creatinine level of each sample.

Fig. 6 shows a comparison of urinary nucleoside levels pre- and post-operation for cancer patients and normal subjects. Contrary to previous reports[17–20], the present results did not show an elevation of modified nucleosides in urines from patients with colorectal cancer.

DISCUSSION

An increase in excretion of urinary uracil in leukaemic patients has been reported by Horrigan[29] and Adams *et al.*[30]. The activity of dihydrouracil dehydrogenase (DHUDH, E.C. 1.3.1.2), which is a rate-limiting enzyme of the pyrimidine degradation system, is decreased in rat hepatoma[31,32], embryonic liver[31,32] and human leukaemia[33]. The elevated uracil level in neoplastic colorectal mucosa observed in this study may be related to the decrease in DHUDH activity.

The decrease in activity of xanthine oxidase (E.C. 1.2.3.2), the rate-limiting enzyme of inosine monophosphate (IMP) catabolism, has also been observed in hepatoma and in other tumours[31,32]. Thus, the increased level of hypoxanthine and xanthine in neoplastic mucosa we observed may be related to the decrease in activity of xanthine oxidase.

Several investigations reported elevation of the modified nucleosides in urines from cancer patients[17–20]. Very recently, it was reported that the urinary pseudouridine levels in patients with lung cancer were significantly higher than those of controls and decreased after surgical operation[34]. To confirm these findings the urinary nucleosides, prefractionated on the affinity gel column, were analyzed by the reversed-phase HPLC technique. However, our results show no elevation of modified nucleosides in the preoperative urines of patients with colorectal cancer as compared with postoperative urines and normal urines, as shown in Fig. 6.

ACKNOWLEDGEMENTS

The authors acknowledge Dr. P. R. Brown (Rhode Island University) for her kind and helpful guidance in HPLC techniques, Dr. K. Kiyoshima and Mr. H. Murao (PL Osaka Health Control Center) for the measurement of creatinine and the supply of some samples, and Director S. Oda and Mr. K. Imaizumi (PL Botanical Institute) for the use of equipment and for advice. This study was supported by a grant from Patriarch Takahito Miki and the "Perfect Liberty" Organization.

REFERENCES

1 M. Zakaria and P. R. Brown, *J. Chromatogr.*, 226 (1981) 267.
2 P. R. Brown (Editor), *HPLC in Nucleic Acid Research: Methods and Applications*, Marcel Dekker, New York, 1984.
3 K. Nakano, *Adv. Chromatogr.*, 25 (1985) in press.
4 A. Floridi, C. A. Palmerini and C. Fini, *J. Chromatogr.*, 138 (1977) 203.
5 E. H. Edelson, J. G. Lawless, C. T. Wehr and S. R. Abbott, *J. Chromatogr.*, 174 (1979) 409.

6 E. G. Brown, R. P. Newton and N. M. Shaw, *Anal. Biochem.*, 123 (1982) 378.
7 P. D. Reiss, P. F. Zuurendonk and R. L. Veech, *Anal. Biochem.*, 140 (1984) 162.
8 P. Durre and J. R. Andreesen, *Anal. Biochem.*, 123 (1982) 32.
9 E. Harmsen, P. Ph. DeTombe and J. W. DeJong, *J. Chromatogr.*, 230 (1982) 131.
10 B. Burnette, C. R. McFarland and P. Batra, *J. Chromatogr.*, 277 (1983) 137.
11 G. K. Bedford and M. A. Chiong, *J. Chromatogr.*, 305 (1984) 183.
12 K. Morimoto, K. Tagawa, T. Hayakawa, F. Watanabe and H. Mogami, *J. Neurochem.*, 38 (1982) 833.
13 D. Pruneau, E. Wulfert, M. Pascal and C. Baron, *Anal. Biochem.*, 119 (1982) 274.
14 H. Martinez-Valdez, R. M. Kothari, H. V. Hershey and M. W. Taylor, *J. Chromatogr.*, 247 (1982) 307.
15 F. S. Anderson and R. C. Murphy, *J. Chromatogr.*, 121 (1976) 251.
16 K. M. Taylor, L. Chase and M. Bewick, *J. Liq. Chromatogr.*, 1 (1978) 849.
17 E. Borek, O. K. Sharma and T. P. Waalkes, in G. Nass (Editor), *Recent Results in Cancer Research*, Vol. 84, Springer, Berlin, Heidelberg, 1983, p. 301.
18 F. Salvatore, A. Colonna, F. Costanzo, T. Russo, F. Esposito and F. Cimino, in G. Nass (Editor), *Recent Results in Cancer Research*, Vol. 84, Springer, Berlin, Heidelberg, 1983, p. 360.
19 J. Speer, C. W. Gehrke, K. C. Kuo, T. P. Waalkes and E. Borek, *Cancer*, 44 (1979) 2120.
20 D. C. Tormey, T. P. Waalkes and C. W. Gehrke, *J. Surg. Oncol.*, 14 (1980) 267.
21 C. W. Gehrke, K. C. Kuo, G. E. Davis, R. D. Suits, T. P. Waalkes and E. Borek, *J. Chromatogr.*, 150 (1978) 455.
22 C. W. Gehrke, K. C. Kuo and R. W. Zumwalt, *J. Chromatogr.*, 188 (1980) 129.
23 K. Nakano, K. Shindo, T. Yasaka and T. Yamamoto, *J. Chromatogr.*, 343 (1985) 21.
24 P. R. Brown, *J. Chromatogr.*, 52 (1970) 257.
25 A. M. Krstulovic, P. R. Brown and D. M. Rosie, *Anal. Chem.*, 49 (1977) 2237.
26 R. A. Hartwick, A. M. Krstulovic and P. R. Brown, *J. Chromatogr.*, 186 (1979) 659.
27 R. A. Hartwick, S. P. Assenza and P. R. Brown, *J. Chromatogr.*, 186 (1979) 647.
28 K. Nakano, S. P. Assenza and P. R. Brown, *J. Chromatogr.*, 233 (1982) 51.
29 D. L. Horrigan, *J. Clin. Invest.*, 33 (1954) 901.
30 W. S. Adams, F. Davis and M. Nakatani, *Am. J. Med.*, 28 (1960) 726.
31 G. Weber, *N. Engl. J. Med.*, 296 (1977) 486.
32 G. Weber, *N. Engl. J. Med.*, 296 (1977) 541.
33 Y. Shioya, Y. Hashimoto, T. Tanaka and S. Irino, *Proc. 43rd Annual Meeting of the Japanese Cancer Assoc., Fukuoka, 1984*, Japanese Cancer Association, Tokyo, 1984, p. 344 (in Japanese).
34 S. Tamura, N. Iwahashi, J. Fujii, N. Ueki, T. Yamamoto, Y. Amuro, K. Nabeshima, T. Hada and K. Higashino, *Proc. 43rd Annual Meeting of the Japanese Cancer Assoc., Fukuoka, 1984*, Japanese Cancer Association, Tokyo, 1984, p. 340 (in Japanese).

Journal of Chromatography, 332 (1985) 139–146
Elsevier Science Publishers B.V., Amsterdam — Printed in The Netherlands

CHROMSYMP. 630

QUANTITATIVE DECONVOLUTION OF HEAVILY FUSED CHROMATOGRAPHIC PEAKS OF BIOLOGICAL COMPONENTS USING A MULTI-WAVELENGTH UV DETECTOR

TADAO HOSHINO
Pharmaceutical Institute, School of Medicine, Keio University, 35 Shinano-Machi, Shinjuku-ku, Tokyo 160 (Japan)
and
TOSHINOBU HONDO*, MASAAKI SENDA, MUNEO SAITO and SIRO TOHEI
JASCO, Japan Spectroscopoic Co. Ltd., 2967-5 Ishikawacho, Hachioji City, Tokyo 192 (Japan)
(First received March 30th, 1985; revised manuscript received May 14th, 1985)

SUMMARY

Quantitative deconvolution of a chromatographic peak with extremely low UV absorption (less than 0.005 A.U.) is demonstrated for the analysis of an anaesthetic (ketamine) in rabbit serum. One ketamine metabolite, nor-ketamine, was deconvoluted from a completely fused peak in the three-dimensional chromatogram by using a highly sensitive multi-wavelength UV detector. After injection of ketamine, the nor-ketamine level in the serum increased to 3 μg/ml, calculated as ketamine, in 120 min.

INTRODUCTION

When a chromatogram is monitored with a spectrophotometric detector, it should be defined as a series of spectra as a function of time. However, a chromatogram must be regarded as a cross-section of a series of spectra along the time axis, owing to lack of suitable instrumentation.

Earlier, attempts were made to use an ordinary spectrophotometer to obtain a spectrum of a sample component in a chromatographic peak by using the stopped-flow technique. However, it was necessary to interrupt the chromatographic elution to obtain the spectra. Chromatography is, in principle, a time-dependent phenomenon and, therefore, such a technique failed to be accepted by chromatographers.

Denton *et al.*[1] reported the use of an oscillating mirror rapid-scanning spectrophotometer as a high-performance liquid chromatographic (HPLC) detector, capable of generating a three-dimensional chromatogram. However, even though the flow cell was as large as 87 μl, the noise levels below 250 nm were fairly high (±0.05 to ±0.2 A.U.)[2]. As micro-particulate packing materials capable of yielding narrow and fast peaks became available, such instrumentation rapidly became obsolete.

0021-9673/85/$03.30

An instrument that incorporated a vidicon detector[3] was reported as an alternative, but this was soon replaced by a solid-state linear photodiode-array detector[4–6]. The use of a photodiode array improved the sensitivity owing to improvements in the efficiency of light energy utilization, because the detector is always irradiated. However, a self-scan type of photodiode array hardly allows real symmetrical double-beam optical arrangement, which results in poor long-term stability. In addition, a current-photodiode array with 128, 256 or 1024 elements does not properly match the available optics, because the 25 μm element spacing interval[7] is too narrow to be used with the entrance slit of a polychromator. If one attempts to obtain the maximum spectral resolution available, in general the image of the cell hole should be focused on the entrance slit of width 25 μm, resulting in extremely poor sensitivity owing to a significant loss of energy on introduction of the light into the polychromator. Therefore, in practice, in order to obtain the necessary sensitivity, outputs of several elements are summed and treated as a single output, which also meets the realistic slit width suitable for collecting light efficiently from the flow cell[4,8].

Recently, we reported a multi-wavelength UV detector incorporating symmetrical double-beam optics and a 32-element discrete-photodiode array, the element width of which is ideally suited to a 1-mm I.D. flow-cell[9,10]. This configuration achieved a noise level of less than $5 \cdot 10^{-5}$ A.U. at 250 nm, $1 \cdot 10^{-4}$ A.U. for the entire wavelength range from 195 to 350 nm and a linear dynamic range up to 1.8 A.U.

Three-dimensional chromatographic data, acquired by a multi-wavelength UV detector, can be manipulated by computer-aided techniques for graphical presention in various fashions, such as three-dimensional, contour and ratio chromatograms. Another aspect of computer-aided techniques is the peak deconvolution of unresolved chromatographic peaks by the use of standard reference spectra[3,9,11–18]. Applications of the peak deconvolution technique have so far been limited to very simple and known components, and practical applications to multi-component samples, such as physiological fluids, have not yet been possible. The reasons that prevent the technique from being extended to such samples include the following shortcomings of existing instruments: (1) low signal-to-noise ratio, which distorts portions of the spectrum having weak absorbance; (2) limited linear dynamic range, which also distorts portions of the spectrum having strong absorbance; and (3) poor stability of the chromatographic and spectral baselines, which distorts the overall shape of the spectrum. The spectral distortion caused by these shortcomings would not permit the peak deconvolution to be carried out at the high and low ends of the sensitivity range.

In order to investigate the applicability of peak deconvolution, it was applied to a peak with extremely low UV absorption (less than 0.005 A.U.) by using a newly developed multi-wavelength UV detector in the analysis of an anaesthetic (ketamine) and its metabolite (nor-ketamine) in rabbit serum.

EXPERIMENTAL

Reagents

Ketamine (Ketalar 50) was obtained from Sankyo (Japan). Methanol and acetonitrile were of LC grade, purchased from Wako (Osaka, Japan).

Nor-ketamine from culture fluid of ketamine with isolated rat hepatocytes was used as a reference[19]

Instruments

A MULTI-320 multi-wavelength UV detector (JASCO, Tokyo, Japan) and a DS-L800 data processor were used with a JASCO TRI ROTAR-VI HPLC system.

Procedure

Ketalar 50 (700 μl) was injected into a rabbit at a level of 10 mg/kg as ketamine, which is equivalent to the dose for human subjects. About 2 ml of blood were drawn at intervals of 3 min for the first 30 min, then the intervals were increased as time elapsed. Each blood sample was centrifuged at 2800 *g* for 10 min. A 0.5-ml volume of the supernatant was added to 1.0 ml of methanol, then the mixture was centrifuged again under the same conditions. A 50-μl volume of the last supernatant was injected into a JASCO Fine Pak SIL C_{18} column (125 × 4.6 mm I.D.), which was eluted with acetonitrile–water (30:70) containing 60 m*M* perchloric acid.

Three-dimensional chromatographic data were acquired by the multi-wavelength detector. A chromatographic peak in which nor-ketamine was fused with another compound was quantitatively deconvoluted into the nor-ketamine peak and a peak originating from the serum. This procedure was performed for each serum and the nor-ketamine concentration obtained was plotted against time.

RESULTS AND DISCUSSION

Chromatographic and spectrometric identification of ketamine and nor-ketamine

In order to examine the retention times of ketamine and nor-ketamine, the ketamine standard and the culture fluid were chromatographed prior to the serum sample.

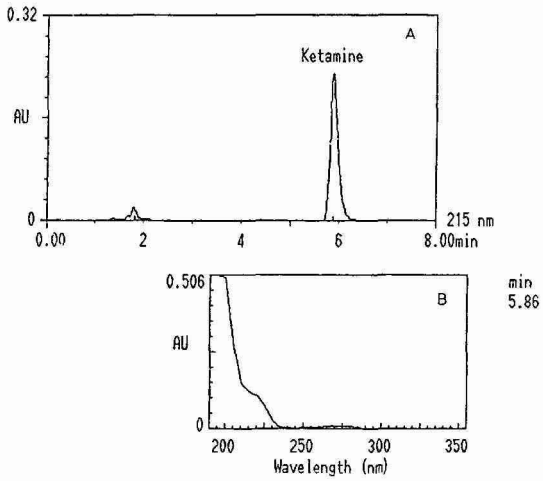

Fig. 1. Chromatogram and spectrum of the ketamine standard. (A) Chromatogram of the ketamine standard, monitored at 215 nm, obtained from the three-dimensional chromatographic data. A 2-μg amount of ketamine was eluted on a JASCO Fine Pak SIL C_{18} (125 × 4.6 mm I.D.) at 5.86 min. (B) UV spectrum taken at the peak. The ketamine standard spectrum has a small shoulder at 220 nm and a broad peak at 275 nm. Eluent: acetonitrile–water (30:70) containing 60 m*M* perchloric acid.

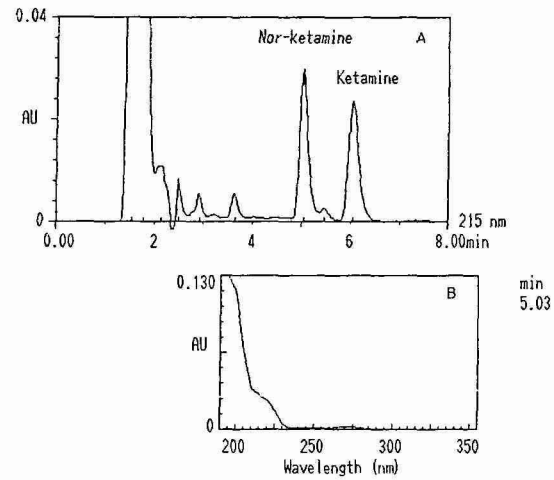

Fig. 2. Chromatogram and spectra of ketamine and nor-ketamine from the culture fluid. Nor-ketamine was eluted at 5.03 min, and its UV spectrum (B), taken at the peak, is also shown. The nor-ketamine spectrum is identical with that of ketamine.

Fig. 1A shows the chromatogram of the ketamine standard monitored at 215 nm obtained from the three-dimensional chromatographic data by the data reduction technique using the data processor. A 2-μg amount of ketamine was eluted at 5.86 min, and its UV spectrum (Fig. 2B), taken at the peak, is also shown. The ketamine spectrum has a small shoulder at 220 nm and a broad peak at 275 nm.

Fig. 2A shows the chromatogram of ketamine and nor-ketamine from the culture fluid. Nor-ketamine was eluted at 5.03 min; its UV spectrum (Fig. 2B), taken at the peak, is also shown. The nor-ketamine spectrum is identical with that of ketamine.

Fig. 3 shows the three-dimensional chromatogram of rabbit serum taken 18 min after the administration of ketamine. A 50-μl volume of the pretreated serum was separated with the same chromatographic system as before. As it is already known that nor-ketamine and ketamine would be eluted at 5.03 and 5.86 min, respectively, peaks were sought near these retention times with spectra equivalent to that of the ketamine standard. It was found that the peak eluted at 5.98 min had a

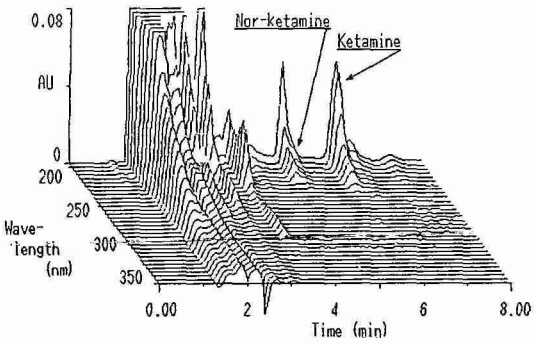

Fig. 3. Three-dimensional chromatogram of rabbit serum taken 18 min after ketamine administration. A 50-μl volume of pretreated serum was separated with the same chromatographic system as before.

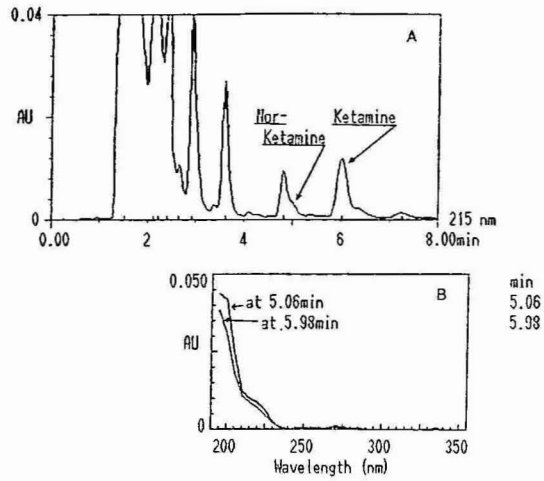

Fig. 4. Chromatogram and spectra of rabbit serum. (A) Chromatogram monitored at 215 nm and (B) spectra taken at 5.06 and 5.98 min. The spectra were obtained by subtracting the spectra taken just before the rise of the 5.06 min peak and the fall point of the 5.98 min peak from the spectra at those times. The 5.98 min peak had a spectrum that agreed with the ketamine standard spectrum, and the portion at 5.06 min of the peak that appeared as a tail also had the same spectrum.

spectrum that agreed with that of the ketamine standard, and a portion of the peak which appeared as a tail at 5.06 min had also the same spectrum.

Fig. 4 shows (A) a chromatogram monitored at 215 nm and (B) spectra taken at 5.06 and 5.98 min, which were obtained from the same chromatographic data. The spectra were obtained by subtracting the spectra taken just before the rise of the 5.06 min peak and the fall of the 5.98 min peak from the spectra at those times in order to eliminate the backgrounds. These spectra were obtained accurately enough to be compared with the standard spectrum. Fig. 5 shows the correlation between a spectrum taken at 5.06 min and the nor-ketamine reference spectrum taken from the culture fluid analysis. The two spectra were in good correlation (γ = 0.994). These

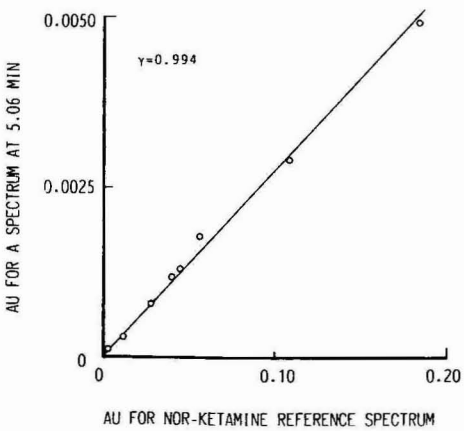

Fig. 5. Correlation between the spectrum at 5.06 min and the nor-ketamine reference peak.

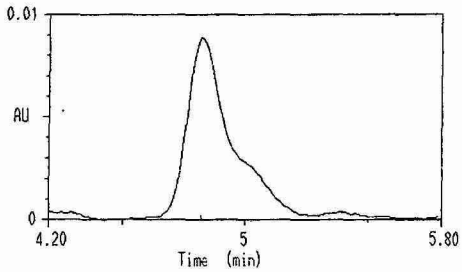

Fig. 6. Observed peak, including nor-ketamine. An enlargement of an observed peak that includes nor-ketamine, is shown.

components did not appear in the chromatogram of the control serum, taken just before the administration of ketamine. However, they were present in those of the sera after administration. In addition, their amounts varied with time. Hence they were confirmed to originate from ketamine. Therefore, the two peaks were chromatographically and spectrometrically identified to be nor-ketamine and ketamine, respectively.

Quantitative deconvolution of the nor-ketamine peak

Fig. 6 shows an enlargement of an observed peak that includes nor-ketamine. It was completely fused into the tailing part of the main peak, which originated from the serum, so that a conventional peak integration method failed to quantitate it. Therefore, peak deconvolution, in which the least-squares method is utilized[10], was performed on the spectral range from 210 to 300 nm and the time range from 4.2 to 5.8 min, using the nor-ketamine reference spectrum and the spectrum of the peak with which nor-ketamine peak is fused. The latter spectrum was obtained from the data for the control serum, taken just before administration of ketamine.

The observed peak 1 was deconvoluted into two peaks, 2 and 3, as shown in Fig. 7. Peak 3 represents the fraction that agrees with the nor-ketamine spectrum. Peak 2 is a fraction originting from the serum. The heavy line shows a residual curve, that is, the square root of the sum of the squares of differences between the observed spectrum and the re-convoluted spectrum from the spectra of peaks 2 and 3. That

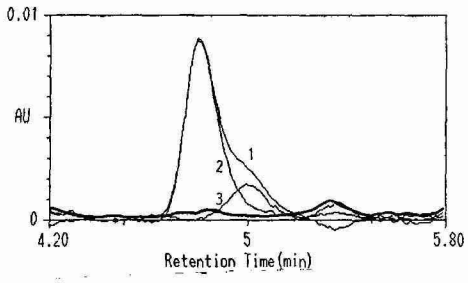

Fig. 7. Quantitative deconvolution of nor-ketamine peak. The peak deconvolution was performed by using the spectrum of the nor-ketamine standard and that of the peak in which nor-ketamine peak is fused. The observed peak 1 was deconvoluted into two peaks, 2 and 3. Peak 3 represents the fraction that agrees with the nor-ketamine spectrum. Peak 2 is a fraction originating from the serum. The heavy line shows the residual curve that indicates the performance of the peak deconvolution (see text).

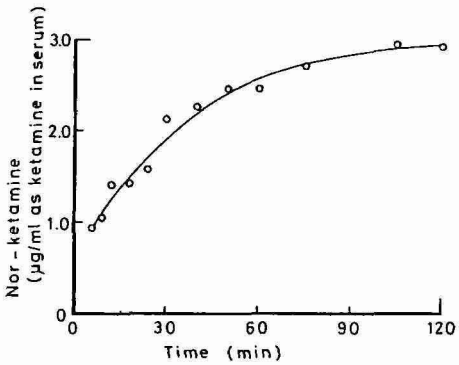

Fig. 8. Time course of nor-ketamine levels. Even though the peak was completely fused and weak, quantitation was carried out succesfully. The time course shows a reasonable curve for a ketamine metabolite. After ketamine injection, the amount of nor-ketamine increased to a level of 3 ± 0.3 μg/ml, calculated as ketamine.

is a good indication of the performance of the peak deconvolution. For the quantitation of nor-ketamine, peak 3 was integrated from 4.70 to 5.20 min. The level of the residual curve remained below $5 \cdot 10^{-4}$ A.U. in this time range. The small peak at 5.34 min on the residual curve represents a component that does not fit the spectra used in the deconvolution.

Fig. 8 shows the time course of nor-ketamine levels in the serum obtained by peak deconvolution. Even though the peak was completely fused and the spectral peak was weak, quantitation was carried out succesfully, as shown. The time course is a reasonable curve for a ketamine metabolite. After ketamine injection, the level of nor-ketamine increased to 3 ± 0.3 μg/ml, calculated as ketamine, in 120 min.

CONCLUSION

A multi-wavelength detection system generally allows the quantitative analysis of chromatographic peaks that include unresolved components by using the peak deconvolution technique. However, the utility of the technique is determined by the performance of the detection system itself, *i.e.*, the attainable precision of the spectral data, rather than the sophistication of the data processor. In general, more data points give a more accurate spectrum, but this is true only when the noise level and the linear dynamic range are independent of the number of data points, in other words, the spectral band width. Further, in practice, excessive amounts of data require excessive processing time or the use of an expensive large computer. Therefore, as a design criterion for a practical multi-wavelength UV detector, there should be good balance between the spectral band width, sensitivity, linear dynamic range, accuracy and precision of spectral data.

These successful results of the application of peak deconvolution in biological component analysis show that a band width of 5 nm, a noise level of $1 \cdot 10^{-4}$, a linear dynamic range up to 1.8 A.U. and a wavelength range of 195–350 nm represent a good example of a well designed system for practical applications.

REFERENCES

1 M. S. Denton, T. P. DeAngelis, A. M. Yacynych, W. R. Heineman and T. W. Gilbert, *Anal. Chem.*, 48 (1976) 20.
2 M. J. Milano, S. Lam and E. Grushka, *J. Chromatogr.*, 125 (1975) 315.
3 A. E. McDowell and H. L. Pardue, *Anal. Chem.*, 49 (1977) 1171.
4 R. E. Dessy, W. D. Reynolds, W. G. Nunn, C. A. Titus and G. F. Moler, *J. Chromatogr.*, 126 (1976) 347.
5 Y. Talmi, *Anal. Chem.*, 47 (1975) 697A.
6 Y. Talmi, *Anal. Chem.*, 47 (1975) 658A.
7 *Product Summary, Solid State Image Sensors*, 055-0014 38003 EG&G RETICON, Sunnyvale, CA.
8 S. A. George, *Pittsburgh Conference, 1984, Abstr. No. 175.*
9 S. Tohei, S. Kohara and M. Saito, *Pittsburgh Conference, 1984, Abstr. No. 179.*
10 T. Hoshino, M. Senda, T. Hondo, M. Saito and S. Tohei, *J. Chromatogr.*, 316 (1984) 473.
11 R. G. Berg, C. Y. Ko, J. M. Clemons and H. M. NcNair, *Anal. Chem.*, 47 (1975) 2480.
12 M. J. Milano, S. Lam, M. Savonis, D. B. Pautler, J. W. Pav and E. Grushka, *J. Chromatogr.*, 149 (1978) 599.
13 L. N. Klatt, *J. Chromatogr. Sci.*, 17 (1979) 225.
14 J. M. Halket, *J. Chromatogr.*, 175 (1979) 229.
15 M. L. Malczewski and E. Grushka, *J. Chromatogr. Sci.*, 19 (1981) 187.
16 M. McCue and E. R. Malinowski, *J. Chromatogr. Sci.*, 21 (1983) 229.
17 A. F. Fell, H. P. Scott, R. Gill and A. C. Moffat, *J. Chromatogr.*, 282 (1983) 123.
18 A. F. Fell, B. J. Clark and H. P. Scott, *J. Chromatogr.*, 316 (1984) 423.
19 T. Hoshino and H. Takahagi, *J. Chromatogr.*, submitted for publication.

Journal of Chromatography, 332 (1985) 147–168
Elsevier Science Publishers B.V., Amsterdam — Printed in The Netherlands

CHROMSYMP. 613

STOICHIOMETRIC DISPLACEMENT OF SOLVENT BY NON-POLAR SOLUTES IN REVERSED-PHASE LIQUID CHROMATOGRAPHY

XINDU GENG* and FRED E. REGNIER*
Department of Biochemistry, Purdue University, West Lafayette, IN 47907 (U.S.A.)
(Received March 30th, 1985)

SUMMARY

This paper proposes a retention model which predicts that the displacement of non-polar solutes from a reversed-phase chromatographic column is accompanied by the adsorption of a stoichiometric number (Z) of solvent molecules. The number of solvent molecules involved in this process is a function of both solute and solvent contact surface areas. Increasing solute contact surface area would increase Z whereas increasing solvent contact surface area would decrease the Z value for a specific solute. The experimental observations presented are consistent with this model.

Further predictions of the model are that (1) plots of log k' *versus* the inverse log of solvent concentration will be non-linear at solvent concentrations where the surface of a reversed-phase support is not fully solvated, and (2) only a portion of the total non-polar surface area of a molecule actually contacts the surface of a reversed-phase support. Non-linearity in plots of log k' *versus* the inverse log of solvent concentration was in fact observed at solvent concentrations where solvation of the reversed-phase support is incomplete.

INTRODUCTION

The problem of predicting solute retention in reversed-phase chromatography (RPC) has occupied the attention of liquid chromatographers for decades. At present the most popular approach is to relate the logarithm of solute capacity factor (k') to the volume fraction (Φ_b) of organic solvent B in the mobile phase[1], as shown in eqn. 1.

$$\log k' = \log k_w - S\Phi_b \quad (1)$$

The intercept ($\log k_w$) is an extrapolated value of the capacity factor in pure water and S is the slope of the plot of log k' *versus* Φ_b. S is said to be an indicator of the

* Visiting Professor from the Department of Chemistry, The Northwestern University, Xian, China.

0021-9673/85/$03.30

strength of pure solvent B as a mobile phase. A larger value of S leads to a faster decrease in k' with increases in Φ_b. The fact that the same volume fraction of two different solvents will produce different k' values with the same solute indicates that S is dependent on the type of solvent.

Although eqn. 1 adequately expresses the relationship of k' to Φ_b for k' values between 0.5 and 10, it has been suggested by Schoenmakers *et al.*[2] that the equation

$$\ln k' = A_g\Phi_b^2 + B_g\Phi_b + C_g + D_g(\Phi_b) \quad (2)$$

provides a more adequate description of the process. The terms A_g, B_g and C_g are constants and $D_g(\Phi_b)$ is a size correction term. This equation fits experimental data at least as well as eqn. 1 and in some cases it is superior. The principal difference is that eqn. 2 shows ln k' to be a quadratic rather than a linear function of solvent composition Φ_b. Non-linearity of ln k' *vs.* Φ_b plots at extremes of k' confirms the assertion that eqn. 2 provides a more adequate description of the process. At present, no reason has been given for non-linearity of ln k' *vs.* Φ_b plots at extremes of k'.

Horváth *et al.*[3] have provided the most detailed analysis of the interaction of small non-polar solutes with solvent. Through application of the solvophobic theory[3] they have been able to account for many of the factors that control solute retention; even making it possible to characterize eluent strength of mixed solvents with different compositions. The basic premise in this treatment is that mobile phase surface tension provides the driving force for retention in RPC. Attenuation of the solute–sorbent and water–water interactions is achieved by the addition of organic solvents. Unfortunately, the relatively large number of surface tension measurements and physicochemical constants required to use the equations developed in this treatment are not always available.

The influence of stationary phase on retention in RPC is well known, yet most retention models do not include the contribution of stationary phase in solute retention. Jandera *et al.*[4] have recently proposed a semi-empirical model based on "interaction indices", in which the importance of stationary phase modifiers and silanol groups are considered. However, the main assumption of this model is that retention in RPC is primarily controlled by interactions in the mobile phase.

Several studies[5–7] have also been carried out on macromolecular retention in RPC. Although the same mechanism is probably involved in the retention of both small and macromolecular species, molecular size has been found to contribute to the retention process. Much smaller changes in mobile phase composition are required for the elution of macromolecules than small molecules[8]. Grego *et al.* proposed[7] that in the case of proteins this is due to the larger contact area of macromolecular solutes than small peptides. In a recent treatment of gradient elution, Larmann *et al.*[9] and Snyder *et al.*[10] showed with polystyrene that the slope (S) of plots of ln k' *versus* Φ_b increases with solute molecular weight. Since S varies with solute size, it may be questioned whether S is truly a measure of solvent strength.

The recent papers[5,6] by Geng and Regnier have proposed that retention of proteins on an alkylsilane support can be described by the equation

$$k' = I/[D_0]^Z \quad (3)$$

where $[D_0]$ is the concentration of the organic solvent in the mobile phase, Z is the number of solvent molecules involved in the displacement of a protein from the reversed-phase surface and I is a constant. This approach is based on the assumption that a stoichiometric number of solvent molecules is required for solute displacement from an RPC column. Instead of examining the forces that promote adsorption, this model is directed more toward contact surface area between the stationary phase and solutes and how solvent stoichiometry may be used to predict contact surface area.

The question of whether there is also a solvent–solute displacement stoichiometry (Z) for small molecules has not been examined. The objectives of this paper are (1) to examine the possibility that eqn. 3 also describes the retention of small molecules in RPC, (2) to determine Z values for a series of low-molecular-weight, non-polar species, (3) to examine the relationship between Z number and non-polar surface area (A_u), (4) to examine the relationship between log I and A_u, (5) to examine the relationship between Z and I and (6) to give a physical meaning to I.

THEORETICAL

The driving force for solvation of an alkylsilane bonded phase is provided by solvophobic effects in the mobile phase. It is probable that the thickness of either the adsorbed solvent or solute layer should in no case be more than a bilayer[11]. Layer thickness probably also depends on the solvent dipole. Solvents such as methanol and ethanol that interact with the alkyl bonded phase in such a way as to provide a gradient between the hydrophobic bonded phase and a hydrophilic mobile phase would be expected to form a monolayer. In contrast, molecules with a smaller dipole could be in the form of a bilayer.

Adsorption of a hydrophobic molecule onto an RPC column can be envisioned as an interaction between non-polar portions of the bonded phase and non-polar areas of the solute[11]. Polar groups of a solute, in contrast, will be directed away from the hydrophobic support toward the more hydrophilic mobile phase. Since this is a surface phenomenon, only a portion (f, to be referred to henceforth as a geometric factor) of either the non-polar surface area (A_m) of a monomeric group within a molecule or of the total non-polar surface area (A_u) of the solute will be involved in interactions with the RPC support surface.

Solvent displacement stoichiometry

The basic premise of this model[5,6] is that there is a stoichiometric relationship between solute adsorption and the number (Z) of solvent molecules displaced from an RPC column. It has been shown[6] that

$$S_m + nL_d \rightleftarrows S_b + (nr+q)D_0 \qquad (4)$$

where S_m is solvated solute in the mobile phase, n is the number of alkyl ligands onto which a solute is adsorbed, L_d is organic displacing agent adsorbed on alkyl ligands, S_b is adsorbed solute, r is the amount of solvent displaced from a single ligand when solute is adsorbed and D_0 is the organic displacing agent in the mobile phase. Letting $(nr+q) = Z$, this displacement process may be expressed in terms of the formation constant (K_1) shown in eqn. 5.

$$K_1 = \frac{[S_b][D_0]^{(nr+q)}}{[S_m][L_d]^n} = \frac{[S_b][D_0]^Z}{[S_m][L_d]^n} \quad (5)$$

Since solute displacement occurs with changes of only a few percent in $[D_0]$, it is assumed that the activity coefficient of the solvent is constant over this range and it is valid to use formation constants to describe these equilibria. This model is simpler than that for macromolecules in that structural transitions and changes in the degree of solvation during elution do not have to be considered with small molecules. The ratio of solute concentration in the stationary phase to that in the mobile phase, $[S_b]/[S_m]$, may be related to chromatographic retention and the phase ratio (φ) of the column through the distribution coefficient (K_D) by the equation

$$[S_b]/[S_m] = K_D = k'/\varphi \quad (6)$$

Substituting k'/φ for $[S_b]/[S_m]$ in eqn. 5 shows that

$$k' = K_1\varphi[L_d]^n \cdot \frac{1}{[D_0]^Z} \quad (7)$$

Since K_1, φ and n are constants and $[L_d]$ is a constant over the range of $[D_0]$ in which $0.5 < k' < 30$ (ref. 6), these constants may be clustered into a single constant, I, where

$$I = K_1\varphi[L_d]^n \quad (8)$$

This allows eqns. 7 and 8 to be combined and written in logarithmic form as

$$\log k' = Z \log 1/[D_0] + \log I \quad (9)$$

Solutes that behave according to this stoichiometric displacement model would be expected to give linear plots of $\log k'$ *versus* $\log 1/[D_0]$, with a slope of Z and intercept of $\log I$.

Relationship between Z and solute surface area

The contact surface area (C_m) of any non-polar monomeric unit within a molecule may be expressed as

$$C_m = f_m A_m \quad (10)$$

where f_m and A_m are the geometric factor and non-polar surface area of the monomer, respectively. The total non-polar contact surface area (C_u) of a molecule with multiple hydrophobic residues will be equal to the sum of the contributions of individual non-polar groups, as seen in eqn. 11:

$$C_u = \sum_{n=1}^{i} f_{mi} A_{mi} \quad (11)$$

The term A_{mi} represents the non-polar surface area of a particular ith group which is experiencing partial contact (f_{mi}) with the support surface, and n is the number of ith non-polar groups in the molecule. Unfortunately it is difficult to determine C_u. Although n can be found by examining the structure of the molecule, and A_{mi} may be obtained by calculating the van der Waals surface area[12], the geometric factor (f_{mi}) is not available. In addition, the geometric factor may vary between species and be dependent on the position of a non-polar group in the molecule.

For convenience, this treatment will be limited to solutes of the same shape in which it is assumed that f_m is the same for all monomeric units of the same type and that

$$C_M = n_m f_m A_m = f_m A_M \tag{12}$$

where n_m is the number of a particular monomeric unit, C_M is the total contact surface area of this type of monomeric unit, and A_M is the total non-polar surface area of these identical monomeric units. It will be shown later using a homologous series as an example, that eqn. 12 makes it possible to develop a relationship between Z and the non-polar van der Waals surface area (A_u).

The total non-polar contact surface area (C_u) of a solute is

$$C_u = C_M + C_E + C_F + C_I \tag{13}$$

where C_M is as defined above, C_E is the contact surface area of all terminal methyl groups, C_F is the contact surface area of all functional groups and C_I is the contact surface area of other moieties in the molecule that serve as points of branching. An expansion of eqn. 11 into its contributing variables is seen in eqn. 14:

$$C_u = n_m f_m A_m + n_e f_e A_e + n_i f_i A_i + n_f f_f A_f \tag{14}$$

where A_m, A_e, A_f and A_i are the non-polar van der Waals surface areas of monomers, end-groups, functional groups and branching groups, respectively. The terms n_m, n_e, n_f and n_i represent the number of each species of functional group, while f_m, f_e, f_f and f_i designate the corresponding geometric factors.

The assumption has been made in eqn. 14 that f_m, f_e and f_f will be independent of the position of a group in a molecule. This may not always be true. Strong electronic, steric or solvent effects of neighboring groups may alter the geometric factor (f) of a group such that its contact surface area will not be equivalent to other identical moieties in the molecule. This point will be further examined later.

In the case of a homologous series with a normal alkyl chain, $n_m > n_e$, $C_M > C_E$, and it will be assumed that $f_m A_m \approx f_e A_e$. This allows the methyl group to be treated as a methylene group and eqns. 13 and 14 to be reduced to

$$C_u = C_{M+E} + C_F + C_I \tag{15}$$

and

$$C_u = n_{(m+e)} f_m A_m + n_f f_f A_f + n_i f_i A_i \tag{16}$$

This means that

$$n_{(m+e)} = f_m A_M / f_m A_m = A_M / A_m \tag{17}$$

where $n_{(m+e)}$ is the combined number of end and monomer groups.

Geometric factors will also limit the contact of solvents with both support and solute surfaces such that

$$C_v = f_v A_v + C_\alpha \tag{18}$$

where C_v is non-polar contact surface area of a solvent, A_v is its total non-polar surface area, f_v is the geometric factor for non-polar groups in the solvent and C_α allows for the contribution made by functional groups when present.

The stoichiometric displacement model holds that when a substance is displaced from a surface, nr molecules of solvent solvate the support surface in an area C_{spt}, and q molecules of solvent solvate the solute in an area C_u. The area of solvation (C_{spt}) on the support would be related to C_v by the equation

$$C_{spt} = \frac{nrC_v}{S_{cs}} + C_\beta \tag{19}$$

where C_β is a constant that accounts for any functional group contributions and S_{cs} represents support surface coverage by solvent molecules, where a value of $S_{cs} = 1$ would indicate a monolayer.

Contact surface area of the solute may also be described in terms of the contact surface area of the solvent:

$$C_u = \frac{qC_v}{S_{cu}} + C_\gamma \tag{20}$$

where S_{cu} represents solvent surface coverage on the solute surface and C_γ is a constant accounting for functional-group contributions. Actual surface area (C_u) should be larger than the average geometric area occupied by solvent unless the solute is adsorbed in multiple layers. For convenience, this treatment uses average geometric area. As long as the surface of the bonded phase and solute are of the same chemical nature, S_{cs} will equal S_{cu}. In the case of more polar solutes, it is possible that $S_{cs} > S_{cu}$. Values of one for S_{cs} and S_{cu} indicate a monolayer. In all cases the two terms will be proportional and it is possible to write

$$S_{cs} = S_{cu} C_\delta \tag{21}$$

where C_δ is a proportionality constant.

The total non-polar contact surface area (C_T) of both the support and solute is

$$C_T = C_{spt} + C_u \tag{22}$$

According to eqns. 19 and 20, it may be shown that

$$C_T = \frac{nrC_v}{S_{cs}} + \frac{qC_v}{S_{cu}} + C_\beta + C_\gamma \tag{23}$$

Recalling from eqn. 5 that $Z = nr+q$, and taking the special case where $S_{cu} = S_{cs}$, eqn. 23 reduces to

$$C_T = \frac{ZC_v}{S_{cu}} + C_\beta + C_\gamma \tag{24}$$

Solution of the general case in which $S_{cs} \neq S_{cu}$ is achieved by assuming that for a homologous series the ratio of displacing agent in the contact surface area on the support (nr) to that in the contact surface area on the solute (q) is a contant (C_ε):

$$C_\varepsilon = \frac{nr}{q} \tag{25}$$

This allows eqn. 23 to be converted into the more general equation

$$C_T = \frac{C_v \cdot q}{S_{cu}}\left[\frac{C_\varepsilon}{C_\delta} + 1\right] + C_\mu \tag{26}$$

where $C_\mu = C_\beta + C_\gamma$.

It may be shown, by solving eqns. 19 and 20 for C_v and setting them equal, that there should be a constant relationship between C_{spt} and C_u in a homologous series; *i.e.* $C_{spt} = C_\eta C_u + C_\rho$ where $C_\eta = C_\varepsilon/C_\delta$ and $C_\rho = (C_\gamma C_\varepsilon/C_\delta) + C_\beta$. In this case (substituting in eqn. 22), $C_T = C_u(1 + C_\eta) + C_\rho$. Using these terms and letting $q = Z/(1 + C_\delta)$, it may be shown through substitution in eqn. 26 that

$$Z = \frac{S_{cu}}{C_v}[C_u C_\sigma + C_\omega] \tag{27}$$

where $C_\sigma = 1 + C_\eta$ and $C_\omega = C_\rho - C_\mu$. Since S_{cu}, C_v, C_σ and C_μ are all constants, this equation may be reduced to

$$Z = sC_u + i \tag{28}$$

where $s = \frac{S_{cu}}{C_v} \cdot C_\sigma$ and $i = \frac{S_{cu}}{C_v} \cdot C_\omega$. This equation shows that, for a non-polar homologous series, it is expected that Z will be directly proportional to non-polar contact surface area (C_u).

Z may also be related to the non-polar surface area (A_u) of a substance, as seen in eqn. 29 by combining eqns. 11 and 28:

$$Z = s \sum_{n=1}^{i} f_{mi} A_i + i \tag{29}$$

In a homologous series such as normal aliphatic hydrocarbons in which there are no functional groups, the geometric factor (f_u) for the molecule is approximately equal to that of the individual monomers (f_{mi}) and $\sum_{n=1}^{i} A_1 = A_u$. Eqn. 29 may be reduced to

$$Z = s f_u A_u + i \tag{30}$$

in this special case. Addition of functional groups in the more general case will provide a constant but different contribution than that of non-polar groups. This functional-group contribution is accommodated in the equation

$$Z = s A_u (f_{mi} a_{mi} + F) + i \tag{31}$$

where a_{mi} is the fraction of the total non-polar surface area contributed by a monomer and F is the functional-group contribution. On the basis of the linear relationship between Z and C_u predicted by eqn. 28, for a homologous series, the same is expected of other solutes. Through the use of eqns. 29 and 31, it should be possible to use Z values and the non-polar surface areas (A_{mi}) to determine values for f_{mi}.

Relationship between I and surface area

Other than being the product of a cluster of constants (see eqn. 8), there is no known relationship between I and the molecular properties of a solute. Since the objective here is to couple contact surface area (C_u) to retention, this treatment will develop a relationship between C_u and I.

The Martin equation is often used to describe retention properties

$$\log k' = A + B n_{(m+e)} \tag{32}$$

of the members of a homologous series where A and B are constants and n is the number of monomeric units in the solute[13]. Total non-polar contact surface area (C_u) of a solute in such a series may be represented as

$$C_u = n_{(m+e)} C_m + C_\psi \tag{33}$$

where C_m is the contact surface area of a single monomeric unit such as a methylene (CH_2) group and $C_\psi = C_F + C_I$. Substituting for $n_{(m+e)}$ in eqn. 32, chromatographic retention in a homologous series may be related to non-polar contact surface area:

$$\log k' = A + B\left[\frac{C_u}{C_m} - \frac{C_\psi}{C_m}\right] \tag{34}$$

When a homologous series is separated isocratically on an RPC column, the log $1/[D_0]$ term in eqn. 9 is a constant (d), and eqns. 9, 28 and 34 may be combined to produce the expression

$$\log I = C_u\left[\frac{B}{C_m} - sd\right] + A - id - \frac{BC_\psi}{C_m} \tag{35}$$

Combining constants in eqn. 35 produces the expression

$$\log I = aC_u + C_\lambda \tag{36}$$

where $a = (B/C_m) - sd$ and $C_\lambda = A - id - (BC_\omega/C_m)$. Through eqn. 11, $\log I$ of a solute may be related to non-polar surface area by the equation

$$\log I = a \sum_{n=1}^{i} f_{mi}A_i + C_\lambda \tag{37}$$

when $f_{mi} \approx f_u$ and $\sum_{n=1}^{i} A_i = A_u$ as in equation 30, then

$$\log I = af_uA_u + C_\lambda \tag{38}$$

In those cases where functional groups are present, functional-group contributions are accommodated by the equation

$$\log I = aA_u(f_{mi}a_{mi} + F) + C_\lambda \tag{39}$$

as in eqn. 31. The slope (a) in eqns. 36–39 indicates that there should be a constant incremental increase in $\log I$ with the addition of each monomeric unit in a homologous series.

Relationship between I and Z

It has been shown in eqns. 28 and 36 that both I and Z may be related to contact surface area (C_u). Solving these equations for C_u and setting them equal shows, after rearranging terms, that

$$\log I = aZ/s - ai/s - C_\lambda = JZ - C_\theta \tag{40}$$

where $J = a/s$ and $C_\theta = ai/s - C_\lambda$. The derivative of this equation, $d(\log I)/dZ = J$, shows that there should be a constant relationship between I and Z for solutes in a homologous series.

Relationship of I to K_D

It has been shown in RPC of proteins[5,6] that species of nearly identical Z values can be resolved in an isocratically eluted system because their intercept terms

(I) differ. It will be assumed here that solutes of the same Z value are of identical contact surface area. In this case, the term $([D_0]^Z/[L_d]^n)$ in eqn. 5 will be identical for both solutes, and it is possible to write

$$(K_1)_A\frac{[S_m]_A}{[S_b]_A} = (K_1)_B\frac{[S_m]_B}{[S_b]_B} \tag{41}$$

The symbols A and B identify the first and second members, respectively, of this solute pair to elute from the column. Since $[S_b]/[S_m] = K_D$ and I is directly proportional to K_1 (eqn. 8), eqn. 41 becomes

$$I_A/(K_D)_A = I_B/(K_D)_B \tag{42}$$

This means that when contact surface area has been normalized, the relative difference between the I terms of solutes will be directly related to the differences between their partition coefficients.

Relationship between I and P

The octanol–water partition coefficient (P) of a molecule is a property used to predict transport across cell membranes. Yalkowsky and Valvani have reported[14] that hydrocarbon surface area (A_{hsa}) of a molecule is proportional to the logarithm of its partition coefficient, where

$$\log P = 0.0275\, A_{hsa} - 0.863 \tag{43}$$

Since A_{hsa} is proportional to non-polar van der Waals surface area (A_u), this allows eqn. 43 to be rewritten as

$$\log P = mA_u - v \tag{44}$$

Combining eqns. 43 and 44 it may be shown that

$$\log I = (a/m)(f_{mi}a_{mi} + F)\log P + (av/m)(f_{mi}a_{mi} + F) + C_\lambda \tag{45}$$

When functional-group contributions are small and $f_{mi}a_{mi} \gg F$, then $a_{mi} \simeq 1$ and $f_{mi} \simeq f_u$. In this special case eqn. 41 may be reduced to

$$\log I = g \log P + C_\theta \tag{46}$$

by letting $g = a/m$ and $C_\theta = (avf_u/m) + C_\lambda$. Eqn. 46 will apply in those cases where a molecule has no functional groups or where the non-polar portion of the molecule is sufficiently large that it dominates retention. Eqns. 45 and 46 suggest that chromatographic methods will be useful in predicting P of large hydrophobic molecules but will fail in the case of solutes containing small functional groups because f_{mi} and F are unknown in eqn. 45.

MATERIALS AND METHODS

Equipment

All separations were carried out on a chromatographic system equipped with a Beckman-Altex (Berkeley, CA, U.S.A.) Model 110 gradient pumping system, a Rheodyne (Berkeley, CA, U.S.A.) Model 7120 injection valve fitted with a 100-μl loop, a Varian Model UV-50 detector operated at 254 nm and a Fisher Recordall (Austin, TX, U.S.A.) series 5000 recorder.

Supports

SynChropak C-1, C-8 and C-18 supports of 6-μm particle diameter were obtained from SynChrom (Linden, IN, U.S.A.). Columns of 50 × 4.6 mm I.D. were slurry-packed using 2-propanol as solvent.

Mobile phases

HPLC grade water was prepared in the laboratory. 2-Propanol and methanol were obtained in HPLC grade from Mallinckrodt (Paris, KY, U.S.A.) HPLC grade acetonitrile was purchased from Fisher (Fair Lawn, NJ, U.S.A.). Mobile phases were prepared with the pumping system of the instrument by mixing a weak solvent (A) with a strong solvent (B) to achieve the desired mobile phase composition. Weak solvents used in these studies were water, water–methanol (80:20; v/v), water–acetonitrile (90:10; v/v) and water–tetrahydrofuran (90:10; v/v). Strong solvents used in these studies were water–methanol (20:80; v/v), water–acetonitrile (40:60; v/v) and water–acetonitrile (40:60; v/v). When pure water was used as the weak solvent the strong solvent was water–methanol (80:20; v/v), water–acetonitrile (90:10; v/v) or water–tetrahydrofuran (90:10; v/v). Mobile phase flow-rate was 1 ml/min in all cases. Columns were equilibrated with 40 ml of mobile phase before any retention measurements were made.

Solutes

All solutes (Table I) were obtained from Aldrich (Milwaukee, WI, U.S.A.) and used at a concentration of 5.0 mg/ml in pure solvent B. Sample volumes were 5–10 μl.

Column permeation volume

The total permeation volume ($k' = 0$) of columns was measured by injecting several microliters of sodium dichromate and calculating the dead volume according to published methods[3].

RESULTS

Testing the model

The relationship between the capacity factor (k') of selected solutes and the organic solvent concentration $1/[D_0]$ with a water–methanol mobile phase and octylsilane stationary phase is seen in Fig. 1 and Table I. With the exception of benzene and toluene (Fig. 1b), the curves in Fig. 1a are linear. The data presented in the figure for nine compounds are representative of the family of 24 compounds studied. Slope

TABLE I

RETENTION DATA FOR SOME ALKYLBENZENES

Solute No.	*Solute*	*Correlation coefficient*	*Slope (Z)*	*Intercept (log I)*	*Standard deviation*
1	Benzene	0.995	1.71	2.09	0.026
2	Bibenzyl	0.999	6.49	8.35	0.024
3	Biphenyl	0.999	4.92	6.28	0.019
4	*m*-Diisopropylbenzene	0.999	6.90	9.02	0.025
5	*p*-Diisopropylbenzene	0.998	7.07	9.26	0.031
6	2,2'-Diphenylpropane	0.999	6.72	8.72	0.020
7	3,3'-Dimethylbiphenyl	0.999	6.79	8.81	0.017
8	4,4'-Dimethylbiphenyl	0.999	6.77	8.79	0.025
9	Mesitylene	0.997	4.38	5.89	0.033
10	*m*-Xylene	0.991	3.59	4.50	0.042
11	*n*-Pentylbenzene	0.999	6.74	8.81	0.024
12	Naphthalene	0.997	3.83	4.83	0.029
13	*n*-Propylbenzene	0.996	4.44	5.73	0.036
14	Pentamethylbenzene	0.996	4.93	6.60	0.033
15	4-Phenyltoluene	0.994	5.37	7.02	0.055
16	*p*-Xylene	0.996	3.36	4.32	0.035
17	*sec*-Butylbenzene	0.997	5.08	6.64	0.032
18	1,2,3,4-Tetramethylbenzene	0.997	4.52	5.95	0.036
19	1,2,3,5-Tetramethylbenzene	0.997	4.57	6.04	0.029
20	1,2,4,5-Tetramethylbenzene	0.995	4.84	6.34	0.036
21	Toluene	0.997	2.65	3.31	0.020
22	1,2,3-Trimethylbenzene	0.997	3.92	5.09	0.025
23	1,2,4-Trimethylbenzene	0.999	4.43	5.72	0.018
24	*o*-Xylene	0.900	3.17	4.09	0.057

(Z) and intercept (I) data for the 24 compounds are presented in Table I. To facilitate discussion of the proposed model, linear and non-linear portions (when applicable) of these curves will be treated separately. The data presented in Table I are derived from the linear portion of these curves. Correlation coefficients for the linear segments of these curves were greater than 0.99 in all cases; indicating that the stoichiometric retention model (eqn. 9) is consistent with the data.

Observations of non-linearity at elution extremes, *i.e.* as k' approaches either zero or large values, have also been made by other workers[1,2] without explanation as to the origin of the phenomenon. A question is whether the stoichiometric retention model is capable of predicting or explaining these deviations. An important condition of the model is that linearity will only be achieved when activity coefficients and the concentration of adsorbed displacing agent [L_d] are constant while [D_0] is varied to effect elution. Variations in activity coefficients or [L_d] would cause both Z and I to very and produce non-linear plots of log k' *vs.* log $1/[D_0]$. McCormick and Karger[15] and Slaats *et al.*[16] have examined the relationship between [L_d] and [D_0] in RPC and found [L_d] to be relatively constant in the 30–80% (v/v) range for methanol–water and in the 50–70% (v/v) range for acetonitrile–water. As the concentration of the displacing agent approached the extremes (0–30 and 80–100%) with methanol–water, [L_d] decreased. This means that the stationary phase in the column

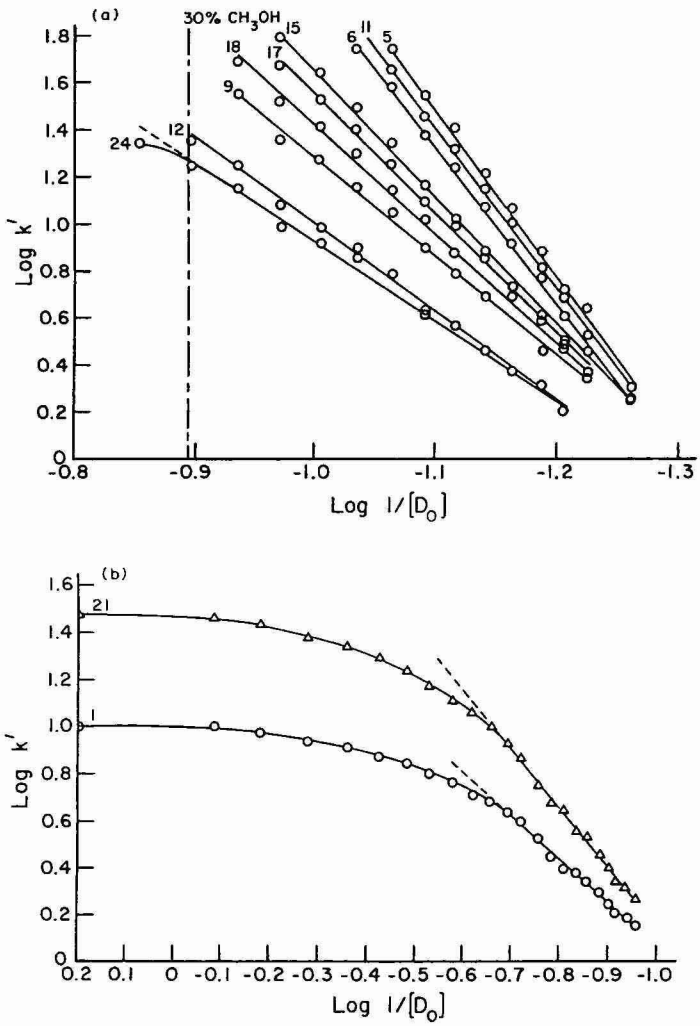

Fig. 1. Plots of log k' *vs.* log $1/[D_0]$ for a non-homologous series of alkylbenzenes. Separations were achieved on a 5.0 × 0.41 cm I.D. SynChropak C_8 column eluted with a methanol–water mobile phase at ambient temperature. Solutes in the figure are numbered and identified in Table I. (a) Data were obtained at methanol concentrations of greater than 30% (v/v); (b) data were derived at less than 30% methanol concentration (v/v).

is changing at the extremes of solvent concentration. In view of the contribution of the stationary phase to retention through $[L_d]$ in the stoichiometric displacement model, the data of McCormick and Karger[15] and Slaats *et al.*[16] would lead to the conclusion that non-linearity is to be expected with methanol and acetonitrile at the extremes of organic solvent concentration $[D_0]$, and that the observed deviations are consistent with variations in $[L_d]$. Support for this concept may also be derived from experimental data in the literature[16,17]. Slaats *et al.*[16] reported non-linearity in plots of ln k' *vs.* $[D_0]$ that can be explained in terms of variations in $[L_d]$. In addition, when

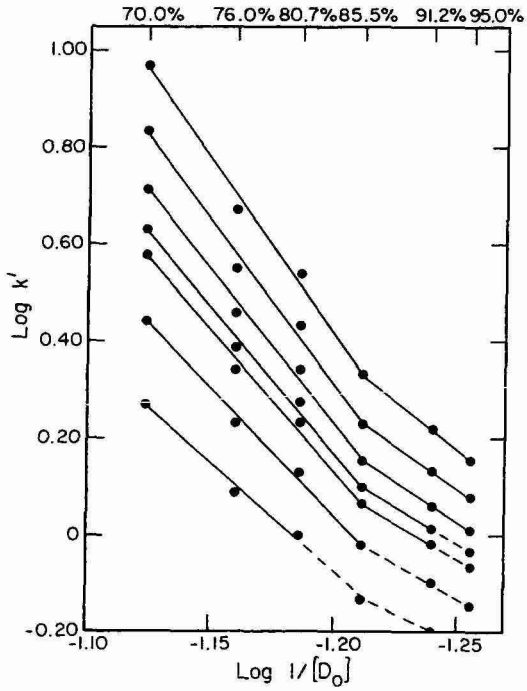

Fig. 2. Plots of log k' *vs.* log $1/[D_0]$ for some aromatic hydrocarbons. Data for this figure were derived from ref. 17. Separations were achieved on a C_{18} column eluted with acetonitrile–water at ambient temperature. Identification of solutes in the figure is as follows: 1 = 1,4-diisopropylbenzene; 2 = *sec*-pentylbenzene; 3 = 1,3-diethylbenzene; 4 = 1,2,3,4-tetramethylbenzene; 5 = 1,3,5-trimethylbenzene; 6 = *n*-propylbenzene; 7 = ethylbenzene.

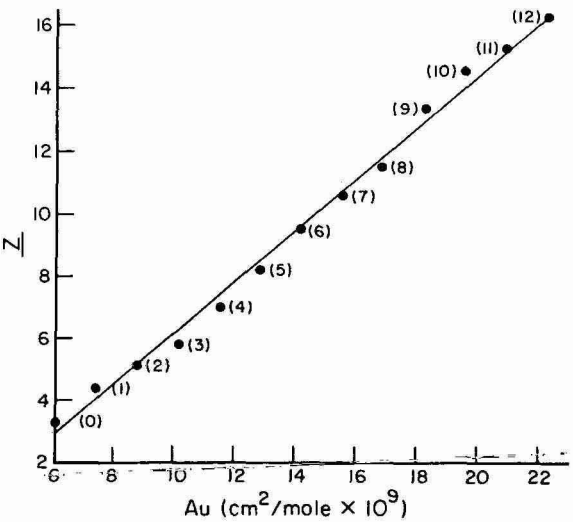

Fig. 3. A plot of Z *vs.* non-polar van der Waals surface area (A_u) for *n*-alkylbenzenes. Retention data for this plot were obtained from ref. 18. Separations were achieved on a C_{18} column eluted with a methanol–water mobile phase at ambient temperature. Solutes ranged from benzene to *n*-dodecylbenzene. The symbols 0 to 12 designate the combined number of methyl and methylene groups in the alkylbenzene.

the data of Jinno and Ishigaki[17] describing retention of non-polar solutes on a reversed-phase column eluted with acetonitrile–water are recalculated and plotted as log k' *vs.* log $1/[D_0]$ (Fig. 2), non-linear portions of the curve are seen to be beyond the 80% (v/v) concentration range[16]. The stoichiometric-displacement model and the experimental data of McCormick and Karger[15], Slaats *et al.*[16] and Jinno and Ishigaki[17] strongly suggest that at least part of the non-linearity observed when retention data are plotted according to eqns. 1, 2 and 9 are the result of variations in $[L_d]$ at both extremes of $[D_0]$. Although changes in the activity coefficient of the mobile phase have not been eliminated as a causitive factor of non-linearity, correlation of non-linearity with changes in $[L_d]$ diminish the possible contribution of activity coefficient.

Relationship of Z to non-polar surface area

The theoretical basis for a relationship between solvent displacement stoichiometry (Z) and non-polar van der Waals surface area (A_u) in a homologous series has been established in eqns. 30 and 31. This relationship was examined with a homologous series of alkylbenzenes by plotting their Z values *versus* the van der Waals surface area (A_u), as shown in Fig. 3*; retention data were taken from the paper by Colin *et al.*[18] and surface areas calculated according to Bondi[12]. As predicted in eqn. 30, there is a linear relationship between Z and A_u. When retention data from a non-homologous series of hydrocarbons were examined in the same manner (Fig. 4), correlation coefficients and standard deviations indicated a poorer fit of the experimental data to eqns. 30 and 31. This is as expected, because the geometric factors f_u and f_{mi} that relate A_{mi} to contact surface area of the various groups in a molecule are not necessarily the same as they are in a homologous series, even though the same monomeric unit is being added to the molecule.

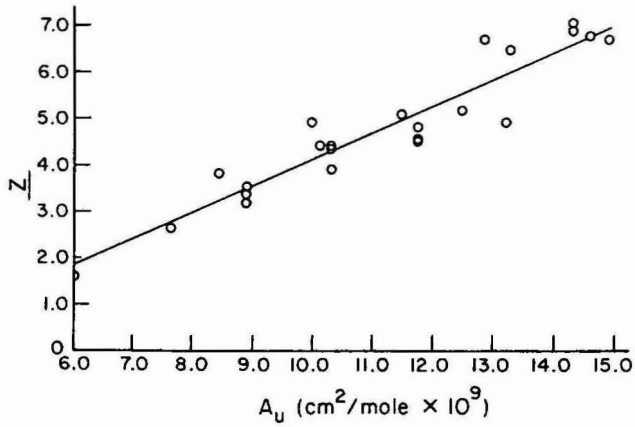

Fig. 4. A plot of Z *vs.* non-polar van der Waals surface area (A_u) for the non-homologous series of alkylbenzenes in Table I. Experimental conditions are given in Fig. 1.

* It should be noted that the Z value for benzene in this figure is different than in Table I. It has been noted previously[1] that the S value in eqn. 1 may also vary between different columns. The reason for this is unknown.

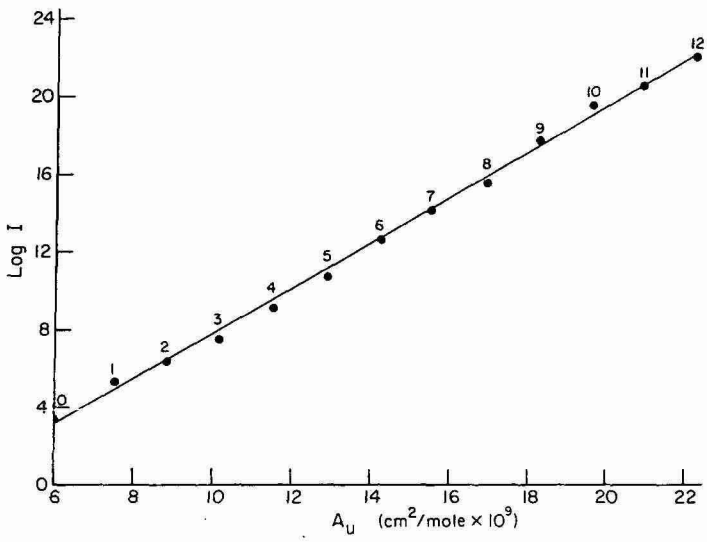

Fig. 5. A plot of log I *vs.* non-polar van der Waals surface area (A_u) for the *n*-alkylbenzenes. Retention data were derived from ref. 18. Experimental conditions are as given in Fig. 3.

Relationship between I and non-polar surface area

Fig. 5 is a plot of log I *vs.* non-polar van der Waals surface area (A_u) of a homologous series of alkylbenzenes. As expected from eqn. 38, this plot is linear and there is general agreement between the model and experimental data. Although not a homologous series, data from the hydrocarbons used in Fig. 4 also exhibit linear behavior as shown in Fig. 6. Again the geometric factors (f_{mi}) of the various groups are sufficiently different that there is some scatter in the plot.

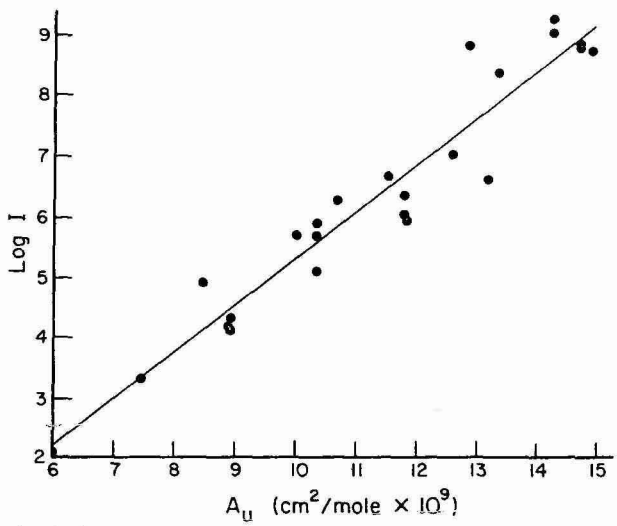

Fig. 6. A plot of log I *vs.* non-polar van der Waals surface area (A_u) for the non-homologous series of alkylbenzenes in Table I. Experimental conditions are given in Fig. 1.

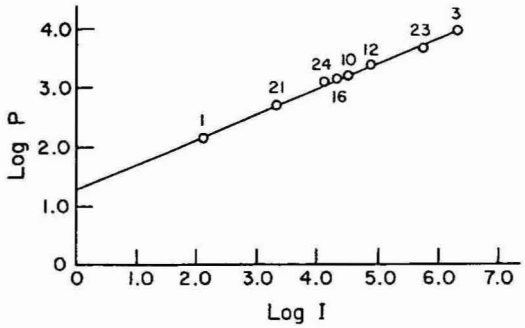

Fig. 7. A plot of log P *vs.* log I for some aromatic hydrocarbons. Octanol–water partition coefficient (P) values were taken from ref. 14. Chromatographic conditions are given in Fig. 1. Solutes are numbered according to Table I.

Relationship between I and P

The Yalkowsky and Valvani treatment[14] of the relationship between hydrocarbon surface area and the partition coefficient (P) of a substance was obtained from the hydrophobic fragment constants of Nauta and Rekker[19]. Because of the ease of calculation, van der Waals surface areas of non-polar portions of solutes were substituted for Rekker constants in these studies. Justification for this was obtained from a plot (data not shown) of octanol–water partition coefficients *versus* A_u; linearity was equivalent to that obtained by Yalkowsky and Valvani[14]. Plots of log I *versus* log P shown in Fig. 7 are linear, as suggested by eqn. 46. Numerical values of 0.445 and 1.2223 were calculated for the slope (g) and intercept (C_θ) respectively. The correlation between log I of this hydrocarbon series on the octysilane column and log P for an octanol–water system is sufficiently good that treating an octylsilane

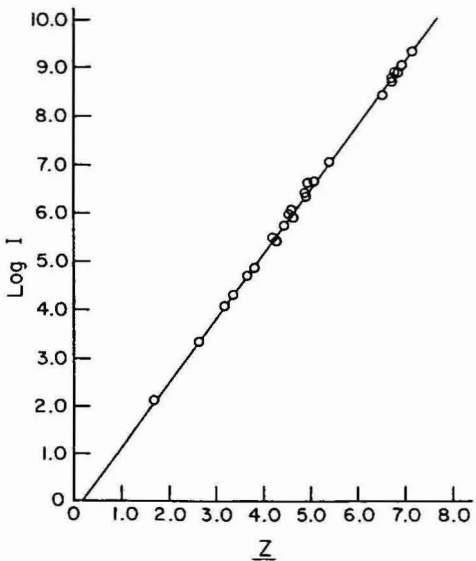

Fig. 8. A plot of log I *vs.* Z for the non-homologous series of alkylbenzenes given in Table I. Experimental conditions are given in Fig. 1.

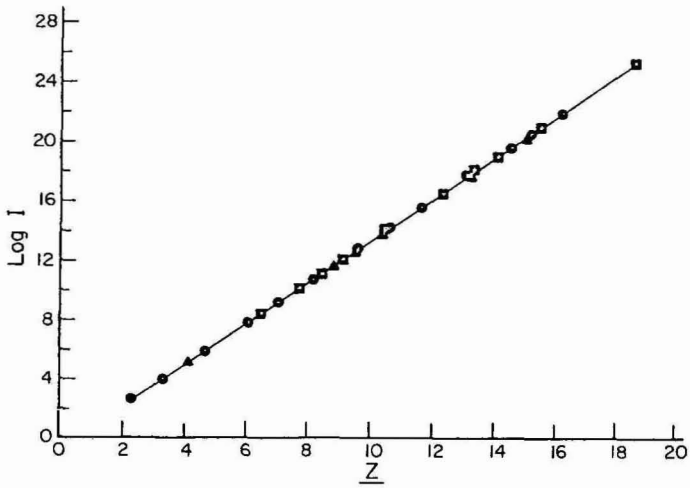

Fig. 9. Plots of log I *vs.* Z for three homologous series. The retention data for this figure were obtained from ref. 18. The chromatographic conditions are given in Fig. 3. Identification symbols: ● = *n*-alkylbenzenes; ▲ = *n*-methyl esters; ■ = *n*-alkanes.

column as a liquid–liquid partition system with non-polar solutes would seem to be valid.

Relationship between I and Z

Since both Z and I have been related to non-polar contact surface area (C_u) in eqns. 28 and 36, respectively, it is to be expected that plots of log I *vs.* Z will be linear with a slope of J, as indicated in eqn. 40. This has been confirmed experimentally, with a non-homologous series of hydrocarbons (Fig. 8) and three homologous series (Fig. 9). Since C_u is used here instead of A_u, and geometric factors (f) do not appear in any of these equations, it is to be expected that a non-homologous series will show linearity equivalent to that of a homologous series, and this is indeed observed in the figures. These plots confirm again that as the number (Z) of solvent molecules involved in displacement increases, the affinity (I) of a solute for the bonded phase increases logarithmically.

The slope J of Fig. 8 for the 24 non-polar compounds from Table I was 1.328 in comparison to 1.384 for the *n*-alkylbenzenes in Fig. 9. These values are relatively close to J values of 1.418 for *n*-alkanes and 1.400 for *n*-methyl esters that may be calculated from the data of other workers[18] with different columns (figures not shown). In all these cases, the monomeric unit was a methylene group (CH_2), and it is seen that the contribution of a monomer to retention is only slightly influenced by the rest of the molecule and the column.

CONCLUSIONS

This paper is the first to examine a model predicting that displacement of small non-polar solutes from an RPC support involves the participation of a stoichiometric number (Z) of solvent molecules. This stoichiometric displacement model predicts

that there is a specific contact surface area of both solvents and solutes with the organosilane bonded phase and that this contact surface area is a fraction of the total non-polar surface area of the molecule. An increase in the non-polar surface area of a solute is accompanied by increasing retention and the number (Z) of solvent molecules required for displacement. In contrast, increasing the surface area of the solvent decreases Z for a particular solute.

The model also predicts that the fraction of the non-polar surface area of a solute that contacts the surface of a support is a function of a series of group specific steric factors within a molecule that limit the contact of individual groups. Total contact surface area of a molecule would be the sum of the contributions of individual groups in a molecule. In all cases experimental data were found to be consistent with this model. Non-linearity in plots of log k' *versus* log $1/[D_0]$ at extremes of $[D_0]$ were concluded to be the result of variations in the concentration of solvent adsorbed on either the support or the solute.

GLOSSARY OF SYMBOLS

$a = (B/C_m) - sd = d(\log I)/dC_u$ from eqn. 36.
a_{mi} is the fraction of the total non-polar surface area contributed by a monomer.
A is a constant in eqn. 32 (see ref. 13 for a more detailed discussion).
A_e represents the non-polar surface area of an end group.
A_f represents the non-polar surface area of a functional group.
A_g is a constant in eqn. 2 (see ref. 2 for a more extensive discussion).
A_{hsa} designates hydrocarbon surface area of a solute according to Yalkowsky and Valvani[14].
A_i represents the non-polar surface area of a branching group.
A_m represents the non-polar van der Waals surface area of a monomeric unit in a solute.
A_M represents the non-polar van der Waals surface area of all monomeric units of a particular type in a solute.
A_{mi} represents the non-polar van der Waals surface area of some ith group in a molecule.
A_u represents the total non-polar van der Waals surface area of a molecule.
A_v represents the total non-polar van der Waals surface area of a solvent molecule.
B is a constant in eqn. 32 (see ref. 13 for a more detailed discussion).
B_g is a constant in eqn. 2 (see ref. 2 for a more extensive discussion).
C_E represents the non-polar contact surface area of all end groups in a molecule.
C_F represents the non-polar contact surface area of all functional groups in a molecule.
C_g is a constant in eqn. 2 (see ref. 2 for a more extensive discussion).
C_I represents the total non-polar contact surface area of branching groups in a molecule.
C_m represents the non-polar contact surface area of a monomer unit in a molecule.
C_M represents the combined non-polar contact surface area of all monomeric units of the same type in a molecule.
C_{M+E} represents the total non-polar constant surface area of all end groups and monomeric units in a molecule.

$C_T = C_{spt} + C_u$, which is the total non-polar surface area that is solvated when a solute desorbs from a column.
C_{spt} represents the non-polar contact surface area on the support surface determined by contact with a solute molecule.
C_u represents the non-polar contact surface of a solute molecule.
C_v represents the non-polar contact surface area of a solvent molecule.
C_α is a constant in eqn. 18 that accounts for solvent functional-group contribution to solvent contact surface area (C_v).
C_β is a constant in eqn. 19 that accounts for functional-group contributions in the solvent to C_{spt}.
C_γ is a constant in eqn. 20 that accounts for functional-group contributions from the solvent to C_u.
$C_\delta = S_{cs}/S_{cu}$
$C_\varepsilon = nr/q$
$C_\mu = C_\beta + C_\gamma$
$C_\eta = C_\varepsilon/C_\delta$
$C_\rho = (C_\gamma C_\varepsilon/C_\delta) + C_\beta$
$C_\sigma = C_\eta + 1$
$C_\omega = C_\rho - C_\mu$
$C_\psi = C_F + C_1$
$C_\lambda = A - id - (BC_\psi/C_m)$
$C_\theta = (avf_u/m) + C_\lambda$
$d = \log 1/[D_0]$ when $[D_0]$ is a constant.
D_g is a constant in eqn. 2 (see ref. 2 for a more extensive discussion).
$[D_0]$ represents desorbing agent concentration in moles/liter.
f is a geometric factor representing the fraction of the total non-polar surface area of a molecular or group that contacts the surface of a reversed-phase support.
F is fractional contribution of functional groups to A_u.
f_e is the geometric factor for an end-group substituent in a molecule.
f_f is the geometric factor for a particular functional group.
f_i is the geometric factor for a branching group in a molecule.
f_m is the geometric factor for a monomeric unit in a molecule.
f_{mi} is the geometric factor for an ith monomeric unit.
f_u is the geometric factor for a molecule.
f_v is the geometric factor for a particular solvent.
$g = a/m$
$i = S_{cu}C_\omega/C_v$
I is a constant which is equal to $K_1\varphi[L_d]^n$.
J is a constant that shows the relationship between incremental changes in log I and Z. $J = d(\log I)/dZ$.
k' is the capacity factor of a solute, where $k' = K_{d\varphi}$.
k_w is the extrapolated value of the capacity factor of a solute in water (ref. 1).
K_D designates the distribution coefficient of a solute, where $K_D = [S_b]/[S_m]$.
K_1 is a formation constant in eqn. 5.
$(K_1)_A$ represents the formation constant for some solute A.
$(K_1)_B$ represents the formation constant for some solute B.
L_d designates desorbing agent adsorbed on the alkylsilane bonded phase.

m is a constant in eqn. 44.
n is the number of alkyl residues onto which a solute is absorbed.
n_e is the number of end groups in a molecule.
n_f is the number of functional groups in a molecule.
n_i is the number of branching points in a molecule.
n_m is the number of monomeric units of the same type in a molecule.
$n_{(m+e)}$ is the combined number of end groups and monomeric units in a molecule.
n_{mi} is the number of ith monomeric units in a molecule.
P designates the octanol–water partition coefficient of a solute.
q is the number of solvent molecules displaced from the contact surface area of the solute when it adsorbs to a reversed-phase support.
r is the number of solvent molecules displaced from a single alkylsilane when solute absorbs.
$s = S_{cu}C/C_v$
S is the slope of eqn. 1 (see ref. 1 for a more extensive discussion).
$[S_b]$ designates solute concentration on the stationary phase in moles/m^2.
$[S_b]_A$ represents the concentration of solute A in the stationary phase.
$[S_b]_B$ represents the concentration of solute B in the stationary phase.
S_{cs} is a constant representing support surface coverage by solvent. Values of 1, 2 and 4 for S_{cs} represent 100, 50 and 25% surface coverage, respectively.
S_{cu} is a constant representing coverage of the contact surface area of a solute molecule by solvent. Values of 1, 2 and 4 for S_{cu} represent 100, 50 and 25% coverage respectively.
$[S_m]$ designates solute concentration in the mobile phase in moles/liter.
$[S_m]_A$ represents the concentration of solute A in the mobile phase.
$[S_m]_B$ represents the concentration of solute B in the mobile phase.
S_s is the slope of the plot of log k' *vs.* v_f according to eqn. 1.
v is a constant in eqn. 44.
V_f is the volume fraction of organic solvent in the mobile phase.
Z is the number of solvent molecules required to displace a protein from the reversed-phase surface.
φ represents the phase ratio of the support which in the case of RPC is the volume of the stationary phase divided by the volume of the mobile phase.
Φ_b designates the volume fraction of organic solvent B in the mobile phase.

ACKNOWLEDGEMENTS

This research was supported by NIH Grant No. GM25431. This is Journal Paper No. 10,269 from the Purdue University Agricultural Experiment Station.

REFERENCES

1 L. R. Snyder, J. W. Dolan and J. R. Gant, *J. Chromatogr.*, 165 (1979) 3.
2 P. J. Schoenmakers, H. A. H. Billiet, R. Tijssen and L. de Galan, *J. Chromatogr.*, 149 (1978) 519.
3 Cs. Horváth, W. Melander and I. Molnár, *J. Chromatogr.*, 125 (1976) 129.
4 P. Jandera, H. Colin and G. Guiochon, *Anal. Chem.*, 54 (1982) 435.
5 X. Geng and F. E. Regnier, *Proc. Am. Soc. Pept. Chem.*, (1984) 727.
6 X. Geng and F. E. Regnier, *J. Chromatogr.*, 296 (1984) 15.

7 B. Grego, F. Lambrou and M. T. W. Hearn, *J. Chromatogr.*, 266 (1983) 89.
8 M. T. W. Hearn and B. Grego, *J. Chromatogr.*, 266 (1983) 75.
9 J. P. Larmann, J. J. DeStefano, A. P. Goldberg, R. W. Stout, L. R. Snyder and M. A. Stadalius, *J. Chromatogr.*, 255 (1983) 163.
10 L. R. Snyder, M. A. Stadalius and M. A. Quarry, *Anal. Chem.*, 55 (1983) 1413A.
11 A. W. Adamson, *Physical Chemistry of Surfaces*, 4th ed., Wiley, New York, 1982.
12 A. Bondi, *J. Phys. Chem.*, 68 (1964) 441.
13 L. R. Snyder and J. J. Kirkland, *Introduction to Modern Liquid Chromatography*, 2nd ed., Wiley, New York, 1979, p. 580.
14 S. H. Yalkowsky and S. C. Valvani, *J. Med. Chem.*, 19 (1976) 727.
15 R. M. McCormick and B. L. Karger, *Anal. Chem.*, 52 (1980) 2249.
16 E. H. Slaats, W. Markovski, J. Fekete and H. Poppe, *J. Chromatogr.*, 207 (1981) 299.
17 K. Jinno and A. Ishigaki, *J. High Resolut. Chromatogr. Chromatogr. Commun.*, 5 (1982) 668.
18 H. Colin, A. M. Krstulovic, M. F. Gonnard, G. Guiochon, L. Yun and P. Jandera, *Chromatographia*, 17 (1983) 9.
19 W. Th. Nauta and R. F. Rekker, *The Hydrophobic Fragmental Constant*, Elsevier, Amsterdam, 1977.

Journal of Chromatography, 332 (1985) 169–179
Elsevier Science Publishers B.V., Amsterdam — Printed in The Netherlands

CHROMSYMP. 634

SEMI-PREPARATIVE HIGH-PERFORMANCE LIQUID CHROMATOGRAPHIC ANALYSIS OF COMPLEX ORGANIC MIXTURES

F. W. KARASEK* and H. Y. TONG
Department of Chemistry, University of Waterloo, Waterloo, Ontario, N2L 3G1 (Canada)
(First received April 8th, 1985; revised manuscript received May 24th, 1985)

SUMMARY

Better understanding of the trace organic pollutants in the environment challenge us to carry on the extensive multi-component identification and quantification in an extremely complex environmental mixture. The analysis of such complex mixtures requires an effective separation method which has a high efficiency, speed, reproducibility, and recovery. This requirement is beyond the ability of any single conventional separation method, and has led to the use of high-performance liquid chromatography separation techniques in the analysis of organic mixtures.

The effectiveness of a semi-preparative high-performance liquid chromatographic separation together with gas chromatography–mass spectrometry for the analysis of organic compounds and for target analysis of dioxins in organic extracts of fly ash particulate samples from municipal incenerators has been demonstrated. The extract is a typically complex environmental mixture containing as many as 600 organic components.

INTRODUCTION

In environmental samples, traces of organic compounds are commonly present in extremely complex matrices and many of these are toxic[1,2]. Hundreds of components are known to be present in the extracts of particulates from diesel exhaust and fly ash from municipal incinerators[3,4]. Utilizing detection techniques with high sensitivity, direct analysis has been limited to a few compounds in such complex samples. More often the interference among components in the mixtures hinders direct multicomponent analysis. Therefore, a preseparation is necessary for the effective analysis of such mixtures.

A number of separation procedures have been reported for subsequent class or individual compound analysis[5–8]. For complex samples and where there is a requirement for extensive identification, the use of high-performance liquid chromatography (HPLC) has definite advantages. HPLC is gaining popularity in the fractionation and clean-up of complex environmental samples[3,9,10].

The organic extract of fly ash from municipal incinerators is extremely complex. Two classes of toxic compounds found are polychlorinated dibenzodioxins

0021-9673/85/$03.30

(PCDDs) and polychlorinated dibenzofurans (PCDFs). Based on our previous work[11,12], a complete procedure is given here to show the effectiveness of HPLC separation for both multicomponent identification and target compound analysis in an extremely complex mixture. Data for extracts of fly ash samples from Canada and Japan are presented.

EXPERIMENTAL

Chemical reagents

Most polycyclic aromatic compound (PAC) standards and all polychlorinated benzene and phthalate ester standards used for compound identification and retention index calculation were of 95–99% purity and obtained from either Aldrich Chem. Co. (Montreal, P,Q., Canada) or Chem. Service Inc. (West Chester, PA, U.S.A.). The standards of 1,2,3,4-tetrachlorodibenzo-*p*-dioxin (1234-TCDD), 1,2,3,4,7,8-hexachlorodibenzo-*p*-dioxin (123478-H_6CDD), 1,2,3,4,6,7,8-heptachlorodibenzo-*p*-dioxin (1234678-H_7CDD), octachlorodibenzo-*p*-dioxin (OCDD) and octachlorodibenzofuran (OCDF) were obtained from Ultra Scientific Inc. (Hope, RI, U.S.A.). The standards of 1,2,3,4,7-pentachlorodibenzo-*p*-dioxin (12347-P_5CDD) and 2,3,7,8-tetrachlorodibenzo-*p*-dioxin (2378-TCDD) were obtained from Cambridge Isotope Laboratories Inc. (Woburn, MA, U.S.A.) and Foxboro/Analabs (North Haven, CT, U.S.A.), respectively.

The solvents used in this study were "distilled in glass", UV grade from Caledon Laboratories (Georgetown, Ontario, Canada).

Fly ash extracts

The Ontario fly ash sample was collected from the electrostatic precipitator of a municipal incinerator in Toronto, Canada. The 435-g sample was Soxhlet-extracted with benzene for 48 h and finally concentrated to 1.8 ml for normal-phase HPLC separation.

A total of 135 g of a Japanese fly ash sample taken from two municipal incinerators in the city of Kyoto was also Soxhlet-extracted with benzene and reduced to 0.2 ml for the HPLC separation.

The extraction and following concentration procedure have been described previously[11].

Normal-phase semi-preparative HPLC separation

The normal-phase HPLC separation was achieved on a Spectra-Physics SP8000 equipped with a SP8400 UV/vis variable wavelength detector and SP4100 integrator. A 10-μm Spherisorb silica column (250 × 9.4 mm; Terochem, Toronto, Canada) was used with a 140-μl sample loop. A 91-min gradient elution program consisting of *n*-hexane, dichloromethane and acetonitrile was employed to separate the raw extract into five fractions. The flow-rate was 5 ml/min. The details of this HPLC separation were described previously[11]. Five fractions were collected and concentrated, and then subjected to extensive detailed analysis by gas chromatography–mass spectrometry (GC–MS) and high-resolution gas chromatography (HRGC).

Reversed-phase semi-preparative HPLC separation

The instrument used for the reversed-phase HPLC separation was a Varian 5000 equipped with a Vista 402 data system, built-in UV detector and Fluorichrom detector. A MicroPak MCH-10 (C_{18}) column (300 × 8 mm; Varian Associates Inc., Walnut Creek, CA, U.S.A.) was used with a 100-μl sample loop. A gradient elution program using acetonitrile and dichloromethane was employed with a flow-rate of 2 ml/min.

Fraction 2, collected from the normal-phase HPLC separation and containing exclusively PCDDs and PCDFs, was subjected to the reversed-phase separation. Six subfractions (SFs) were separately collected during 27 min and concentrated for the target analysis of PCDDs and PCDFs. The detailed description of this reversed-phase HPLC separation has been reported previously[12].

Qualitative analysis of HPLC fractions

Five fractions obtained from the normal-phase HPLC separation were subjected to analysis by GC–MS and HRGC for compound identification. The GC–MS analyses were performed mainly on a Hewlett-Packard 5987 GC–MS–data system equipped with a 30 m × 0.32 mm I.D. DB-5 FSCC column (J & W Scientific, Rancho Cordova, CA, U.S.A.). The electron-impact ionization mode was operated at 70 eV. This system allows a comprehensive library search of unknown spectra against 70 000 stored reference spectra.

Retention indices based on polycyclic aromatic hydrocarbon reference compounds have also been used to facilitate compound identification[13]. The retention indices of unknown compounds in samples were obtained on a Hewlett-Packard 5880A gas chromatograph equipped with a flame ionization detector and the same FSCC column used for GC–MS analysis.

Quantitative analysis of PCDDs and PCDFs in HPLC subfractions

The subfractions 2–6 were subjected to quantitative analysis for PCDDs and PCDFs by HRGC and GC–MS with selected ion monitoring (SIM). These analyses were performed on the HP5880 GC and HP5987 GC–MS instruments, respectively. PCDDs and PCDFs in each subfraction were first confirmed by the mass chromatograms of their M^+, $[M+2]^+$ and $[M+4]^+$ ions, and then quantified on the basis of the peak area of the $[M+2]^+$ ion mass chromatogram relative to that for the standards injected[12].

The identification of PCDDs and PCDFs in gas chromatograms of subfractions was achieved by comparison of those flame ionization detector traces to their corresponding total ion-current traces obtained from GC–MS analysis. PCDD and PCDF standards were injected in order to obtain response factors for quantitative analysis. The analysis of PCDDs and PCDFs in this study was not completely isomer-specific due to the unavailability of standards for all the individual isomers.

RESULTS AND DISCUSSION

A scheme of the complete procedure for the analysis of organic compounds in a fly ash sample is given in Fig. 1. This procedure can be divided into two major parts: first, normal-phase HPLC separation for an extensive identification of com-

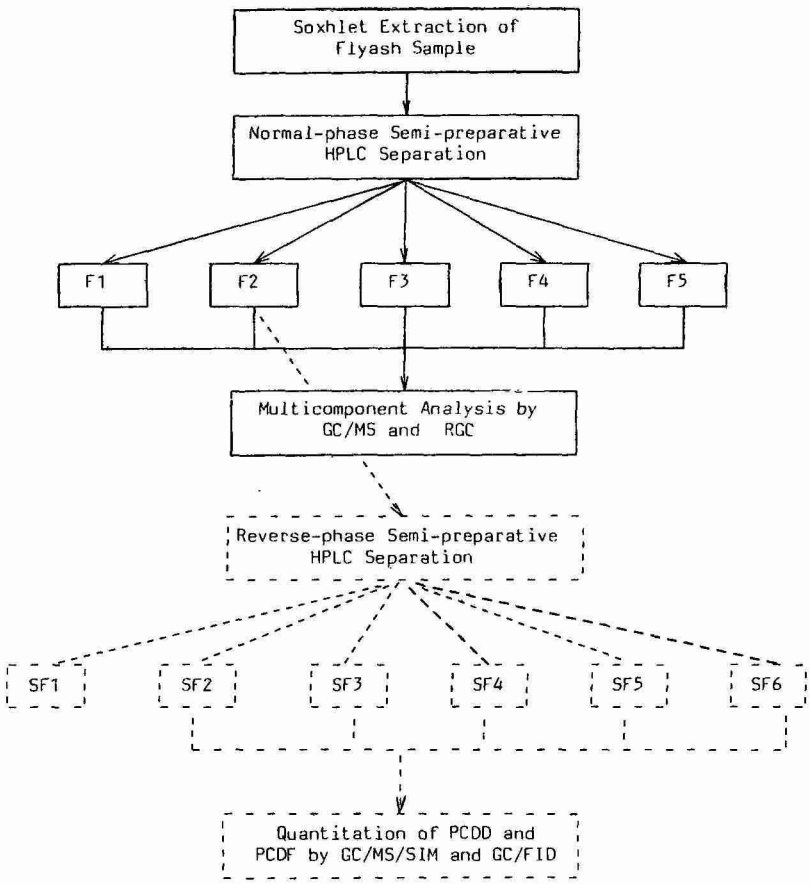

Fig. 1. Scheme of the complete procedure for the multicomponent analysis (solid line), and PCDD–PCDF target analysis of a fly ash sample.

pounds, and secondly, reversed-phase HPLC separation for a target analysis of PCDDs and PCDFs in a fly ash sample.

Fig. 2 illustrates the normal-phase HPLC separation of the Kyoto fly ash sample. This separation sorted organic compounds into non-polar, medium polar and polar categories. Five fractions (F1 to 5) were collected. Numerous components in the raw extract were grouped into different organic compound classes. The interferences among the co-eluting components had been greatly reduced in each fraction. More components could be seen and a better identification could be achieved after the components in the raw extract had been divided into several fractions.

The gas chromatogram of fraction 2 of the Kyoto sample is shown in Fig. 3. Some typical compounds identified in this fraction as well as the identification method used are listed in Table I.

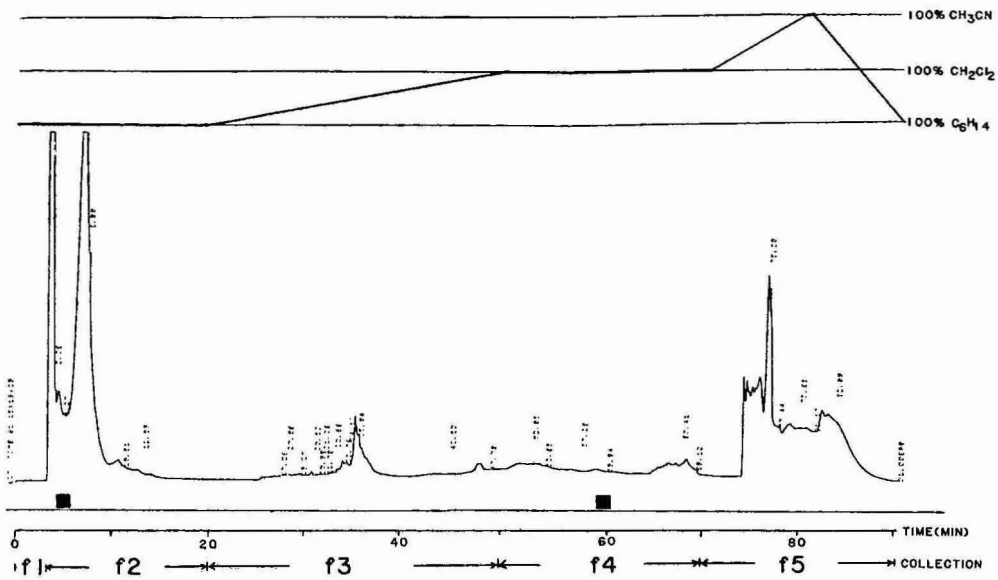

Fig. 2. Normal-phase HPLC separation of the Kyoto fly ash extract: gradient elution program (upper trace); UV chromatogram (middle trace); and fraction collection interval. For the HPLC conditions, see Experimental section.

A more complete identification of a number of organic compounds was made for five fractions of Ontario fly ash and some of the typical compounds are illustrated in Table II. More than 600 organic components were observed in the GC traces of five fractions of Ontario fly ash, more than 200 of which have been identified. Such

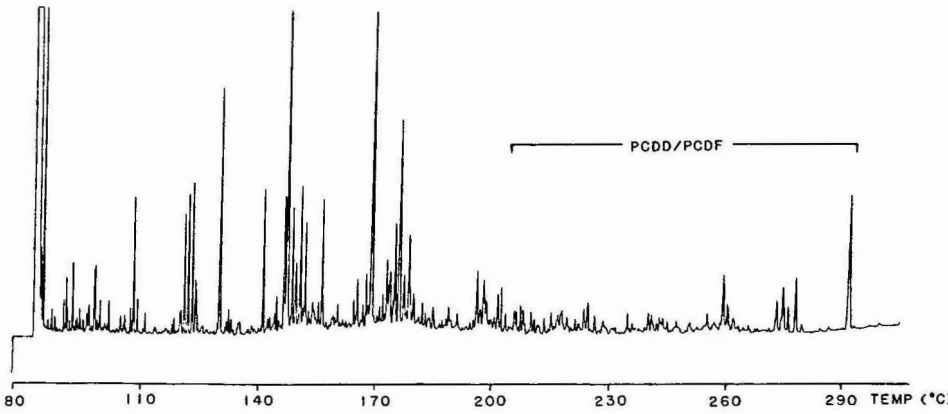

Fig. 3. Gas chromatogram of HPLC fraction 2 of the Kyoto fly ash extract. Chromatographic conditions: column 30 m × 0.32 mm I.D. DB-5 FSCC; temperature, 80°C for 1 min, programmed to 300°C at 3°C/min; flame ionization detection. The elution region for PCDDs and PCDFs (which have more than four chlorine atoms) is shown.

a comprehensive identification of organic compounds will provide a great deal of information for the better understanding of the impact of fly ash pollution on the human environment.

In the normal-phase HPLC separation, PCDDs and PCDFs are exclusively eluted in fraction 2 together with more than 100 other components. PCDDs and PCDFs are two series of compounds formed by chlorine atom substitution on the dibenzo-*p*-dioxin and dibenzofuran parent molecules. Owing to the different numbers and patterns of substitution, there are 75 PCDD and 135 PCDF isomers. When they are present together, these isomers are eluted in a narrow temperature range on the gas chromatogram. Such serious peak overlapping makes component identification very difficult and quantification by GC data impossible. In many reported clean-up procedures, even after separation, the analysis of PCDDs and PCDFs is usually achieved with a highly selective system such as GC–MS–SIM.

To facilitate an isomer-specific analysis or an analysis using non-selective detectors, a further isolation of PCDDs and PCDFs in fraction 2 of Ontario fly ash

TABLE I

COMPOUNDS IDENTIFIED IN HPLC FRACTION 2 OF THE KYOTO FLY ASH EXTRACT

Compound	*MW*	*Retention index*	*Identification method**
Trimethylbenzene	120	177.24	a
Dichlorobenzene	146	179.21	a
Naphthalene	128	200.00	a,b,c,d
Trichlorobenzene	180	204.34	a,d
Dimethylnaphthalene	142	217.46	a,b
Tetrachlorobenzene	214	222.05	a,b,c,d
Biphenyl	154	231.38	a,b,c,d
Ethylnaphthalene	156	234.26	a,b,c
Methylbiphenyl	168	250.27	a,b,c
Pentachlorobenzene	248	256.22	a,b,c,d
Hexachlorobenzene	282	289.55	a,b,c,d
Tetrachlorophenol	230	296.69	a,b,d
Phenanthrene	178	300.00	a,b,c,d
Tetrachloroacenaphthalene	288	307.23	a,b,c
Methylanthracene	192	323.28	a,b,c,d
Phenylnaphthalene	204	331.30	a,b,d
Tetrachlorodibenzodioxin	320	375.46	a,b,d
Chrysene	228	400.01	a,b,c,d
Pentachlorodibenzofuran	338	405.74	a,b,d
Pentachlorodibenzodioxin	354	408.84	a,b,d
Hexachlorodibenzodioxin	388	427.34	a,b,d
Heptachlorodibenzofuran	406	461.57	a,b,d
Heptachlorodibenzodioxin	422	465.07	a,b,d
Octachlorodibenzodioxin	456	493.40	a,b,c,d

* a, Identified by sample mass spectra; b, identified by retention indices; c, identified by standard compounds injected; d, can be found in ref. 11.

TABLE II

COMPOUNDS IDENTIFIED IN FRACTIONS 1–5 OF ONTARIO FLY ASH

Compound	*MW*	*Identification method**
Fraction 1		
C_{12}–C_{39} *n*-alkane	170–548	
C_{14}–C_{25} *n*-alkene	196–350	
Fraction 2		
Tetramethylbenzene	134	a
Trichlorobenzene	180	a
Naphthalene	128	a,b,c
Methylnaphthalene	142	a
Tetrachlorobenzene	214	a
Biphenyl	154	a
Ethylnaphthalene	156	a
Dimethylnaphthalene	156	a
Acenaphthylene	152	a
Methylbiphenyl	168	a
Dibenzofuran	168	a
Pentachlorobenzene	248	a
Trimethylnaphthalene	170	a,b
Nonylbenzene	204	a
Trichlorophenol	196	a
Bromotetrachlorobenzene	292	a
Decylbenzene	218	a
Hexachlorobenzene	282	a
Methylfluorene	180	b
Bromodichloromethylphenol	254	a
Dibenzothiophene	184	a,b,c
Tetrachlorophenol	230	a
Phenanthrene	178	a
Tetrachloroacenaphthylene	288	a
Dihydropyrene or dihydrofluoranthene	204	a
Dichlorodibenzofuran	236	a
Methylphenanthrene	192	a
Tetrachlorobenzene dicarbonitrile	264	a
Methylanthracene	192	a
Dichlorodibenzodioxin	252	a
Phenylnaphthalene	204	a
Chlorophenylethynylbenzene	212	a
Ethylphenanthrene	206	a
Trichlorodibenzofuran	270	a
Fluoranthene	202	a
Pentachloronaphthalene	298	a
Trichlorodibenzodioxin	286	a
Pyrene	202	a
Tetrachlorobiphenyl	290	a
Tetrachlorodibenzofuran	304	a
Tetrachlorodibenzodioxin	320	a
Hexachloronaphthalene	332	a
Benzo[*ghi*]fluoranthene	226	a
Pentachlorobenzofuran	338	a
Pentachlorodibenzodioxin	354	a
Hexachlorodibenzofuran	372	a

(*Continued on p. 176*)

TABLE II (*continued*)

Compound	*MW*	*Identification method**
Hexachlorodibenzodioxin	388	a,c
Nonachlorobiphenyl	460	a
Decachlorobiphenyl	494	a
Heptachlorodibenzofuran	406	a
Heptachlorodibenzodioxin	422	a,c
Octachlorodibenzodioxin	456	a,c
Fraction 3		
Dimethylbenzofuran	146	a
Benzoic acid	122	a
Naphthaldehyde	156	a
1,2-Diphenylethane	182	a
Biphenylamine	169	a
Diphenylmethanone	182	a
Diphenylpropane	196	a
9-Fluorenone	180	a,b,c
Bis(methylphenyl)diazene	210	a
Phenyl benzoate	198	a
1,3-Diphenyl-2-propen-1-one	208	a
Terphenyl	230	a,b
Chloro-9-fluorenone	214	a
4H-Cyclopenta[*d,e*]phenanthren-4-one	204	a
Dichloro-9-fluorenone	248	a
1-Chloro-9,10-anthraquinone	242	a
Trichloro-9-fluorenone isomer	282	a
7H-Benz[*d,e*]anthracen-7-one (or 11-benzo[*a*]fluorenone)	230	a
Methylphenylindole	207	a
Triphenylene	228	a,b
Chrysene	228	a,b,c
Tetrachloro-9-fluorenone	316	a
Diisooctyl phthalate	390	a
Methylphenyl-1H-indole	207	a
Benzo[*c,d*]pyrenone	254	a
Pentachloro-9-fluorenone isomer	350	a
Quaterphenyl	306	a,b
Benzo[*e*]pyrene	252	a,b,c
1,7-Diphenylnaphthalene	280	a
Benzo[*a*]pyrene	252	a,b,c
Fraction 4		
1-(Methylphenyl)ethanone	134	a
Biphenylamine isomer	169	a
Xanthen-9-one	196	a,c
Dibutyl phthaalate	278	a
9,10-Anthraquinone	208	a,c
Diisooctyl phthalate	390	a
Fraction 5		
Diethyl phthalate	222	a
Caffeine	194	a
Dibutyl phthalate	278	a
Benzo[*c*]cinnoline	134	a

* For a,b,c see Table I.

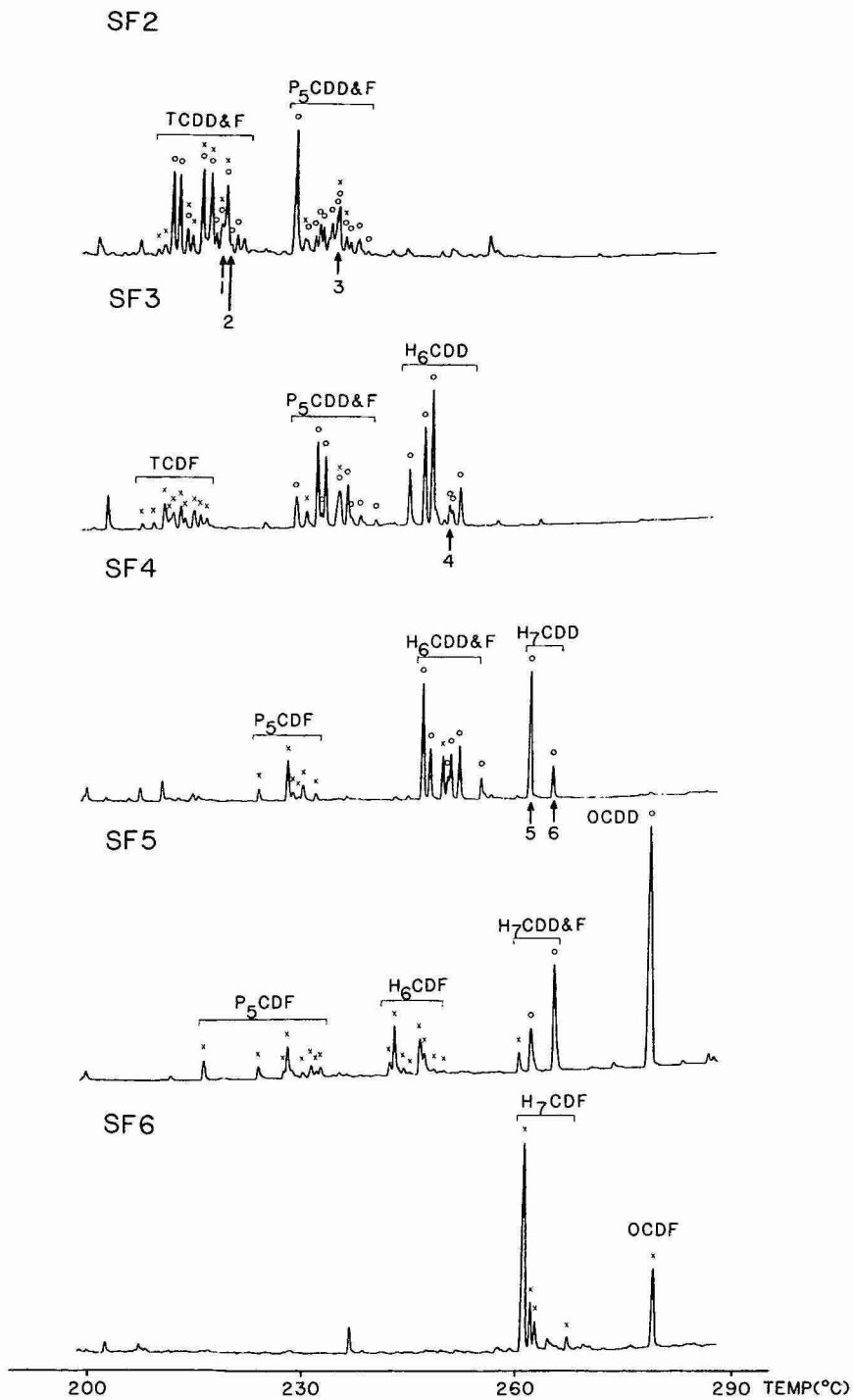

Fig. 4. GC traces (flame ionization detection) showing the distribution of PCDDs and PCDFs among subfractions 2–6 from the reversed-phase HPLC separation. Conditions as in Fig. 3. ○, PCDD; ×, PCDF. GC retention times: 1 = 1234-TCDD; 2 = 2378-TCDD isomer; 3 = 12347-P_5CDD; 4 = 123478-H_6CDD; 5 = 1234578-H_7CDD isomer; 6 = 1234678-H_7CDD isomer.

was carried out by reversed-phase HPLC. Six subfractions (SF1 to 6) were obtained. Fig. 4 shows the distribution pattern of PCDDs and PCDFs among SF2 to SF6. In this diagram, PCDDs and PCDFs are labelled differently. The method used for identification has been described in the Experimental section and also discussed elsewhere[12]. Most of the other components in fraction 2 were found in SF1.

Many PCDDs were separated from their corresponding PCDFs, and some positional isomers of PCDDs (or PCDFs) with the same number of chlorine atoms were distributed into different subfractions. This further spread of PCDDs and PCDFs into different subfractions and good isolation of PCDDs and PCDFs from almost all other organic components greatly facilitates their isomer-specific identification and quantification. This separation is also an important improvement in the analysis of PCDDs and PCDFs in a complex mixture using a non-selective detector. The quantitation of PCDDs and PCDFs in Ontario fly ash using GC–MS–SIM and GC analysis with flame ionization detection has been given elsewhere[12]. After this two-step HPLC separation, the results obtained by GC–MS–SIM and GC are reasonably consistent[12].

Recoveries of higher than 90% for some typical PAC, PCDD and PCDF standards have been reported for these normal- and reversed-phase HPLC separations[3,11,12]. The HPLC separations described also provide a good reproducibility.

CONCLUSIONS

The data obtained provide evidence for the effectiveness of semi-preparative HPLC when used as a separation technique for the analysis of organics in an extremely complex mixture. Using different combinations of mobile phases and columns, a large number of components can be separated into different classes or groups as needed. In this way, the complexity of each HPLC fraction or subfraction and the interferences among components are dramatically reduced. Consequently, more components can be identified and a better quantitation can be achieved by the subsequent analysis. High separation efficiency and recovery, and good reproducibility, are much more easily obtained in HPLC separations.

ACKNOWLEDGEMENT

This work was financially supported by the Natural Sciences and Engineering Research Council of Canada.

REFERENCES

1 C. E. Searle (Editor), *Chemical Carcinogens*, ACS Monogr. 173, American Chemical Society, Washington, DC, 1976.
2 P. W. Jones and P. Leber, *Polynuclear Aromatic Hydrocarbons: Third International Symposium on Chemistry and Biology — Carcinogenesis and Mutagenesis*, Ann Arbor Science, Ann Arbor, MI, 1978.
3 H. Y. Tong, J. A. Sweetman, F. W. Karasek, E. Jellum and A. K. Thorsrud, *J. Chromatogr.*, 312 (1984) 183.
4 G. A. Eiceman, R. E. Clement and F. W. Karasek, *Anal. Chem.*, 51 (1979) 2344.
5 M. L. Lee, M. Novotny and K. D. Bartle, *Anal. Chem.*, 48 (1976) 405.
6 J. M. Daisey and M. H. Leyko, *Anal. Chem.*, 51 (1979) 24.

7 M. L. Yu and R. A. Hites, *Anal. Chem.*, 53 (1981) 51.
8 S. F. Hrudey, R. Perry and R. A. Wellings, *Environ Res.*, 7 (1974) 294.
9 T. Nielsen, *Anal. Chem.*, 55 (1983) 286.
10 T. Romanowski, W. Funcke, J. König and E. Baltanz, *Anal. Chem.*, 54 (1982) 1285.
11 H. Y. Tong, D. L. Shore, F. W. Karasek, P. Helland and E. Jellum, *J. Chromatogr.*, 285 (1984) 423.
12 H. Y. Tong, D. L. Shore and F. W. Karasek, *Anal. Chem.*, 56 (1984) 2442.
13 M. L. Lee, D. L. Vassilaros, C. M. White and M. Novotny, *Anal. Chem.*, 51 (1979) 768.

Journal of Chromatography, 332 (1985) 181–188
Elsevier Science Publishers B.V., Amsterdam — Printed in The Netherlands

CHROMSYMP. 628

DETERMINATION OF THIAMINE AND ITS PHOSPHATE ESTERS IN HUMAN AND RAT BLOOD BY HIGH-PERFORMANCE LIQUID CHROMATOGRAPHY WITH POST-COLUMN DERIVATIZATION

MIEKO KIMURA* and YOSHINORI ITOKAWA
Department of Hygiene, Faculty of Medicine, Kyoto University, Kyoto 606 (Japan)
(First received April 2nd, 1985; revised manuscript received May 10th, 1985)

SUMMARY

A method for the determination of thiamine and thiamine phosphate esters in human and rat blood by liquid chromatography with post-column derivatization, and distribution of thiamine and its phosphate esters in human and various animals is demonstrated. Blood is deproteinized and centrifuged. Aliquots of the samples are applied to a μBondapak C_{18} column attached to a high-performance liquid chromatograph. Addition of potassium ferricyanide sodium hydroxyide solution to the column effluent with a proportioning pump converts thiamine phosphate into fluorophores, the intensities of which are measured with a spectrofluorophotometer. In human blood, thiamine pyrophosphate was present in the greatest concentration, followed by thiamine triphosphate; thiamine monophosphate and thiamine were present in small amounts. In rat blood, thiamine pyrophosphate was found in the largest amount, followed by thiamine monophosphate. Thiamine triphosphate and thiamine were present in small amounts.

INTRODUCTION

Various biochemical tests have been developed for the detection of thiamine deficiency, including measurements of thiamine in blood or urine or of erythrocyte transketolase activity[1]. A close correlation exists between the development of thiamine deficiency and the decreasing excretion of thiamine as measured in 24-h urine samples[1,2]. However, the determination of thiamine status by the use of untimed urine samples may be inaccurate[3], and it is not usually feasible to collect 24-h urine samples. Measurement of the activity of erythrocyte transketolase, a thiamine-dependent enzyme, is considered to be a convenient and sensitive method for detecting thiamine deficiency[4,5]. However, in these assay methods, effects of other non-thiamine dependent enzymes cannot be excluded. Moreover, erythrocyte transketolase frequently fails to respond to the *in vitro* addition of TPP in patients with nervous or hepatic diseases, even in the presence of severe thiamine deficiency[6,7]. The determination of total thiamine in blood is assumed to be the most accurate way of evaluating the nutritional status of thiamine in humans.

0021-9673/85/$03.30

Berger *et al.*[8] discovered that a fluorescent substance (thiochrome) was formed from thiamine by reaction with potassium hexacyanoferrate(III) in alkaline solution, and later Fujiwara and Matsui[9] found that thiochrome was produced when thiamine was mixed with cyanogen bromide. Both of these reactions have been widely used for the determination of the total thiamine content of blood. However, in these methods, at least 3 ml of blood are necessary for accurate determination, and technical difficulties are involved.

In view of this, we have developed a simple and sensitive method for determining the total thiamine content of blood[10] and the erythrocyte transketolase activity using high-performance liquid chromatography (HPLC)[11] with post-column derivatization.

In animal tissues, there exist four different forms of thiamine: free thiamine, thiamine monophosphate (TMP), thiamine pyrophosphate (TPP) and thiamine triphosphate (TTP).

Recently, several microquantitative methods for the determination of thiamine and its phosphate esters by HPLC have been developed[12–19]. We have previously reported a reversed-phase HPLC method with post-column derivatization for separating and determining thiamine phosphate esters[20]. Here, we describe an improved method for the determination of as little as 30 fmol of thiamine and its phosphate esters in human and animal blood.

EXPERIMENTAL

Apparatus

The following instruments were used: pump for HPLC, Model LC-3A; sample injector, Model SIL-1A; column, μBondapak C_{18} (25 cm × 4 mm I.D.); proportioning pump with Tygon tubing for thiochrome reactions, PRR-2A; detector, RF500-LCA spectrofluorophotometer (excitation wavelength 375 nm; emission maximum, 450 nm; square-shaped flow cell of 12 μl capacity); recorder and computer, R-112 and chromatopac C-RIA. The column was obtained from Waters Assoc. (Milford, MA, U.S.A.) and all other equipment from Shimadzu (Kyoto, Japan).

Reagents

Thiamine hydrochloride was obtained from Wako (Osaka, Japan) and TMP and TPP from Sigma (St. Louis, MO, U.S.A.). TTP was donated by the Central Research Division of Takeda Chemical (Osaka, Japan). All other chemicals were of the best grade commercially available. De-ionized, distilled water was used to prepare all reagents.

For the mobile phase, we used a 0.2 *M* solution of NaH_2PO_4 in 0.3% aqueous acetonitrile. For post-column conversion of phosphate esters into fluorophores, we used a 0.1% solution of $K_3Fe(CN)_6$ in 15% NaOH[10].

Preparation of samples

Collect human, rat, mouse, guinea pig, rabbit, dog, pigeon and chick blood with a heparinized syringe. Centrifuge the blood quickly after collecting at 1100 *g* for 15 min to separate erythrocytes from plasma. To 0.2 ml of 10% trichloroacetic acid in a 1.5-ml polyethylene centrifuge tube, add 0.2 ml of blood, erythrocytes or

plasma and vortex mix vigorously, then centrifuge at 35 000 *g* for 5 min. Use the supernatant solution as the sample.

Procedures

Inject 100 μl of the sample into the chromatograph. The flow-rate of the mobile phase is 1.0 ml/min. Add hexacyanoferrate(III)–sodium hydroxide solution to the column effluent at 0.5 ml/min with a proportioning pump to convert thiamine phosphate esters into thiochrome phosphates. Measure and record with the spectrofluorophotometer. For quantification compare the peak heights of the samples with a standard calibration graph for thiamine and its phosphate esters.

We also chromatographed samples without adding the potassium hexacyanoferrate(III) to check the blank values.

Animal experiments

Use male Wistar rat weighing approximately 150 g. Administer thiamine (10 mg/kg body weight) intraperitoneally or orally. Collect blood at 0, 5, 15, 30, 60, 120 and 180 min after administration and measure thiamine and its phosphate esters in these samples. Also, collect blood and incubate it at 37°C on a water-bath without or with thiamine *in vitro*. At 0, 5, 15, 30, 60, 120 and 180 min after incubation measure the thiamine and its phosphate esters in the blood.

RESULTS AND DISCUSSION

Elution profiles for a standard solution of thiamine, TMP, TPP and TTP, a human blood sample and a blank (without thiochrome reaction) are shown in Fig. 1 TTP, TPP, TMP and thiamine were each detected as single peaks, with retention times of 3.1, 3.8, 5.0 and 8.0 min, respectively. In the blood sample, TTP, TPP and TMP were detected as single peaks, but thiamine was usually not detected. Moreover, the blood contained three fluorescent peaks other than thiochrome, with retention times of 2.0, 6.25 and 12.0 min, but no substance was found to be eluted at the position where the peaks for TTP, TPP, TMP and thiamine would be eluted. Thiamine and its phosphate esters were not detected in the solution after passing it through a zeolite column[9], which adsorbs thiamine and its phosphate esters.

Fig. 2 shows the calibration graph obtained for standard solutions of thiamine, TMP, TPP and TTP. The detection limit is 30 fmol of thiamine and its phosphate esters. Fig. 1 illustrates elution profiles for a human blood sample to which TTP, TPP, TMP and thiamine had been added. Analytical recoveries of 1 pmol each of added thiamine and its phosphate esters in samples of blood taken from normal humans were 95.0–100.2%. In normal blood, the concentration of TPP was highest, followed by TTP; TMP and thiamin were hardly detectable. In erythrocytes, only TTP and TPP were found; TMP and thiamine were not detected. Plasma, on the other hand, contained small amounts of TMP and thiamine, but no TTP and TPP. In blood kept at room temperature for 1 h after collection, the TTP content decreased in proportion to the time interval, but no significant changes in TPP, TMP and thiamine contents were observed.

Fig. 3 illustrates elution profiles for whole blood, erythrocytes and plasma samples of a rat. In the whole blood, TTP, TPP, TMP and thiamine were detected

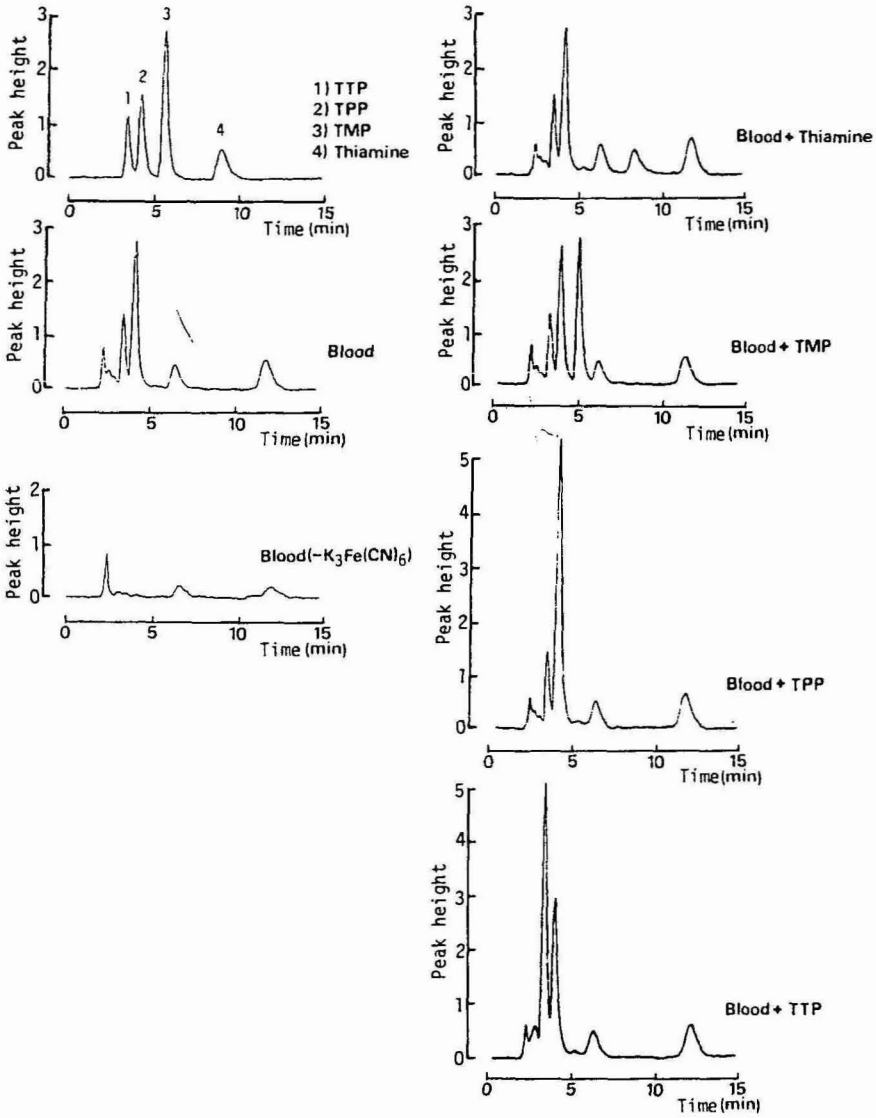

Fig. 1. Elution profiles for standard solutions of thiamine, TMP, TPP and TTP; a human blood sample, a human blood sample without thbiochrome reaction and human blood samples supplemented with thiamine, TMP, TPP and TTP.

as single peaks. TTP and TPP were found in the erythrocytes, and larger amounts of TMP and thiamine were detected in the rat plasma than in the human sample. The finding that a considerable amount of TMP was found in rat plasma is consistent with the results of Rindi *et al.*[21]. Concentrations of thiamine and its phosphate esters in whole blood of various species are shown in Table I. It is worth noting that a large amount of TMP was found in the blood of various animals. These results suggest

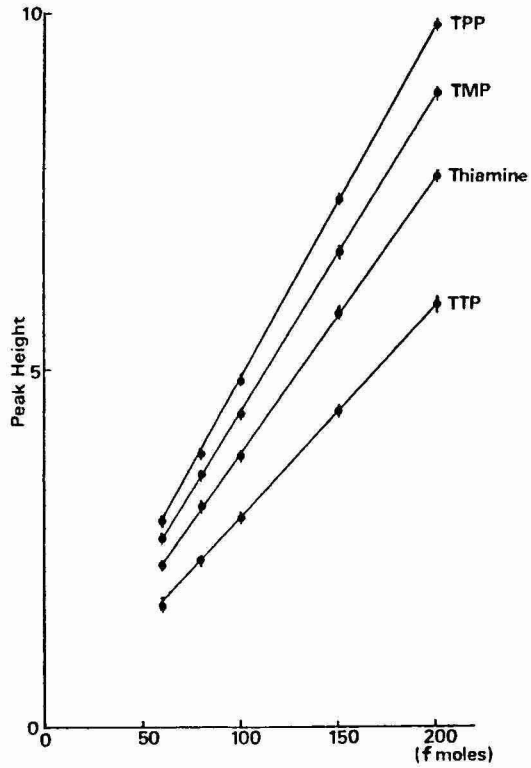

Fig. 2. Calibration graphs obtained for standard solutions of thiamine, TMP, TPP and TTP.

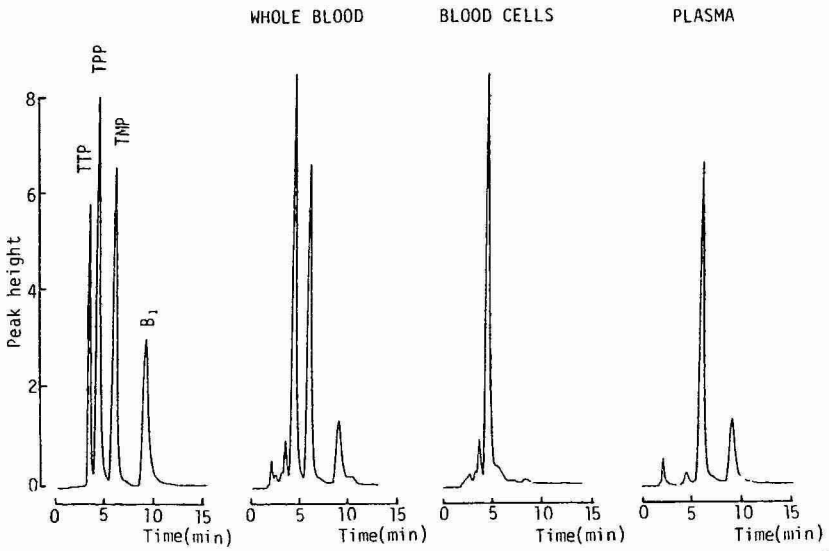

Fig. 3. Elution profiles for a standard solution, whole blood, blood cells and plasma of a rat.

that the distribution of thiamine and its phosphate esters in blood will differ according to the animal species or thiamine nutritional status.

A 10-mg amount of thiamine hydrochloride was administrated i.p. or orally to rats *in vivo*, and blood was collected at various intervals after administration. The changes in concentration of thiamine and its phosphate esters in whole blood are shown in Fig. 4A and B. With i.p. administration, the thamine concentration increased quickly up to a very high level ($4 \cdot 10^{-6}$ *M*) within 5 min, then decreased.

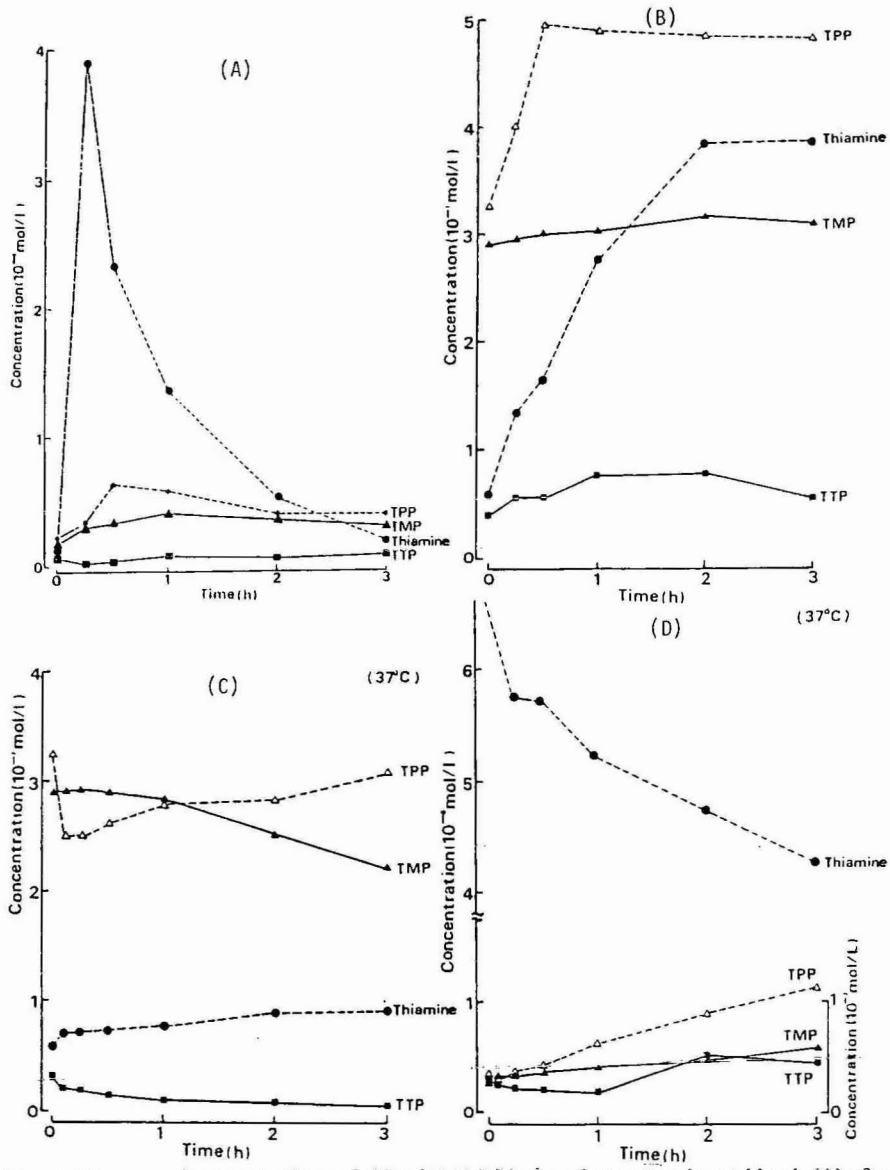

Fig. 4. Changes of concentrations of thiamine and its phosphate esters in rat blood: (A) after thiamine administration i.p. *in vivo*; (B) after thiamine administration orally *in vivo*; (C) blood kept at 37°C *in vitro*; (D) blood kept at 37°C after thiamine administration *in vitro*.

TABLE I

THIAMINE AND ITS PHOSPHATE ESTERS CONCENTRATION IN BLOOD OF VARIOUS ANIMALS (n = 3)

Blood	*Concentration (10^{-7} mol/l)*			
	Thiamine	*TMP*	*TPP*	*TTP*
Mouse	4.86 ± 0.33	4.92 ± 0.41	7.80 ± 0.56	0.50 ± 0.02
Rat	1.03 ± 0.10	4.42 ± 0.31	3.45 ± 0.25	0.42 ± 0.02
Guinea pig	0.66 ± 0.03	1.28 ± 0.11	7.16 ± 0.21	0.55 ± 0.03
Rabbit	0.07 ± 0.00	1.79 ± 0.09	4.06 ± 0.34	0.62 ± 0.04
Dog	0.20 ± 0.01	0.39 ± 0.01	1.34 ± 0.08	0.24 ± 0.02
Pigeon	0.22 ± 0.01	1.28 ± 0.10	6.79 ± 0.36	0.23 ± 0.01
Chick	0.22 ± 0.01	0.32 ± 0.02	1.23 ± 0.06	0.11 ± 0.01

The TPP and TMP concentrations increased gradually. On the other hand, with of oral administration, the thiamine concentration increased gradually and reached a peak after 2 h. TPP increased more quickly than thiamine, and TTP and TMP did not change much. Fig. 4C and D also shows the changes in the concentrations of thiamine and its phosphate esters in rat blood *in vitro*. Rat blood was collected and placed in a test-tube in a 37°C water-bath. The TPP level decreased over 5 min, then increased again gradually; the TMP and thiamine levels increased. When thiamine was added to rat blood, its concentration decreased quickly and the TTP, TPP and TMP levels increased slowly.

We had previously reported two methods for post-column derivatization in separating and measuring thiamine and its phosphate esters by HPLC. In the first method[13] we used an ion-exchange column (Shimadzu ISA-07/S2504) and in the second[20] a reversed-phase column (μBondapak C_{18}). With the ion-exchange column, thiamine phosphates were eluted in the order thiamine, TMP, TPP and TTP. The elution peak of TTP was, accordingly, broad and difficult to quantify. In the second method, TTP was eluted first, clearly separated from other, non-specified eluted substances. Therefore, we used this method and column to determine the concentration of TTP in blood. The sensitivity for determination of thiamine phosphates is such that they can be measured in 0.1 ml of human or other animal blood. Although the presence of TTP and TMP in human blood has never been reported previously, we could have confirmed with this method that they are present, and these facts suggest that TMP or TTP may have important biological roles, unknown until now. This method will be useful in studying the clarification of the mechanism of action and metabolism of thiamine and its phosphate esters.

REFERENCES

1 Y. Itokawa, *J. Appl. Nutr.*, 29 (1977) 5.
2 N. Shimazono and E. Katsura (Editors), *Beriberi and Thiamine*, Vitamin B Research Committee of Japan, Kyoto, Japan, 1965, p. 64.
3 W. A. Krehl and R. E. Hodges, *Amer. J. Clin. Nutr.*, 17 (1965) 191.
4 J. C. Somogyi, *J. Nutr. Sci. Vitaminol.*, 22, Suppl. (1976) 29.
5 M. Brin, M. Tai, A. S. Ostashever and H. Kalinsky, *J. Nutr.*, 71 (1960) 273.

6 J. Fennelly, O. Frank, H. Baker and C. M. Leevy, *1Amedr. J. Clin. Nutr.*, 20 (1967) 946.
7 A. Konttineu, A. Louhija and G. Hartel, *Ann. Med. Exp. Fenn.*, 48 (1970) 172.
8 G. Berger, F: Bergel and A. R. Todd, *Nature (London)*, 136 (1935) 259.
9 M. Fujiwara and K. Matsui, *Anal. Chem.*, 25 (1953) 810.
10 M. Kimura, T. Fujita and Y. Itokawa, *Clin. Chem.*, 28 (1982) 29.
11 M. Kimura and Y. Itokawa, *J. Chromatogr.*, 239 (1982) 707.
12 K. Ishii, K. Sarai, H. Sanemori and T. Kawasaki, *Anal. Biochem.*, 97 (1979) 191.
13 M. Kimura, T. Fujita, S. Nishida and Y. Itokawa, *J. Chromatogr.*, 188 (1980) 417.
14 H. Sanemori, H. Ueki and T. Kawasaki, *Anal. Biochem.*, 102 (1980) 451.
15 B. C. Hemming and C. J. Gubler, *J. Liq. Chromatogr.*, 3 (1980) 1697.
16 D. M. Hilker and A. J. Clifford, *J. Chromatogr.*, 231 (1982) 433.
17 J. Bontemps, L. Bettendorff, J. Lombet, C. Grandfils, G. Dandrifosse, E. Schoffeniels, F. Nevejans and J. Crommen, *J. Chromatogr.*, 295 (1984) 486.
18 K. Ishii, K. Sarai, H. Sanemori and T. Kawasaki, *J. Nutr. Sci. Vitaminol.*, 25 (1979) 517.
19 J. Bontemps, P. Philippe, L. Bettendorff, J. Lombet, G. Dandrifosse, E. Schoffeniels and J. Crommen, *J. Chromatogr.*, 307 (1984) 283.
20 M. Kimura, B. Panijpan and Y. Itokawa, *J. Chromatogr.*, 245 (1982) 141.
21 G. Rindi, L. de Giuseppe and G. Sciorelli, *J. Nutr.*, 94 (1968) 447.

Journal of Chromatography, 332 (1985) 189–194
Elsevier Science Publishers B.V., Amsterdam — Printed in The Netherlands

CHROMSYMP. 624

ENERGY EFFECTS IN THE RETENTION OF AROMATIC ACIDS IN LIQUID CHROMATOGRAPHY

T. HANAI
Gasukuro Kogyo Inc., 237-2 Sayamagahara, Iruma 358 (Japan)
(First received March 25th, 1985; revised manuscript received May 13th, 1985)

SUMMARY

The reversed-phase liquid chromatographic behaviour of phenols and aromatic acids was studied using an octadecyl-bonded silica gel as the stationary phase and acidic acetonitrile–water mixtures as the mobile phase. The retentions of these compounds can be predicted from their Van der Waals volumes and energy effects. The energy effects are classified according to π and hydrogen-bonding energies. The inclusion of dissociation constants, derived from Hammett's equation, in the above approach makes it possible to predict the retention times of ionized aromatic acids.

INTRODUCTION

Several approaches have been used to develop systems for the prediction of retention times in reversed-phase liquid chromatography. These have included alkyl chain length, connectivity index, number of double bonds, localization and delocalization energies, Hansch's π constants and Rekker's hydrophobic fragmental constants. Of these parameters, Rekker's hydrophobic fragmental constants (log P values)[1] were useful for predicting the retention times of several groups of compounds in systems with octadecyl-bonded silica gels as the stationary phase and pH-controlled acetonitrile–water mixtures as the mobile phase[2–5].

However, each group of compounds required individual standard compounds in order to obtain the constants of the equations that were used for the calculation of the retention time, the resolution and the concentration of acetonitrile as an organic modifier. This meant that if a compound had two or more different types of substituents, the retention time predicted from one set of equations was often far from the observed value. The system based on the partition coefficient between octanol and water was, therefore, not adequate for producing an optimized system for mixtures of different types of compounds. Further investigations have used basic physico-chemical parameters such as Van der Waals volumes, π-energies, hydrogen-bonding energies and dissociation constants. In systems with octadecyl-bonded silica gels and pH-controlled acetonitrile–water mixtures, the retention times of non-ionizable compounds, such as *n*-alkanes, polyaromatic hydrocarbons, alkylbenzenes and halogenated benzenes, have been well predicted from the Van der Waals volume and

0021-9673/85/$03.30

π-energy effects[6,7]. The retention of phenols has been calculated from the following equation:

$$\log k' \text{ (Ar–OH)} = \log k'(\text{VWV}) - \log k' (\pi) - \log k'(\text{HB})$$

where $\log k'$(Ar–OH) is the capacity ratio of a substituted phenol, $\log k'$(VWV) is obtained from the Van der Waals volume, $\log k'(\pi)$ is the π-energy effect of a phenyl group and $\log k'$(HB) is the hydrogen bonding effect of the hydroxy group of phenol[8]. This approach has now been applied to produce an optimization system for aromatic acids in liquid chromatography.

EXPERIMENTAL

The details of the instrument used were described previously[5] and the chemicals used are listed in Table I. The octadecyl-bonded silica gel column was an ERC-1000, kindly donated by ERMA Optical Works (Tokyo, Japan). The column temperature was 40°C. The Van der Waals volumes were calculated by Bondi's method[9] and the values of the energy effect of phenols were obtained from a previous paper[8].

RESULTS AND DISCUSSION

The $\log k'$ values measured are listed in Table I together with the values of the energy effect. The relationship between $\log k'$ and Van der Waals volumes was linear. However, the slopes for the different groups of compounds were not exactly the same, *e.g.*, hydrophobic groups had higher slopes. The difference in slopes could be explained by enthalpy effects[10]. The energy effect of each compound could easily be calculated if a linear relationship between Van der Waals volumes and $\log k'$ values for *n*-alkanes could be obtained. However, the retention times of *n*-alkanes were very long with eluents containing low concentrations of an organic modifier. Thus, such plots could not be obtained easily for aromatic acids, the retention times of which were relatively short. Therefore, a linear relationship for alkylphenols between their $\log k'$ values and their Van der Waals volumes was first obtained. The capacity ratios of *n*-alkanes were then calculated from their Van der Waals volumes and from the values of the energy effect of phenols.

The slope of the linear relationship for *n*-alkanes was further adjusted by the addition of the enthalpy effect[10]. The difference between the observed energy effect of phenols and the reference values was less than 5%. The energy effect of aromatic acids was obtained from the last equation and their $\log k'$ values. The values are given in Table I.

The hydrogen-bonding energy effect of a carboxyl group of benzoic acid is about 2 kcal/mole higher than that of a phenolic hydroxy group. The difference between the energy effects of benzoic acid and phenylacetic acid is about 2 kcal/mole, and that between phenylacetic acid and 3-phenylpropionic acid or 4-phenylbutyric acid is small. A similar result was obtained for indole acids. In addition, the retention times of ionized aromatic acids were predicted from their $\log P$ values and their dissociation constants[11,12]. This equation was modified to

$$k' = (k'_{\text{max}} + k'_{\text{min}} K_a/[\text{H}^+])/(1 + K_a / [\text{H}^+])$$

where the maximum capacity ratios (k'_{max}) were calculated from their Van der Waals volumes and their energy effects instead of their log P values. The pK_a values were calculated from a modified Hammett equation[12]. The minimum capacity ratios (k'_{min}), *i.e.*, the capacity ratios of totally ionized acids, were close to zero and could not be predicted, so the values were obtained experimentally in the eluent of pH 7.000. The result is shown in Fig. 1.

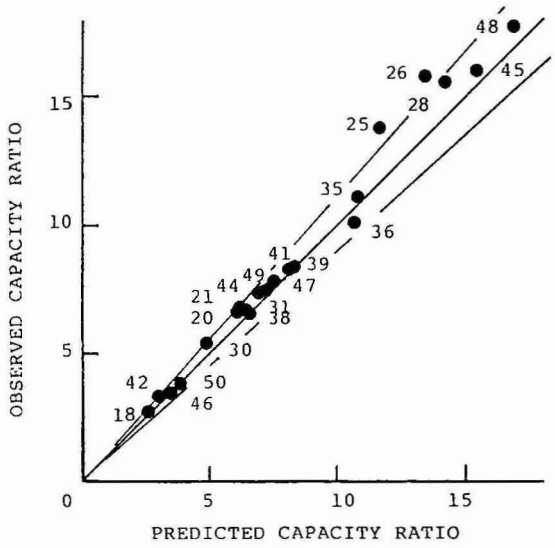

Fig. 1. Predicted and observed capacity ratios of aromatic acids at pH 4.500. Experimental conditions: column, ERC-1000 (ODS), 15 cm × 6.0 mm I.D.; eluent, 0.05 *M* sodium phosphate (pH 4.500) containing 25% of acetonitrile; column temperature, 40°C. The numbers adjacent to the symbols are the same as in Table I. The two lines on either side of the central line indicate a 10% error (n = 21).

The difference between the predicted and observed capacity ratios was 10%. The error for 3,4- and 3,5-dimethylbenzoic acids (Nos. 25 and 26 in Fig. 1) was more than 10%, but the error for 3,4-dimethylbenzoic acid should depend on the value of the π-energy effect but not the dissociation constant.

The following equation was obtained between the predicted and observed capacity ratios:

$$k'_{obs} = a/k'_{pre} + b$$

where k'_{obs} and k'_{pre} are the observed and predicted capacity ratios, respectively, and constants a and b are 1.132 and −0.2038, respectively. The correlation coefficient (n = 21) was 0.990 and the average error was 4.78%. Only 3,5-dichlorobenzoic acid (No. 36 in Fig. 1) had an error of more than 10%. However, the error for this acid at pH 1.900 was very small, and therefore should be due to the dissociation constant.

TABLE I

COMPOUNDS STUDIED AND THEIR PHYSICAL PARAMETERS

Experimental conditions: column, ERC-1000 (ODS), 15 cm × 6.0 mm I.D.; eluent, 0.05 *M* phosphoric acid in acetonitrile–water mixtures; column temperature, 40°C.

Compound	*VWV**	*E***	*pK*$_a$***	*log k'* *% acetonitrile*					*E*§
				20	*25*	*30*	*35*	*40*	
1 Phenol	53.88	7.883	–	–	0.5186	–	0.2738	–	7.963
2 2-Methylphenol	65.03	8.259	–	1.086	0.8723	0.6924	0.5691	0.4596	8.410
3 3-Methylphenol	65.03	–	–	1.040	0.8242	0.6932	0.5137	0.4047	8.643
4 4-Methylphenol	65.03	8.704	–	1.038	0.8248	0.6922	0.5094	0.4027	8.653
5 2,3-Dimethylphenol	76.18	9.116	–	1.393	1.143	0.9872	0.7851	0.6526	9.197
6 2,4-Dimethylphenol	76.18	–	–	1.427	1.172	1.013	0.8058	0.6713	9.057
7 2,5-Dimethylphenol	76.18	9.013	–	1.427	1.172	1.015	0.8127	0.6734	9.045
8 2,6-Dimethylphenol	76.18	8.524	–	1.409	1.174	1.026	0.8320	0.7047	8.984
9 3,4-Dimethylphenol	76.18	9.762	–	1.320	1.067	0.9725	0.7007	0.5714	9.570
10 3,5-Dimethylphenol	76.18	9.489	–	1.385	1.126	0.9615	0.7487	0.6179	9.337
11 2,3,5-Trimethylphenol	87.33	9.851	–	1.735	1.449	1.259	1.020	0.8979	9.844
12 2,3,6-Trimethylphenol	87.33	9.360	–	1.717	1.454	1.270	1.047	0.8986	9.844
13 2,4,6-Trimethylphenol	87.33	9.175	–	1.758	1.487	1.303	1.072	0.9208	9.644
14 2,3,5,6-Tetramethylphenol	98.48	10.13	–	–	–	–	1.263	1.092	10.46
15 2-Ethylphenol	75.26	9.192	–	1.487	1.232	0.9985	0.8647	0.7259	8.627
16 3-Ethylphenol	75.26	–	–	1.490	1.155	0.9902	0.7800	0.6426	8.946
17 4-Ethylphenol	75.26	9.122	–	1.432	1.168	0.9994	0.7858	0.6466	8.946
18 Benzoic acid	65.36	–	4.200	0.8271	0.6065	0.4489	0.2794	0.1557	10.00
19 2-Methylbenzoic acid	76.51	–	–	1.140	0.8853	0.7058	0.5117	0.3712	10.76
20 3-Methylbenzoic acid	76.51	–	4.270	1.216	0.9444	0.7507	0.5399	0.3957	10.51
21 4-Methylbenzoic acid	76.51	–	4.340	1.177	0.9263	0.7516	0.5248	0.3803	10.61
22 2,4-Dimethylbenzoic acid	87.66	–	–	1.535	1.228	1.007	0.7733	0.6084	11.27
23 2,5-Dimethylbenzoic acid	87.66	–	–	1.356	1.231	1.007	0.7715	0.6092	11.43
24 2,6-Dimethylbenzoic acid	87.66	–	–	1.137	0.8348	0.7064	0.5068	0.3740	13.00
25 3,4-Dimethylbenzoic acid	87.66	–	4.440	1.225	1.209	0.9072	0.7315	0.5674	11.62
26 3,5-Dimethylbenzoic acid	87.66	–	4.340	1.456	1.288	1.050	0.8032	0.6334	11.16
27 2,4,6-Trimethylbenzoic acid	98.81	–	–	1.527	1.228	1.011	0.7782	0.6125	13.44
28 4-Ethylbenzoic acid	86.74	–	4.350	1.598	1.284	1.049	0.8090	0.6310	10.85

29 2-Chlorobenzoic acid	74.84	–	–	0.9933	0.7629	0.5878	0.4075	0.2691	11.09
30 3-Chlorobenzoic acid	74.84	–	3.380	1.011	1.082	0.7626	0.6548	0.5016	9.715
31 4-Chlorobenzoic acid	74.84	–	3.960	1.370	1.097	0.8897	0.6700	0.5135	9.419
32 2,4-Dichlorobenzoic acid	84.32	–	–	1.587	1.289	1.067	0.8306	0.6585	10.30
33 2,5-Dichlorobenzoic acid	84.32	–	–	1.489	1.206	0.9944	0.7687	0.6032	10.70
34 2,6-Dichlorobenzoic acid	84.32	–	–	1.049	0.8365	0.6796	0.4977	0.3669	12.48
35 3,4-Dichlorobenzoic acid	84.32	–	3.600	1.847	1.517	1.258	0.9914	0.8063	9.223
36 3,5-Dichlorobenzoic acid	84.32	–	3.460	1.929	1.588	1.338	1.077	0.8818	8.791
37 2-Bromobenzoic acid	77.96	–	–	1.077	0.8317	0.6490	0.4595	0.3215	11.35
38 3-Bromobenzoic acid	77.96	–	3.810	1.470	1.175	0.9595	0.7300	0.5647	9.641
39 4-Bromobenzoic acid	77.96	–	3.980	1.505	1.195	0.9792	0.7475	0.5821	9.522
41 2-Chlorophenylacetic acid	85.07	–	–	1.188	0.9203	0.7209	0.5165	0.3676	12.34
42 4-Chlorophenylacetic acid	85.07	–	4.216	1.364	1.081	0.8601	0.6359	0.4739	11.57
42 Phenylacetic acid	79.55	–	4.300	–	0.6309	–	–	–	12.88
43 2-Tolylacetic acid	86.74	–	–	1.144	0.8849	0.6904	0.4916	0.3478	12.83
44 3-Tolylacetic acid	86.74	–	4.325	1.233	0.9625	0.8761	0.5503	0.4017	12.51
45 4-Phenyl-*n*-butylic acid	96.05	–	4.719	1.517	1.212	0.9807	0.7441	0.5714	13.05
46 L(+)-Mandelic acid	80.18	–	3.380	0.2384	0.0492	−0.0804	−0.2516	−0.3393	16.03
47 *trans*-Cinnamic acid	82.32	–	4.380	1.263	0.9754	0.7629	0.5476	0.3906	11.56
48 4-Methylcinnamic acid	93.47	–	4.492	1.650	1.314	1.060	0.8171	0.6241	12.08
49 3-Phenyl-*n*-propionic acid	86.04	–	4.579	1.190	0.9200	0.7323	0.5281	0.3782	12.49
50 Indole-3-acetic acid	91.65	–	4.750	0.8907	0.6270	0.2058	0.2384	0.1023	15.42
51 Indole-3-propionic acid	114.11	–	–	1.214	0.9130	0.6889	0.4650	0.3003	18.19
52 Indole-3-butylic acid	121.34	–	–	1.492	1.153	0.8953	0.6511	0.4584	18.44
53 Hippuric acid	96.15	–	–	0.2225	0.0116	−0.1430	−0.3132	−0.4259	19.31
Void volume (elution volume of Na_2NO_3, ml)				1.950	1.992	1.860	1.926	1.800	
Dead volume of instrument (ml)				0.067	0.116	0.067	0.116	0.067	

* Van der Waals volume calculated by Bondi's method[9].
** Energy effect (kcal/mol) from ref. 8.
*** Dissociation constant from ref. 12.
§ Energy effect obtained from the observed log k' values.

CONCLUSION

The retention times of aromatic acids with an eluent of given pH can be obtained from their Van der Waals volumes, energy effects and dissociation constants. The remaining difficulty is the substituent effect in estimating the energy effect. Hammett's σ and Taft's σ^* constants did not bear a linear relationship to their log k' values. Hammett's σ constant was useful only for calculating the dissociation constant, even though the estimated dissociation constants for multi-substituted compounds were uncertain because not many data have been reported.

ACKNOWLEDGEMENT

I thank to Mr. A. Gyukurogi for technical assistance.

REFERENCES

1 R. F. Rekker, *The Hydrophobic Fragmental Constant,* Elsevier, Amsterdam, 1977.
2 T. Hanai, *Chromatographia,* 12 (1979) 77.
3 T. Hanai, K. C. Tran and J. Hubert, *J. High Resolut. Chromatogr. Chromatogr. Commun.,* 4 (1981) 454.
4 T. Hanai, K. C. Tran and J. Hubert, *J. Chromatogr.,* 239 (1982) 527.
5 T. Hanai and J. Hubert, *J. High Resolut. Chromatogr. Chromatogr. Commun.,* 6 (1983) 20.
6 T. Hanai and J. Hubert, *J. Chromatogr.,* 290 (1984) 197.
7 T. Hanai and J. Hubert, *J. Chromatogr.,* 291 (1984) 81.
8 T. Hanai and J. Hubert, *J. Chromatogr.,* 302 (1984) 89.
9 A. Bondi, *J. Phys. Chem.,* 68 (1964) 441.
10 T. Hanai and J. Hubert, *Chromatographia,* 19 (1985) 266.
11 T. Hanai, K. C. Tran and J. Hubert, *J. Chromatogr.,* 239 (1982) 385.
12 T. Hanai and J. Hubert, *J. High. Resolut. Chromatogr. Chromatogr. Commun.,* 7 (1984) 524.

Journal of Chromatography, 332 (1985) 195–201
Elsevier Science Publishers B.V., Amsterdam — Printed in The Netherlands

CHROMSYMP. 610

THE ABBÉ REFRACTOMETER AS A LIQUID CHROMATOGRAPHIC DETECTOR USING AN IMAGE SENSOR FOR BOUNDARY LOCATION

SATORU EGASHIRA
Faculty of General Education, Ehime University, Bunkyocho, Matsuyama, 790 (Japan)
(First received March 14th, 1985; revised manuscript received April 11th, 1985)

SUMMARY

A novel refractive index detector for liquid chromatography using a flow-through Abbé refractometer cell and image sensor is described. The Abbé refractometer has some advantages such as independence of the intensity of the light, a wide dynamic range and a small cell volume (less than 3.5 μl).

A linear diode array image sensor was used to determine the critical angle of refraction. As the output of the sensor is essentially discrete, interpolation to locate accurately the position of the boundary is required. The least-squares method was used in real time for this purpose. A change in the refractive index of 10^{-5} units was detected with this apparatus.

INTRODUCTION

Fresnel and deflection-type refractive index (RI) detectors are widely used in liquid chromatography and an interference type refractometer has also been reported recently[1]. This paper describes a trial of a new type of RI detector based on the Abbé refractometer.

The Abbé refractometer is a total reflection type of refractometer that gives RI by measurement of the critical angle of refraction of light through the interface between the liquid sample and a glass prism. The refractometer has the advantage of being unaffected by the intensity of the light source, giving a wide dynamic range and requiring a small-bore cell (less than 3.5 μl). However, it is difficult to determine the critical angle accurately and to convert it into an electrical signal by using analogue sensors. Accordingly, a linear diode array image sensor was used for this purpose.

PRINCIPLES

Fig. 1 shows the optical system used in the apparatus. Light from the source is scattered by a rough-surface prism and is refracted at the interface between the liquid and a smooth-surface prism. The critical angle of refraction, θ, is given by

$$\theta = \sin^{-1}(n/n_0) \quad (1)$$

0021-9673/85/$03.30

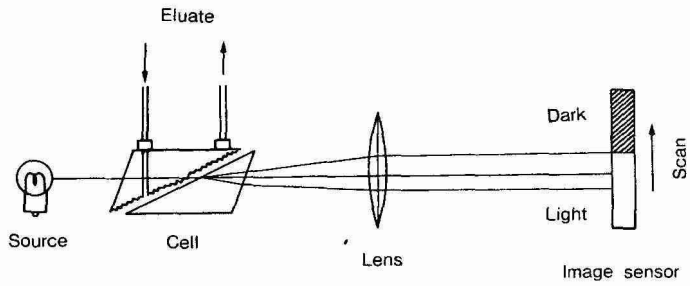

Fig. 1. Optical system.

where n and n_0 are the refractive index of the liquid and the prism, respectively.

The refracted light is transmitted into the smooth-surface prism and focused on the window of the image sensor with the aid of a lens. The critical angle is determined by locating the bondary of the light and dark areas on the window.

As the boundary location is given in terms of the segment number of the sensor, the physical resolution is limited by the dimensions and the apertures of the diode segments. Interpolation by a least-squares method was used in real time to locate the boundary accurately.

The profile of the output signal from the sensor around the boundary is shown schematically in Fig. 2. The curve of the profile should be represented by the Fresnel equation, and the boundary position of the light and dark areas should theoretically be detected as the intersection of the curve and the baseline at x_0. However, experimentally, less noisy outputs were obtained with an appropriate threshold, y'_0, giving the boundary position at x'_0. The threshold near the inflection point of the curve was found to give the minimum noise.

The linear part of the curve around its inflection point was approximated with the following first-order equation:

$$y = ax + b \tag{2}$$

where y is the height of the curve (arbitrary units) and x is the segment number of

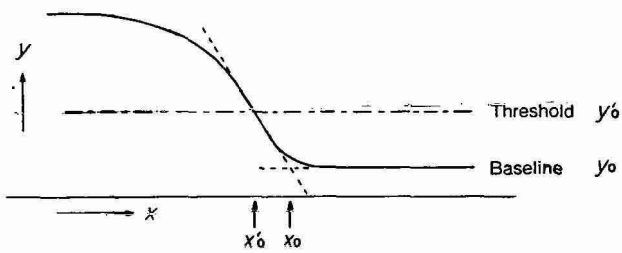

Fig. 2. Output signal of image sensor around the critical angle.

the sensor. The parameters a and b were obtained with the least-squares method as follows.

The normal equations obtained from eqn. 2 are

$$\left.\begin{aligned} A_1 a + B_1 b &= C_1 \\ A_2 a + B_2 b &= C_2 \end{aligned}\right\} \tag{3}$$

where

$$A_1 = 1/6\ N(N+1)(2N+1) \tag{4}$$

$$A_2 = B_1 = 1/2\ N(N+1) \tag{5}$$

$$B_2 = N \tag{6}$$

$$C_1 = \sum_{i=1}^{N} x_i y_i \tag{7}$$

$$C_2 = \sum_{i=1}^{N} y_i \tag{8}$$

and N is the number of samples used in the least-squares treatment.

The parameters a and b are obtained by solving eqn. 3 as

$$a = (B_2 C_1 - B_1 C_2)/(A_1 B_2 - A_2 B_1)$$

and

$$b = (A_1 C_2 - A_2 C_1)/(A_1 B_2 - A_2 B_1)$$

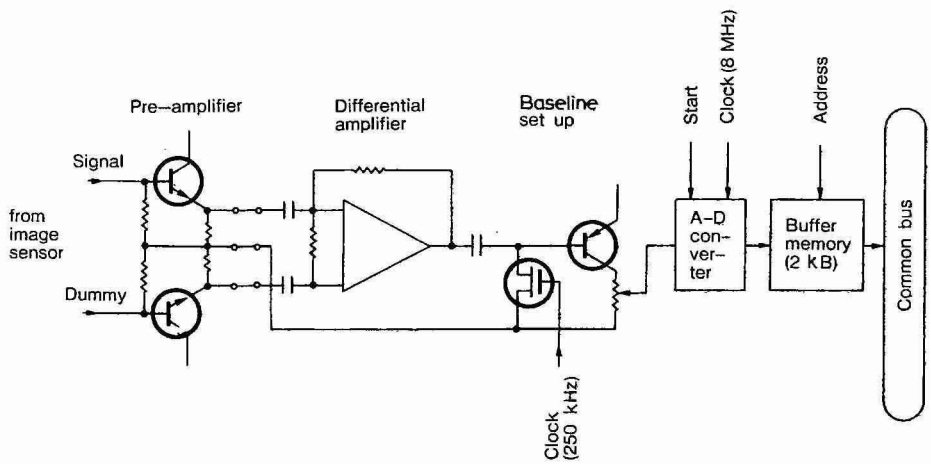

Fig. 3. Electrical circuits around the image sensor.

Applying the parameters to eqn. 2, the x coordinate (segment number) of the intersect, x_0, is given as

$$x_0 = \frac{y_0(A_1B_2 - A_2B_1) - (C_2A_1 - C_1A_2)}{C_1B_2 - C_2B_1} \tag{9}$$

where y_0 is height of the baseline. When we use the threshold instead of the baseline, x_0 and y_0 are replaced by x'_0 and y'_0.

The sensitivity of diode segments vary in the range ± 10% and dark output varies for each segments. Corrections for these variations are carried out before the least-squares treatments.

APPARATUS

The optical equipment of the Model 678 automatic urine analyser (Hitachi, Tokyo, Japan) is used in the optical part with a minor modification (Fig. 1). Eluate from the chromatographic column flows in the space between the smooth- and the rough-surface prisms.

A linear charge-coupled device image sensor (LZ-2020, 2048 segments; Sharp, Osaka, Japan) was used as the optical sensor. Electrical circuits around the image sensor are shown in Fig. 3.

The output of the sensor is amplified by a pre-amplifier and mixed with the dummy output by a differential amplifier. Then, after setting up the electrical baseline, the signal is sent to 8-bit analogue-to-digital (A–D) converter (TDC1002J, TRW LSI Products, Redondo Beach, CA, U.S.A.). The sampling interval is 0.1 sec and the

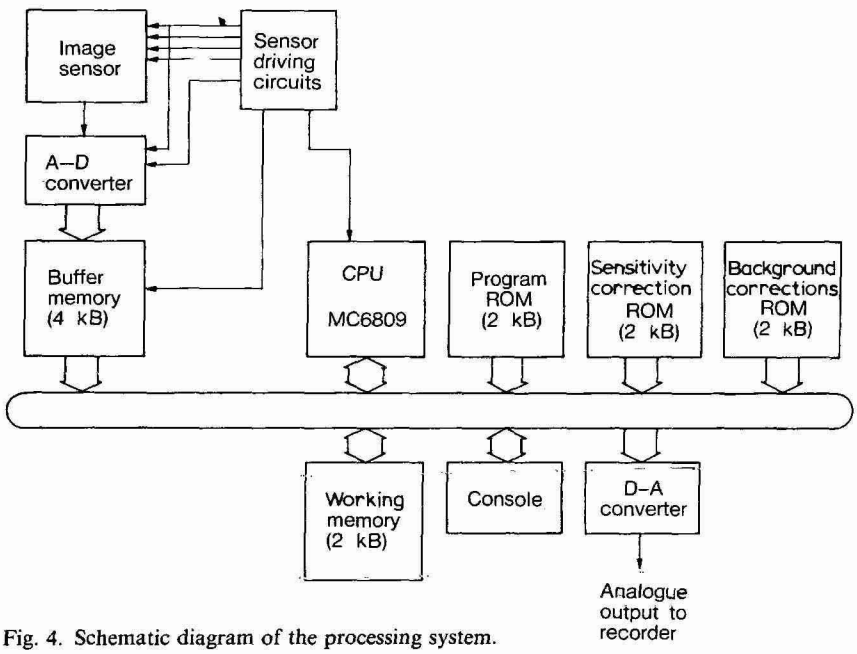

Fig. 4. Schematic diagram of the processing system.

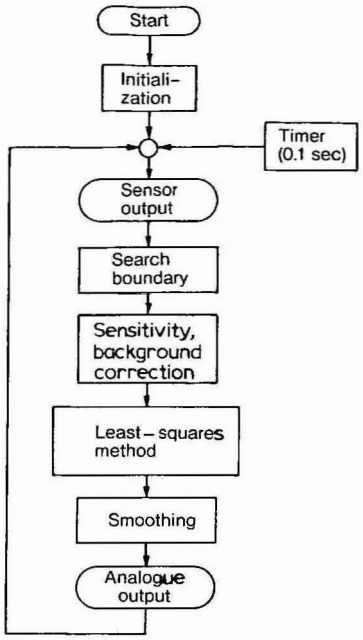

Fig. 5. Flow chart of processing.

conversion time is 1 μsec with an 8-MHz clock. The digital data are stored on a 2 kbyte (kB) buffer memory to permit accessing by the central processor.

Fig. 4 is a schematic diagram of the whole system. As the central processor (CPU), an MC6809 microprocessor (Motorola Semiconductor Products, U.S.A.) is used. The digital outputs of the A–D converter, stored on the buffer memory, are

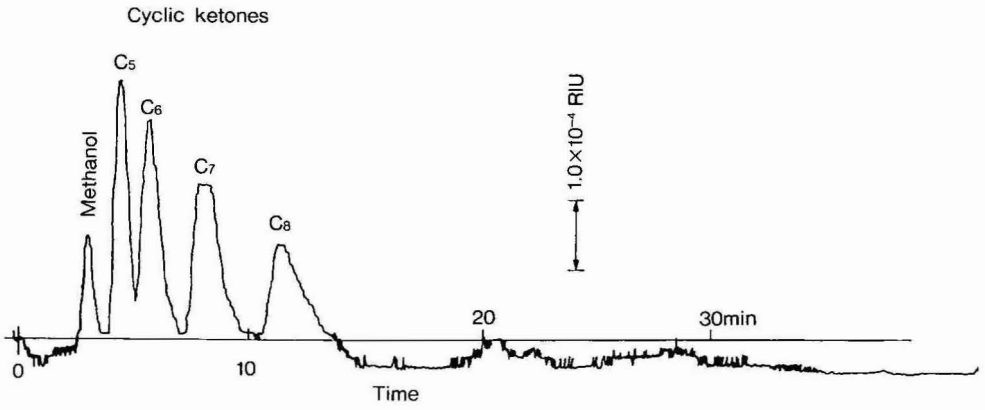

Fig. 6. Separation of cyclic ketones on a column of Develosil ODS-5 (250 × 2.6 mm I.D.) with 50% (v/v) methanol. Flow-rate: 0.5 ml/min.

read out by the CPU. The approximate position of the boundary is detected by a preliminary search. Then, after correction for the dark output and sensitivity of the sensor segments, the numerical treatment by the least-squares method is performed.

Each 2 kB of read-only memory (ROM) was provided to store the factors for the correction of the sensitivity and the dark output. Another 2 kB ROM and 2 kB random access memory were used as program and working memory, respectively, for the data processing.

The results of the numerical treatment are converted into an analogue signal again, and sent to a pen recorder to give the chromatographic elution curve. Smoothing by the moving average method is used prior to A–D conversion if necessary. A processing flow chart is shown in Fig. 5.

The sensor driving circuits supply several kinds of clock pulses for the image sensor, the CPU and the A–D converter, and address signals for buffer memory accessing.

RESULTS AND DISCUSSION

Cyclic ketones (1 mg of each) and cyclic terpenes (1 mg of each) were separated on Develosil ODS-5 (Nomura Chemical Co., Seto, Japan), as shown in Figs. 6 and 7, respectively.

Eqn. 1 represents a non-linear response of the detector. However, it was found experimentally that the system gives almost a linear output over the range $n = 1.33–1.40$. It took 10 msec for scanning of the image-sensor and about 200 msec for numerical processing.

One eighth of the aperture of the diode segments of the sensor could be read out by the above treatment. This corresponds to 10^{-5} refractive index units (RIU).

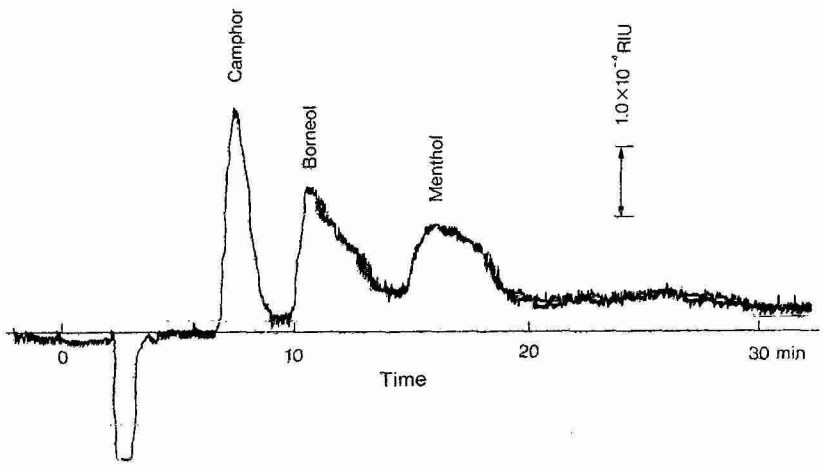

Fig. 7. Separation of cyclic terpenes. Solvent: 70% (v/v) methanol. Other conditions as in Fig. 6.

The noise level was nearly equal to the limit of read out, *i.e.*, 10^{-5} RIU. It was found experimentally that the noise level was lowest when the threshold, y'_0, was set at the inflection point of the sensor output *vs.* position (Fig. 2).

Smoothing by the moving average method also reduced the apparent noise. Thus Figs. 6 and 7 used both the moving average method and a threshold set at the inflection point.

It has been shown here that the sensitivity of the flow-through Abbé RI detector could be improved by numerical treatment. The sensitivity, determined by the 10^{-5} RIU noise level, does not show the inherent limits of the detector. The effective sensitivity of the system could be improved by reducing the noise with more sophisticated hardware or software.

ACKNOWLEDGEMENT

I thank Dr. Kyoichi Ozawa (Hitachi, Tokyo, Japan) for providing the optical assembly of the apparatus.

REFERENCE

1 M. N. Munk, in T. M. Vickrey (Editor), *Liquid Chromatography Detectors*, Marcel Dekker, New York, 1983, p. 165.

Journal of Chromatography, 332 (1985) 203–209
Elsevier Science Publishers B.V., Amsterdam — Printed in The Netherlands

CHROMSYMP. 627

COUNTER-ION EFFECTS IN PARTITION CHROMATOGRAPHY

H. F. WALTON
Chemistry Department and Cooperative Institute for Research in Environmental Sciences (CIRES), University of Colorado, Campus Box 449, Boulder, CO 80309 (U.S.A.)
(First received March 25th, 1985; revised manuscript received May 7th, 1985)

SUMMARY

The inorganic counter-ion of an ion-exchange resin affects retention of organic solutes in several ways, such as the formation of co-ordination complexes, ion–dipole interaction, ionic hydration and hydrogen bonding. To study these effects the retention of sugars and sugar alcohols, amino acids and hydroxy acids has been measured on a column of polystyrene-based cation-exchange resin, carrying these counter-ions: Li^+, K^+, Ca^{2+}, La^{3+}. The eluent was water or, in some cases, a salt solution. To correlate retention with complex stability the solubility of calcium sulfate was measured in solutions of the ligands mannitol, sorbitol, glycine, α- and β-alanine. We concluded that the calcium complexes are about as stable in the ion-exchange resin as in aqueous solution.

INTRODUCTION

The inorganic counter-ion affects the retention of organic compounds on ion-exchange resins in various ways. Most studies have been made with cation exchangers, where the most obvious effect is the formation of co-ordination complexes between the metal ions and organic ligands; this is the basis of ligand-exchange chromatography. Other interactions affect retention too, and one of these is ionic hydration. We have reported[1] on the partition of polar organic compounds between aqueous solutions and cation-exchange resins of the polystyrene type, containing alkali-metal and alkaline-earth cations, and we noted two effects that act in opposite directions. For many solutes, retention increases in the order K < Na < Li. For phenolic compounds the opposite order was observed. We attributed the effects to the "free" water in the resin polymer, that is, the imbibed water that is not attached to the cation as water of hydration. The proportion of "free" water apparently increases in the order Li < Na < K. "Free" water makes the polymer gel a poorer solvent for organic compounds, decreasing their absorption, but on the other hand it can form hydrogen bonds with phenols and other hydroxylic compounds and so increase their absorption.

If this theory is correct, the retention of compounds that contain many hydroxyl groups, like sugars and sugar alcohols, should increase with the counter-ion in the order Li < Na < K. We have found this to be the case.

0021-9673/85/$03.30

Cation-exchange resin columns carrying potassium ions[2,3] have been used for the chromatography of carbohydrates, and so have sodium-form resin[4], but today, one of the common methods for analyzing carbohydrate mixtures is chromatography on a calcium-loaded ion-exchange resin with water as the eluent[5–10]. Calcium-form resins retain polyols relatively strongly, and the mechanism of retention is undoubtedly the formation of co-ordination complexes. If the orientation of hydroxyl groups is favorable to complex formation, retention is strong[11], and it is stronger with lanthanum counter-ions than with calcium[11,12]. The retention of all sugars and sugar alcohols in such systems is increased by adding alcohol or acetonitrile to the mobile phase, and there is a considerable body of literature on their chromatography in alcohol–water mixtures[13].

The chromatography of sugars and sugar alcohols on a calcium-form resin is an example of ligand-exchange chromatography with weak complexes. Complex formation is not the only mechanism that influences retention. We know that the stability of metal–ligand complexes may be very different in the resin from what it is in solution[14]. The Cu(II)–ethylenediamine complexes, for example, are ten times more stable in a sulfonated polystyrene cation exchanger than in aqueous solution[15].

In this investigation we measured the retentions on a cation-exchange resin of a number of sugars and sugar alcohols, as well as other alcohols and amino acids and hydroxy acids, substances that are commonly associated with sugars in nature. We compared four counter-ions, Li^+, K^+, Ca^{2+} and La^{3+}. At each run we injected a small volume of dilute salt solution, for example $LiNO_3$ with the lithium-loaded column, to mark the interstitial volume of the column and fittings; it was assumed, and verified by using different salt concentrations, that the salt was excluded from the resin by the Donnan equilibrium. To find the total volume of water in the column, inside and outside the resin, we injected deuterium oxide as a tracer. The difference between the deuterium oxide peak and the salt peak gave the internal water volume, the volume of water inside the resin beads. We estimated the stability constants of certain complexes by measuring the solubility of calcium sulfate, first in pure water, then in solutions of amino acids and sugar alcohols. One aim of the investigation was to see whether these complexes were more stable in the resin than in solution.

EXPERIMENTAL

The resin and the column

The resin was Benson BCx6 (Benson, Reno, NV, U.S.A.) a sulfonated polystyrene, 6% cross-linked, particle size 7–10 μm. It was packed into a glass column (Glenco, Houston, TX, U.S.A.) 30 cm × 6.3 mm I.D., water jacketed with adjustable bed supports, rated to 1000 p.s.i. internal pressure. Column temperature was maintained at 60°C by a Lauda heater-circulator pump (Brinkman Instruments, Westbury, NY, U.S.A.); the flow-rate was generally 0.5 ml min^{-1}. The ionic capacity of the column was found by converting it into the hydrogen form with 0.5 *M* nitric acid, then washing it with water and displacing the hydrogen ions with calcium nitrate; the displaced acid was titrated with sodium hydroxide. Also, the calcium-loaded column was flushed with dilute nitric acid to displace the calcium ions, which were then titrated with EDTA. The two measurements agreed closely; the ionic capacity was 16.6 milliequivalents, or 8.30 mmol Ca^{2+}

After each change of counter-ion the column was washed with water, and the bed supports were adjusted to leave no void space at the ends of the resin bed. The bed length was *ca.* 23 cm, but varied from one counter-ion to another. The retention volume of deuterium oxide tracer, noted below, indicates the swelling and shrinkage of the resin.

Chromatographic system

This consisted of an M-45 pump and R-401 refractive index detector (Waters Assoc., Milford, MA, U.S.A.), a six-port injector (Rheodyne, Cotati, CA, U.S.A.) and the glass column described above.

Solubility measurements

The solubility of calcium sulfate dihydrate was measured in water and in solutions of five ligands in order to estimate the stabilities of the calcium–ligand complexes. A buret with a glass-wool plug at the bottom was packed with small crystals of calcium sulfate dihydrate to give a column *ca.* 10 cm long, and the aqueous solution was allowed to flow through the column at *ca.* 1 ml min^{-1}; it was recirculated until the calcium-ion concentration, measured by EDTA titration, became constant; two passes through the column were generally enough. The experiments were carried out at room temperature, 21 ± 1°C; closer temperature control seemed unnecessary, since the solubility of calcium sulfate changes by only 0.5% per degree centigrade. To obtain the desired particle size, the calcium sulfate was prepared by dissolving commercial calcium sulfate in hot 1 *M* hydrochloric acid, filtering and neutralizing the excess acid by the hydrolysis of urea added to the boiling solution (the method of "precipitation from homogeneous solution").

RESULTS

Retention volumes

The retention volumes are given in Table I. They are shown as multiples of the retention volume of deuterium oxide, because the bed volume changed as one counter-ion was substituted for another. The footnote to Table I shows the measured retention volumes of deuterium oxide. The internal volume of the resin changed from one counter-ion to another, being least with La^{3+}, greatest with Li^{+}.

For La^{3+} the salt peak does not truly represent the interstitial volume, for it emerges at a greater volume than sucrose. There is some penetration of the resin by lanthanum nitrate. The reason for this penetration is presumably ion association.

All the sugars gave a single, symmetrical peak, indicating that mutarotation was complete and rapid at the column temperature.

Sugars, sugar alcohols

Table I shows the trends between the counter-ions. The increase in retention of sugars and sugar alcohols on going from Li^{+} to K^{+} can be ascribed to an increase in "free" water available for hydrogen bonding, as we discussed in the Introduction. In the calcium-form resin there is less total water and much less "free" water than in the potassium-form resin, for Ca^{2+} is strongly hydrated; hence the drop in retention of glucose and sucrose. The retention of the sugar alcohols, mannitol and sor-

TABLE I

COMPARISON OF RETENTIONS WITH DIFFERENT COUNTER-IONS

Deuterium oxide = 1.00; column temperature, 60°C except where marked. Volume retentions of deuterium oxide were lithium, 5.81 ml; potassium, 5.62 ml; calcium, 5.58 ml; lanthanum, 4.95 ml.

Counter-ion *Salt peak*	Li^+ *0.385*	K^+ *0.47*	Ca^{2+} *0.50*	La^{3+} *0.72*
Sucrose	0.52	0.605	0.57	0.60
Lactose	–	–	0.56	0.60
Glucose	0.58	0.76	0.67	0.65
Sorbose	–	–	0.80	0.71
Fructose	0.59	0.83	0.82	0.77
Arabinose	–	–	0.90	0.77
Xylose	–	0.82	0.77	0.71
Ribose	0.72	0.94	1.43	2.05
Glycerol	0.77	0.82	0.96	1.10
Pentaerythritol	0.75	0.73	0.90	1.08
Mannitol	0.64	0.73	1.10	1.44
Sorbitol	0.665	0.74	1.36	2.60
Malic acid	0.37	0.46	1.20	>12*
Tartaric acid	–	0.45	1.52	>12*
Citric acid	–	0.45	–	>12*
Glycine	1.49	1.02	1.81	6.25*
α-Alanine	1.43	0.94	1.55	5.56*
β-Alanine	1.72	1.29	2.19	>12*

* Column temperature, 72°C.

bitol (glucitol), rises sharply, as does that of ribose. Complex formation with Ca^{2+} is clearly indicated. The four hydroxyl groups of ribose in its pyranose form are oriented on the same side of the ring in such a way as to favor co-ordination; a potentiometric study[16] showed that ribose associates with calcium ions with a stability constant of 1.6 l mol^{-1}, while the association of the pentoses xylose and arabinose was much weaker.

Lanthanum ions not only form stronger complexes than calcium[17], but discriminate better between mannitol and sorbitol[12], and between ribose and other sugars.

Returning to the lithium- and potassium-form resins, we see that sugars and sugar alcohols are partially excluded from the resins, that is, that the ratio of sugar to water inside the resin is less than that outside. Steric exclusion may be a factor, but a more likely reason is the limited opportunity for hydrogen bonding within the resin.

Amino acids, hydroxy acids

Table I shows that the three amino acids tested are attached to the resin and that retention by lithium-form resin is stronger than retention by potassium-form resin. Again we can invoke the concept of "free" water. Hydrogen bonding is not a factor here, but rather the hydrophobic interaction with the resin matrix, which is

stronger with lithium-resin because there is less "free" water. Hydrophobic interaction is also indicated by these results, not included in Table I: on calcium-form resin, retention volumes of valine, 1.87; serine, 1.71; threonine, 1.57 (deuterium oxide = 1). Further, 1-butanol was retained at volume 1.52 (deuterium oxide = 1), while methanol, ethanol and 2-propanol all eluted close to deuterium oxide.

In the bonding of amino acids to the resin, the obvious effect is their strong retention by the calcium- and lanthanum-resins. In previous papers[18] we have noted the strong absorption of dipolar ions by rssins loaded with Ca^{2+} and La^{3+} and suggested an interaction between the dipoles and strong electrostatic fields existing between polyvalent metal ions and unoccupied fixed ions of the resin. If this mechanism is important, amino acid complexes in the resin should be much stronger in the resin than in aqueous solution. Results described below indicate that calcium complexes are *not* more stable in the resin than in solution, but the lanthanum complexes may well be more stable.

The retention of amino acids could be occurring by cation exchange, even though the eluent was water and the amino acids were close to their isoelectric pH. There was evidence that β-alanine might be retained by cation exchange, with accompanying displacement of calcium ions. When repeated injections were made, the retention volumes increased and the peaks became very asymmetrical. This condition was cured by an injection of calcium nitrate solution. If 0.1 *M* calcium nitrate was used as the eluent instead of pure water, stable, reproducible retention volumes were obtained with all the amino acids. These are the volumes listed in Table I. Volumes in pure water were *ca.* 5% greater than in 0.1 *M* calcium nitrate, and those in 0.25 *M* calcium nitrate were *ca.* 10% less. We attempted to use these data to calculate the stability of the calcium-ligand complexes in solution.

The retention of hydroxy acids was also measured in 0.1 *M* calcium nitrate, and the results clearly indicated complex formation. On lanthanum-form resin the retention of hydroxy acids was very strong indeed.

Calculations of stability constants

From the solubility of calcium sulfate. The solubility data are shown in Fig. 1. The manner of plotting was suggested by the work of Kirkwood[19] on the activities of solutions of dipolar ions. Complex formation raises the solubility, and the order of solubilities shown in Fig. 1 is the same as the order of retention of the five ligands on calcium-form resin. The graphs are almost linear at low ligand concentrations, and if we ignore activity coefficients or (more legitimately) assume them to cancel, we can calculate stability constants as follows:

Let s and s_0 be the solubilities of calcium dihydrate in the presence and absence of ligand; let L represent the ligand, and K_{sp} be the solubility product of calcium sulfate dihydrate; then,

$$[Ca^{2+}] + [CaL^{2+}] = s = [SO_4^{2-}] = K_{sp}/[Ca^{2+}];\ K_{sp} = s_0^2;$$

therefore: $[Ca^{2+}] = s_0^2/s$, and $[CaL^{2+}] = \dfrac{s^2 - s_0^2}{s}$

$$\text{Stability constant of } CaL^{2+} = \frac{s^2 - s_0^2}{s_0^2} \times \frac{1}{[L]}$$

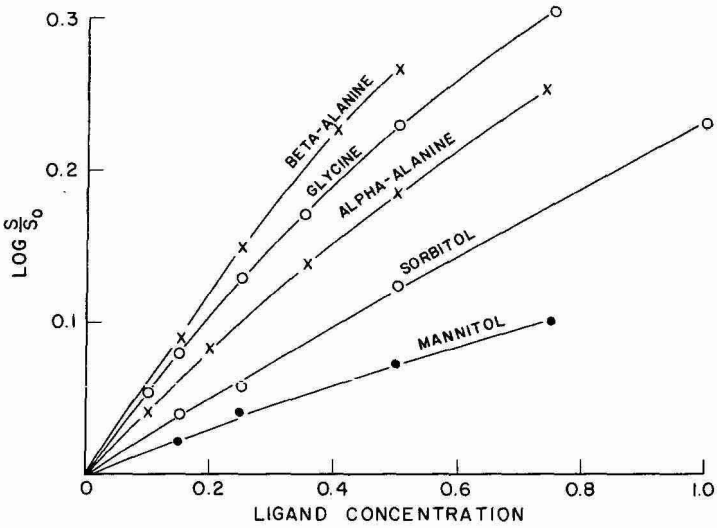

Fig. 1. Effect of dissolved ligands on the solubility of calcium sulfate dihydrate at 21°C: s = solubility in ligand solution; s_0 = solubility in water; ligand concentrations in molarities.

The stability constants thus deduced are (l mol^{-1}): mannitol, 0.7; sorbitol, 1.2; α-alanine, 2.1; glycine, 2.6; β-alanine, 3.2. The measured solubility, s_0, was 0.0153 M. The fraction of ligand bound to calcium is small, and in this calculation, [L] was taken as the concentration of ligand added.

We showed the net charge of the ligand as zero, even for the amino acids. At high pH, Ca^{2+} and other metal ions displace a proton from amino acid molecules and yield a singly charged complex ion. Stability constants for such complexes are well documented, but we were working at neutral pH, and to show that a proton was not displaced, we added calcium nitrate crystals to solutions of amino acids around a glass electrode; only minimal pH changes were observed, from 6.50 to 6.55 with 0.25 M glycine, 6.55 to 6.10 with 1 M β-alanine. We thus conclude that the amino acid complexes are ion–dipole pairs.

From the effect of calcium nitrate solutions on chromatographic retention. The retention volumes of amino acids and sorbitol are reduced if calcium salt is added to the water eluent, because complexes are now formed in solution as well as in the resin, and we hoped to use this effect to measure stability constants. However, the effect is small, and its interpretation is complicated by the shrinkage of the resin beads when the salt is added. For the calcium–glycine complex we calculated a stability constant between 0.7 and 1.4 l mol^{-1}, depending on whether we did or did not allow for the change in resin volume. All we can say about these estimates are that they are of the right magnitude.

Stability within the resin. From Table I retention volume of sorbitol on calcium-form resin is 1.36 (deuterium oxide = 1), and the inter-particle void volume is 0.50. Let us suppose that if sorbitol did not form a complex, its retention would be the same as that of glucose, namely 0.67. The corresponding capacity factors, k', are: sorbitol, 1.72; glucose, 0.34. We may infer that the internal concentrations of complexed and uncomplexed sorbitol are in the ratio (1.72 − 0.34) to 0.34, or 4.0:1. The

internal concentration of calcium ions is 8.3 mmol in 2.8 ml (see above), or 3.0 molal. The stability constant is thus 1.33. Thus the complex is about as stable in the resin as it is in solution. Similar calculations for amino acids are more complicated, for we cannot estimate what the retention would be without complexation, but they lead to the same conclusion, namely, that the complexes in the resin are not markedly more stable nor less stable than they are in aqueous solution.

CONCLUSIONS

Retention data are presented that have analytical interest. They confirm in general, but not in detail, the results of other workers[11,12] and show that calcium is the best counter-ion for separating pentose and hexose sugars, while lanthanum is better for sugar alcohols or polyols. They offer the possibility of analyzing mixtures of sugars with fruit acids (hydroxy acids) and amino acids on the same column without previously removing the acids from the sample. Hydroxy acids are bound very strongly to the lanthanum-loaded column, but if the proper eluent is found, a lanthanum column may be useful for analyzing such acids.

On the theoretical or mechanistic side, we have found no great differences between complex stabilities in the resin and those in water, though such differences may well exist in lanthanum-loaded resins. Ion–dipole association is shown to exist between calcium ions and amino acids in solution and in the resin.

ACKNOWLEDGEMENTS

The assistance of Gregory Tipsword in making some of the measurements is gratefully acknowledged. I am indebted to the Cooperative Institute for Research in Environmental Sciences, University of Colorado, for facilities granted to a retired faculty member.

REFERENCES

1 D. S. Dieter and H. F. Walton, *Anal. Chem.*, 55 (1983) 2109.
2 R. M. Saunders, *Carbohydrate Res.*, 7 (1968) 76.
3 J. Wong-Chong and F. A. Martin, *Sugar Azucar*, 75 (1980) 40, 64; *C.A.*, 93 (1980) 116271p, 206460d.
4 T. Kawamoto and R. Okada, *J. Chromatogr.*, 258 (1983) 284.
5 S. J. Angyal, G. S. Bethell and R. J. Beveridge, *Carbohydrate Res.*, 73 (1979) 9.
6 L. E. Fitt, W. Hassler and D. E. Just, *J. Chromatogr.*, 187 (1980) 381.
7 J. Dokladalova, A. Y. Barton and E. A. Mackenzie, *J. Ass. Offic. Anal. Chem.*, 63 (1980) 664.
8 L. A. Th. Verhaar and B. F. M. Kuster, *J. Chromatogr.*, 210 (1981) 279.
9 C. Vidal-Valverde, B. Olmedilla and C. Martin-Villa, *J. Liquid Chromatogr.*, 7 (1984) 2003.
10 J. G. Haust, R. E. Leegr, R. R. Rojas, D. L. Henrix, D. Friday and H. James, *J. Chromatogr.*, 261 (1983) 65.
11 R. W. Goulding, *J. Chromatogr.*, 103 (1975) 229.
12 L. Petrus, V. Bilak, E. Kuniak and L. Stankovic, *Chem. Zvesti*, 34 (1980) 530.
13 O. Samuelson, in J. Marinsky (Editor), *Ion Exchange —A Series of Advances*, Marcel Dekker, New York, 1969, Vol. 2, Ch. 5.
14 R. H. Stokes and H. F. Walton, *J. Amer. Chem. Soc.*, 76 (1954) 3327.
15 A. Maes, P. Peigneur and A. Cremers, *J. Chem. Soc., Farad. Trans. I*, 74 (1978) 182.
16 L.-G. Ekström and A. Olin, *Acta Chem. Scand.*, A31 (1977) 838.
17 S. J. Angyal, *Tetrahedron*, 30 (1974) 1695.
18 J. Otto, C. M. De Hernandez and H. F. Walton, *J. Chromatogr.*, 247 (1982) 91.
19 J. G. Kirkwood, *J. Chem. Phys.*, 2 (1934) 351.

Journal of Chromatography, 332 (1985) 211–217
Elsevier Science Publishers B.V., Amsterdam — Printed in The Netherlands

CHROMSYMP. 615

ELECTROKINETIC CHROMATOGRAPHY WITH 2-O-CARBOXYMETHYL-β-CYCLODEXTRIN AS A MOVING "STATIONARY" PHASE

SHIGERU TERABE*, HIROTO OZAKI, KOJI OTSUKA and TEIICHI ANDO
Department of Industrial Chemistry, Faculty of Engineering, Kyoto University, Sakyo-ku, Kyoto 606 (Japan)
(Received March 28th, 1985)

SUMMARY

Preliminary results are presented on a new type of liquid chromatography, based on inclusion complex formation in a solution of a β-cyclodextrin derivative having an ionized group, 2-O-carboxymethyl-β-cyclodextrin (β-CMCD), combined with electrokinetic migrations. Only the host–guest interaction between β-CMCD and the solute operates as the distribution process, and electroosmosis and electrophoresis in an open-tubular capillary filled with a β-CMCD solution permit differential migrations between the host and guest molecules. Separations of some aromatic isomers are shown, and retention parameters and the distribution coefficient are discussed.

INTRODUCTION

One of the two phases constituting a chromatographic system between which a solute is distributed is usually fixed rigid in a column and is therefore called the stationary phase. It is, however, not always necessary for the stationary phase to be held immovable in the column; a relative displacement of the two phases is sufficient for chromatographic separations. Micellar solubilization chromatography[1–3], or more generally electrokinetic chromatography[3], is an example where the two chromatographic phases move in the column with different velocities.

In electrokinetic chromatography where a solution of an ionic surfactant is filled in an open-tubular glass capillary and is subjected to free zone electrophoresis, the whole solution is transported by the electroosmotic flow with an approximately flat velocity profile in a direction determined by the sign of the zeta potential at the solution–glass interface. On the other hand, the ionic micelle is concurrently moved by the electrophoretic attraction generally in the direction opposite to the electroosmotic flow. As the electroosmotic flow is usually much stronger than the electrophoretic migration of the micelle[2,3], the micelle is also transported in the same direction as the whole solution but with a slower velocity than the latter. A mixture of solutes added to the micellar solution at one end of the tube can be separated while it moves towards the other end according to the extent to which each component is incorporated into the micelle by the micellar solubilization phenomenon.

0021-9673/85/$03.30

This concept of chromatography can be readily extended to the utilization of some specific interactions, *e.g.*, complexation or clathration. This paper presents preliminary results on electrokinetic chromatography with an ionic cyclodextrin derivative that can be expected to form inclusion complexes with a variety of organic molecules; 2-O-carboxymethyl-β-cyclodextrin (β-CMCD) was employed as a substitute for the chromatographic phase corresponding to the micelle in the above-mentioned chromatographic system.

Recently, cyclodextrins have attracted wide attention in high-performance liquid chromatography (HPLC), *e.g.*, cyclodextrins chemically bonded to silica gel as stationary phases have revealed interesting features for the separation of aromatic isomers[4,5] and optical isomers[6]. In these chemically bonded cyclodextrin phases, adsorption by spacer groups employed to link the cyclodextrin to the silica gel could be involved in the distribution process in addition to the formation of inclusion complexes of cyclodextrins with the solutes[4,5]. In electrokinetic chromatography, however, the cyclodextrin derivative is free in the solution and, therefore, only inclusion complex formation or host–guest interaction should be operating as the distribution process, although inclusion by ionic cyclodextrins may be slightly different from that by electrically neutral cyclodextrins.

EXPERIMENTAL

Reagents and materials

β-Cyclodextrin was purchased from Nakarai Chemical (Kyoto, Japan). All compounds employed as samples and reagents used for the preparation of the cyclodextrin derivative and for the preparation of the chromatographic solution were of analytical-reagent grade and used without further purification.

Preparation of 2-O-carboxymethyl-β-cyclodextrin (β-CMCD)

β-CMCD was synthesized by the reaction of sodium iodoacetate with an excess of β-cyclodextrin anion in dimethyl sulphoxide (DMSO) according to the method described by Kitaura and Bender[7] for the preparation of carboxymethyl-α-cyclodextrin (α-CMCD), and isolated by the method described by Gruhn and Bender[8] with some modifications, *viz.*, DEAE Toyopearl 650M (Toyo Soda, Tokyo, Japan) was employed instead of DEAE-Sephadex A-25 and 0.02 *M* phosphate buffer solution (pH 4.6) was delivered into the column as an isocratic eluent. Each eluate fraction was subjected to HPLC analysis with a DEAE-5500PW column (15 cm × 6 mm I.D.) (Toyo Soda) and a 0.02 *M* phosphate buffer solution (pH 3.85). Fractions containing β-CMCD were collected, concentrated by evaporation and desalted with a Sephadex G-10 (Pharmacia, Uppsala, Sweden) column to give an aqueous solution of the sodium salt of β-CMCD. β-CMCD was isolated by lyophilization and its molecular structure was confirmed by NMR spectroscopy as described below.

About 40 mg of the sodium salt of β-CMCD were dissolved in *ca.* 0.5 ml of ^2H_2O and proton NMR spectra at 90 MHz and carbon-13 NMR spectra at 22.49 MHz were measured at room temperature by using tetramethylsilane as an external standard. The proton NMR spectrum of β-CMCD was similar to that reported for α-CMCD[8]. Two peaks at δ 5.34 (1H, doublet, J = 4 Hz) and δ 4.21 (2H, singlet) were apparently observed, distinct from the spectrum of β-cyclodexrin recorded

under the same conditions. These peaks can be assigned to the C_1 anomeric proton on the carboxymethylated glucose unit and methylene protons of the carboxymethyl group in the order cited above.

Only two weak peaks were recognized in the carbon-13 NMR spectrum of β-CMCD other than those observed for β-cyclodextrin[9], *i.e.*, δ 100.0 and δ 70.4, which may be assigned to C_1 and C_3, respectively, of the glucose unit having the substituent. Major peaks of C_1 and C_3 were observed at δ 101.9 and δ 72.2, respectively. The absorption peak due to the saturated carbon of the carboxymethyl group seemed to overlap with the peak due to C_5 (δ 71.9), because only the C_5 peak was stronger than the others. Whereas the major peak of C_2 appeared at δ 73.1, the absorption by the C_2 of the glucose unit having the substituent could not be detected. Probably it accidentally coincides with that due to C_4 (δ 81.1).

Apparatus

Electrokinetic chromatography was performed at room temperature with an apparatus similar to that previously described[2]. The current supply of a Shimadzu IP-2A isotachophoretic analyser was used, which could deliver a constant current up to 500 μA at below 25 kV. The on-column detection technique was employed with a Jasco Uvidec-100-V spectrophotometric detector with a modified slit, as described elsewhere[2]. Proton NMR spectra were recorded on a Varian EM-390 and carbon-13 NMR spectra on a Jeolco FX-90Q NMR spectrometer.

Procedure

The chromatographic solution was prepared by dissolving β-CMCD in 0.1 *M* phosphate buffer solution (pH 7.0) consisting of sodium salts alone. The two solutions at the two electrodes were interchanged at an appropriate interval to avoid changes in pH owing to the electrolysis of water. The apparatus was operated at the constant current of 50 μA. All the solutes were injected as methanol solutions. Other chromatographic procedures were the same as those described elsewhere[2].

RESULTS AND DISCUSSION

Retention data obtained in this work are listed in Table I. The retention time of unretained solutes, t_0, was regarded as being equal to that of methanol used as the solvent for the solutes. On the assumption that methanol cannot be included at all by β-CMCD, the velocity of methanol band should be identical with that of the aqueous phase that is moved by electroosmosis[3]. The observed variations in t_0 shown in Table I for identical solutions are considered to be due to temperature fluctuations and/or slight changes in the pH of the solution as a result of the electrolysis of water. As the tube is filled with β-CMCD solution of a constant concentration, it is necessary for the measurement of the velocity of β-CMCD to label β-CMCD with a UV-absorbing molecule. Iodine was employed as a candidate for the tracer of β-CMCD, but the iodine peak could not be recognized when it was injected in the same way as the other samples. The chromatogram for the separation of cresol isomers is shown in Fig. 1 and that for the separation of xylidine isomers in Fig. 2.

The solutes listed in Table I can be assumed to be electrically neutral under the experimental conditions used, except for nitrophenols. These neutral solutes were

TABLE I

RETENTION TIMES, CAPACITY FACTORS* AND DISTRIBUTION COEFFICIENTS** OF SUBSTITUTED BENZENES

Conditions as in Fig. 1. Three to six solutes listed under the same run number were injected as a mixture.

No.	*Solute*	t_0 *(min)*	t_R *(min)*	$\bar{k}'$	K
1	Acetophenone	15.6	18.5	1.00	49
	Anisole		18.8	1.19	58
	Methyl benzoate		19.6	1.88	92
	Ethyl benzoate		19.9	2.23	109
	Propyl benzoate		20.4	3.04	149
	Butyl benzoate		20.7	3.71	182
2	*o*-Cresol	15.6	18.1	0.78	38
	m-Cresol		18.6	1.04	51
	p-Cresol		19.3	1.55	76
3	*m*-Nitroaniline	16.1	18.6	0.75	37
	o-Nitroaniline		18.9	0.89	44
	p-Nitroaniline		20.8	2.54	124
4	*o*-Chloroaniline	15.8	18.7	0.96	47
	m-Chloroaniline		18.9	1.08	53
	p-Chloroaniline		19.7	1.68	82
5	*m*-Dinitrobenzene	14.5	15.5	0.29	14
	p-Dinitrobenzene		15.7	0.36	18
	o-Dinitrobenzene		16.6	0.78	38
6	*m*-Nitrophenol	15.3	18.9	–***	–
	o-Nitrophenol		20.3	–***	–
	p-Nitrophenol		22.5	–***	–
7§	*m*-Nitrophenol	9.8	10.4	–	–
	p-Nitrophenol		12.3	–	–
	o-Nitrophenol		14.2	–	–
8§§	*m*-Nitrophenol	8.0	8.6	–	–
	o-Nitrophenol		12.2	–	–
	p-Nitrophenol		13.0	–	–
9	3,5-Xylidine	15.6	16.4	0.18	9
	2,6-Xylidine		17.0	0.35	17
	2,3-Xylidine		17.4	0.48	24
	2,5-Xylidine		18.1	0.77	38
	2,4-Xylidine		18.3	0.86	42
	3,4-Xylidine		18.6	1.02	50
10	3,5-Xylenol	15.4	17.6	0.68	33
	2,6-Xylenol		17.6	0.68	33
	2,5-Xylenol		18.5	1.18	58
	2,4-Xylenol		18.8	1.41	69
	2,3-Xylenol		19.1	1.67	82
	3,4-Xylenol		19.4	2.00	98

* An electrophoretic mobility of $9.03 \cdot 10^{-3}$ mm^2 sec^{-1} V^{-1} for β-CMCD was adopted in calculating t_{CD}.

** As specific volume of 0.671 ml g^{-1} for β-CMCD was assumed in calculating V_{CD}.

*** See text.

§ α-Cyclodextrin (0.032 *M*) was employed instead of β-CMCD.

§§ Phosphate buffer (0.1 *M*, pH 7.0) containing no cyclodextrin was used.

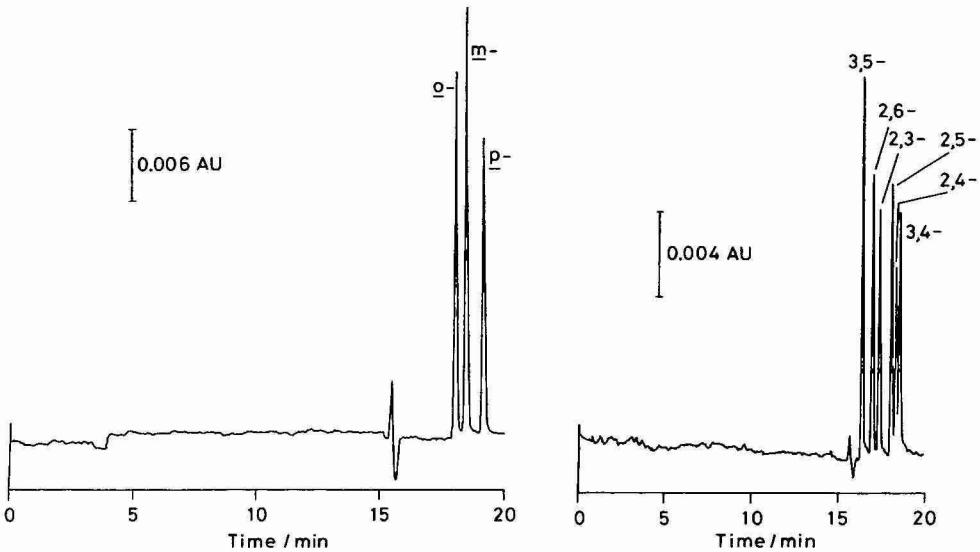

Fig. 1. Electrokinetic chromatogram of cresol isomers. Chromatographic solution, 0.025 *M* β-CMCD in 0.1 *M* phosphate buffer (pH 7.0); separation tube, 650 × 0.05 mm I.D.; length of the tube used for separation, 500 mm; current, 50 μA; total applied voltage, *ca.* 12 kV; detection wavelength, 210 nm.

Fig. 2. Electrokinetic chromatogram of xylidine isomers. Conditions as in Fig. 1.

not separated by electrophoresis alone when 0.032 *M* α-cyclodextrin was used in place of β-CMCD. The lower solubility of β-cyclodextrin than α-cyclodextrin in water is the reason why β-cyclodextrin was not used in the blank experiment. The fact that the separation of these isomers was effected when β-CMCD was present in the solution clearly implies that the inclusion of solutes by β-CMCD takes part in the distribution process. The order of elution of isomers of cresol, nitroaniline and dinitrobenzene is the same as that reported[4,5] in HPLC with β-cyclodextrin-bonded stationary phases. It should be noted that isomers of xylidine or xylenol were successfully separated even if 3,5- and 2,6-xylenols were not resolved. These results suggest that this method is promising for separating isomers of substituted benzenes.

The isomers of nitrophenol were separated in every instance shown in Table I (Nos. 6, 7 and 8), and these results can be explained as follows. In the absence of cyclodextrins (Table I, No. 8), the isomers were separated only by electrophoresis of free isomers in the phosphate buffer, that is, the isomers were eluted in decreasing order of their pK_a values. When α-cyclodextrin was added to the buffer solution (Table I, No. 7), the *p*-isomer was included by α-cyclodextrin to a much greater extent than the other isomers and the electrophoretic mobility was reduced, causing reversal of the order of elution between the *o*- and *p*-isomers. Comparison of the results with α-cyclodextrin (Table I, No. 7) and β-CMCD (Table I, No. 6) reveals that the *p*-isomer was also included by β-CMCD more strongly than the *o*-isomer.

The capacity factor, $\bar{k}'$, which is defined as the ratio of the total number of moles of the solute included by β-CMCD, n_{CD}, to those in the aqueous phase, n_{aq}, *i.e.*, $\bar{k}' = n_{CD}/n_{aq}$, is related to the retention time, t_R, for electrically neutral solutes

by the following equation, which is similar to that derived for electrokinetic chromatography with micellar solutions[3]:

$$\tilde{k}' = \frac{t_R - t_0}{t_0 (1 - t_R/t_{CD})} \tag{1}$$

where t_{CD} is the elution time of β-CMCD and indicates a longer limit of retention times for electrically neutral solutes. As shown in eqn. 1, the values of both t_{CD} and t_0 are required for calculation of the capacity factor. This means that the possible range of the retention time should be known in order to determine the capacity factor in this method.

In order to measure the elution time of β-CMCD, an experimental approach was used in addition to the tracer method mentioned above. A *ca.* 0.015 *M* aqueous solution of β-CMCD was injected and detected by UV absorption at 200 nm under the same conditions as those given in Table I, except that 0.1 *M* phosphate buffer solution (pH 7.0) containing no β-CMCD was used instead of that containing β-CMCD. The current was kept at 50 μA, but the voltage increased to 15 kV from the 12 kV observed with the 0.025 *M* β-CMCD solution. The electroosmotic velocity was measured with methanol added to the aqueous β-CMCD solution. The electrophoretic mobility of β-CMCD in the 0.1 *M* phosphate buffer solution (pH 7.0) was $9.03 \cdot 10^{-3}$ mm^2 sec^{-1} V^{-1}. The estimated value of t_{CD}/t_0 from the above value of the electrophoretic mobility was about 1.4 under the conditions given in Table I.

Capacity factors calculated by eqn. 1 from the retention time and t_0 listed in Table I and the values of t_{CD}/t_0 estimated from the electrophoretic mobility of β-CMCD described above are also given in Table I, together with the distribution coefficient, *K*, which was obtained according to

$$\tilde{k}' = K \cdot \frac{V_{CD}}{V_{aq}} \tag{2}$$

where V_{aq} and V_{CD} are the volumes of the aqueous phase and β-CMCD, respectively, in the tube. The specific volume of β-CMCD required in order to know V_{CD} was assumed to be equal to that of α-cyclodextrin (0.671 ml g^{-1})[10]. It should be stressed that the capacity factors and hence the distribution coefficients listed in Table I are approximate values because the estimated value of t_{CD} is adopted in the calculation.

The resolution equation in electrokinetic chromatography is given by considering eqn. 1[3]:

$$R_s = \frac{\sqrt{N}}{4}\left(\frac{\alpha - 1}{\alpha}\right)\left(\frac{\tilde{k}'}{1 + \tilde{k}'}\right)\left[\frac{1 - t_0/t_{CD}}{1 + (t_0/t_{CD})\,\tilde{k}'}\right] \tag{3}$$

where R_s is the resolution, *N* is the plate number and α is the separation factor. In eqn. 3, capacity factors for two closely eluted peaks are assumed to be approximately equal. The resolution expressed by eqn. 3 is apparently a function not only of *N*, α and $\tilde{k}'$, but also of t_0/t_{CD}. As discussed in a previous paper[3], the capacity factor that gives the maximum resolution at constant values of the other parameters is dependent

on the ratio t_0/t_{CD}. As the value of t_0/t_{CD} is estimated to be about 0.7, as discussed above, the maximum value at $\tilde{k}' = 1.1$ can be predicted to be about 0.07 for the product of the last two terms of the right-hand side of eqn. 3, which depend only on the capacity factor among four terms. This large value of 0.7 for t_0/t_{CD} in this method results in a much poorer resolution in comparison with electrokinetic chromatography with micellar solutions where t_0/t_{mc} lies in the range[3] 0.2–0.3, where t_{mc} is the elution time of the micelle and corresponds to t_{CD}. The low electrophoretic mobility of β-CMCD, which results from the small ratio of the charge number to the molecular weight, must be the reason for the large value of t_0/t_{CD} and it is therefore desirable to introduce more charges into a molecule in order to improve the resolution in this method.

Plate number calculated from peak area, peak height and retention time are 120 000–130 000 in the chromatogram shown in Fig. 1. These numbers correspond to plate heights of about 4 μm. These plate heights are considerably higher than the 2–3 μm observed for chromatograms with micellar solutions[3], the reason for which remains to be clarified.

CONCLUSION

The method described is an example of chromatography with a homogeneous solution and electrokinetic migrations, supplementing that with micellar solutions reported previously[3]. It demonstrates the possibility of widening the scope of electrokinetic chromatography. Only the formation of inclusion complexes or the host–guest interaction between the cyclodextrin derivative and the solute, both of which are free in the solution, operates as the distribution process. This method seems very promising, especially for separating aromatic isomers, although much remains to be done before practical application.

ACKNOWLEDGEMENT

This research was supported in part by the Nissan Science Foundation.

REFERENCES

1 T. Nakagawa, *Newsl., Div. Colloid Surf. Chem., Chem. Soc. Jap.*, 6, No. 3 (1981) 1.
2 S. Terabe, K. Otsuka, K. Ichikawa, A. Tsuchiya and T. Ando, *Anal. Chem.*, 56 (1984) 111.
3 S. Terabe, K. Otsuka and T. Ando, *Anal. Chem.*, 57 (1985) 834.
4 K. Fujimura, T. Ueda and T. Ando, *Anal. Chem.*, 55 (1983) 446.
5 Y. Kawaguchi, M. Tanaka, M. Nakae, K. Funazo and T. Shono, *Anal. Chem.*, 55 (1983) 1852.
6 W. L. Hinze, T. E. Riehl, D. W. Armstrong, W. DeMond, A. Alak and T. Ward, *Anal. Chem.*, 57 (1985) 237.
7 Y. Kitaura and M. L. Bender, *Bioorg. Chem.*, 4 (1975) 237.
8 W. B. Gruhn and M. L. Bender, *Bioorg. Chem.*, 3 (1974) 324.
9 K. Takeo, K. Hirose and T. Kuge, *Chem. Lett.*, (1973) 1233.
10 P. C. Manor and W. Saenger, *J. Amer. Chem. Soc.*, 96 (1974) 3630.

Journal of Chromatography, 332 (1985) 219–226
Elsevier Science Publishers B.V., Amsterdam — Printed in The Netherlands

CHROMSYMP. 617

ELECTROKINETIC CHROMATOGRAPHY WITH MICELLAR SOLUTIONS

SEPARATION OF PHENYLTHIOHYDANTOIN-AMINO ACIDS

KOJI OTSUKA*, SHIGERU TERABE and TEIICHI ANDO
Department of Industrial Chemistry, Faculty of Engineering, Kyoto University, Sakyo-ku, Kyoto 606 (Japan)
(Received March 25th, 1985)

SUMMARY

A mixture of 22 phenylthiohydantoin-amino acids was separated by electrokinetic chromatography with a sodium dodecyl sulphate (SDS) solution and a 650 × 0.05 mm I.D. fused-silica tube. This chromatography is based on micellar solubilization and electrokinetic migration in an open-tubular capillary. The retention times of the solutes could be controlled by changing the SDS concentration, the applied voltage or the length of the separation tube. Dodecyltrimethylammonium bromide (DTAB) solutions were also employed. The separation characteristics with SDS solutions were completely different from those with DTAB solutions. The resolutions were better with the former than with the latter solution, but for some solutes the latter gave better results.

INTRODUCTION

Micellar solubilization chromatography[1–3], or more generally electrokinetic chromatography[3], is a new type of chromatography based on micellar solubilization and electrokinetic migration. In this method, micellar solubilization operates as the partition mechanism, that is, a solute is distributed between the micelle and the aqueous phase, and the electroosmotic flow of a solution filled in an open-tubular capillary and the electrophoretic migration of the ionic micelle make possible differential displacement between the micelle and the aqueous phase. Although micelles are understood to be dynamic structures and are called a pseudo-phase, this technique can be regarded as belonging to a branch of liquid–liquid partition chromatography having no solid support. We have previously described[3] the fundamental characteristics of this method from the viewpoints of electrokinetic migration, chromatographic parameters and the micellar solubilization phenomenon.

In previous work[2,3], we employed solutes that were electrically neutral under the experimental conditions used. If a solute can be ionized, the chromatographic behaviour of the ionized solute should be different from that of the neutral solute, because the ionized solute is subjected to electrophoretic attraction in addition to the

0021-9673/85/$03.30

electroosmotic migration of the whole solution when it exists in the aqueous phase. The electrophoretic attraction for the ionized solute should also be effective when the solute is incorporated into the micelle as well as that for the ionic micelle. This kind of electrophoretic effect on the ionized solute should be taken into account in order to achieve a good separation of a complex mixture containing ionized species.

Phenylthiohydantoin (PTH)-amino acids, which are amino acid derivatives resulting from the Edman degradation of peptides and proteins, are important materials for determining amino acid sequences. Since Zimmerman *et al.*[4] first introduced high-performance liquid chromatography (HPLC) for separating PTH-amino acids, several studies have been published in which various kinds of techniques were used for HPLC. Isocratic[5–10] and binary gradient[11–16] elution were performed with acidic eluents, in some instances at high temperatures. In any event, however, some disadvantages were noted, such as long analysis times, complexity of the operation or failure of complete separation. Recently, it has been shown that the use of micro HPLC under the conditions of isocratic elution and room temperature operation can shorten the analysis time[17], but satisfactory separation was not obtained.

In this paper, the separation of PTH-amino acids is described to demonstrate the applicability of electrokinetic chromatography with micellar solutions. Some strategies for improving the resolution with this technique are also considered.

EXPERIMENTAL

The same apparatus as described previously[2,3] was used. As a chromatographic column, a 650 × 0.05 mm I.D. or an 1150 × 0.05 mm I.D. fused-silica tube was employed. The temperature of the thermostated oven was maintained at 35°C.

All the reagents and samples were used as received. Sodium dodecyl sulphate (SDS) solutions were prepared by dissolving SDS in 0.05 *M* sodium dihydrogen phosphate–0.0125 *M* sodium tetraborate buffer solution (pH 7.0). Dodecyltrimethylammonium bromide (DTAB), supplied by Tokyo Kasei Kogyo (Tokyo, Japan), was dissolved in 0.1 *M* tris(hydroxymethyl)aminomethane–0.1 *M* hydrogen chloride buffer (Tris–HCl buffer) (pH 7.0). PTH-amino acids, obtained from Wako (Osaka, Japan), were dissolved in acetonitrile–water (1:1) or in acetonitrile and stored at −20°C. Sudan III or Yellow OB (Tokyo Kasei Kogyo) was used after dissolution in surfactant solution or methanol.

The experimental procedure was the same as that described previously[2].

RESULTS AND DISCUSSION

Fig. 1 shows an electrokinetic chromatogram of a mixture of 22 PTH-amino acids with 0.05 *M* SDS solution. In this chromatogram, the peaks of all the solutes in the mixture were separately recognized. However, four pairs of peaks were poorly resolved: Thr (T)–Ser (S), Val (V)–Met (M), Leu (L)–Trp (W) and Phe (F)–Nle (n-L). Here, three- or one-letter abbreviations for the amino acid are used to indicate the corresponding PTH-amino acid. As noted previously[2], the capacity factor, $\tilde{k}'$, of an electrically neutral solute in this chromatography is given by

$$\tilde{k}' = \frac{t_R - t_0}{t_0(1 - t_R/t_{mc})} \quad (1)$$

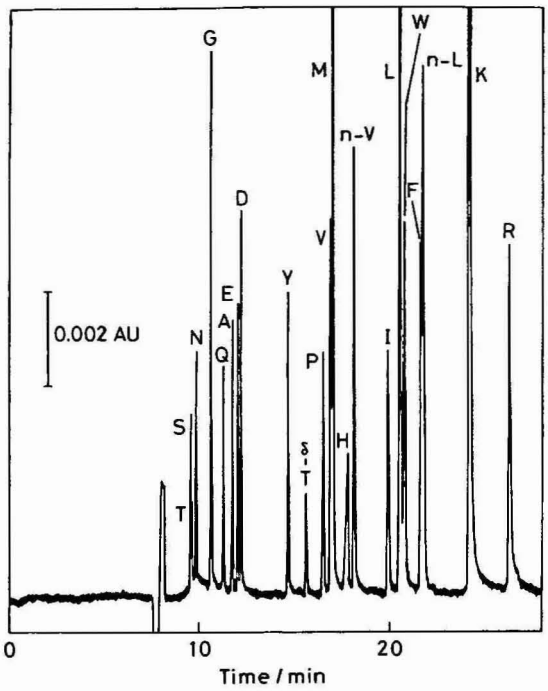

Fig. 1. Electrokinetic chromatogram of a mixture of 22 PTH-amino acids. Micellar solution, 0.05 *M* SDS in phosphate–borate buffer (pH 7.0); separation tube, 650 × 0.05 mm I.D.; length of the tube used for separation, 500 mm; total applied voltage, *ca.* 10 kV; current, 14 μA; detection wavelength, 260 nm; temperature of oven, 35°C. The peaks are labelled with one-letter abbreviations for the amino acid.

where t_R, t_0 and t_{mc} are the elution times of the solute, the insolubilized solute and the micelle, respectively. Here, the symbol, $\tilde{k}'$ is used instead of k', which is widely accepted in conventional HPLC[3]. In the experiments, t_0 was regarded as the retention time of methanol and t_{mc} that of Sudan III or Yellow OB[3]. The resolution, R_s, of two adjacent peaks whose capacity factors are $\tilde{k}'_1$ and $\tilde{k}'_2$ is expressed as follows[3]:

$$R_s = \frac{\sqrt{N}}{4}\left(\frac{\alpha - 1}{\alpha}\right)\left(\frac{\tilde{k}'}{1 + \tilde{k}'}\right)\left[\frac{1 - t_0/t_{mc}}{1 + (t_0/t_{mc})\tilde{k}'}\right] \quad (2)$$

where N is the plate number, α is the separation factor and $\tilde{k}'$ is approximately given by $\tilde{k}' = \tilde{k}'_1 = \tilde{k}'_2$. The term t_0/t_{mc} is a specific parameter for electrokinetic chromatography which shows the width of the total range of elution[3], and in Fig. 1 its value was about 0.25: t_0 = 470 sec and t_{mc} = 1860 sec. We have already shown[3] that R_s should be maximal at $\tilde{k}'$ = 2.0 for the value of t_0/t_{mc} = 0.25. In the chromatogram shown in Fig. 1, the retention time corresponding to $\tilde{k}'$ = 2.0 is about 16 min. The value of $\tilde{k}'$ of a solute changes linearity with the concentration of the surfactant and with the applied voltage[3]: an increase in the concentration of surfactant or a decrease in the applied voltage causes an increase in the value of $\tilde{k}'$. Therefore, for pairs of peaks that are eluted at a time far from the optimum, *e.g.*, pairs

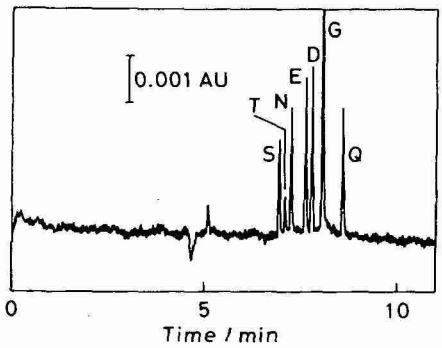

Fig. 2. Electrokinetic chromatogram of a mixture of some PTH-amino acids, showing shorter retention times in Fig. 1. Micellar solution, 0.10 *M* SDS; total applied voltage, *ca.* 15 kV; current, 31 μA. Other conditions as in Fig. 1.

such as Ser–Thr, Leu–Trp or Phe–Nle, we can adjust the $\tilde{k}'$ to more appropriate values by changing the SDS concentration and/or the applied voltage, and expect to obtain better resolutions than those given under the conditions used in Fig. 1.

For the pair Ser–Thr, whose $\tilde{k}'$ value is small (*ca.* 0.33) in Fig. 1, an increase in the SDS concentration gave a better separation, as shown in Fig. 2, where the Ser–Thr pair is completely resolved. It should be noted in Fig. 2 that Glu (E) and Asp (D) were eluted faster than Gly (G) and Gln (Q), in contrast to the elution order in Fig. 1. The result can be interpreted by considering two effects on the retention of PTH-amino acids in this chromatography: one is the micellar solubilization phenomenon in combination with electrophoresis of micelles and the other is electrophoresis of an ionized solute. Both PTH-Glu and -Asp have a free carboxyl group but PTH-Gly and -Gln do not. That is, PTH-Gly and -Gln are transported in the tube with a velocity $v_s(n)$, which is given by[3]

$$v_s(n) = \frac{1 + (t_0/t_{mc})\tilde{k}'_n}{1 + \tilde{k}'_n} \cdot v_{eo} \tag{3}$$

where $\tilde{k}'_n$ is the capacity factor for the electrically neutral solute and v_{eo} is the electroosmotic velocity, which is equal to the migration velocity of the unretained solute. On the other hand, PTH-Glu and -Asp can be considered to be ionized under the conditions given in Fig. 2, so that these solutes are subjected to the electrophoretic attraction to the positive electrode in addition to the electrokinetic chromatographic migration expressed by eqn. 3. By assuming that the electrophoretic velocity of the micelle, $v_{ep}(mc)$, remains constant, even when the micelle solubilizes the ionized solute, the migration velocity of the ionized solute, $v_s(i)$, is represented by

$$v_s(i) = v_{eo} + \frac{1}{1 + \tilde{k}'_i} \cdot v_{ep}(i) + \frac{\tilde{k}'_i}{1 + \tilde{k}'_i} \cdot v_{ep}(mc) \tag{4}$$

where $\tilde{k}'_i$ is the capacity factor for the ionized solute and $v_{ep}(i)$ is the electrophoretic velocity of the ionized solute itself when it exists in the aqueous phase. Here, it should

be noted that the sign of the migrating direction is taken into account. As the migration velocity of the micelle, v_{mc}, is given by[3]

$$v_{mc} = v_{eo} + v_{ep}(mc) \tag{5}$$

eqn. 4 can easily be rewritten as

$$v_s(i) = \frac{1 + (t_0/t_{mc})\bar{k}'_i}{1 + \bar{k}'_i} \cdot v_{eo} + \frac{1}{1 + \bar{k}'_i} \cdot v_{ep}(i) \tag{6}$$

where the direction of $v_{ep}(i)$ is the reverse of that of v_{eo} or $v_s(i)$. Comparison of eqn. 3 with eqn. 6 reveals that an increase in capacity factor, which is caused by an increase in the SDS concentration, should decrease the velocity of the non-ionized solute, $v_s(n)$, to a greater extent than that of the ionized solute, $v_s(i)$, because the second term in eqn. 6 becomes smaller in absolute value with an increase in $\bar{k}'_i$. As had been expected, the retention times of PTH-Gly and -Gln could be made longer than those of PTH-Glu and -Asp by increasing the SDS concentration, as shown in Figs. 1 and 2.

For other poorly resolved pairs in Fig. 1, *i.e.*, Leu–Trp and Phe–Nle, which were eluted with larger $\bar{k}'$ (4.9 and 5.8) than the optimum values, a decrease in SDS concentration was required in order to attain better separations. The chromatogram in Fig. 3 shows that a decrease in SDS concentration from 0.05 to 0.02 *M* brought about better resolutions of both pairs than those observed in Fig. 1.

The pair Val–Met was not completely separated in Fig. 1, although it was eluted with the nearly optimum value of $\bar{k}' = 2.6$. We tried to improve the resolution of this pair by doubling the length of the initially used column to 100 cm. Under these conditions, the number of theoretical plates should be twice and the resolution about 1.4 times as large as those in Fig. 1. The two peaks were successfully separated, as shown in Fig. 4.

Dodecyltrimethylammonium bromide (DTAB), which is a cationic surfactant, was also used to examine the effect of surfactant molecules on the separation of

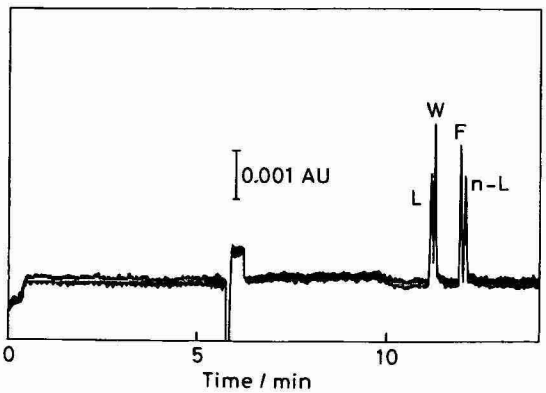

Fig. 3. Electrokinetic chromatogram of a mixture of PTH-Leu, Trp, -Phe and -Nle. Micellar solution, 0.02 *M* SDS; total applied voltage, *ca.* 12.5 kV; current, 13 μA. Other conditions as in Fig. 1.

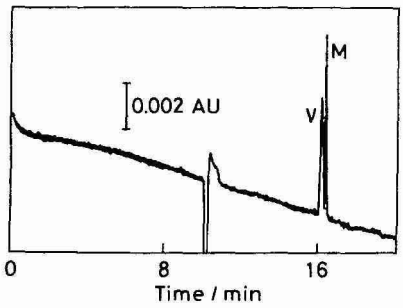

Fig. 4. Electrokinetic chromatogram of a mixture of PTH-Val and -Met. Separation tube, 1150 × 0.05 mm I.D.; length of the tube used for separation, 1000 mm; total applied voltage, *ca.* 25 kV; current, 17 μA. Other conditions as in Fig. 3.

PTH-amino acids. The directions of both electroosmotic flow and electrophoretic migration of the DTAB micelle were the opposite of those in SDS solutions: the direction of the electroosmotic flow was from the negative to the positive electrode and that of the electrophoretic migration of the DTAB micelle was from positive to negative. These observations can be explained in terms of the reversal of the signs of the zeta potentials at the fused-silica wall and the micelle when DTAB is substituted for SDS. In fact, the zeta potential of the quartz/DTAB solution has been reported[18] to be positive if the concentration of DTAB is higher than 10^{-4} *M*, and the micelle of DTAB apparently has positive charges. The chromatogram shown in Fig. 5 is an example of the separation of PTH-amino acids with 0.05 *M* DTAB solution. It is

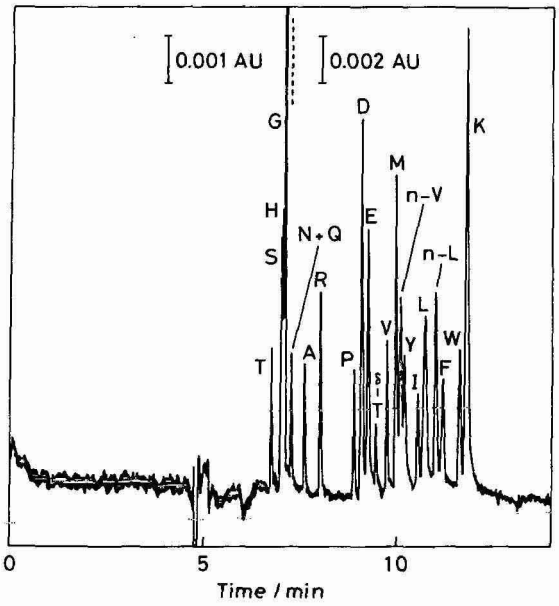

Fig. 5. Electrokinetic chromatogram of a mixture of 22 PTH-amino acids. Micellar solution, 0.05 *M* DTAB in Tris–HCl buffer (pH 7.0); total applied voltage, *ca.* 15 kV; current, 37 μA. Other conditions as in Fig. 1.

TABLE I

COMPARISON OF VARIABLES* OF ELECTROKINETIC MIGRATION BETWEEN SDS AND DTAB SOLUTIONS

Separation tube, 650 × 0.05 mm I.D.; total applied voltage, *ca.* 15 kV; temperature of oven, 35°C.

Surfactant	*Concentration (M)*	*I (μA)*	v_{eo} *(mm sec*$^{-1}$*)*	v_{mc} *(mm sec*$^{-1}$*)*	t_0/t_{mc}
SDS	0.03	19.4	1.76	0.522	0.298
	0.05	22.1	1.71	0.494	0.288
	0.10	30.4	1.68	0.363	0.217
DTAB	0.03	32.2	1.73	0.733	0.425
	0.05	37.4	1.70	0.698	0.412
	0.10	45.5	1.71	0.651	0.380

* I, current; v_{eo}, electroosmotic velocity; v_{mc}, migration velocity of micelles.

worth noting that any pair of solutes that were eluted as partially overlapping peaks under the conditions employed in Fig. 1 was completely resolved in the chromatogram shown in Fig. 5, although some other solutes were not separated in Fig. 5 even with concentrations of DTAB different from 0.05 *M*.

In Table I, some migration variables in elektrokinetic chromatography for the SDS and DTAB solutions are presented . The current in each surfactant solution increased with increase in the concentration of the surfactant[3]. A higher current is observed in the DTAB solution than in the SDS solution at the same concentration of the surfactants. The differences in these values seem to be due to the differences in the buffer solutions used, borate–phosphate and Tris–HCl, rather than to the difference in the surfactants themselves. The electroosmotic velocities, v_{eo}, were almost constant, regardless of the surfactant concentration, but the migration velocities of micelles, v_{mc}, decreased with increase in the micellar concentration in both SDS and DTAB solutions. These facts can be explained in terms of the change in the viscosity of the solutions and the temperature rise due to Joule heat[3]. As a specific parameter in electrokinetic chromatography, we obtained smaller values for t_0/t_{mc} in the SDS solutions than in DTAB solutions at any concentration. From the viewpoint of the maximum resolution, a smaller value of t_0/t_{mc} is advantageous, and this is probably the main reason why the SDS solution gave a better resolution as a whole than the DTAB solution for the 22 PTH-amino acids.

In conclusion, a satisfactory separation of 22 PTH-amino acids was achieved by electrokinetic chromatography with a micellar solution and an open-tubular capillary, and this indicates the high resolving power of this chromatographic technique.

ACKNOWLEDGEMENT

This work was partly supported by a Grant-in-Aid for Scientific Research (No. 59550512) from the Ministry of Education, Science and Culture, Japan.

REFERENCES

1 T. Nakagawa, *Newsl., Div. Colloid Surf. Chem., Chem. Soc. Jap.*, 6, No. 3 (1981) 1.
2 S. Terabe, K. Otsuka, K. Ichikawa, A. Tsuchiya and T. Ando, *Anal. Chem.*, 56 (1984) 111–113.
3 S. Terabe, K. Otsuka and T. Ando, *Anal. Chem.*, 57 (1985) 834–841.
4 C. L. Zimmerman, E. Appella and J. J. Pisano, *Anal. Biochem.*, 75 (1977) 569–573.
5 M. Abrahamsson, K. Gröningsson and S. Castensson, *J. Chromatogr.*, 154 (1978) 313–317.
6 S. M. Rose and B. D. Schwartz, *Anal. Biochem.*, 107 (1980) 206–213.
7 G. E. Tarr, *Anal. Biochem.*, 111 (1981) 27–32.
8 S. M. Kim, *J. Chromatogr.*, 247 (1982) 103–110.
9 P. Pucci, G. Sannia and G. Marino, *J. Chromatogr.*, 270 (1983) 371–377.
10 M. R. Silver, T. D. Trosper, M. R. Gould, J. E. Dickson and G. A. Desotelle, *J. Liq. Chromatogr.*, 7 (1984) 559–568.
11 A. S. Bhown, J. E. Mole, A. Weissinger and J. C. Bennett, *J. Chromatogr.*, 148 (1978) 532–535.
12 P. W. Moser and E. E. Rickli, *J. Chromatogr.*, 176 (1979) 451–455.
13 N. D. Johnson, M. W. Hunkapiller and L. E. Hood, *Anal. Biochem.*, 100 (1979) 335–338.
14 L. E. Henderson, T. D. Copeland and S. Oroszlan, *Anal. Biochem.*, 102 (1980) 1–7.
15 R. Somack, *Anal. Biochem.*, 104 (1980) 464–468.
16 D. Hawke, P.-M. Yuan and J. E. Shively, *Anal. Biochem.*, 120 (1982) 302–311.
17 T. Takeuchi, M. Yamazaki and D. Ishii, *J. High Resolut. Chromatogr. Chromatogr. Commun.*, 7 (1984) 101–102.
18 P. Somasundaran, T. W. Healy and D. W. Fuerstenau, *J. Phys. Chem.*, 68 (1964) 3562–3566.

Journal of Chromatography, 332 (1985) 227–236
Elsevier Science Publishers B.V., Amsterdam — Printed in The Netherlands

CHROMSYMP. 616

RECENT PROGRESS IN GEL PACKING MATERIALS AND DETECTORS FOR MODERN LIQUID CHROMATOGRAPHY IN JAPAN

HIROYUKI HATANO
Department of Chemistry, Faculty of Science, Kyoto University, Kyoto 606 (Japan)
(Received March 26th, 1985)

SUMMARY

Developments in rigid polymer gels for size exclusion, ion-exchange and reversed-phase chromatography are described, especially products which are commercially available in Japan. New detectors for high-performance liquid chromatography are reviewed.

HISTORICAL INTRODUCTION

In 1958 I set up The Research Group of Automatic Liquid Chromatography in Japan, the aim of which is to modernize liquid chromatographic techniques and to promote liquid chromatographic research. It meets once a year and has held workshops with leaders in liquid chromatography every summer since 1963.

The first contribution by this group to the automation of liquid chromatography was in developing the Hitachi Model KLF-1 automatic liquid chromatograph which is equipped with a two-wavelength spectrophotometric detector, and was reported in 1961[1] and 1962[2]. This instrument had an automatic fractionation mode and the detector enabled the selection of two wavelengths from 200 to 750 nm for simultaneous spectrophotometric detection and recording after colour development (chemical reaction).

I had previously published a book on automatic amino acid analysis[3]. An automatic amino acid analyzer (Hitachi Models KLA-1 and KLA-2)[4], equipped with three constant-flow delivery pumps and a three-wavelength flow-photometric detector utilizing a continuous-flow mode, was produced by myself and my colleagues immediately afterwards. The photometric detector was used at 570, 440 and 640 nm. The wavelength of 570 nm was most effective for detection of ninhydrin colour reaction with ordinary alpha-amino acids, 440 nm was for imino acids, proline and hydroxyproline and 640 nm for measurements of one-third the intense absorbance of large amounts of eluted amino acids.

Since 1964, The Research Group has published a series of books on automatic and modern liquid chromatography[5–11] and since 1977, data books[12] on high-performance liquid chromatography (HPLC), under the sponsorship of The Japan Society for Promotion of Science and of The Promotion Bureau of Science and Technology.

0021-9673/85/$03.30

In 1973, further development of a coulometric detector was reported by Muto and Takata[13] and of a spectrofluorimetric detector for HPLC by Hatano *et al.*[14]. These efforts[15,16] eventually led to the U.S.–Japan Seminar of Advanced Techniques of Liquid Chromatography, held at Boulder, Colorado, in 1978[17] and to Micro-capillary Techniques in Liquid Chromatography, held at Honolulu in Hawaii in 1982[18] under the sponsorship of The National Science Foundation, U.S. and of The Japan Society for Promotion of Science. The 18th International Symposium on Advances in Chromatography was held at Tokyo in 1982[19], and The International Symposium on High Performance Liquid Chromatography was held at Kyoto in 1985[20], under the sponsorship of The Japan Society for Promotion of Science and of The Science Council of Japan. These meetings were also co-sponsored by The Chemical Society of Japan, The Japan Society for Analytical Chemistry, The Japanese Biochemical Society, The Agricultural Chemical Society of Japan, Japan Analytical Instrumental Manufacturer's Association and the Nissan and the Inoue Science Foundations. Several books on modern liquid chromatography have been published by members of this Research Group[21–26].

Recently, a quite unique detector, an electron spin resonance spectrometric detector, was linked with a high-performance liquid chromatograph[27], which enabled the separation not only of stable free radicals but also trapped spin adducts of unstable radicals, produced in chemical reactions and biological processes. A review paper on liquid chromatographic detectors[28] was read in Melbourne. Developments in ion chromatography were reported by Hanaoka *et al.*[29]. Several distinguished works on miniaturization of columns and instruments have been reported by Ishii and co-workers since 1977[30–33], on microbore packed columns by Tsuda and Novotny[34] and by Rokushika and Hatano[35]. The combination of a high-performance liquid chromatograph with a mass spectrometer[36,37], with ion-selective electrodes[38] and with spectroscopic detection system[39] were proposed.

GEL PACKING MATERIALS AND COLUMN TECHNOLOGY

Various porous polymer gels for size exclusion and ion-exchange chromatography have been reported[40–44] These aqueous and non-aqueous materials are commercially available as Hitachi gels from Hitachi, Shodex gels from Showa Denko Co., as Shim-pack gels from Shimadzu, as TSK gels from Toyo Soda Co., as Asahi gels from Asahi Kasei Co., as Fine-pak gels from Jasco Co. and as MCI gels from Mitsubishi Kasei Co.

Polystyrene gels are copolymers of polystyrene–divinylbenzene, and polyester gels comprise polyacrylate, polymethacrylate or polyvinyl acetate. Polyacrylamide has been used as a base material for soft gel packings. The other gels are hydroxymethyl, carboxyl, quaternary ammonium and sulphonated derivatives of the copolymers. These gels have large surface areas, over 300 m^2/g, pore sizes of 40–1000 Å and particle sizes of 5–20 μm. All of these gels can be used with both aqueous methanol and non-aqueous hexane–methanol mobile phases in normal or reversed-phase chromatography[45].

The separation behaviours of biologically active molecules on these gel columns are characteristic and the biological activities of molecules are completely recoverable. Moderate separations and effective recoveries can be obtained on size

exclusion gel columns. Ion-exchange resins have been used for separation of relatively small molecules such as amino acids and nucleic acid constituents. Recently, improved ion exchangers have been introduced for separation of large molecules such as proteins and nucleic acids. Progress in the separation of biomolecules has also been reported in reversed-phase liquid chromatography. Developments in high-performance columns[46] and packing materials[47] have been described.

GEL PACKING MATERIALS FOR SEPARATION OF PROTEINS AND NUCLEIC ACIDS

Proteins and nucleic acids are polyvalent ionic compounds with high molecular weights and which sometimes show oligomeric association in solution. The ionic dissociation of such molecules enables their separation by ion exchange, the high molecular sizes by size exclusion and the large hydrophobic molecular skeletons by reversed-phase chromatography.

Porous polymer gel packings for HPLC columns can be classified into three groups: wholly inorganic silica, wholly organic synthetic polymer and silica chemically bonded to organic molecules. For high resolution, the gel packing should comprise homogeneous spherical fine particles with extremely small particle diameters, homogeneous pore size and even homogeneous pore depth. Among these properties, it is important that the pore size is relatively large for separation of large biomelecules and loading capacity is as large as possible for the preparation of large amounts of biomolecules, *e.g.*, capacity of a gel packing with a pore size of 300 Å is about 50–100 kilodaltons). The column size, length and internal diameter, is relatively less important for the separation of large biomolecules, contrary to the separation of small molecules such as amino acids and nucleic bases. Gel packing materials for size exclusion chromatography are classified into soft gel, semi-hard gel and hard gel depending upon their mechanical strength. The polystyrene–divinylbenzene copolymer is a semi-hard gel and is useful for high-performance size exclusion chromatography. All TSK gel Type H, Shodex gel A, Shimadzu gel HSG and Hitachi Gelko GL materials are polystyrene gels and are used for non-aqueous gel permeation chromatography of synthetic polymer compounds, the molecular weights of which are $< 10^8$. TSK gel Type PW (polyacrylate), Type Phenyl-PW (polyacrylate phenyl derivative), Shodex OH-pak (glyceryl methacrylate), Asahi-pak Typ GS (polyvinyl alcohol), Shim-pack HSG-W and Hitachi GL-W520 materials are used for aqueous gel filtration chromatography of proteins and nucleic acids, the exclusion limits of which are $< 10^5$. Toyo-Pearl Type HW is an hydrophilic vinyl polymer and is used for the exclusion limit ranges from 10^3 to 10^7, for preparation of biopolymers[48].

It is important that the biological activities of molecules such as enzymes and hormones should not be lost during the separation procedures. The wholly organic synthetic polymer gel might be most effective for the separation of such compounds.

SIZE EXCLUSION GELS FOR PROTEIN AND NUCLEIC ACID SEPARATION

Porous synthetic polymer gels of methacrylate, amide and polyvinyl resin, and porous silica gels, have been used for aqueous gel filtration of proteins and nucleic acids. Pressure-resistant and less adsorptive aqueous polymer gels are presented in Table I[49,50]. The most suitable pore size for the separation of proteins is probably

TABLE I

HARD POLYMER GELS (COMMERCIALLY AVAILABLE IN JAPAN) FOR AQUEOUS SIZE EXCLUSION CHROMATOGRAPHY OF PROTEINS AND NUCLEIC ACIDS

Type	*Gel material*	*Trade-name*	d_p *(μm)*	*Pore size (Å)*	*Exclusion limit*	*Supplier*
Synthetic polymer	Hydrophilic methacrylate	MCI gel CQP10	10	100		Mitsubishi-Kasei
		30	10	300		
	Glyceryl methacrylate	Shodex OH-PakQ 801	10		2×10^3	Showa Denko
		802	10		5×10^3	
		OH-pakB 803	15		1×10^5	
		804	15		5×10^5	
		805	15		5×10^6	
		806	15		10^7	
	Hydrophilic acrylate polymer	TSK gel PW				Toyo Soda
		G-1000	10		10^3	
		2000	10		5×10^3	
		3000	10		5×10^4	
		4000	10		3×10^5	
		5000	10		1×10^6	
		6000	10		10^7	
		TSK gel PW_{XL}				
		G-2500	6			
		3000	6		8×10^5	
		4000	10		4×10^6	
		5000	10		1×10^7	
		6000	13		2×10^8	
		GM-PW_{XL}	13		2×10^8	
		G-Oligo-PW	6			
		G-DNA-PW	10			
	Hydrophilic vinyl polymer	Toyo Pearl EW-35			5×10^3	
		Toyo Pearl HW series (6 grades)			1×10^4 ~ 5×10^7	
	Polyvinyl alcohol	Asahi-pak GS310, 320	9		4×10^4	Asahi Kasei
		GS510, 520	9		3×10^5	
	Hydrophilic porous polymer	Gelko GL-W520			6×10^3	Hitachi
		530			5×10^4	
		550			2×10^6	
		Shim-Pack HSG-30W				Shimadzu
Porous silica	Glycerylpropyl-silica	Shodex Protein WS 802	9	150	2×10^4	Showa Denko
		803	9	300	8×10^5	
	Hydroxy-silica	Shim-pack Diol-150	5	150	2×10^5	Shimadzu
		Diol-300	5	300	1×10^6	
	Hydrophilic silica	MCI GEL CQS10	9–11	90 ~ 110		Mitsubishi-Kasei
		S30	9–11	250 ~ 350		
		TSK gel SW				Toyo Soda
		G-2000	10	130	6×10^4	
		3000	10	240	3×10^5	
		4000	10	450	1×10^6	

100–500 Å and the exclusion limits of the gel packings should be selected according to the nature of the sample mixtures.

Glycerylpropylsilica is slightly adsorptive, leading to deviations from a linear

relationship between retention volumes and logarithms of molecular weights. Such gels have been improved for sufficient recoveries of biological activities of proteins[51].

A successful separation of lipoproteins on TSK gel columns was reported and compared with the results achieved by ultracentrifugation, and the medical significance of the separated lipoproteins was classified in relation to liver disease[52].

The separation of oligonucleotides has been reported[53] using the Asahipak GS320 columns. Oligonucleotides in a mixture of three kinds of deoxyhexamer (dCGTCCA, dTGTCCA and dGGTCCA), and of ribosomal ribonucleic acids (rRNA) in a mixture of 23S (MW 1 100 000), 16S (MW 550 000) and 5S (MW 160 000) rRNA particles were separated on Asahi-pak GS320 and GS520 columns respectively. It has been shown that these gel packings are very useful in the developing fields of genetics and biotechnology.

ION EXCHANGERS FOR PROTEIN AND NUCLEIC ACID SEPARATION

The most useful ion exchanger for separation of proteins and nucleic acids is sulphonated polystyrene, which has been used for analysis of the amino acid constituents of proteins, nucleic bases, nucleosides and nucleotides of nucleic acids. The automatic amino acid analysis carried out on the ion-exchange resin column at Moore's laboratory in 1958 was a significant event in the fields of instrumental liquid chromatography and of protein chemistry. Protein separation had been performed by ion-exchange chromatography since 1954. However, the strongly acidic cation exchanger adsorb proteins and nucleic acids irreversibly owing to the hydrophobicity of their polystyrene structures. Porous glass chemically bonded to aminopropyltrimethoxysilane also adsorbs non-specifically owing to residual silanol groups on its surface. High-performance ion-exchange separations are performed by using ion exchangers coated with a thin epoxy resin layer or with polyamine films. Three kinds of ion exchangers are now available; pellicular coated ion exchanger on inactive carrier; wholly porous silica containing introduced ion-exchangeable groups and synthetic polymer gels containing ion-exchangeable groups. Ion exchangers for rapid and high-performance separations should be mechanically strong enough to withstand a linear velocity of 1 mm/sec, exhibit reversible adsorption for high recoveries, have large exchange capacity for preparative separations (pore diameter 30–100 nm, pore depth 0.5–1.0 ml/g), be stable over wide ranges of pH, be homogeneously spherical in shape with diameter 5–10 μm and, of course, be in expensive even for large preparative columns. The ion exchangers available for separation of proteins, amino acid and nucleic acids are presented in Table II[45,51].

The TSK gel 2SW is suitable for separation of peptides, nucleotides and other relatively small molecules, and also of oligomers. TSK gel 3SW and Shodex gel Ax-pak U424 are used for separation of proteins and enzymes. The polyacrylate or polymethacrylate polymer gels are better for separation of proteins and enzymes rather than the polystyrene–divinylbenzene copolymer gels owing to lower adsorption of proteins. The TSK and Shodex gels comprise fine particles of small diameter, 5–10 μm. However, the macroporous gels with larger particle diameters of 30–70 μm are better for preparative separations of larger biomolecules.

The TSK gel 5PW series have large pore sizes of about 1000 Å and are very efficient in separating proteins and nucleic acids. Beautiful separation patterns of

TABLE II

HARD POLYMER GELS (AVAILABLE IN JAPAN) FOR ION-EXCHANGE CHROMATOGRAPHY OF PROTEINS, AMINO ACIDS AND NUCLEIC ACIDS

Type	*Material trade-name*	*Functional group*	d_p *(μm)*	*Exchange capacity (mequiv./g)*	*Pore size (Å)*	*Supplier*
Wholly porous silica	TSK gel DEAE 2SW	$-N(C_2H_5)_2$	5	>0.3	130	Toyo Soda
	CM 3SW	$-COOH$	10	>0.3	240	
	DEAE 3SW	$-N(C_2H_5)_2$	10	>0.3	240	
	Shodex Axpak U424	Polyamine	10	>0.3	300	Showa Denko
Porous polymer gel	TSK gel SP5PW	$-SO_3-$	10,15	>0.3	1000	Toyo Soda
	DEAE 5PW	$-N(C_2H_5)_2$	10,15	>0.3	1000	
Polystyrene–divinylbenzene	Hitachi resin 2600 series	$-SO_3-(Na^+)$	13–17			
	Shodex CX pak	$-SO_3-(Na^+)$				Showa Denko
	Shim pack ISC-07	$-SO_3-$	7			Shimadzu
	MCI gel CK	$-SO_3-$	5,7			Mitsubishi-Kasei
	Jasco AA pak	$-SO_3$	5			Jasco

mixtures of oligo deoxynucleotides have been obtained on TSK gel DEAE-PW500[53]. The mixtures contained eight kinds of oligodeoxynucleotides from the hexamer to the 26-residue oligomers: dCATGGT, dCTAAATC, dCGGGATTTGA, dCGACCCGGGT, dCATCTTCATGGC, unknown sequential 16-residual oligomer, dCCIAAITCCATCCAICCITAIGC, dCCIAAITCCATCCAICCCATITAITC, where D = deoxy, C = cytidine, A = adenine, G = guanine, I = inosine and T = thymine. Some polystrene–divinylbenzene copolymers in Table II, such as the Hitachi 2600 series, etc., are efficient ion exchangers for analysis of amino acids.

REVERSED-PHASE GELS FOR PROTEIN AND NUCLEIC ACID SEPARATION

Hydrophobic and hydrophilic interactions among chemically bonded reversed-phase packings, aqueous mobile phase solvents with organic modifiers and amphoteric molecules of proteins and nucleic acids are extremely complicated in solution and result in complex separation behaviours on reversed-phase gel columns. Many kinds of reversed-phase packings have been used for efficient separation of nucleic bases, nucleosides and nucleotides (Table III)[50].

Cytochrome *c*, myoglobin, ribonuclease, lysozyme, α-chymotrypsin and α-chymotrypsinogen were separated on the TSK gel Phenyl-5PW[49]. This gel packing is an aqueous polymer chemically bonded to phenyl groups. It is very efficient for protein separation, although the separation mechanism is likely to be more complicated than solvophobic interaction in the reversed phase.

DETECTORS AND SYSTEMS FOR MODERN LIQUID CHROMATOGRAPHY

A new ion-selective electrode detector with an hydrophobic ion-exchange resin

TABLE III

CHEMICALLY BONDED REVERSED-PHASE PACKING MATERIALS AVAILABLE IN JAPAN

Polarity	*Trade-name*		d_p *(μm)*	*Functional group*	*Supplier*
None	Hitachi gel	#3050	10–15	Octadecylsilane	Hitachi
		#3053	4–6		
		#3056	4–6		
		#3063	5		
	Yana pak	ODS-N	5	Octadecylsilane	Yanaco
		ODS-A	7		
		ODS-T	10		
	Yanaco Pel	ODS	30–40		
	Fine-pak	SIL C_{18}	5,10	Octadecylsilane	Jasco
		C_{18}T	10	(capping)	
	ODS pak F	series	5,10	Octadecylsilane	Showa Denko
	Develosil	ODS	3,5,7,10	Octadecylsilane	Nomura Kagaki
			10–20,		
			15–30		
	Cosmosil	$5C_{18}$	5	Octadecylsilane	Nakarai Kagaku
		$5C_{18}$-P	5		
	TSK gel	ODS-120	5,10	Octadecylsilane	Toyo Soda
		120T	5,10	(capping)	
	Fine pak	SIL C_8	10	Octylsilane	Jasco
	Cosmosil	$5C_8$	5	Octylsilane	Nakarai Kagaku
	Develosil	C_8	3,5,7,10	Octylsilane	Nomura Kagaku
			10–20		
			15–30		
	Shim-pack	PC_8	10	Octylsilane	Shimadzu
	Cosmosil	5PH	5	Phenyl	Nakarai Kagaku
	Fine pak	SIL C_2	10	Ethyl	Jasco
	Fine pak	SIL C	10	Dimethylsilane	Jasco
	Yanapak	DMS	5	Dimethylsilane	Yanaco
	Cosmosil	5TMS	5	Trimethylsilane	Nakarai Kagaku
	Shim-pack	TMS	5	Trimethylsilane	Shimadzu
	TSK gel	TMS-250	10	Trimethylsilane	Toyo Soda
Weak	Fine pak	SIL OH	10	Hydroxyl	Jasco
	TSK gel	OH-120	5,10	Hydroxyl	Toyo Soda
Medium	Fine pak	SIL CN	10	Nitrile	Jasco
	Yana pak	CN	10	Nitrile	Yanaco
	Yanaco Pel	CN	35	Nitrile	Yanaco
	Cosmosil	5CN-R		Nitrile	Nakarai Kagaku
	Yanaco Pel	PA		Polyamide	Yanaco
High	Shim-pack	PNH_2	10	Amino	Shimadzu
	Yanaco Pel	NH_2	35	Amino	Yanaco
	Yana pak	NH_2	10	Amino	
	Shodex	NH pak		Amino	Showa Denko
	Fine-pak	SIL NH_2	10	Aminopropyl	Jasco
	TSK gel	NH_2-60	5,10	Aminopropyl	Toyo Soda
	Bile pak		10		Jasco
	Catechol pak		5		Jasco

membrane has been reported[38]. Hydrophobic anion-exchange resin membranes based on homogeneous cross-linked polystyrene membrane were used. The membranes showed good selectivity and high sensitivity for HPLC. A highly sensitive twin-electrode voltammetry detector for HPLC was developed by Kurahashi and co-workers[54], and a dual electrochemical detector for micro-HPLC by Goto *et al.*[55]. The latter had two working electrodes (anode and cathode) and was employed for the selective detection of catecholamine. A rapid determination could be performed by means of cyclic semi-differential voltammetry. The detector was utilized for the selective determination of catecholamine in human urine. Miniaturization of a electrical conductivity detector for a new micro-packed column ion chromatograph with a hollow-fibre suppressor has been achieved using a new micro-scale detection cell[35]. Other types of detectors are a streaming current detector and a spray detector for detection of nanogram amounts of carboxylic acids[56]. The spray detector showed almost equally high sensitivities for the detection of underivatized free and conjugated bile acids and their sulphates. The detection limit was about 100 μg, and a linear response was obtained for the injected amounts in the range 0.1–10 μg.

A time-resolved laser fluorescence detector was developed for highly sensitive detection in micro-HPLC by Imasaka *et al.*[57]. A sub-nanosecond tunable dye-laser pumped by a transversely excited atmospheric pressure nitrogen-laser was combined with the time-resolved detection system, which consisted of a microchannel plate photomultiplier, a sampling oscilloscope and a microcomputer for data processing. This system had a time resolution of 1.4 nsec, and was used for determination of trace amounts of polynuclear aromatic hydrocarbons.

Various detection systems have been employed with HPLC for qualitative and quantitative measurements of separated compounds. A HPLC–ESR (electron spin resonance) system was described above[27]. This instrument is very useful for free-radical chemistry, and many kinds of new radicals produced upon γ-irradiation of amino acids, peptides, nucleic bases, nucleosides and nucleotides in aqueous solution were discovered and characterized by Hatano and co-workers[58–61]. An extremely highly-sensitive infra-red spectrometer for HPLC was reported by Mori *et al.*[62]. The sensitivity of the detection system was at least 40 times greater than that of conventional instruments, for acrylonitrile–styrene and styrene–methyl methacrylate copolymers. Inductively coupled argon-plasma-emission spectrometric detection for HPLC was developed by Morita *et al.*[63], and inductively coupled plasma-atomic-emission spectrometric detection for micro-HPLC by Jinno and Tsuchida[39]. A Raman spectroscopic detector for HPLC was reported by Koizumi *et al.*[64] and by Iriyama *et al.*[65]. A capillary flow cell and argon-ion laser were used for the Raman spectroscopic detection of 2,4-dinitrophenylhydrazone derivatives of aliphatic aldehydes. The detection limit was about 100 ng for formaldehyde derivatives. A cold vapour atomic absorption spectrometer was used with success for HPLC determination of mercuric compounds by Fujita and Takabatake[66]. Recent excellent work on LC spectrometry was performed with the buffer-memory[67,68]. A vacuum nebulizing interface for HPLC–mass spectrometry was used successfully by Tsuge[69].

These developments in column packing materials and detection techniques have made significant contributions to separation procedures and to their applications in various fields of chemical and biological sciences.

REFERENCES

1 S. Egashira, *Japan Analyst*, 10 (1961) 693*.
2 H. Hatano, *Hitachi Sci. Instr. News*, 5 (1962) 141*.
3 H. Hatano, *Automatic Amino Acid Analysis*, Kagaku-dojin Co., Kyoto, 1959*.
4 H. Hatano, S. Egashira, K. Ozawa and S. Ganno, *Hitachi Hyoron*, 44 (1962) 2068*.
5 H. Hatano (Editor), *Liquid Chromatography*, Vol. 1, Nankodo Co., Tokyo, 1964*.
6 H. Hatano (Editor), *Liquid Chromatography*, Vol. 2, Nankodo Co., Tokyo, 1965*.
7 H. Hatano (Editor), *New Liquid Chromatography*, Nankodo Co., Tokyo, 1969*.
8 H. Hatano (Editor), *High Speed Liquid Chromatography*, Nankodo Co., Tokyo, 1973*.
9 H. Hatano (Editor), *Applied Liquid Chromatography*, Nankodo Co., Tokyo, 1976*.
10 H. Hatano (Editor), *New High Speed Liquid Chromatography*,Nankodo Co., Tokyo, 1977*.
11 H. Hatano (Editor), *High Resolution Chromatography*, Nankodo Co., Tokyo, 1983*.
12 H. Hatano (Editor), *Data Books of High Performance Liquid Chromatography*, Vols. 1–25, International Publishing and Consulting Co., Tokyo, 1978–1983*.
13 G. Muto and Y. Takata, *Anal. Chem.*, 45 (1973) 1864.
14 H. Hatano, Y. Yamamoto, M. Saito, E. Mochida and S. Watanabe, *J. Chromatogr.*, 83 (1973) 373.
15 H. Hatano, *Res./Dev.*, 24 (4) (1973) 28.
16 H. Hatano, *Res./Dev.*, 26 (5) (1975) 46.
17 A. P. Graffeo and N. H. C. Coode, *J. Chromatogr. Sci.*, 17 (1979) 202.
18 M. Novotny and D. Ishii (Editors), *Microcolumn Separation Methods*, Elsevier, Amsterdam, 1985.
19 A. Zlatkis (Editor), *Advances in Chromatography*, University of Houston, Houston, 1982.
20 E. Heftmann (Editor), *International Symposium on High-Performance Liquid Chromatography, Kyoto, 1985, J. Chromatogr.*, Vol. 332 (1985).
21 H. Hatano, M. Hori, S. Rokushida and F. Murakami, *Liquid Chromatography and Application*, Kodansha, Tokyo, 1974*.
22 H. Hatano and T. Hanai, *Experimental High Performance Liquid Chromatography*, Kagaku-dojin, Kyoto, 1977*.
23 S. Egashira, *Liquid Chromatography*, Sankyo Publ. Co., Tokyo, 1977*.
24 T. Hashimoto (Editor), *Packing Material (Stationary Phase)*, Musashino Book Co., Tokyo, 1978*.
25 S. Hara and A. Tsuji (Editors), *Modern Liquid Chromatography*, Nanzando, Tokyo, 1978*.
26 T. Yamabe (Editor), *Introduction to High Performance Liquid Chromatography*, Saiwai Book Co., Tokyo, 1978*.
27 S. Rokushika, H. Taniguchi and H. Hatano, *Anal. Lett.*, 8 (1975) 205.
28 H. Hatano, in A. J. C. Nicholson (Editor), *Detectors and Chromatography*, Australian Science and Industry Association, Melbourne, 1983.
29 Y. Hanaoka, T. Murayama, S. Muramoto, T. Matsuura and A. Nanba, *J. Chromatogr.*, 239 (1982) 537.
30 D. Ishii, K. Asai, K. Hibi, T. Jonokuchi and M. Nagaya, *J. Chromatogr.*, 144 (1977) 157.
31 D. Ishii, K. Hibi, K. Asai and M. Nagaya, *J. Chromatogr.*, 151 (1978) 341.
32 D. Ishii, A. Hirose, K. Hibi and Y. Iwasaki, *J. Chromatogr.*, 157 (1978) 43.
33 M. Goto, E. Sakurai and D. Ishii, *J. Chromatogr.*, 238 (1982) 357.
34 T. Tsuda and M. Novotny, *Anal. Chem.*, 50 (1978) 271.
35 S. Rokushika, Z. Y. Qui and H. Hatano, *J. Chromatogr.*, 260 (1983) 81.
36 T. Takeuchi, Y. Hirata and Y. Okuyama, *Anal. Chem.*, 50 (1978) 659.
37 S. Tsuge, Y. Hirata and T. Takeuchi, *Anal. Chem.*, 51 (1979) 166.
38 T. Imato, A. Jyo and N. Ishibashi, *Anal. Chem.*, 52 (1980) 1893.
39 K. Jinno and H. Tsuchida, *Anal. Lett.*, 15 (1982) 427.
40 T. Yamabe and S. Takai, *Seisan Kenkyu*, 22 (1970) 485*.
41 T. Yamabe and S. Takai, *Hitachi Sci. Instr. News*, 15 (1972) 10*.
42 S. Takai and T. Yamabe, *Bunseki Kiki*, 10 (1972) 153*.
43 T. Yamabe, N. Takai and H. Nakamura, *J. Chromatogr.*, 104 (1975) 359.
44 S. Rokushika, T. Ohkawa and H. Hatano, *J. Chromatogr.*, 176 (1979) 456.
45 H. Hatano, in F. Bruner (Editor), *The Science of Chromatography (J. Chrom. Library, Vol. 32)*, Elsevier, Amsterdam, Oxford, New York, Tokyo, 1985, pp. 165–178.

* In Japanese.

46 H. Hatano, *Bunseki*, 10 (1984) 721*.
47 Y. Kato and T. Hashimoto, *Bunseki*, 10 (1984) 725*.
48 H. Hatano (Editor), *Report of the Physical and Chemical Property Data, Liquid Chromatography Data*, Vol. 5, Promotion Bureau, Science & Technology Agency, 1984*.
49 K. Makino and H. Hatano, in P. L. Dubin (Editor), *Size Exclusion Chromatography*, Elsevier, Amsterdam, 1985, in press.
50 H. Hatano, H. Wada, K. Makino, T. Takeuchi, K. Noguchi and Y. Yanagihara, *Abstracts of 9th International Symposium on Column Liquid Chromatography, Edinburgh, 1985*, p. 163.
51 F. Yamamoto and H. Hatano, *Protein, Nucleic Acid, Enzyme* (Tanpakushitsu, Kakusan, Kohso), Kyoritsu Publ. Co., Tokyo, 1985, in press*.
52 M. Ozaki, H. Itakura, K. Shinaishi and I. Hara, *Clin. Chem.*, 29 (1983) 768.
53 K. Makino, H. Wada, H. Ozaki, T. Takeuchi and H. Hatano, *Proceedings of 9th International Symposium on Column Liquid Chromatography, Edinburgh, 1985*, p. 297.
54 O. Hiroshima, S. Ikenoya, T. Naito, K. Kusube, M. Omae, K. Kawabe, S. Ishikawa, H. Hoshida and T. Kurahashi, *Chem. Pharm. Bull.*, 31 (1983) 3571.
55 M. Goto, E. Sakurai and D. Ishii, *J. Chromatogr.*, 238 (1982) 357.
56 S. Terabe, K. Yamamoto and T. Ando, *J. Chromatogr.*, 239 (1982) 515.
57 T. Imasaka, K. Ishibashi and N. Ishibashi, *Anal. Chim. Acta*, 142 (1982) 1.
58 F. Moriya, K. Makino, N. Suzuki, S. Rokushika and H. Hatano, *J. Phys. Chem.*, 84 (1980) 3085.
59 F. Moriya, K. Makino, N. Suzuki, S. Rokushika and H. Hatano, *J. Phys. Chem.*, 84 (1980) 3614.
60 S. Kominami, S. Rokushika and H. Hatano, *Int. J. Radiat. Res.*, 30 (1976) 525.
61 S. Kominami, S. Rokushika and H. Hatano, *Radiat. Res.*, 72 (1977) 89.
62 S. Mori, A. Wada, F. Kaneuchi, A. Ikeda, M. Watanabe and K. Mochizuki, *J. Chromatogr.*, 246 (1982) 215.
63 M. Morita, T. Uehiro and K. Fuwa, *Anal. Chem.*, 52 (1980) 351.
64 H. Koizumi, H. Kojima and Y. Suzuki, *Japan Analyst*, 30 (1981) 99.
65 K. Iriyama, Y. Ozaki, K. Hibi and T. Ikeda, *J. Chromatogr.*, 254 (1983) 285.
66 M. Fujita and E. Takabatake, *Anal. Chem.*, 55 (1983) 454.
67 K. Jinno, C. Fujimoto and D. Ishii, *J. Chromatogr.*, 239 (1982) 625.
68 C. Fujimoto, K. Jinno and Y. Hirata, *J. Chromatogr.*, 258 (1983) 81.
69 S. Tsuge, *Fresenius' Z. Anal. Chem.*, 311 (1982) 674.

Journal of Chromatography, 332 (1985) 237–242
Elsevier Science Publishers B.V., Amsterdam — Printed in The Netherlands

CHROMSYMP. 626

USE OF TOYOPEARL AS A SUPPORT FOR THE IMMOBILIZATION OF UREASE

ICHIRO SASAKI, KEISUKE MAKINO* and TAMIO TAKEUCHI
Department of Polymer Science and Engineering, Faculty of Textile Science, Kyoto Institute of Technology, Matsugasaki, Sakyo-ku, Kyoto 606 (Japan)
and
HIROO SASAKI
Central Research Laboratory, Toyo Soda Manufacturing Co., Tonda, Shinnanyo, Yamaguchi 746 (Japan)
(First received March 29th, 1985; revised manuscript received May 13th, 1985)

SUMMARY

A packing material for size-exclusion chromatography, Toyopearl, which was derivatized by introducing amino groups, was found to be a good support for the immobilization of urease. The immobilized enzyme had an optimum pH of 7, the same value as for intact urease. In the use of the enzyme, packed in PTFE tubing (*ca.* 8 cm × 0.7 mm I.D.) in a flow system, the addition of ethylenediaminetetraacetic acid (EDTA) to the eluent was found to be essential. With phosphate buffers containing EDTA, a constant high value of the enzyme activity could be obtained for 21 days at 37°C.

INTRODUCTION

By the application of enzymatic reactions to clinical analysis[1,2], the diagnosis of various diseases has become more accurate and faster. The recent introduction of immobilized enzymes[3–6] has furthered this trend and possible the reuse of expensive enzymes. This unique and powerful method will be needed to overcome the current problem that the number of clinical samples to be examined is increasing more rapidly than that the number of clinical chemists.

Another useful tool recently introduced into clinical medicine is high-performance liquid chromatography (HPLC)[7,8]. These two methods are often combined to produce a more effective method for complex biological samples[9]. In this case, the samples are separated by HPLC and the targeted molecules, which have been isolated from biological contaminants, are subsequently converted into easily detectable compounds by an immobilized enzyme, packed into a column. However, the substrate remaining on the immobilized enzyme column after the measurements can often inhibit the enzyme activity. For example, when controlled-pore glass is used as a support, damage to the enzyme can be caused by substrates remaining on the column through the interaction with free silanols on the support. Also agarose, which is

0021-9673/85/$03.30

preferred as a support for this purpose and is known to be less prone to interaction with components in biological samples, is so soft that the system can hardly be used at a practical, high flow-rate.

In this study, we have examined the applicability of Toyopearl, which has been used as a semirigid gel in size-exclusion chromatography[10,11] and is known to be less adsorptive for components in the samples, as a base matrix for the immobilization of the enzyme. Toyopearl has also been used as a support in affinity columns[12] and has shown excellent properties for biological samples. The enzyme bound to the support in the present investigation was urease (urea amidohydrolase, E.C. 3.5.1.5), and the immobilized enzyme was used for the detection of urea in a flow system.

EXPERIMENTAL

Urease was purchased from E. Merck (Darmstadt, F.R.G.). Toyopearl HW-55S was obtained from Toyo Soda (Tokyo, Japan). The amino derivatization of the gel was performed according to the method reported previously[12]. All other chemicals were purchased from Nakarai Chemicals (Kyoto, Japan) and used without further purification.

Water was purified by a Milli R/Q water purifier (Millipore, Bedford, MA, U.S.A.). The concentration and pH of the phosphate buffer were 50 m*M* and 7, respectively, unless otherwise specified.

An aqueous solution of urease was prepared by dissolving 0.2 g of urease in 5 ml of phosphate buffer and allowing it to stand for 2 h at 5°C. Precipitates were removed by centrifugation at 7880 *g* for 30 min at 4°C. The samples were obtained as supernatants.

The immobilization of urease on the gels was carried out according to the method reported previously for urease bound to alkylaminosilane glass beads[1]. The gel (1 g), which was washed with water, was activated with 25 ml of an aqueous glutaraldehyde solution (2.5%). The suspension was degassed *in vacuo* for 30 min at room temperature and then allowed to stand for 1 h under atmospheric conditions. After the reaction, this activated gel was washed with water. The prepared urease solution (15 ml) was added to the activated gel, followed by degassing for 30 min at room temperature. The immobilization was carried out by shaking the sample under atmospheric conditions for 24 h at 5°C. After the coupling reaction, the suspension was washed with phosphate buffer and then dried *in vacuo* for 1 h at room temperature. The immobilized urease was stored dry in a refrigerator at 5°C.

For the determination of the activity of the immobilized urease in the batch system, the amount of ammonium ion released by the enzyme was determined by the urease indophenol method, in which urea was used as a substrate. Two reagents were used: solution A containing 12.5 g of phenol and 62.5 mg of sodium nitroprusside per l; solution B containing 1.56 g of sodium hydroxide and 4 ml of 10% sodium hypochlorite solution per l. The determination was carried out as follows. A test sample (5 ml) of substrate was prepared by dissolving 1 g of urea in phosphate buffer. The solution was preincubated for 15 min at 37°C. Subsequently, 20 mg of immobilized urease gel were added. The suspension was incubated for 2 min at 37°C in a shaking incubator. After incubation, the suspension was filtered immediately through a Millex-HA filter (Millipore). To the filtrate (10 μl), 2 ml of solution A and

then 2.5 ml of solution B were added. This mixture was kept for 50 min at 50°C in a shaking incubator. After incubation, the absorbance at 560 nm was measured. A calibration curve used for the calculation of the activity was obtained by use of different concentrations of ammonium chloride and by plotting the concentrations against the observed absorbance.

The column of immobilized urease was prepared as follows. Pre-swollen, immobilized urease gel (200 mg) was suspended in 1.5 ml of phosphate buffer. This slurry was packed in PTFE tubing (50 cm × 0.7 mm I.D.). One end of this column was connected to a pump, Model 5SK25GK-A (Milton Roy Co., Philadelphia, PA, U.S.A.), the other end was plugged with glass wool to retain the gel, and then a stainless-steel tube was attached. Pumping was continued until the gel had settled completely. The column of immobilized urease thus prepared was installed in a flow system in which the column was placed immediately after the sample injector and the column outlet was connected directly to the fraction collector. The determination of the concentration of ammonium ion in the column effluent was performed as follows. A quantity (1 ml) of the effluent was collected immediately after the injection of the sample and then 2.0 ml of solution A and 2.5 ml of solution B were added to the effluent. After the same treatment as that used for the batch system, the absorbance was measured.

RESULTS AND DISCUSSION

First, the effect of the functional groups at the gel surface on the resulting activity of the immobilized urease (IU) was examined. Under the conditions given in the Experimental section, urease was immobilized, by use of glutaraldehyde on two different types of Toyopearl gel: HW-55S, which has hydroxyl groups, and its amino derivative. The resulting activities (U/g IU) were 1.84 and 1520 for Toyopearl HW-55S and its amino derivative, respectively. One unit (U) of enzyme hydrolyzes 1 μmol of urea per minute at 37°C under the conditions described in the Experimental section. The higher activity obtained with the amino derivative suggests that the introduction of amino groups into the gel is essential for immobilization in which glutaraldehyde is used as a spacer. Therefore, the amino derivative of Toyopearl was used as a support for the immobilization in further studies.

The effect of the concentration of the urease solution was then explored. Different concentrations of urease solution were used for the immobilization on 1 g of gel, activated prior to use with glutaraldehyde, and the activity of the immobilized enzyme was determined. The maximum activity was achieved when 15 ml of urease solution (40 g/l) were used with 1 g of gel. A further increase in the amount of enzyme did not lead to an increase in the activity. Although the use of higher concentrations of urease may shorten the reaction time between urease and the gel, activated with glutaraldehyde, our attempts did not lead to better results because of extensive precipitation of urease. Since this precipitation blocks the column, a 40 g/l urease solution was selected for immobilization in the present study.

The effect of the reaction time for the immobilization of urease on the activity of the IU obtained was also explored in order to optimize the immobilizing conditions. A 15-ml volume of urease solution (40 g/l) was used for immobilization on 1 g activated gel, and the activity of the IU thus prepared was determined for each

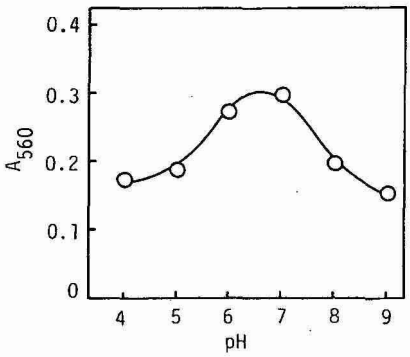

Fig. 1. Relationship between the activity of immobilized urease and pH of the urea solution. The activity is expressed in terms of the absorbance of stained solutions at 560 nm. Conditions: immobilized urease, 20 mg; urea, 1 g; concentration of urea in sample, 200 g/l; temperature, 37°C; reaction time, 2 min.

different reaction time. The maximum activity of IU was obtained with a reaction time of 12 h; longer reaction times did not result in an increased activity of IU. For this study, a reaction time of 24 h was selected. Consequently, in the present work, all reactions were carried out under the following conditions: activated gel, 1 g; volume of urease solution (40 g/l), 15 ml; reaction time between urease and the activated gel, 24 h; temperature, 5°C.

The optimum pH for the enzymatic activity of IU was determined as follows. After enzymatic reaction at different pH values the activity was determined spectroscopically. The change in activity obtained with the pH is depicted in Fig. 1. From the results, the optimum pH for the IU was found to be *ca.* 7. It has been reported that the optimum pH for the enzymatic reaction of intact urease in solution lies between 6.4 and 7.6[13]. Thus, the optimum pH is unchanged by immobilization. This may suggest that slight changes in the enzyme environment, caused by the remaining unreacted amino groups on IU, do not affect the activity.

In practical applications of IU in clinical medicine the enzyme may be stored in slurry form for certain periods before use. Therefore, the change in activity during wet storage was investigated. IU was stored at 5°C in phosphate buffer for 30 days,

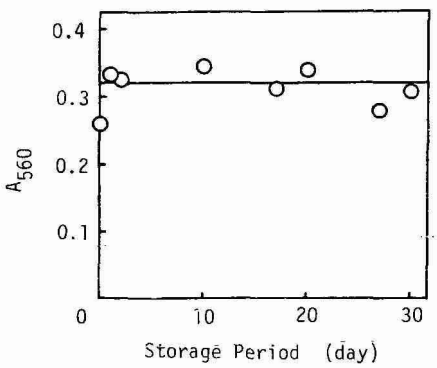

Fig. 2. Relationship between the storage period of wet immobilized urease and its activity. Details as in Fig. 1.

and the residual activity of an aliquot of IU (*ca.* 20 mg) was determined at intervals during that period by the method given in the Experimental section. A new aliquot was used for each measurement. The change in activity is shown in Fig. 2. This result demonstrates that the activity of IU did not decrease in cold phosphate buffer over this period and that the urease immobilized on Toyopearl can be used in clinical practice.

For continuous detection of urea, IU was packed in a column (*ca.* 80 × 0.7 mm) of PTFE tubing and was installed in the flow system. A calibration curve was constructed by introducing samples containing various concentrations of urea into the system and measuring the amount of ammonium ion released in the effluent. The samples volume was 25 μl. The flow-rate of the phosphate buffer, containing ethylenediaminetetraacetic acid (EDTA, 0.2 g/l), used as a carrier, was 0.5 ml/min. The temperature was controlled with a column oven at 37°C. Fractions (1 ml) were collected immediately after the injection and subsequently determined for released ammonium ion. The results in Fig. 3 show a good linear relationship between the concentration of urea (up to *ca.* 0.6 g/l) in the samples and absorbance of the effluent. The highest concentration of urea in normal human sera is *ca.* 0.4 g/l. Therefore, urease immobilized on Toyopearl with glutaraldehyde can be used for the detection of urea in normal human sera in either a flow-injection system or in a post-column detection system for HPLC, because the detection limit of the IU column can be increased by using a longer column.

Since a great number of samples is often analyzed in clinical laboratories, high

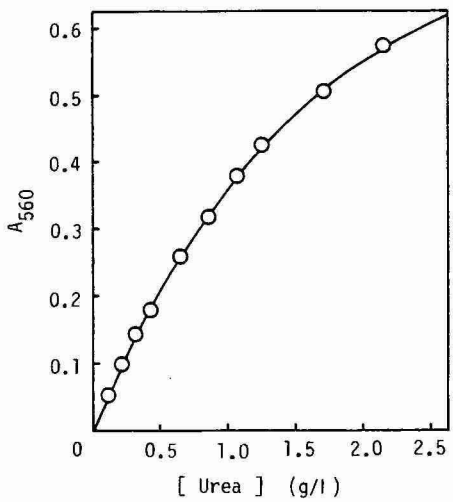

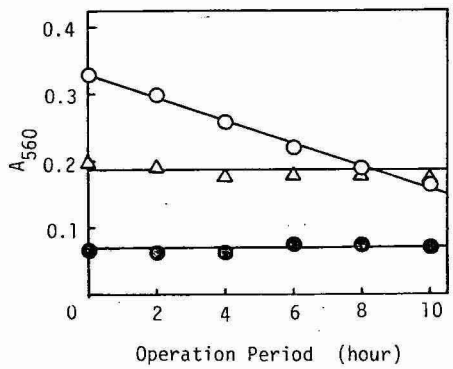

Fig. 3. Relationship between the concentration of urea in the sample loaded on the immobilized urease column and the absorbance at 560 nm of the stained effluents. Conditions: volume injected, 25 μl; column, *ca.* 80 × 0.7 mm; flow-rate, 0.5 ml/min; temperature, 37°C; carrier, phosphate buffer containing EDTA (0.2 g/l); fraction, 1.0 ml. Fractions were stained by reaction with solutions A and B and the absorbance monitored at 560 nm.

Fig. 4. Change in the activity of the immobilized urease column during continuous use for 10 h. Conditions: column, *ca.* 80 × 0.7 mm; concentration of urea in the sample, 0.4 g/l; volume injected, 25 μl; carrier and temperature, phosphate buffer at 37°C (○), phosphate buffer containing EDTA (0.2 g/l) at 25°C (●) and at 37°C (△). Other conditions as in Fig. 3.

stability of the enzyme is required in order to obtain reliable data. Therefore, the operational stability of the IU column (*ca.* 80 × 0.7 mm) was examined over 10 h by assaying samples every 2 h. The IU column was installed in the flow system, 25 μl of a solution containing 0.4 g/l urea were injected and the released ammonium ion was measured. The results are shown in Fig. 4. When phosphate buffer alone was used as a carrier at 37°C the activity of the IU column was found to decrease gradually to almost half of its original value after 10 h. However, the activity of this column could be restored several times, although not completely, by injecting phosphate buffer containing EDTA. Therefore, an EDTA-treated column was subsequently used for the assay with phosphate buffer, containing EDTA, at 37 and 25°C. When phosphate buffer containing 0.2 g/l EDTA was used as a carrier, the activity of the IU column was found to be unchanged after 10 h at 37 and 25°C, as shown in Fig. 4. These results suggest that the decrease in the activity of the IU column with phosphate buffer alone was caused by inhibition due to small amounts of metal in the solution, and that this undesirable contaminant can be removed by adding EDTA to the solution. By comparing the results at 37 and 25°C, it was found that at 37°C a higher sensitivity of detection was obtained, and that more reliable data could be obtained by use of a longer column, with EDTA in the carrier, at this temperature.

Another important factor for a practical column reactor is the reproducibility of over a long period. The column was installed in the flow system, and an assay carried out every day. Between assays, the column was stored with a carrier in a refrigerator at 5°C. The column (*ca.* 80 × 0.7 mm) was used with phosphate buffer containing EDTA (0.2 g/l), 25 μl of urea solution (0.4 g/l) were injected at 37 and 25°C and the amount of ammonium ion released was detected. At both temperatures the activity of each IU column was found to be constant for 25 and 21 days, respectively. During these periods, 62 injections were performed at each temperature.

In conclusion, Toyopearl was found to be highly useful as a support for the immobilization of urease. The immobilized enzyme column could be used in a flow-injection system or as a post-column reactor for HPLC and, therefore, could facilitate speedy and accurate analyses.

REFERENCES

1 T. Murachi, *Rinsho Kensa Rinzi Zokan* (in Japanese), Igaku Shoin, Tokyo, 1978.
2 H. U. Bergmeyer, *Methods of Enzymatic Analysis*, Academic Press, New York, 2nd ed., 1974.
3 H. H. Weetall and L. S. Hersh, *Biochim. Biophys. Acta*, 185 (1969) 464.
4 M. Tabata, J. Endo and T. Murachi, *J. Appl. Biochem.*, 3 (1981) 84.
5 J. Endo, M. Tabata and T. Murachi, *Clin. Chim. Acta*, 95 (1979) 411.
6 G. Johansson and L. Ögren, *Anal. Chim. Acta*, 84 (1976) 23.
7 M. Okazaki, K. Shiraishi, Y. Ohno and I. Hara, *J. Chromatogr.*, 223 (1981) 285.
8 M. Okazaki, N. Hagiwara and I. Hara, *J. Chromatogr.*, 231 (1982) 13.
9 S. Okuyama, N. Kokubun, S. Higashidate, D. Uemura and Y. Hirata, *Chem. Lett.*, (1979) 1443.
10 Y. Kato, K. Komiya and T. Hashimoto, *J. Chromatogr.*, 247 (1982) 184.
11 T. Irimura, M. Nakajima, N. D. Ferrante and G. L. Nicolson, *Anal. Biochem.*, 130 (1983) 461.
12 I. Matsumoto, Y. Ito and N. Seno, *J. Chromatogr.*, 239 (1982) 747.
13 J. E. Varner, in P. D. Boyer, H. Lardy and K. Myrbäch (Editors), *The Enzymes*, Vol. 2, Academic Press, New York, 1960, p. 247.

Journal of Chromatography, 322 (1985) 243–253
Elsevier Science Publishers B.V., Amsterdam — Printed in The Netherlands

CHROMSYMP. 631

BEHAVIOUR OF SINGLE-STRANDED OLIGODEOXYRIBONUCLEOTIDES ON A DEAE-5PW ANION-EXCHANGE COLUMN

HIROAKI OZAKI, HIROO WADA, TAMIO TAKEUCHI and KEISUKE MAKINO*
Department of Polymer Science and Engineering, Faculty of Textile Science, Kyoto Institute of Technology, Matsugasaki, Sakyo-ku, Kyoto 606 (Japan)
TOSHIKAZU FUKUI*
Faculty of Pharmaceutical Sciences, Osaka University, Yamadaoka, Suita, Osaka 565 (Japan)
and
YOSHIO KATO
Central Research Laboratory, Toyo Soda Manufacturing Co., Tonda, Shinnanyo, Yamaguchi 746 (Japan)
(First received March 29th, 1985; revised manuscript received May 15th, 1985)

SUMMARY

The separation of large, single-stranded oligodeoxyribonucleotides, prepared by chemical synthesis, was carried out on a DEAE-5PW anion-exchange column with eluents containing only volatile salts. It was found that gradient elution is essential and that a high resolution can be achieved at elevated temperatures (*ca.* 50°C). Also, neutral pH of the eluents was found to be desirable for the separation. Under optimum conditions, a linear relationship between the elution volumes and the number of bases in the substrates was observed.

INTRODUCTION

Because of the recent rapid development of gene manipulation, the preparation of various DNA fragments carrying genetic information has become extremely important in biochemistry. Such DNA fragments, oligodeoxyribonucleotides, are commonly obtained by chemical synthesis[1–3], enzymic digestion of DNA[4] and reverse transcription from mRNA[5]. Traditionally, the purification and identification of such oligodeoxyribonucleotides have been carried out by open-column chromatography[6,7], gel electrophoresis[8] or thin-layer chromatography[9,10]. However, there has not been a satisfactory method for purification when the samples to be purified are single-stranded oligodeoxyribonucleotides, synthesized chemically. Contamination of a sample having a finely designed base sequence with impurities that have sequences similar to or almost identical with that of the sample often prevents complete ligation

* Present address: Research Laboratory, Dainippon Pharmaceutical Company, Enoki 33-94, Suita, Osaka 564, Japan.

0021-9673/85/$03.30

of the sample from building up a targeted large DNA. Also, by use of a DNA sample containing undesirable DNAs, proper *E. coli* transformation is made less efficient.

High-performance liquid chromatography (HPLC), by means of which a number of biologically important materials have been isolated, has not been effectively utilized in this field. In particular, there have been few applications of HPLC to larger, single-stranded DNA fragments[11,12]. Even then, satisfactory practical procedures were not reported. The samples studied were very simple, the column material was toxic to cells and the salts used in the mobile phases were all difficult to remove from the fractions after the separation.

In this study, we investigated the separation of large single-stranded oligodeoxyribonucleotides by anion-exchange chromatography with a newly developed DEAE-5PW column. The eluent used was a solution containing only salts that can be removed from the fractions by lyophilization.

EXPERIMENTAL

The oligodeoxyribonucleotides used were synthesized chemically by the liquid-phase triester method described previously[2,13,14]. The sequences of the samples are listed in Table I. Ammonium acetate and ammonium formate of analytical-reagent grade were purchased from Nakarai Chemicals (Kyoto, Japan). Water was purified by a Milli R/Q water purifier (Millipore, Bedford, MA, U.S.A.).

TABLE I

BASE SEQUENCES OF THE OLIGODEOXYRIBONUCLEOTIDES USED AND THEIR ABBREVIATIONS

Substrate	*No. of bases*	*Abbreviation*
dCATGGT	6	6b
dTCAAATC	7	7b
dCGGATTTGA	9	9b
dCGACCCGGGT	10	10b
dCATCTTCATGGC	12	12b
–	16	16b
dCCIAAITCCATCCAICCITAIGC	23	23b
dCCIAAITCCATCCAICCCATITAITC	26	26b

The high-performance liquid chromatograph was a Model HLC-803D (Toyo Soda, Tokyo, Japan), equipped with a GE-4 gradient system (Toyo Soda) and a thermostatically controlled column oven. The column effluents were monitored at 260 nm with a UV-8 Model II variable-wavelength UV detector (Toyo Soda). A commercially available anion-exchange column (7.5 cm × 7.5 mm I.D.) of DEAE-5PW (Toyo Soda) was utilized.

Eluents were degassed immediately prior to use by a combination of sonication and evacuation. The injection volume of the samples was 20 μl. The concentration of the samples was made as low as possible and therefore the highest sensitivity of the detector was used.

RESULTS AND DISCUSSION

As a preliminary study, separation was carried out under isocratic conditions. The solutes used were 7b, 10b, 16b and 26b (Table I). The ammonium acetate concentrations in the eluent were 1 and 0.9 *M*. This slight difference in concentration produced great differences in the elution volumes of the solutes, as shown in Fig. 1. The elution volume of 26b, which was eluted most slowly in the chromatogram shown in Fig. 1A, was 7.6 ml when the salt concentration was 1 *M* and 23.4 ml at 0.9 *M* (see Fig. 1B). On the other hand, 7b appeared at almost the same elution position at both salt concentrations. From these results, gradient elution was found to be essential for improved separation.

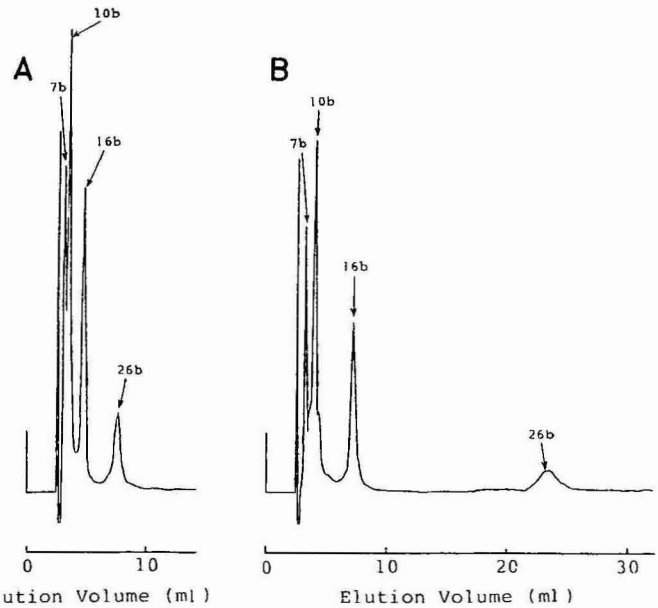

Fig. 1. Isocratic elution profile of single-stranded oligodeoxyribonucleotides. Conditions: column, DEAE-5PW; eluent, aqueous solution of ammonium acetate; concentration of eluent, (A) 1 *M* and (B) 0.9 *M*; flow-rate, 1 ml/min; temperature, 50°C.

The effect of differences in the salt on retention behaviour was also investigated. Fig. 2 shows a typical separation of a sample containing several types of single-stranded oligodeoxyribonucleotides, obtained by gradient elution with linearly increasing ammonium acetate concentrations. All of the solutes could be separated satisfactorily. In addition, it was found that the elution volumes of the solutes increased with an increase in the number of bases. These results indicate that by controlling the ammonium acetate gradient system, optimization of the separation of oligodeoxyribonucleotides can be achieved. The small humps on the baseline are probably due to the high sensitivity of the detector.

Another volatile salt, ammonium formate, which is frequently used in bio-

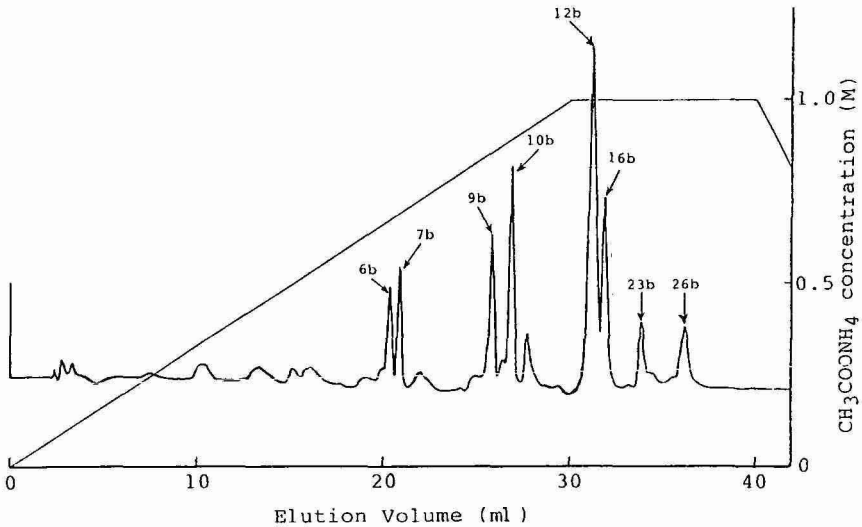

Fig. 2. Separation of single-stranded oligodeoxyribonucleotides. Eluent, linear gradient from 0.01 to 1 *M* ammonium acetate in 30 min and then isocratic elution (1 *M*) used after 30 min. Other conditions as in Fig. 1.

chemistry, was also used. When the same sample was chromatographed with that solvent, an elution profile similar to that shown in Fig. 2 was observed, as depicted in Fig. 3. This salt may possibly also be effective for the separation of these samples, but in this study all of the subsequent experiments were carried out with the use of ammonium acetate.

The effects of flow-rate on the retention behaviour of the solutes were examined, and the results are summarized in Table II. The gradient system used for the measurements was varied according to the flow-rates, as shown in the table. Changes in flow-rate made little difference to the retention positions and elution profile. Therefore, a flow-rate of 1 ml/min. which shortens the analysis time, was used.

The changes in the retention behaviour of the samples at different temperatures were studied. The relationship between the number of bases in the samples and their elution volumes observed at different temperatures is depicted in Fig. 4. The elution volumes were obtained by use of a linear gradient system (see Fig. 4). Good separation of oligodeoxyribonucleotides containing up to twelve bases was obtained at 35°C. At elevated temperatures, improvements in the separation could be achieved. In particular, the resolution of substrates with more than sixteen bases was improved. However, the slope of the curves for the samples with more than sixteen bases was still shallow under the applied linear gradient conditions. Therefore, in order to increase the retention of the larger oligodeoxyribonucleotides, isocratic elution was used after the application of a gradient with the same slope for 30 min. The results are shown in Fig. 5, where it is demonstrated that at higher temperatures a better resolution could be obtained under these conditions. This implies that the separation of single-stranded DNA fragments is strongly dependent on both temperature and the gradient system.

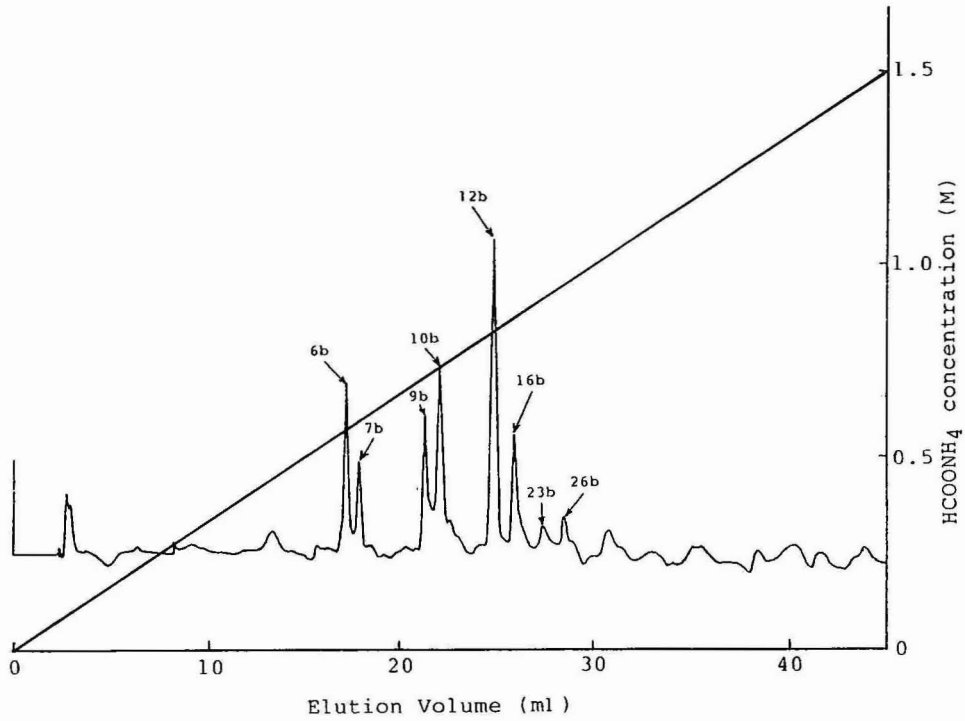

Fig. 3. Separation of single-stranded oligodeoxyribonucleotides. Eluent, linear gradient from 0.01 to 1.5 *M* ammonium formate in 45 min. Other conditions as in Fig. 1.

Fig. 6 summarizes the results from a more detailed study of the effect of temperature on the retention of the samples. Great variations in the elution volumes at different temperatures were observed for each sample. These results indicate that the elution volumes of each oligodeoxyribonucleotide, except 12b, will increase as the temperature is increased, and this effect is greater for samples with a larger number of bases. The unusual behaviour of 12b seen in Fig. 6 is still unexplained.

In the same experiments, changes in temperature were also found affect the peak widths of the substrates studied. The peak widths at half-height, obtained from

TABLE II

EFFECT OF FLOW-RATE

Eluent: linear gradient from 0.01 to 1 *M* ammonium acetate in 60 min and then 1 *M* (A) in 30 min and finally 1 *M* (B). Other conditions as in Fig. 1.

Flow-rate (ml/min)	*Gradient programme*	*Elution volume (ml)*							
		6b	*7b*	*9b*	*10b*	*12b*	*16b*	*23b*	*26b*
0.5	A	19.6	20.4	25.1	26.5	30.5	31.3	32.8	35.3
1.0	B	20.4	20.9	25.8	26.9	31.2	31.9	33.9	36.2

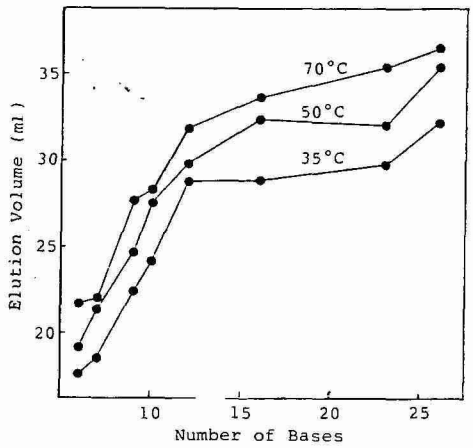

Fig. 4. Relationship between the number of bases and the elution volumes of oligodeoxyribonucleotides at different temperatures. Eluent, linear gradient from 0.01 to 1.5 *M* ammonium acetate in 45 min. Other conditions as in Fig. 1.

the chromatograms in Fig. 6, are listed in Table III. At higher temperatures, the value was small for samples with a smaller number of bases than 16b, whereas 23b and 26b produced wider peaks. From these results, measurement at 50°C can be considered to be suitable for all the nucleotides studied. Also, it was found that the effect of temperature was considerable when there were complementary components in the samples. A typical chromatographic change observed in such a case is depicted in Fig. 7, where 7b (dTCAAATC) and 9b (dCGGATTTGA) were selected as samples complementary with each other. In Fig. 7A, the separation of a mixture containing 7b and 10b (dCGACCCGGGT), obtained at 16°C, is shown. The relative peak-height ratio of 7b to 10b was 1.11. However, on addition of 9b to this mixture, the ratio

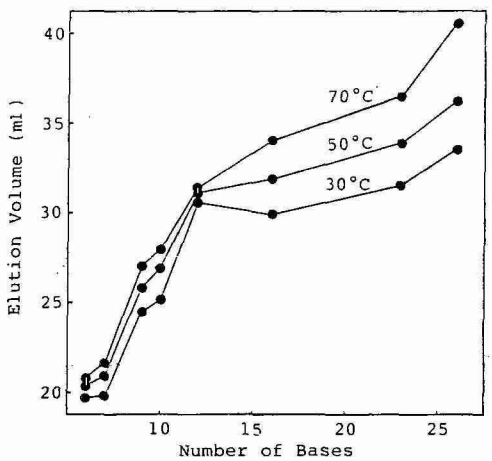

Fig. 5. Relationship between the number of bases and the elution volumes of oligodeoxyribonucleotides at different temperatures. Conditions as in Fig. 2.

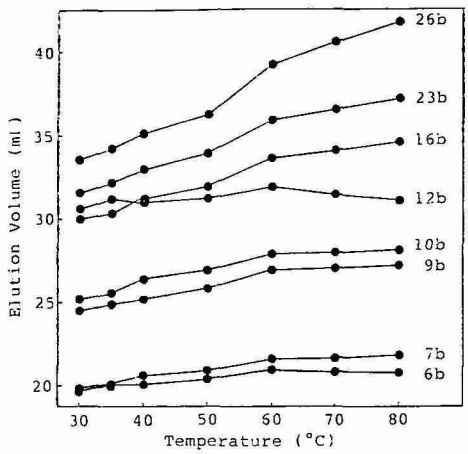

Fig. 6. Effect of temperature on the retention of single-stranded oligodeoxyribonucleotides. Other conditions as in Fig. 2.

TABLE III

PEAK WIDTH AT HALF-HEIGHT OBTAINED FOR THE OLIGODEOXYRIBONUCLEOTIDES AT DIFFERENT TEMPERATURES

Conditions as in Fig. 6.

Temperature (°C)	*Peak width at half-height (ml)*							
	6b	*7b*	*9b*	*10b*	*12b*	*16b*	*23b*	*26b*
35	0.32	0.30	0.34	0.38	0.50	0.36	0.42	0.34
40	0.30	0.28	0.32	0.32	0.44	0.34	0.40	0.44
50	0.30	0.28	0.34	0.28	0.40	0.36	0.36	0.50
60	0.26	0.24	0.30	0.32	0.40	0.32	0.44	0.68
70	0.26	0.24	0.28	0.32	0.38	0.34	0.50	0.72
80	0.22	0.22	0.24	0.30	0.36	0.34	0.54	0.80

changed to 0.93, as shown in Fig. 7B. This implies that 7b and 9b are composed of a double-stranded fragment and, therefore, the height of 7b decreased. This result indicates that at low temperatures, effective purification of such molecules is difficult. The peak of the double-stranded fragment could not be observed in this experiment. On increasing the temperature to 50°C, the change in height of 7b disappeared. As shown in Fig. 7C and D, the relative ratio was 0.73 for both the peak-height measurements. This strongly suggests that with single-stranded DNA fragments containing approximately ten bases, an elevated temperature is required to prevent the formation of double strands, which interferes with accurate measurements. Also, as there is a possibility that oligodeoxyribonucleotides may be hydrolysed at high temperatures, separation at about 50°C is reasonable.

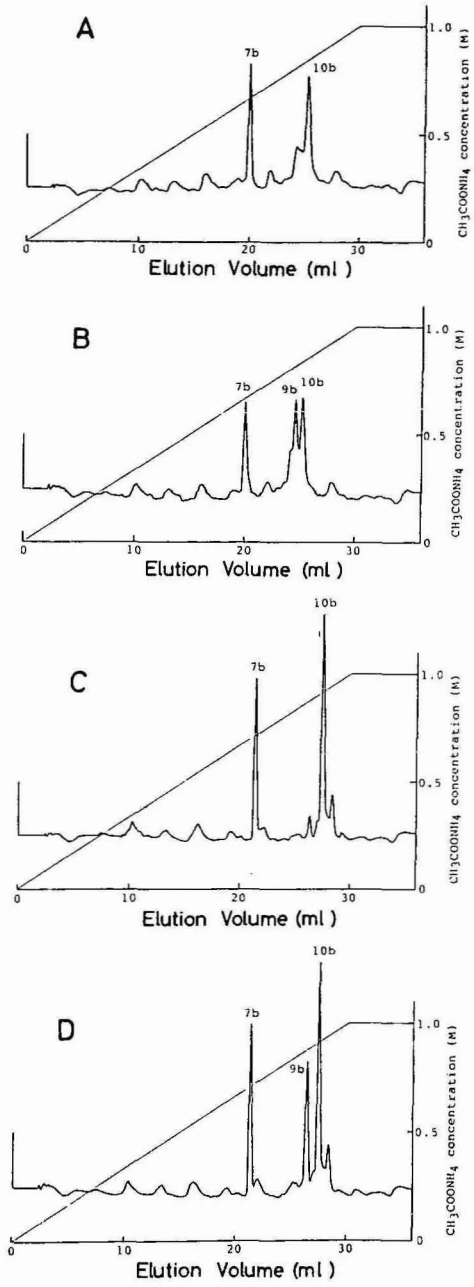

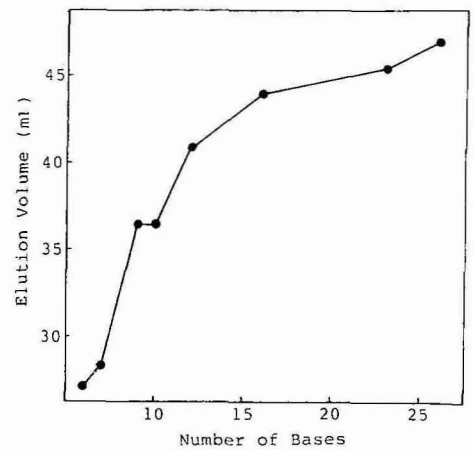

Fig. 7. Elution profiles of samples containing 7b (dTCAAATC) and 10b (dCGACCCGGGT). (A) and (C), obtained in the absence of 9b (dCGGATTTGA), which is complementary to 7b; (B) and (D), obtained in the presence of 9b. (A) and (B), measured at 16°C: (C) and (D), measured at 50°C. Other conditions as in Fig. 2.

Fig. 8. Relationship between the number of bases and the elution volumes of single-stranded oligodeoxyribonucleotides obtained at pH 5 by use of a linear gradient from 0.01 to 2.5 *M* ammonium acetate–acetic acid buffer (pH 5) in 75 min. Other conditions as in Fig. 1.

The effect of the pH of the eluent on retention was also studied. The chromatographic behaviour of the samples was found to vary when the pH of the eluent was changed. At pH 5, the retention became much higher than that observed at the pH of the eluent that contained only ammonium acetate (6.4–7.0). Therefore, a much higher concentration of the salt was required in order to achieve a similar retention of the solutes. In order to obtain the relationship represented in Fig. 8, a high final

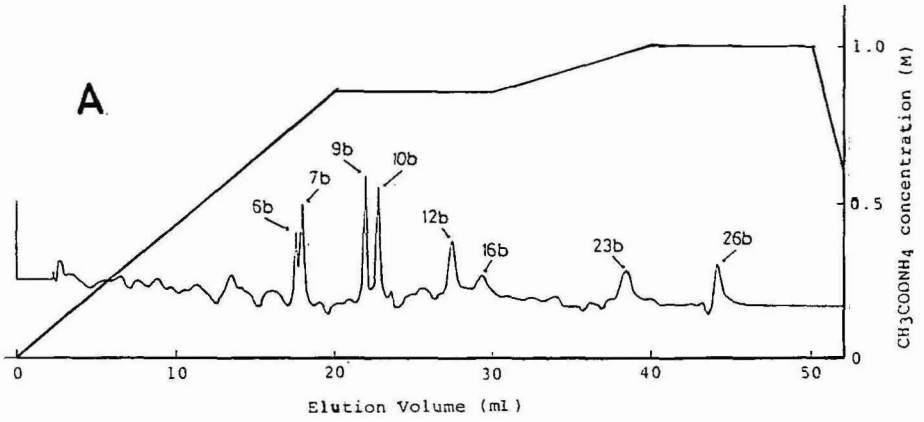

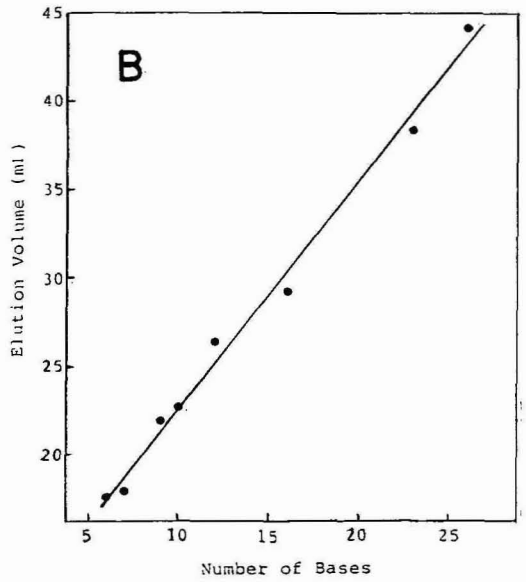

Fig. 9. (A) Separation of single-stranded oligodeoxyribonucleotides under the optimum gradient conditions shown. (B) Relationship between the number of bases and elution volumes of single-stranded oligodeoxyribonucleotides with the gradient system shown in (A). Other conditions as in Fig. 1.

concentration (*ca.* 2.0 *M*) was required for gradient elution, whereas at pH 7, 1 *M* was sufficient. This result implies that it is disadvantageous to lower the pH for the separation of such substrates. Also, a higher pH may lead to hydrolytic degradation of the samples. Consequently, a neutral pH was considered to be best for the separation of the substrates on DEAE-5PW.

Considering all the results, a gradient condition was designed so that a linear relationship between the number of bases and the elution position of the samples could be obtained. A typical separation obtained under optimum conditions is shown in Fig. 9A. The relationship between the elution volume and the number of bases in the samples obtained under the conditions used in this analysis is shown in Fig. 9B.

The separation of sequential isomers, the number of bases in which is the same, was performed in order to establish the extent of the deviation in retention between the isomers. The substrates were separated from each other but were eluted closely, as shown in Fig. 10. The observed separation was small in comparison with those for the samples containing a different number of bases. This indicates that the method used here is sufficient for the purification of single-stranded DNA fragments with different chain lengths and that it can even be used for the isolation of some sequential isomers.

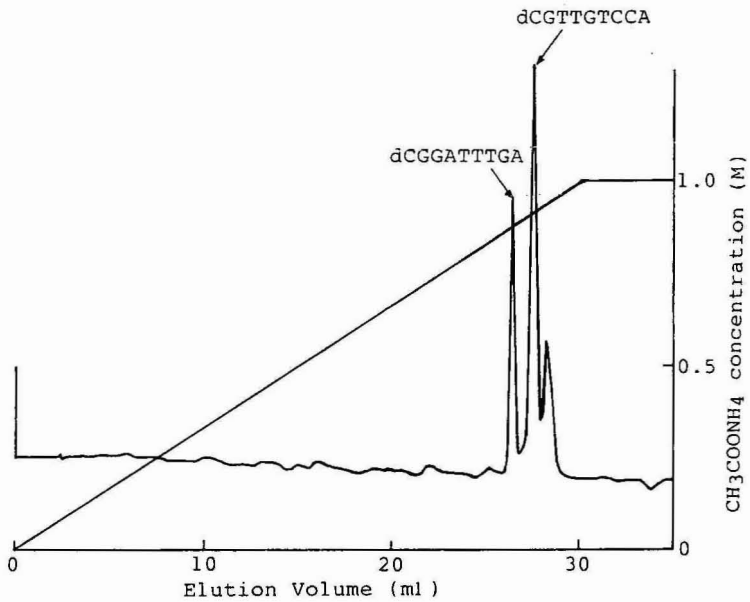

Fig. 10. Separation of sequential isomers containing nine bases. Conditions as in Fig. 2.

The results obtained suggest that anion-exchange chromatography with a DEAE-5PW column and eluents containing only volatile salts is highly efficient for the separation of single-stranded oligodeoxyribonucleotides with chain lengths up to *ca.* 26 base numbers.

REFERENCES

1 M. D. Matteucci and M. H. Caruthers, *J. Amer. Chem. Soc.*, 103 (1981) 3185.
2 E. Ohtsuka, M. Ikehara and D. Söll, *Nucleic Acids Res.*, 10 (1982) 6553.
3 L. J. McBride and M. H. Caruthers, *Tetrahedron Lett.*, 24 (1983) 254.
4 S. D. Putney, S. J. Benkovic and P. R. Schimmel, *Proc. Nat. Acad. Sci. U.S.*, 78 (1981) 7350.
5 D. F. Smith, P. F. Searle and J. G. Williams, *Nucleic Acids Res.*, 6 (1979) 487.
6 M. J. Gait and R. C. Sheppard, *Nucleic Acids Res.*, 4 (1977) 1135.
7 C. F. Crampton, F. R. Rankel, A. M. Benson and A. Wade, *Anal. Biochem.*, 1 (1960) 249.
8 A. M. Maxam and W. Gilbert, *Proc. Nat. Acad. Sci. U.S.*, 74 (1977) 560.
9 H. Domdey and H. J. Gross, *Anal. Biochem.*, 98 (1979) 346.
10 E. Y. Chen and B. A. Roe, *Anal. Biochem.*, 89 (1978) 45.
11 J. D. Pearson and F. E. Regnier, *J. Chromatogr.*, 255 (1983) 137.
12 W. Haupt and A. Pingoud, *J. Chromatogr.*, 260 (1983) 419.
13 K. Itakura, N. Katagiri and S. A. Narang, *Can. J. Chem.*, 52 (1974) 3689.
14 E. Ohtsuka, Y. Taniyama, R. Marumoto, H. Sato, H. Hirosaki and M. Ikehara, *Nucleic Acids Res.*, 10 (1982) 2597.

Journal of Chromatography, 322 (1985) 255–263
Elsevier Science Publishers B.V., Amsterdam — Printed in The Netherlands

CHROMSYMP. 618

RETENTION MECHANISM OF NUCLEOTIDES, NUCLEOSIDES AND THEIR BASES ON POLYVINYL ALCOHOL

HIROO WADA
Department of Polymer Science and Engineering, Faculty of Textile Science, Kyoto Institute of Technology, Matsugasaki, Sakyo-ku, Kyoto 606 (Japan)
(First received March 29th, 1985; revised manuscript received April 22nd, 1985)

SUMMARY

The basic chromatographic properties of a polyvinyl alcohol (PVA) column material were investigated. By pH titration, it was found that the PVA gel surface was negatively charged. The chromatographic behaviour of nucleotides on the gel was compared with that on an ODS column and found to be similar. However, the behaviour of nucleosides and bases were quite different from that on the ODS column. Since the retention characteristics of both types of solutes on the PVA column could be explained reasonably by the solvophobic theory, this result may suggest that the behaviour of these solutes on the ODS column is unusual. The difference in retention between AMP isomers and cAMP can be explained by the differences in their conformations.

INTRODUCTION

In order to detect and identify molecules of biological importance in living bodies, various types of chromatography have been utilized. The columns used most frequently in size exclusion and reversed-phase chromatographies are silica-based. Since the effect of the remaining free silanol groups is known to be undesirable for some compounds[1–3], the development of other matrix-based columns has been extensive. However, except for a few columns, these columns had undesirable properties such as strong interactions with the samples. Therefore, it is extremely important to know the basic chromatographic characteristics of newly developed columns, particularly when the columns are based on polymer gels because their characteristics are highly dependent on the matrix. For instance, a number of carboxyl groups are known to remain on polymethyl methacrylate gel. Therefore, ionic interactions can occur between functional groups on the gel matrix and those of the solutes.

Polyvinyl alcohol (PVA) gel is a new type of column packing material introduced independently by Showa Denko and then Asahi Kasei, and was previously employed for size exclusion chromatography. However, the basic properties of the column have not yet been fully investigated. It has been demonstrated[4–6] that the retention mode of PVA columns for large molecules such as carbohydrates, polyeth-

0021-9673/85/$03.30

ylene glycols[4] and proteins[6] is size exclusion, while for small molecules such as fatty acids, peptides with molecular weights less than 500, nucleotides, etc., the retention mode is similar to that of reversed-phase chromatography[5]. However, a determination of the detailed fundamental retention mechanism could not be made, although there was a possibility that the gel surface was slightly charged. Therefore, in order to reveal the overall retention mechanism of PVA columns, each chromatographic factor should be identified and studied in more detail. Major factors to be investigated first are the effects of the hydrophobic properties and charge of the surface of the PVA gel.

In reversed-phase chromatography the retention mechanism can be explained largely by the solvophobic theory[7,8] which describes how the hydropohobic interaction between the hydrophobic surface of the gel and the solutes, in the aqueous phase, can be produced. However, the retention behaviour of nucleotides, nucleosides and their bases is exceptional[9–11]. For instance, a nucleoside is retained more strongly than its base on an ODS column, although the former has higher hydrophilicity due to the hydroxyl groups in the ribose ring compared to the latter. The unusual behaviour of these two series of compounds has not been explained unambiguously.

In the present study, therefore, in order to demonstrate that the solvophobic theory cannot also be used to explain the behaviour of solutes on ODS columns, the chromatography of nucleotides, nucleosides and their bases on the PVA packing material was investigated in detail and the results obtained compared to those on ODS columns.

EXPERIMENTAL

The nucleotides, nucleosides and their bases employed as samples are listed in Table I. They were purchased from Sigma Chemical Co. (St. Louis, MO, U.S.A.), Kohjin Co. (Tokyo, Japan) and Yamasa (Chiba, Japan). Other chemicals were obtained from Nakarai Chemicals (Kyoto, Japan). Water was purified by a MILI R/Q water purifier (Millipore, Bedford, MA, U.S.A.).

An HLC-803 high-speed liquid chromatograph (Toyo Soda, Japan) equipped with an UVIDEC 100 UV spectrometer (Jasco, Japan) was employed. The column effluents were monitored at 260 nm. The Asahipak GS-320 column (50 cm × 7.6 mm I.D.) containing 9-μm microparticulate polyvinyl alcohol gel was obtained from Asahi Chemical Ind. Co. (Tokyo, Japan). A pH titration was performed by use of a Horiba digital pH meter F-7_{LC} (Kyoto, Japan).

RESULTS AND DISCUSSION

Previous papers described the highly complicated retention mechanism of peptides on the PVA column[5]. For example, the increase in the retention of the peptides caused by the addition of a salt indicated the occurrence of hydrophobic interactions between the solutes and the gel matrix. However, the retention volumes of the same substrates were found to be small for hydrophobic interaction and also were small even when they had been separated by size exclusion chromatography. This suggested the coexistence of a repulsion effect due to the charges on the solutes and the gel matrix.

TABLE I

COMPOUNDS USED AND THEIR ABBREVIATIONS

A = Sigma Chemical Company; B = Kohjin; C = Yamasa.

Compound	*Abbreviation*	*Source*
Adenine	Ade	B
Adenosine	Ado	B
Adenosine 5′-phosphate	(5′-)AMP	B
Adenosine 2′-phosphate	2′-AMP	A
Adenosine 3′-phosphate	3′-AMP	C
Adenosine 5′-diphosphate	ADP	C
Adenosine 5′-triphosphate	ATP	C
Adenosine 3′,5′-cyclic phosphate	cAMP	B
Guanine	Gua	B
Guanosine	Guo	B
Guanosine 5′-phosphate	GMP	B
Guanosine 5′-diphospohate	GDP	A
Guanosine 5′-triphosphate	GTP	C
Cytosine	Cyt	B
Cytidine	Cyd	B
Cytidine 5′-phosphate	CMP	A
Cytidine 5′-diphosphate	CDP	C
Cytidine 5′-triphosphate	CTP	A
Uracil	Ura	B
Uridine	Urd	B
Uridine 5′-phosphate	UMP	A
Uridine 5′-diphosphate	UDP	A
Uridine 5′-triphosphate	UTP	A
Thymine	Thy	B
Thymidine	Thd	C
Thymidine 5′-phosphate	TMP	B
Thymidine 5′-diphosphate	TDP	A
Thymidine 5′-triphosphate	TTP	A

First, therefore, in order to explore the dissociative characteristic of the PVA gel surface, a pH titration was carried out on a suspension of the gel. A 1.0-g amount of dried PVA gel was suspended in 50 ml of water and the suspension was titrated with 0.005 *M* hydrochloric acid. Pure water was used as a reference. Prior to the experiment both the samples were adjusted to pH 11.30 by addition of 0.1 *M* sodium hydroxide. During the titration the samples were stirred continuously with a magnetic stirrer. The results are presented in Fig. 1. Below pH 7.0, the titration curve obtained for the suspension of PVA gel was found to deviate from that for pure water, implying that there are dissociable groups on the PVA gel surface, although the amount of such groups is quite small. The pK_a value of the charged group lies between 4 and 5.

The effect of the surface charge was then investigated, using pyrimidine and purine compounds as samples. In reversed-phase chromatography, the pK_a values of these substrates are known to be an important factor for the retention. Therefore, experiments were carried out by changing the pH of the eluents.

First, 5′-monophosphate nucleotides (AMP, GMP, UMP, CMP and TMP)

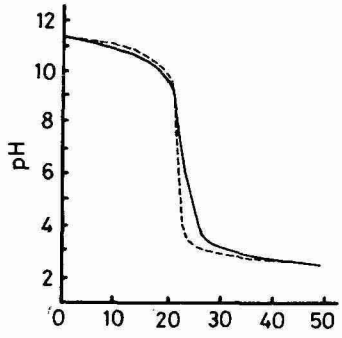

Fig. 1. Titration curves for a suspension (1 g per 50 ml) of PVA gel (—) and for pure water (50 ml) (– – –). Before the pH titration the suspension and pure water were adjusted to pH 11.30 by addition of 0.1 *M* hydrochloric acid.

were studied. The change in the elution volumes with pH is shown in Fig. 2. It was found that purine nucleotides were eluted more slowly than pyrimidine nucleotides, except that TMP was eluted later than AMP at pH 3.0. The largest elution volumes for 5′-monophosphate nucleotides other than 5′-AMP were obtained at pH 3.0 and the retention decreased with increasing pH of the eluent; the largest elution volume of 5′-AMP was obtained at pH 5.0 and the highest values for CMP occurred at both pH 3.0 and 5.0. These results can be explained in terms of the structural changes in the ionogenic groups of the substrates upon changing the pH. In the case of 5′-monophosphate nucleotides other than AMP and CMP, the extent of the dissociation of phosphate groups led to a decrease in retention because the purine ring of GMP (pK_a for N-7 is 2.4) is uncharged at pH 3.0 and the two pyrimidine nucleotides (UMP and TMP) do not have dissociable groups other than the phosphate group at this pH. The nitrogen (N-1) of the adenyl ring of AMP (pK_a 3.8) is positively charged at

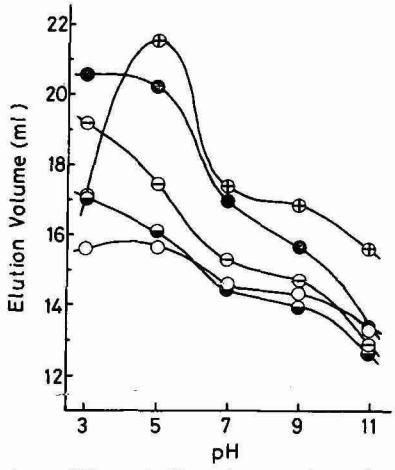

Fig. 2. Effect of pH on the retention volume of monophosphate nucleotides: ⊕—⊕, AMP; ⊙—⊙, GMP; ⊖—⊖, TMP; ◒—◒ UMP; ○—○, CMP. Conditions: flow-rate, 1 ml/min; sample volume, 20 μl; detection, UV at 260 nm; temperature, ambient.

pH 3.0. Hence the solute surface may be covered largely with an aqueous phase because of the formation of its cationic form resulting from the protonation at N-1. At pH 5.0, the adenyl ring of AMP is uncharged. Since the decrease in the hydrophilicity of the adenyl ring caused by its neutralization can result in an increase in the hydrophobic interaction of the solute with the matrix, the retention volume of AMP at pH 5.0 is larger than that at pH 3.0. A similar trend in retention was observed for 5'-CMP. The pyrimidine ring of CMP (pK_a for N-3 is 4.5) is positively charged at pH 3.0. Therefore, CMP cannot be retained strongly on the gel surface at this pH. The small retention of AMP and CMP at pH 3.0 implies that the ionic interaction between negative charge of the gel and positive charge of the solutes is not sufficiently large to compete with the rapid elution caused by the decrease in hydrophobicity due to the positive charge. This is evident because at pH 3.0 the gel surface is mostly neutralized (pK_a 4–5).

Di- and triphosphate nucleotides were also chromatographed with eluents at different pH values. The retention volumes of these substrates are summarized in

TABLE II

EFFECT OF pH ON THE ELUTION VOLUMES (ml) OF NUCLEOTIDES, NUCLEOSIDES AND THEIR BASES

Conditions: flow-rate, 1 ml/min; detection, UV at 260 nm; sample volume, 20 μl; temperature, ambient.

Compound	*pH*				
	3	*5*	*7*	*9*	*11*
Adenine	20.72	63.06	78.16	71.46	48.88
Adenosine	23.32	57.28	65.50	59.02	61.20
AMP	16.92	21.56	17.36	16.90	15.60
ADP	14.88	16.06	15.12	14.88	13.92
ATP	13.96	14.32	14.00	13.80	13.10
Guanine	26.82	48.48	47.28	41.44	25.02
Guanosine	34.10	37.16	39.84	31.84	24.08
GMP	20.56	20.26	16.96	15.70	13.44
GDP	16.40	15.96	15.10	14.24	12.78
GTP	14.96	14.40	14.14	13.48	12.36
Cytosine	16.28	20.00	22.22	21.96	23.20
Cytidine	16.56	21.26	22.36	23.58	21.64
CMP	15.58	15.66	14.52	14.36	13.40
CDP	14.34	13.80	13.60	13.22	12.12
CTP	13.58	12.98	13.04	12.88	12.20
Uracil	25.64	25.48	25.20	23.38	17.76
Uridine	23.38	23.72	24.58	21.00	15.86
UMP	17.08	16.08	14.40	13.98	12.60
UDP	14.80	13.92	13.60	13.22	12.12
UTP	13.86	13.08	13.12	12.70	11.84
Thymine	32.52	32.42	32.52	31.30	20.56
Thymidine	32.22	32.36	34.20	30.00	18.96
TMP	19.22	17.48	15.26	14.72	12.84
TDP	15.54	14.26	13.86	13.58	12.20
TTP	14.28	13.22	13.20	12.96	11.90

Table II. Triphosphate nucleotides were eluted more rapidly than diphosphate nucleotides and both series of solutes were eluted faster than monophosphate nucleotides. This is because of the larger number of phosphate groups in the samples which can influence the hydrophilicity and solubility of the solutes. The retention orders of the substrates in each series of nucleotides were analogous to those of the monophosphate nucleotides. These results are similar to these obtained for the nucleotides on an ODS column[9,12,13].

Analogous experiments were carried out for nucleosides and their bases. The results are also listed in Table II. All the elution volumes obtained at each pH were large compared to those of the nucleotides. This is because of the lack of the highly hydrophilic phosphate moiety in these substrates and because increased hydrophobicity leads to a decrease in the solubility of the solute and to longer retention. The overall retention order of the substrates at pH 3.0 can be explained as follows. The guanyl ring of Guo (pK_a for N-7 is 1.6) is uncharged at this pH. Therefore, the solutes have substantial hydrophobic interaction between the purine ring and the gel. Since the hydrophobicity of Thy is considered to be larger than that of Ura because of the methyl group on the ring, Thy and Thd were retained more strongly than Ura and Urd, respectively. Thd and Urd have a ribose ring which can result in an increased solubility of these solutes. Therefore, the nucleosides were eluted more rapidly than the bases. Half of the nitrogen (N-7) of Gua (pK_a for N-7 is 3.2) is positively charged at pH 3.0. Therefore, the solubility of this solute is still relatively high at this pH. For this reason, Gua was eluted before Guo, Thd and Thy. Probably, because of the weak hydrophobicity of the pyrimidine ring, Ura and Urd were eluted before Gua. The purine rings of Ade and Ado have pK_a values of 4.15 and 3.5 respectively for N-1 and are mainly in the ionic form at pH 3.0. Therefore, these two compounds were eluted more rapidly than the above six compounds and their elution order, Ade and Ado, was a function of the extent of the adenyl ring being positively charged at N-1. This means that the effect of the charge on the decrease in retention is larger than that of the hydrophilic ribose ring. Cyt and Cyd (pK_a values for N-3 are 4.5 and 4.15, respectively) were eluted most rapidly because they were chiefly in the positively charged form and because of the weak hydrophobicity of the ring.

Also, it was found that the elution order of the nucleosides at various pH values is dependent on the order of the bases at the same pH, which is analogous to that for the nucleotides. Also, a characteristic retention order was observed between each nucleoside and its base. At pH 3.0, the orders for each pair were Ade < Ado, Gua < Guo, Cyt < Cyd, Ura > Urd and Thy > Tyd, and at pH 7.0, Ade > Ado, Gua > Guo, Cyt < Cyd, Ura > Urd and Thy < Thd. On the other hand, in a previous study of the same pairs on ODS columns, different elution orders were obtained[9–14]. Especially, at pH 7.0, the orders were completely opposite to those on PVA columns. This extremely characteristic elution behaviour of solutes on the PVA column at pH 7.0 is caused by reversed-phase retention. Since the retention order of the solutes on the PVA gel can be explained reasonably as mentioned above, the order on ODS columns is rather unusual. At pH 7.0, part of the surface of the PVA column is covered with negative charges, which may explain the difference in behaviour from that of the free silanol groups of the ODS column.

The effect of the charged groups on the retention of ionic compounds was also explored for samples such as AMP isomers (5′-, 3′- and 2′-AMP) and 3′,5′-cyclic

TABLE III

EFFECT OF pH ON THE ELUTION VOLUMES (ml) OF cAMP AND AMP ISOMERS

Conditions as in Table II.

Compound	*pH*		
	3.0	*5.0*	*7.0*
5'-AMP	16.80	23.86	19.42
2'-AMP	17.36	24.64	20.44
3'-AMP	18.34	29.42	22.24
cAMP	21.06	43.38	49.56

AMP (cAMP). These substrates were chromatographed at pH 3.0, 5.0 and 7.0. There were two notable differences in the retention between cAMP and the isomers and between the isomers as shown in Table III. cAMP always had a retention larger than those of the three isomers in the pH range applied. Also, the difference in the retention between cAMP and the isomers was much larger at pH 5.0 and 7.0 compared to that at pH 3.0. The conformation of cAMP and the three isomers are illustrated in Fig. 3. In cAMP, the phosphate group is fixed on the ribose ring by the two ester bonds and therefore has little contact with the adenyl ring which has a positive charge at N-1. On the other hand, the phosphate groups of the three isomers are attached to ribose rings through only one ester bond and can rotate relatively freely. For all the four samples, the adenyl rings are considered to participate in hydrophobic interactions with the gel matrix, while the phosphate groups interrupt these interaction through their hydrophilicity, which increases the solubility of the solutes. Also repulsive force arising from the negative charges on the solutes and the gel matrix may decrease the retention. Thus, cAMP, in which hydrophilicity of the phosphate group can hardly affect the hydrophobic influence of the adenyl ring because of the long distance between these groups, has larger retention than the isomers.

The combination of the charges on the phosphate group and on N-1 of the adenyl ring can also contribute to the retention mechanism. Since the phospohate moiety of cAMP is attached to the ribose ring by two ester bonds, it can only have charge of -1 at pH 3.0, 5.0 and 7.0 (pK_a of cAMP phosphate is *ca.* 2). On the other hand, the phosphate groups of the three isomers have a charge of -1 at pH 3.0 and 5.0 (pK_a of primary dissociation is less than 1) and -2 at pH 7.0 (pK_a for the secondary dissociation is *ca.* 6) and can rotate so freely that they can interact with the

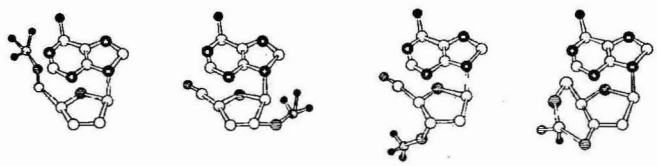

Fig. 3. Conformations of cAMP and the AMP isomers. ○ = Carbon, ● = nitrogen, ◍ = oxygen and ◉ = phosphorus.

positively charged adenyl rings. The extent of the interaction of the AMP isomers with the gel matrix is strongly dependent on the position of these freely rotating phosphate groups. At pH 3.0, the adenyl rings of cAMP and the isomers have a charge of +1 at N-1 (the pK_a value for N-1 is 3.7–3.8). Therefore, the hydrophobic interaction of the solutes with the gel matrix caused by the adenyl ring is weakened by the hydrophilic interference of the positive charge at N-1 of the adenyl rings. The solubility increase caused by the charge at N-1 decreases the retention of all the solutes on the PVA column and results in a decrease in the difference in retention between cAMP and the three isomers. In this case, the interaction between the positive charge of the adenyl ring and the negative charge of the gel matrix cannot compete with the hydrophilic effect because the extent of the negative charge on the gel is small at pH 3.0. Therefore, at pH 3.0, all the four solutes had smaller retentions than at pH 5.0 and 7.0 and the difference in retention between cAMP and the isomers was not large. At higher pH (5.0 and 7.0), the retention of all the solutes was larger than that at pH 3.0. At these pH values, the nitrogen (N-1) of the adenyl rings of cAMP and the isomers is now uncharged. The hydrophobic interaction between the adenyl ring and the gel matrix is strengthened by the increase in hydrophobicity of the ring in its neutral form. Also, particularly at pH 7.0, a large difference in retention between cAMP and the AMP isomers was observed compared to the difference at pH 3.0. This can be explained by considering the charges and the conformational characteristics of the solutes. At pH 7.0 the secondary dissociation of the phosphate groups of all the AMP isomers has taken place. Therefore, the charge on the phosphate moiety of the AMP isomers is −2, while cAMP still has a charge of −1 on the phosphate moiety. The presence of the additional negative charge on the phosphate groups increases the hydrophilicity and solubility of the samples, weakening the interaction of the adenyl ring with the gel matrix and resulting in lower retention. On the other hand, for cAMP there the negative charge on the phosphate moiety is −1 at the three pH values. Therefore, the hydrophilicity of cAMP arising from the phosphate group is unchanged at these pH values while the hydrophobicity is much increased by neutralizing the adenyl ring.

Next, the dissociation of the gel matrix was considered. Because the pK_a value for this dissociation was determined to be 4–5, the surface of the gel is considered to be negatively charged at pH 5.0 and 7.0, while at pH 3.0 it is neutral. Therefore, at pH 5.0 and 7.0, there is a repulsive force between the negatively charged solutes and the gel surface. This force may be higher for the AMP isomers than cAMP because of the larger number of negative charges on the isomers. For the above reasons, the retention of cAMP increased much more than that of the AMP isomers upon raising the pH of the eluent. Consequently, at pH 5.0, the difference in the extent of the repulsive force between the negative charges on the gel surface and on the phosphate group and in the extent of the hydrophilic interference of the phosphate group with the hydrophobic interaction of adenyl ring results in the difference in the retention volume between cAMP and the AMP isomers. In addition to the above two differences which governed retention of the solute, at pH 7.0, secondary dissociation of the phosphate groups of the isomers was involved.

The difference in retention between the three isomers can also be explained as follows. Since the structure of the adenyl ring and the phosphate group is not substantially different between the isomers at the three pH values, almost equal retention

is expected for these solutes at each pH. As seen in Table III, however, the retention order of these substrates as always 5'-, 2'- and 3'-AMP. Therefore, a slight difference in the overall structure of the solutes may be used to account for the difference in the retention. As shown in Fig. 3, of the isomers, the phosphate group of 5'-AMP is nearest to the adenyl ring. In the case of 3'-AMP, the phosphate moiety is kept away from the aenyl ring because its rotation is restricted by the hydroxymethyl group of the ribose ring. The accessibility of the phosphate group of 2'-AMP to the adenyl ring can be considered to represent intermediate between these two cases. Thus, the differences in the extent of the hydrophilicity of the adenyl ring, arising out of the accessibility of the phosphate group, can explain the elution order of 5'-, 2'- and 3'-AMP.

The largest elution volumes obtained for all the AMP isomers at pH 5.0 can be explained by the increase in hydrophobicity of the adenyl ring due to the formation of the neutral form of the adenyl ring (at N-1), as described in the explanation of the retention of 5'-AMP. In the case of cAMP, since N-1 of the adenyl ring is uncharged and secondary dissociation of phosphate group does not take place at pH > 5.0, the elution volume increased with increasing pH. The trend in the elution order obtained on the PVA column is similar to that on ODS.

In summary, the negative charge formed on the PVA gel surface had little effect on the overall retention of the solutes studied. The effect of the charge on the solute retention was also quite different from that observed on ODS columns. For substrates having no phosphate groups, nucleosides and their bases, this negative charge gave rise to an elution order which can be explained in terms of the solvophobic theory, while the order obtained on ODS columns is not readily explained by this theory. The trend observed on the PVA column for substrates having phosphate groups was found to be similar to that on ODS columns. Considering the above results, it may be concluded that the negative charge on the PVA matrix does not produce undesirable and incomprehensible interactions between the solutes and the gel, which have often been observed with ODS columns and cannot easily be explained.

ACKNOWLEDGEMENTS

The author is deeply grateful to Professors H. Hatano, T. Takeuchi and K. Makino for valuable discussion.

REFERENCES

1 A. Nahum and Cs. Horváth, *J. Chromatogr.*, 203 (1981) 53.
2 K. E. Bij, Cs. Horváth, W. R. Melander and A. Nahum, *J. Chromatogr.*, 203 (1981) 65.
3 H. Engelhardt and H. Müller, *J. Chromatogr.*, 218 (1981) 395.
4 H. Wada, H. Ozaki, K. Makino, T. Takeuchi and H. Hatano, *Anal. Lett.*, 16(B19) (1983) 1537.
5 H. Wada, *Chromatographia*, 18 (1984) 550.
6 H. Wada, K. Makino, T. Takeuchi, H. Hatano and K. Noguchi, *J. Chromatogr.*, 320 (1985) 369.
7 Cs. Horváth, W. R. Melander and I. Molnár, *J. Chromatogr.*, 125 (1976) 129.
8 Cs. Horváth, W. R. Melander and I. Molnar, *Anal. Chem.*, 49 (1977) 142.
9 F. S. Anderson and R. C. Murphy, *J. Chromatogr.*, 121 (1976) 251.
10 P. R. Brown and E. Grushka, *Anal. Chem.*, 52 (1980) 1210.
11 P. J. M. Van Haastert, *J. Chromatogr.*, 210 (1981) 229.
12 Cs. Horváth and W. R. Melander, *Am. Lab. (Fairfield, Conn.)*, (1978) 17.
13 D. L. Ramos and A. M. Schoffstall, *J. Chromatogr.*, 261 (1983) 83.
14 M. Zakaria, P. R. Brown and E. Grushka, *Anal. Chem.*, 55 (1983) 457.

Journal of Chromatography, 332 (1985) 265–268
Elsevier Science Publishers B.V., Amsterdam — Printed in The Netherlands

CHROMSYMP. 620

HIGH-PERFORMANCE LIQUID CHROMATOGRAPHY OF ANTIPYRETICS ON CHEMICALLY MODIFIED POROUS GLASS

YOSHIKAZU MATSUSHIMA*, YOSHIKO NAGATA, KEIKO TAKAKUSAGI and MIKI NIYOMURA
Kyoritsu College of Pharmacy, Shibakoen 1-5-30, Minato-ku, Tokyo 105 (Japan)
and
NOBUHARU TAKAI
Institute of Industrial Science, University of Tokyo, Roppongi 7-22-1, Minato-ku, Tokyo 106 (Japan)
(First received March 30th, 1985; revised manuscript received May 1st, 1985)

SUMMARY

An octadecylsilyl porous glass was prepared and used as the packing for reversed-phase high-performance liquid chromatography. Five antipyretic drugs (aspirin, caffeine, guaiacol glycerol ether, 3-hydroxy-*p*-butyrophenetidine, and phenacetin) were separated in 2 min with a mobile phase of 20% acetonitrile at a flow-rate of 3.0 ml/min. A pharmaceutical preparation, containing aspirin, phenacetin, caffeine and chlorpheniramine maleate was analysed in 2 min with a mobile phase of acetonitrile–water–acetic acid (20:79:1). The packing seems promising for the rapid analysis of pharmaceuticals and biomedical compounds.

INTRODUCTION

There is an urgent need for new packing materials in order to achieve rapid chromatographic separation of pharmaceuticals and biomedical materials. To meet this dimand, we prepared chemical modifications of porous glass as packing materials[1]. Porous glass has been used in the chromatographic purification of proteins[2–5]. Antipyretics were successfully separated by the use of an octadecylsilyl porous glass (ODS glass) as the packing for reversed-phase high-performance liquid chromatography (HPLC). HPLC on ODS glass has not been described so far in the literature. The present paper describes results that suggest that this packing material saves much time in the analysis compared with conventional materials.

EXPERIMENTAL

Preparation of ODS glass

Porous Vycor glass with a pore size of 350 Å was treated with concentrated nitric acid, rinsed, and allowed to react with octadecylchlorosilane in boiling toluene for 3 h. The results of elemental analysis showed that the modified glass contained

0021-9673/85/$03.30

6.46% carbon. By treatment with trimethylchlorosilane, unchanged silanol groups in the modified glass were inactivated.

The electronograph and the BET method indicated that the distribution of pore size was fairly small.

ODS glass with a particle size distribution of 10–15 μm was packed into a 150 × 4 mm I.D. stainless-steel column by a high-pressure slurry technique.

Chemicals

Acetonitrile and acetic acid were purchased from Wako (Tokyo, Japan). Antipyretics and their preparations used in the study were pharmaceuticals standardized according to the 10th edition of the *Japanese Pharmacopoeia*. Water used as a solvent was freshly distilled and deionized. Other chemicals were of reagent grade. Vycor glass was obtained from Fuji Photofilm (Tokyo, Japan).

Apparatus

A Hitachi Model 655 high-performance liquid chromatograph, equipped with a Rheodyne Model 7125 valve and a Hitachi Model 655A UV monitor, operated at 254 nm, was used. Pharmaceuticals were dissolved in 80% acetonitrile–water and injected into the chromatograph with a Hamilton syringe. The system was operated at room temperature.

RESULTS AND DISCUSSION

Five antipyretic drugs, aspirin, caffeine, guaiacol glycerol ether, 3-hydroxy-*p*-

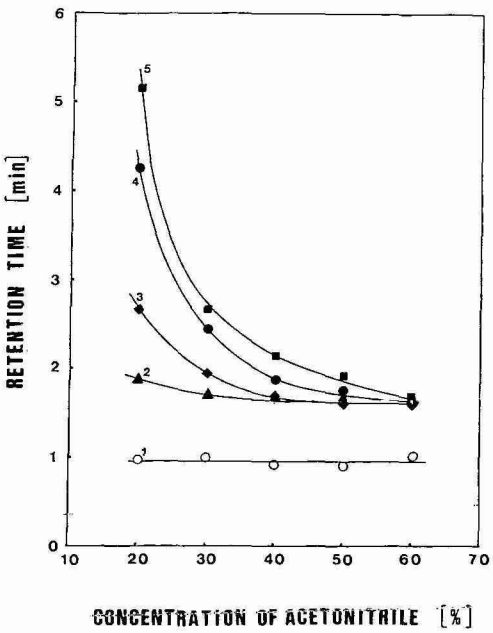

Fig. 1. Effect of the acetonitrile concentration in the mobile phase on the retention times of aspirin (1), caffeine (2), guaiacol glycerol ether (3), 3-hydroxy-*p*-butyrophenetidine (4) and phenacetin (5).

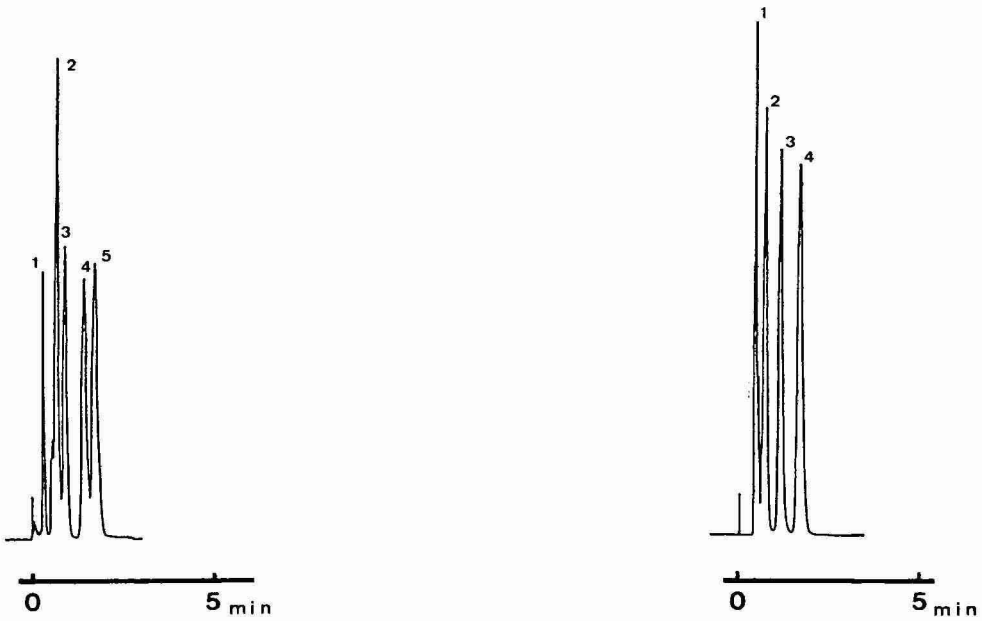

Fig. 2. Chromatogram of a mixture of aspirin (1), caffeine (2), guaiacol glycerol ether (3), 3-hydroxy-*p*-butyrophenetidine (4) and phenacetin (5).

Fig. 3. Chromatogram of the preparation containing chlorpheniramine maleate (1), caffeine (2), aspirin (3), and phenacetin (4).

butyrophenetidine and phenacetin, were chromatographed at room temperature at a flow-rate of 1.0 ml/min. The mobile phases were mixtures of acetonitrile and water, degassed by sonication. The results are shown in Fig. 1. With mobile phases containing more than 40% acetonitrile, the retention times of the five drugs were close together, and they were not separated.

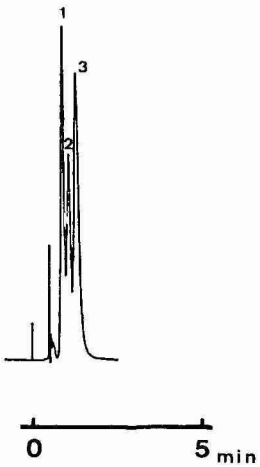

Fig. 4. Chromatogram of a mixture of salicylamide (1), aspirin (2) and salicylic acid (3).

With a mobile phase of 20% acetonitrile, the variation of retention times at different flow-rates was studied. The five peaks were well separated with flow-rates in the range 1.0–3.0 ml/min. Fig. 2 is a chromatogram obtained at a flow-rate of 3.0 ml/min, indicating that mixtures of the five drugs can be analysed in 2 min.

Pulvis aspirini, phenacetini et coffeini compositus (Compound Aspirin, Phenacetin and Caffeine Powder) is a pharmaceutical preparation standardized by the 10th *Japanese Pharmacopoeia*. It contains aspirin, phenacetin, caffeine and chlorpheniramine maleate. Determination of these four ingredients was required for the analysis of this preparation. The peaks of aspirin and chlorpheniramine maleate partially overlapped with acetonitrile–water (20:80) as the mobile phase. To facilitate complete separation, 1% of acetic acid was added to the mobile phase: this addition increased the retention time of aspirin. With acetonitrile–water–acetic acid (20:79:1), the ingredients of the preparation can be separated, as shown in Fig. 3. The separation of aspirin and its derivatives with this mobile phase was also possible. Fig. 4 is a chromatogram of a mixture of aspirin, salicylamide and salicylic acid.

The results shown in Figs. 2–4 indicate that the antipyretic agents can be analysed in 2 min. ODS glass seems to be a promising packing material for the rapid analysis of pharmaceuticals and biomedical compounds. Further studies are in progress in our laboratories.

REFERENCES

1 T. Yoden, N. Isoo, N. Takai, Y. Kuromatsu, H. Masuda, Y. Nagata, S. Sugata and Y. Matsushima, *27th Symposium on Liquid Chromatography, Kyoto, 1984.*
2 D. E. S. Truman, A. G. Brown and K. V. Rao, *Exp. Eye Res.*, 12 (1971) 304.
3 R. C. Collins and W. Haller, *Anal. Biochem.*, 54 (1973) 47.
4 M. J. Frenkel and R. J. Blagrove, *J. Chromatogr.*, 111 (1975) 397.
5 A. A. Ansari and R. G. Mage, *Anal. Biochem.*, 74 (1976) 118.

Journal of Chromatography, 332 (1985) 269–273
Elsevier Science Publishers B.V., Amsterdam — Printed in The Netherlands

CHROMSYMP. 621

ANALYSIS OF ANTIPYRETICS BY SEMIMICRO LIQUID CHROMATOGRAPHY

YOSHIKAZU MATSUSHIMA*, YOSHIKO NAGATA, MIKI NIYOMURA and KEIKO TAKAKUSAGI
Kyoritsu College of Pharmacy, Shibakoen 1-5-30, Minato-ku, Tokyo 105 (Japan)
and
NOBUHARU TAKAI
Institute of Industrial Science, University of Tokyo, Roppongi 7-22-1, Minato-ku, Tokyo 106 (Japan)
(First received March 30th, 1985; revised manuscript received May 1st, 1985)

SUMMARY

Using semimicro columns (150 × 1 mm I.D.) of octadecyl silica and styrene–divinylbenzene porous polymer, antipyretic drugs were analyzed by means of high-performance liquid chromatography. The antipyretics studied were sulpyrin, caffeine, guaiacol glycerol ether, acetaminophen, 3-hydroxy-*p*-butyrophenetidine, methyl *p*-hydroxybenzoate, phenacetin, mefenamic acid, aspirin, salicylamide, salicylic acid, *o*-ethoxybenzamide, theobromine, theophylline and their preparations. The semimicro columns are economical in solvents in chromatographic analysis.

INTRODUCTION

High-performance liquid chromatography (HPLC) on micro or semimicro columns has aroused interest, since it enables the analysis time and amounts of samples and solvents to be reduced[1–5]. In addition, HPLC with semimicro columns requires no or only minor changes to the conventional chromatographic system. The present paper is concerned with the application of semimicro columns (150 × 1 mm I.D.) to the analysis of antipyretics and their pharmaceutical preparations. The packing materials used were octadecyl silica gel and styrene–divinylbenzene porous polymer.

EXPERIMENTAL

Column preparation

The octadecyl silica gel used was Hitachi-Gel 3057 (particle size 3 μm, Hitachi Co.). ODS Silica (200 mg) was dispersed in 1.0 ml of 2-propanol, containing 0.1 ml of dioxane. The slurry was packed into a 150 × 1 mm I.D. stainless-steel column at a pressure of 400 kg/cm² for 30 min with methanol.

The porous polymer used was Hitachi-Gel 3011. A 200-mg amount was dispersed in 1.7 ml of methanol by sonication and packed into a semimicro column at a pressure of 200 kg/cm² for 1 h with methanol.

0021-9673/85/$03.30

Chemicals

The chemicals and solvents used were of reagent grade and obtained from commercial sources. Antipyretics and their preparations were pharmaceuticals standardized according to the 10th edition of the *Japanese Pharmacopoeia*. Water used as solvent was freshly distilled and deionized.

Apparatus

A Hitachi Model 655-15 high-performance liquid chromatograph, equipped with a Rheodyne valve for semimicro columns and a Hitachi Model 655-0510 UV monitor operated at 254 nm, was used. The pharmaceuticals were dissolved in 80% aqueous acetonitrile for the ODS silica column and in methanol for the porous polymer column. A volume of 1.0 μl was injected into the chromatograph with a Hamilton syringe. The system was opoerated at room temperature.

RESULTS AND DISCUSSION

Seven antipyretic drugs, sulpyrin, caffeine, guaiacol glycerol ether, acetaminophen, 3-hydroxy-*p*-butyrophenetidine, methyl *p*-hydroxybenzoate and phenacetin, were chromatographed on the ODS silica column at a flow-rate of 30 μl/min. The mobile phases were mixtures of acetonitrile and water, degassed by sonication. The results are summarized in Fig. 1. With mobile phases containing more than 40% acetonitrile, the retention times of the seven drugs were similar, and they were not separated.

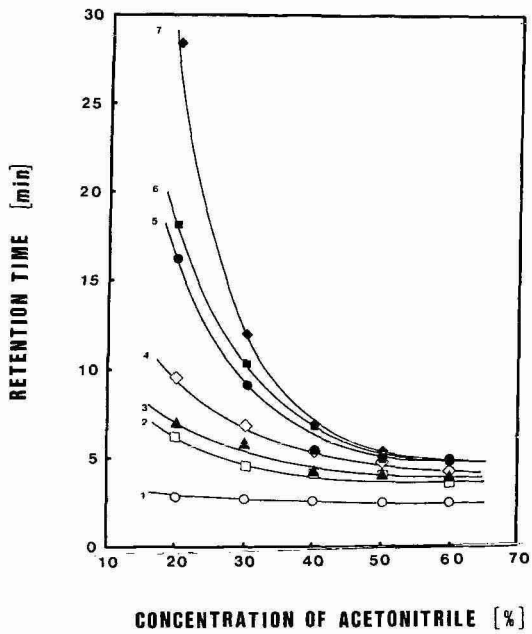

Fig. 1. Effect of acetonitrile concentration in the mobile phase on the retention times of sulpyrin (1), caffeine (2), guaiacol glycerol ether (3), acetaminophen (4), 3-hydroxy-*p*-butyrophenetidine (5), methyl *p*-hydroxybenzoate (6) and phenacetin (7).

With a mobile phase of acetonitrile–water (25:75), a mixture of sulpyrin, caffeine, guaiacol glycerol ether, methyl *p*-hydroxybenzoate and phenacetin was eluted at various flow-rates, ranging from 10 to 50 μl/min. The five peaks were well separated at all flow-rates in this range. The time required for the elution was 55 min with a flow-rate of 10 μl/min, 20 min with 30 μl/min and 10 min with 50 μl/min. The amount of mobile phase required was *ca.* 550 μl. Fig. 2 shows a chromatogram obtained at a flow-rate of 30 μl/min.

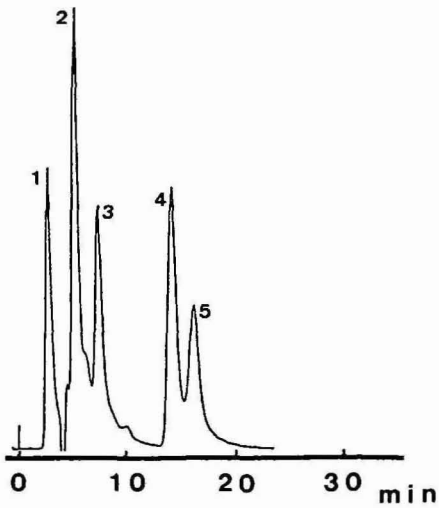

Fig. 2. A chromatogram of a mixture of sulpyrin (1), caffeine (2), guaiacol glycerol ether (3), methyl *p*-hydroxybenzoate (4) and phenacetin (5).

With the porous polymer semimicro column, the antipyretic drugs were chromatographed with three mobile phases at a flow-rate of 30 μl/min. The mobile phases were methanol, methanol containing 1% acetic acid and methanol containing 1% aqueous ammonia. The retention times are listed in Table I.

Pulvis aspirini, phenacetini et coffeini (aspirin, phenacetin and caffeine powder) is a pharmaceutical preparation standardized according to the 10th edition of the *Japanese Pharmacopoeia*. The three ingredients of the preparation were well separated with methanol containing 1% aqueous ammonia as the mobile phase at a flow-rate of 30 μl/min. The chromatogram is shown in Fig. 3.

A preparation containing acetaminophen, caffeine and *o*-ethoxybenzamide (ethenzamide) is a popular antipyretic pharmaceutical. The three drugs were well separated with any of the three mobile phases.

Methanol containing 1% aqueous ammonia was most suitable for the separation of a mixture of aniline antipyretics, acetaminophen, phenacetin, 3-hydroxy-*p*-butyrophenetidine and mefenamic acid. The peak of mefenamic acid was smaller or not detectable with other mobile phases. A mixture of xanthine drugs, caffeine, theobromine and theophylline, was also separated with a mobile phase containing ammonia.

TABLE I

RETENTION TIMES (min) OF ANTIPYRETICS

	Mobile phase		
	Methanol (100%)	*Methanol–1% acetic acid*	*Methanol–1% ammonia*
Aniline antipyretics			
Acetoaminophen	4.48	4.54	3.26
Phenacetin	5.84	5.68	5.70
3-Hydroxy-*p*-butyrophenetidine	5.18	5.20	5.24
Mefenamic acid	–	14.40	3.16
Salicylic acid antipyretics			
Aspirin	8.04	5.06	3.52
Salicylamide	4.98	5.00	3.16
Salicylic acid	–	7.10	3.56
o-Ethoxybenzamide	5.84	5.86	5.86
Pyrazolones			
Sulpyrin	3.42	8.58	3.62
Xanthines			
Caffeine	8.16	8.08	8.06
Theobromine	5.56	5.62	5.18
Theophylline	6.24	5.94	3.00

The results described indicate that semimicro columns can be used for the analysis of antipyretic agents. Such columns are economical in chromatographic solvents and seem promising for analysis of pharmaceuticals and biomedical compounds.

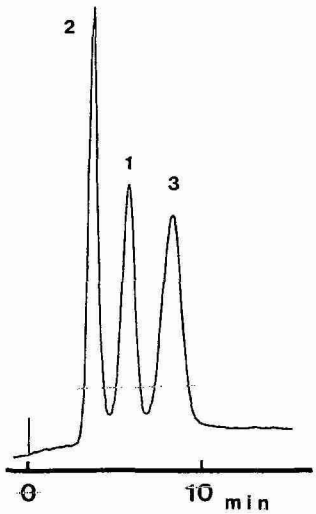

Fig. 3. A chromatogram of a preparation containing aspirin (1), phenacetin (2) and caffeine (3).

REFERENCES

1 R. P. W. Scott and P. Kucera, *J. Chromatogr.*, 169 (1979) 51.
2 R. P. W. Scott and P. Kucera, *J. Chromatogr.*, 185 (1979) 27.
3 R. P. W. Scott, P. Kucera and H. Munroe, *J. Chromatogr.*, 186 (1979) 475.
4 F. J. Yang, *J. Chromatogr.*, 236 (1982) 265.
5 W. Th. Kok, U. A. Th. Brinkman, R. W. Frei, H. B. Hanekamp, F. Nooitgedacht and H. Poppe, *J. Chromatogr.*, 237 (1982) 357.

Journal of Chromatography, 332 (1985) 275–282
Elsevier Science Publishers B.V., Amsterdam — Printed in The Netherlands

CHROMSYMP. 635

SINGLE-COLUMN SEPARATION OF AMINOETHYLCYSTEINE AND OTHER AMINO ACIDS

SHIGETAKE GANNO*, YOSHIMASA HAMANO and JUNKO KOBAYASHI
Naka Works, Hitachi Ltd., 882 Ichige, Katsuta, Ibaraki 312 (Japan)
and
TAKEHARU MASAKI
Faculty of agriculture, Ibaraki University, Ami-machi, Inashiki-gun, Ibaraki 300-03 (Japan)
(First received April 5th, 1985; revised manuscript received May 21st, 1985)

SUMMARY

Analytical conditions for aminoethylcysteine were established with the use of a single-column amino acid analyser equipped with a 150 × 4 mm I.D. column packed with Hitachi custom ion-exchange resin 2617 (5 μm). Using three buffer solutions, twenty amino acids including aminoethylcysteine were separated for analysis. This method was applied to the acid hydrolysate produced by aminoethylation of insulin and lysozyme. The results showed that the method is effective not only for the determination of cysteine but also for acquiring better quantitative data on other amino acids.

INTRODUCTION

The sulphydryl enzyme papain is inactivated through oxidation of cysteine to cystine by oxidative cleavage, and the processing of cystine, which has a disulphide bridge (S–S) in its molecule, has remained a major problem in the analysis of amino acid compositions forming proteins. It has resulted in uneven, incomplete reactions between proteinase and various reagents, and has also required the utmost care in acquiring accurate quantitative values for cysteine and cystine, which is one of the components of proteins.

The S–S bond is cleaved mainly by the following two methods. The first is oxidative cleavage with performic acid, the cystine and cysteine forming a cysteic acid, which can then be subjected to quantitative analysis. However, it requires highly sophisticated techniques and is incapable of determing tryptophan. In the other method, the S–S bond is reducibly cleaved by a reducing agent such as 2-mercaptoethanol, with alkylation to prevent further reaction.

The alkylating agents includes monoiodoacetic acid, acrylonitrile, 4-vinylpyridine and ethyleneimine [or N-(indoethyl)trifluoroacetamine]. Each of them produces cysteines such as S-carboxymethylcysteine, S-cyanoethylcysteine, S-pyridylcysteine and S-aminoethylcysteine. Among these, the S-aminoethylcysteine (AEC) resembles

0021-9673/85/$03.30

lysine in structure, and thus makes enzyme cleavage possible at the AEC position in addition to the lysine or arginine position. This feature greatly facilitates the determination of the arrangement of amino acid components.

In amino acid component analysis, it has been reported that AEC cannot be separated by the conventional method[1]; it can be separated with a basic column using the dual-column method[2,3], and in this instance the analysis should be carried out twice on acidic neutral components and basic components.

It is necessary to have as much sample as possible in order to achieve a high sensitivity for such trace components. Considered from this viewpoint, the single-column method must be regarded as a very efficient method because it requires only half the amount sample.

EXPERIMENTAL

Materials and reagents

S-2-Aminoethyl-L-cysteine hydrochloride, porcine insulin crystals and lysozyme egg white (crystallized six times) were purchased from Sigma (St. Louise, MO, U.S.A.), Shimizu Pharmaceuticals (Tokyo, Japan) and Seikagaku Kogyo (Tokyo, Japan), respectively. Ethyleneimine, purchased from Sogo Pharmaceuticals (Kanagawa, Japan), was used after being distilled. We also purchased urea and 2-mercaptoethanol, of special grade for biochemical analysis, from Nakarai Chemicals (Kyoto, Japan).

Mercaptoethanesulphonic acid purchased from Pierce (Chester, U.K.). All other reagents were of analytical-reagent grade from Wako (Tokyo, Japan).

TABLE I

PREPARATION OF BUFFER SOLUTIONS FOR STANDARD PROTEIN HYDROLYSATE ANALYSIS

Parameter	*Buffer*			
	(1) PH-1, 0.2 M Na	*(2) PH-3, 0.2 M Na*	*(3) PH-4, 1.2 M Na*	*PH-RG (regenerating), 0.2 M Na*
Distilled water	700 ml	700 ml	700 ml	700 ml
Sodium citrate dihydrate	7.74 g	15.7 g	26.67 g	–
Sodium hydroxide	–	–	–	8.0 g
Sodium chloride	7.07 g	2.92 g	54.35 g	–
Citric acid monohydrate	17.7 g	10.50 g	6.10 g	–
Ethanol	60 ml	–	–	–
Benzyl alcohol	–	10.0 ml	5.0 ml	–
Thiodiglycol	5 ml	5 ml	–	–
Brij-35*	4 ml	4 ml	4 ml	4 ml
pH (nominal)	3.3	4.3	4.9	–
Total volume	1 l	1.1 l	1 l	1 l
Caprylic acid	0.1 ml	0.1 ml	0.1 ml	0.1 ml

* Used as dissolved at a ratio of 25 g/100 ml. (Dissolve by heating.)

Chromatographic conditions

We used a Hitachi Model 835 high-speed amino acid analyser[4]. The column (150 × 4 mm I.D.) was packed with Hitachi custom ion-exchange resin 2617 (5 μm). The analytical temperature was set at 40–50°C (stepwise).

Table I shows the eluents used. Aminoethylinsulin was separated into A and B chains with a Hitachi Model 655 high-performance liquid chromatograph with a 150 × 4 mm I.D. column packed with Hitachi Gel 3063 (ODS-silica, 5 μm, 300 Å pore size).

The gradient elution method was adopted with eluents A and B, where A is 0.1% trifluoroacetic acid (TFA) and B is 0.1% TFA–19.9% water–80% isopropyl alcohol–acetonitrile (70:30, v/v).

Sample preparation

Aminoethylation. A 20-mg amount of porcine insulin (3.5 μmol) was dissolved in 1.7 ml of 0.7 *M* Tris–HCl buffer (pH 8.6) containing 0.2% EDTA and 8 *M* urea for aminoethylation. Nitrogen was purged from the insulin, followed by addition of 110 μl (1.47 mmol) of 2-mercaptoethanol, then the solution was reduced at 40°C for 4 h. A total of 420 μl (8.0 mmol) of ethyleneimine was added to the insulin in three separate portions and the solution was incubated at 30°C for 1 h. The pH was then adjusted to 3.0 with acetic acid, followed by dialysis with 0.01 *M* acetic acid and lyophilization, giving 16.4 mg of aminoethylinsulin (AE-insulin). Lysozyme was also aminoethylated[5] as for insulin.

Hydrolysis. Insulin, AE-insulin, A and B chains of AE-insulin and AE-lysozyme were hydrolysed with 6 *M* hydrochloric acid 110°C for 22 h. In order to recover

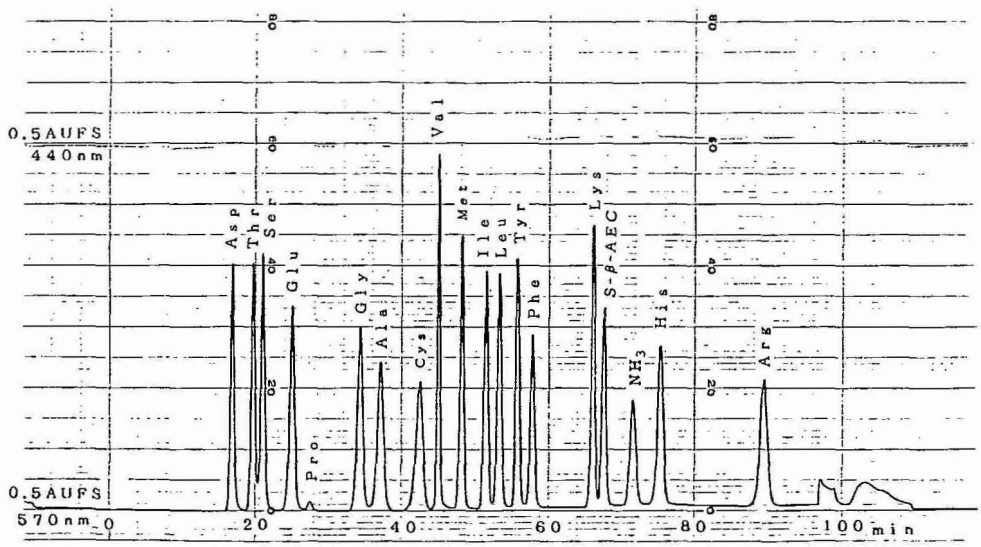

Fig. 1. Analytical chromatogram for amino acids containing AEC. Column: 150 × 4 mm I.D., Hitachi custom ion-exchange resin 2617. Temperature programme: 50°C to 40°C (50 min) to 50°C (60 min). Flow-rates: 0.225 ml/min buffer solution with 2650 NH_3 trap column, 0.3 ml/min ninhydrin solution. Buffer change: PH-1 (0–16 min), PH-3 (16–34 min), PH-4 (34–80 min), PH-RG (80–92 min), PH-1 (92–120 min).

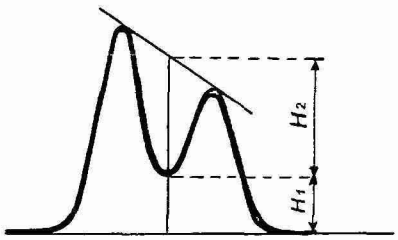

Fig. 2. Calculation of resolution. Resolution (%) = $[H_2/(H_1 + H_2)] \cdot 100$, where H_1 = depth of valley between two adjacent peaks and H_2 = average height of two adjacent peaks.

the tryptophan of AE-lysozyme, it was hydrolysed with mercaptoethanesulphonic acid at 110°C for 22 h.

RESULTS AND DISCUSSION

Separation of AEC and other amino acids

Fig. 1 shows the separation of lysine and AEC by adding 10% ethanol to the third buffer solution and measuring the difference in concentration of the resin surface. The calculation method shown in Fig. 2 indicated that the resolution of lysine and AEC is as high as 94%. The resolution can be further improved by adding 10% ethanol to the second buffer solution. However, the results for isoleucine–leucine and cystine–valine, etc., become poor.

If ornithine is present in the hydrolysate to be used as a sample, *e.g.*, gramicidine, it overlaps with lysine, and no separation will occur under those conditions (10% ethanol). Fig. 3 shows the shift of the elution point of the basic amino acid when 5% water, ethanol and isopropyl alcohol are added to the remaining 5%.

Determining the resolution of Orn–Lys, Lys–AEC and Trp–Arg, the separation of Orn–Lys was the highest (97%) when water was added, and those of Lys–AEC and Trp–Arg were as high as 69% and 94%, respectively, when isopropyl alcohol was added. The test also indicated that all rates of separation are relatively good when isopropyl alcohol is added. Fig. 4 shows the analytical chromatograms of amino acids containing AEC.

When isopropyl alcohol, ethanol, dioxane or tetrahydrofuran (THF) are added in amounts up to 10% to the third buffer solution, Orn and Lys are not separated, *i.e.*, the resolution of Lys and AEC is as high as 94% when 10% ethanol is added.

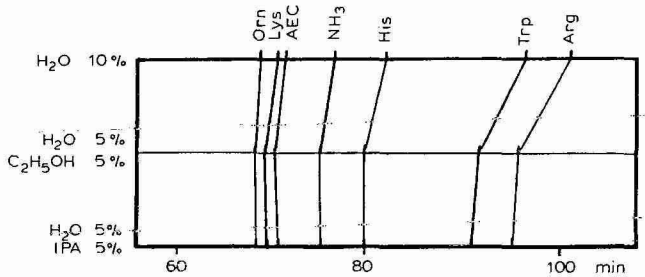

Fig. 3. Shift of basic amino acids on adding alcohols.

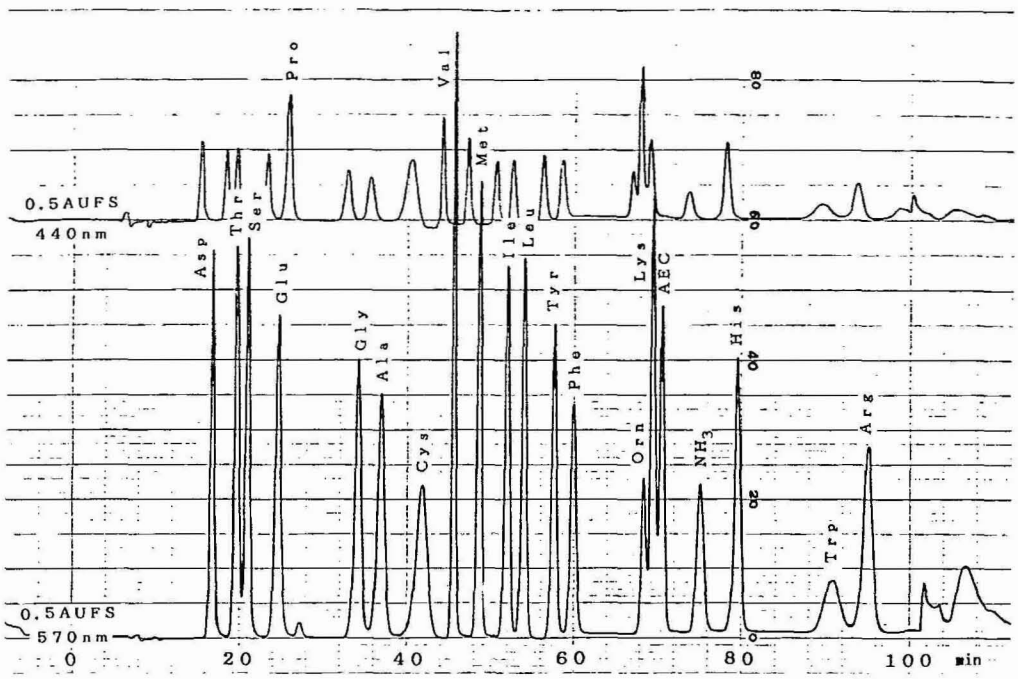

Fig. 4. Analytical chromatograms of amino acids containing Orn, AEC and Trp.

When 10% THF is added the resolution is relatively high (89%), but "leading" is seen on the arginine peak so that this peak overlaps with that of histidine because tryptophan is eluted too fast.

Application to protein

The A and B chains of 2.7 mg of AE-insulin were separated by reversed-phase high-performance liquid chromatography (HPLC) and each was then hydrolysed for amino acid analysis. Fig. 5 shows a chromatogram of 270 μg of AE-insulin obtained by reversed-phase HPLC.

Table II shows the analytical results for amino acid compositions obtained on insulins that had been aminoethylated and not modified by the aminoethylation.

Fig. 6 shows the analytical chromatogram for amino acids present in AE-insulin. In the non-aminoethylated insulin the Ile and Val values are considerably lower than the theoretical values. This indicates that hydrolysis for 22 h at 110°C is not sufficient to hydrolyse them completely. The incomplete separation can be demonstrated by the appearance of unknown peaks other than amino acids, which appear to be partially hydrolysed peptides.

On the other hand, the Ile and Val values of AE-insulin are very close to the theoretical values although the insulin had been hydrolysed under the same conditions. This indicates that the insulin was hydrolysed almost completely by aminoethylation, giving smaller peptides, without applying the conventional external insertion method.

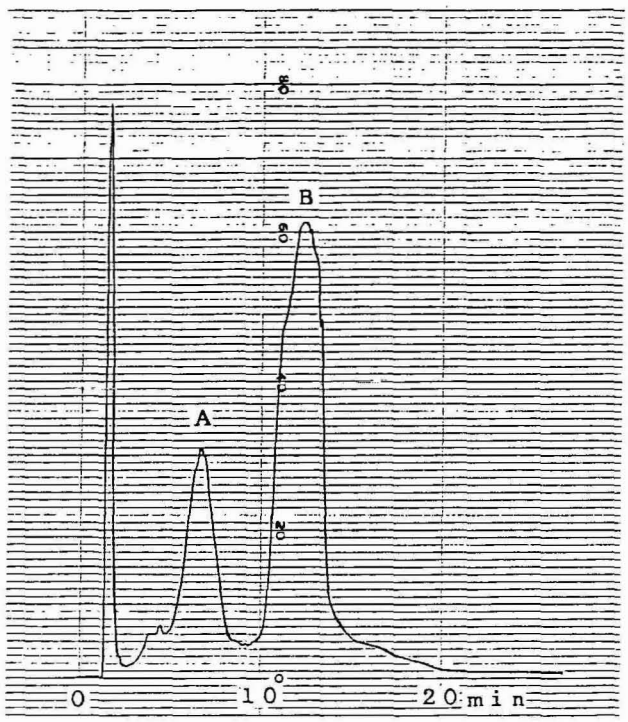

Fig. 5. Chromatogram of (A) A chains and (B) B chains in aminoethylated insulin (270 μg). Column: 150 × 4 mm I.D., Hitachi Gel 3063. Flow-rate: 1.0 ml/min. Eluent: (A) 0.1% TFA in water; (B) 0.1% TFA–19.9% water–80% isopropyl alcohol–acetonitrile (7:3), gradient elution.

TABLE II

ANALYTICAL RESULTS FOR AMINO ACIDS IN INSULIN

Amino acid	*Aminoethylinsulin*				*Insulin*	
	Analytical		*Theoretical*		*Analytical*	*Theoretical*
	A chain	*B chain*	*A chain*	*B chain*		
Asp	2.1	1.1	2	1	3.0	3
Thr	1.0	1.0	1	1	2.1	2
Ser	1.8	1.1	2	1	2.7	3
Glu	4.0	3.1	4	3	6.3	7
Pro	–	1.3	0	1	0.9	1
Gly	0.6	3.0	1	3	4.4	4
Ala	0.0	2.1	0	2	2.1	2
Cys	–	–	0	0	2.0	6
Val	0.7	2.7	1	3	2.2	4
Ile	1.6	0.1	2	0	0.8	2
Leu	2.1	4.1	2	4	5.3	6
Tyr	1.9	1.9	2	2	3.8	4
Phe	0.8	2.6	0	3	3.4	3
Lys	–	0.9	0	1	1.1	1
AEC	3.2	1.8	4	2	–	0
His	–	1.6	0	2	1.6	2
Arg	–	1.0	0	1	1.0	1

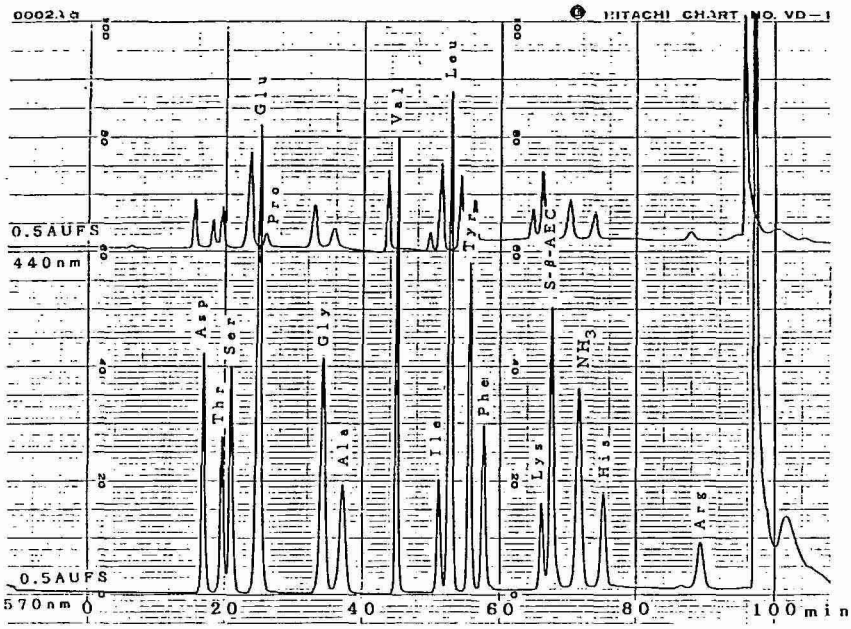

Fig. 6. Amino acid analysis of AE-insulin.

TABLE III

ANALYTICAL RESULTS FOR AMINO ACIDS IN AE-LYSOZYME HYDROLYSATE

Amino acid	*AE-lysozyme hydrolysate*		
	6 N HCl	*Mercaptoethanesulphonic acid*	*Theoretical*
Asp	21.0	21.0	21
Thr	7.0	7.0	7
Ser	9.8	8.9	10
Glu	5.2	5.2	5
Pro	2.1	1.1	2
gly	12.3	12.9	12
Ala	12.3	12.2	12
Val	5.1	6.2	6
Met	1.6	1.8	2
Ile	5.2	5.8	6
Leu	8.2	8.2	8
Tyr	3.0	3.2	3
Phe	3.0	3.5	3
Lys	5.3	5.8	6
AEC	7.7	6.0	8
His	1.0	1.4	1
Trp	2.7	5.5	6
Arg	11.0	10.6	11

As can be seen from Table II, the Glu value is low, *i.e.*, the acid was decomposed considerably in the hydrolysis stage.

Table III shows the ratio of amino acid components when AE-lysozyme was hydrolysed with 6 *M* hydrochloric acid and mercaptoethanesulphonic acid. In both instances the values obtained were similar to the theoretical values.

When hydrolysis was performed with mercaptoethanesulphonic acid, the yields of Trp, Ile, Val and Lys were much higher than those of Pro and AEC. Note that the hydrolysis with mercaptoethanesulphonic acid was performed about 1 month later than that with 6 *M* hydrochloric acid, so the aminoethyl group in the AE-lysozyme hydrolysate might have decomposed before performing the hydrolysis. This can be understood by the fact that the concentration of S-β-AEC aqueous solution is reduced by about 20% after 1 month even if it was stored in a refrigerator.

REFERENCES

1 K. A. Piez and L. Morris, *Anal. Biochem.*,1 (1960) 187.
2 D. H. Spackman, W. H. Stein and S. Moore, *Anal. Chem.*,30 (1958) 1190.
3 M. A. Raftery and R. D. Cole, *J. Biol. Chem.*, 241 (1966) 3457.
4 K. Fujita, S. Takechi and S. Ganno, *Analysis of Food and Beverages*, Vol. 1, Academic Press, New York, 1979, p. 81.
5 S. C. Rall, R. E. Bolinger and R. D. Cole, *Biochemistry*, 8 (1969) 2486.

Journal of Chromatography, 332 (1985) 283–286
Elsevier Science Publishers B.V., Amsterdam — Printed in The Netherlands

CHROMSYMP. 619

SEPARATION OF ASCORBIC ACID, DEHYDROASCORBIC ACID, DIKETOGULONIC ACID AND GLUCOSE BY ISOCRATIC ELUTION FROM A COLUMN OF A HYDROPHILIC GEL

TOKUICHIRO SEKI* and YOSHIHISA YAMAGUCHI
College of Bio-Medical Technology, Osaka University, 1-1, Machikaneyama-cho, Toyonaka Osaka 560 (Japan)
and
KOHJI NOGUCHI and YUZO YANAGIHARA
Asahi Chemical Industry Co., Ltd., 1-3-2, Yakoo Kawasaki-ku, Kawasaki-shi, Kanagawa 210 (Japan)
(Received April 6, 1985)

SUMMARY

High-performance liquid chromatography on an Asahipak GS-320 hydrophilic gel column with tartrate buffer (0.015 *M*, pH 3.0) containing 2 m*M* ethylenediaminetetraacetate and 0.05% β-thiodiglycol as the eluent allowed the separation of glucose, diketogulonic acid, dehydroascorbic acid and ascorbic acid within 30 min. Fluorimetric monitoring of these compounds in the eluate with benzamidine at alkaline pH and at 90°C in the presence of potassium sulphite allowed the determination of nanogram amounts of ascorbic acid, dehydroascorbic acid and diketogulonic acid. This method was applied to the determination of ascorbic acid in fruit juice.

INTRODUCTION

The separation of ascorbic acid, dehydroascorbic acid, diketogulonic acid and their C-5 epimers has been performed by ion-exchange chromatography on a weakly basic ion exchanger using acetonitrile–0.05 *M* potassium dihydrogen phosphate solution (3:1, v/v) as eluent[1] and a mobile phase containing less organic component was used for the determination of ascorbic acid and isoascorbic acid in fruit juice[2]. The separation of these compounds was also possible by ion-pair chromatography on a reversed-phase column[3,4]. Ascorbic acid in eluates has been detected electrochemically[5,6] and from its characteristic absorption at 265 nm[1–4]. The formation of a fluorophor by condensation of dehydroascorbic acid with *o*-phenylenediamine[7,8] was utilized for pre-column derivatization to determine dehydroascorbic acid and isodehydroascorbic acid in foodstuffs by a high-performance liquid chromatography (HPLC) method[9].

We have recently found that pyrimidine bases that have a six-membered ring with a conjugated double bond could be separated from each other by isocratic

0021-9673/85/$03.30

elution from a column of a hydrophilic gel, Asahipak GS-320, using an aqueous buffer as the eluent[10]. As ascorbic acid has a five-membered ring with a conjugated double bond, we tried to separate ascorbic acid from dehydroascorbic acid and diketogulonic acid, and a good separation was obtained at pH 3.0 using dilute tartrate buffer containing ethylenediaminetetraacetate (EDTA) and β-thiodiglycol as the mobile phase. A fluorimetric method using benzamidine as the post-column derivatizing agent[11] allowed the simultaneous determination of ascorbic acid, dehydroascorbic acid, diketogulonic acid and glucose.

EXPERIMENTAL

Materials and solutions

All chemicals were of analytical-reagent grade (Yashima Pharmaceutical, Osaka, Japan) and water was of ultrapure grade prepared by reverse osmosis (RO-pure 40; Barnstead, Boston, MA, U.S.A.), ion exchange and charcoal adsorption of organic matter (NANOpure-II; Barnstead).

The mobile phase was prepared by dissolving 4.5 g of tartaric acid, 1.5 g of EDTA and 1 g of β-thiodiglycol in 2 l of ultrapure water and adjusting the pH to 3.0 with 4 *M* sodium hydroxide solution. The solution was filtered through a membrane filter (pore size 0.45 μm) and degassed under vacuum before use.

The primary stock solution of ascorbic acid was prepared by dissolving 20 mg of ascorbic acid in 100 ml of mobile phase. Secondary standards were prepared by diluting the stock solution with the mobile phase to give solutions containing 1, 2, 4, 10 or 20 mg/l of ascorbic acid. These standard solutions were prepared daily.

Dehydroascorbic acid was prepared by oxidation of ascorbic acid with bromine water. Ten milligrams of ascorbic acid were dissolved in 10 ml of water and bromine water was added drop by drop until a slight yellow colour remained. Excess of bromine was destroyed by addition of three drops of a 2% (w/v) solution of β-thiodiglycol and the pH of the mixture was adjusted to 2.5 with 0.5 *M* sodium hydroxide solution. The mixture was diluted with water to 50 ml and an aliquot of the solution was diluted with mobile phase to give a solution of 4 mg/l. This was analysed immediately.

Diketogulonic acid was prepared by hydrolysis of dehydroascorbic acid.

The solution of oxidized ascorbic acid described above was neutralized to pH 7 with 0.5 *M* sodium hydroxide at 30°C. The solution was then diluted to 50 ml with water and an aliquot of the solution was diluted with mobile phase to give a solution of 2 mg/l.

Reagent A was a solution of benzamidine hydrochloride (0.02 *M*) and reagent B was potassium borate buffer of pH 10 (0.25 *M*) containing 0.25 *M* potassium sulphite.

Equipment

The chromatography system consisted of a constant delivery pump (Trirotar III; Jasco, Japan), an automatic injector (Model KSST 60J; Kyowa Seimitsu, Japan) and a column of hydrophilic gel (Asahipak GS-320, 50 × 0.76 cm I.D.; Asahi Chemical, Japan). A dual-head pump (Model SP-024-2; Jasco) was used to pump the reagents and mix them with the eluate. A Model FP-210 spectrophotometer (Jasco, Japan) equipped with a flow cell (volume 15 μl) was used to monitor fluorescence.

Preparation of mixed bed column

Amberlite CG-50 was graded according to size, washed as described previously[12] and converted into the hydrogen ion form. Amberlite XAD-2 was washed with methanol on a glass filter until the absorbance of the effluent became 0.2 and then washed with water. Equal volumes of Amberlite CG-50 and XAD-2 were mixed, washed with mobile phase and stored in it. The mixed resin was poured into a chromatographic tube (10 × 0.6 cm I.D. with a 5-ml reservoir) and allowed to settle under gravity to form a resin bed 2 cm high.

Purification of fruit juice

A 1-ml volume of orange juice was placed on a mixed-bed column and, after the sample had passed into the column, it was washed with 4 ml of mobile phase. The effluent was collected in a 50-ml measuring flask and diluted with mobile phase to 50 ml. A volume of 10 μl of the sample was used for analysis.

Chromatographic separation and fluorimetric determination

A 10–50-μl volume of standard or sample solution was injected into an Asahipak GS-320 column maintained at 30°C. The mobile phase was pumped at a flow-rate of 1.0 ml/min and the eluate was mixed using a T-shaped connector with a 1:1 mixture of reagents A and B. Reagents A and B were pumped with a dual-head pump at a flow-rate of 0.4 ml/min each and mixed using a T-shaped connector. The mixture was heated at 90°C in a PTFE tube (length 30 m, I.D. 0.5 mm, O.D. 1.5 mm) immersed in a water-bath. Fluorescence was measured with excitation at 325 nm and emission at 400 nm.

RESULTS AND DISCUSSION

As shown in Fig. 1, glucose, diketogulonic acid, dehydroascorbic acid and ascorbic acid were eluted in that order within 30 min. Optimum of the four com-

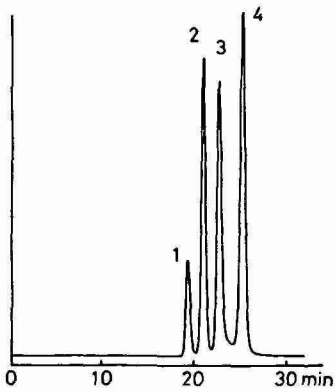

Fig. 1. Elution pattern of glucose, diketogulonic acid, dehydroascorbic acid and ascorbic acid. Peaks: 1 = glucose (3000 ng); 2 = diketogulonic acid (33 ng); 3 = dehydroascorbic acid (30 ng); 4 = ascorbic acid (120 ng). As 1–2% of dehydroascorbic acid and diketogulonic acid were detected in freshly prepared samples of ascorbic acid and dehydroascorbic acid, respectively, the heights of peaks 2 and 3 will be greater than those given by pure samples.

pounds was achieved at pH 3.0. The elution volumes of diketogulonic acid and ascorbic acid were sensitive to changes in the pH of the mobile phase, but those of glucose and dehydroascorbic acid were not. Therefore, at lower pH, the separation of glucose from diketogulonic acid and ascorbic acid from dehydroascorbic acid was improved, whereas diketogulonic acid and dehydroascorbic acid were eluted closer together. At higher pH, the reverse was observed. The optimum pH for the reaction of ascorbic acid with benzamidine to form fluorescent compound(s) was 9.1–9.2. The peak height of ascorbic acid was reproducible. When 40 ng of ascorbic acid were injected, the mean peak height was 83.5 ± 1.2 mm (S.D.) (six determinations), and a linear relationship between peak height and amount of ascorbic acid injected was observed over the range 5–500 ng.

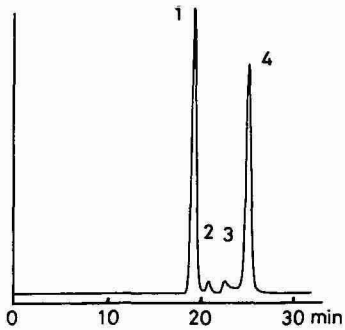

Fig. 2. Elution pattern of an extract of orange juice. Volume of extract injected, 10 μl. Peaks as in Fig. 1.

The elution pattern of the orange juice extract is shown in Fig. 2. The elution volume of the last peak corresponds to that of ascorbic acid, and from the peak height of the last peak the amount of ascorbic acid in the orange juice was calculated to be 40 mg per 100 ml. As ascorbic acid is eluted isocratically from Asahipak GS-320, regeneration of the column is not necessary. Therefore, this method will be useful for the routine determination of ascorbic acid in juice samples. The application of this method to the determination of ascorbic acid, dehydroascorbic acid and diketogulonic acid in other biological samples will be reported later.

REFERENCES

1 L. W. Doner and K. B. Hicks, *Anal. Biochem.*, 115 (1981) 225.
2 J. Geigert, D. S. Hirano and S. L. Neidleman, *J. Chromatogr.*, 206 (1981) 396.
3 J. W. Finley and E. Duang, *J. Chromatogr.*, 207 (1981) 449.
4 J. M. Coustard and G. Sudroud, *J. Chromatogr.*, 219 (1981) 338.
5 L. A. Pachla and P. T. Kissinger, *Methods Enzymol.*, 62 (1979) 15.
6 W. D. Mason, E. N. Amick and W. Heft, *Anal. Lett.*, 13 (1980) 817.
7 J. R. Kirk and N. Ting, *J. Food Sci.*, 40 (1975) 463.
8 D. C. Egberg, R. H. Potter and J. C. Heroff, *J. Ass. Offic. Anal. Chem.*, 60 (1977) 126.
9 A. J. Speek, J. Schrijver and W. H. P. Schreurs, *J. Agr. Food Chem.*, 32 (1984) 352.
10 K. Yasukawa, M. Kasai, Y. Yanagihara and K. Noguchi, in T. Fujii (Editor), *Nucleic Acids Symposium Series*, No. 15, IRL Press, Oxford, 1984, p. 109.
11 T. Seki, Y. Yamaguchi, M. Kamimori and H. Sato, *Studies in Natural Science and Health Technology*, College of Bio-Medical Technology and Nursing, Osaka University, Osaka, 1982, Vol. 10, p. 51 (in Japanese).
12 T. Seki and H. Wada, *J. Chromatogr.*, 114 (1975) 227.

Journal of Chromatography, 332 (1985) 287–295
Elsevier Science Publishers B.V., Amsterdam — Printed in The Netherlands

CHROMSYMP. 639

HIGH-PERFORMANCE LIQUID CHROMATOGRAPHIC ANALYSIS OF PEPTIDES ON AN ASAHIPAK GS-320 COLUMN PACKED WITH HYDROPHILIC POLYMER GEL

KEIKO YASUKAWA*, MASAO KASAI, YUZO YANAGIHARA and KOHJI NOGUCHI
Technology and Development Department, Ion Exchange Membrane Administration, Asahi Chemical Industry Co., Ltd., 1-3-2, Yakoo Kawasaki-ku, Kawasaki-shi 210 (Japan)
(First received April 8th, 1985; revised manuscript received May 28th, 1985)

SUMMARY

Investigation of the chromatographic characteristics of various amino acids and peptides on an Asahipak GS-320 column, developed for high-performance gel filtration chromatography, revealed that these substances, which possess hydrophobic sites, are retained by adsorption and eluted in order of increasing hydrophobicity. The use of organic solvents as eluents was studied and practical separations of amino acids and peptides by isocratic elution were obtained.

INTRODUCTION

The analysis of peptides by high-performance liquid chromatography (HPLC) is generally performed on reversed-phase columns containing chemically bonded silica gels[1]. In previous papers[2,3] we described practical separations of sera, urine and erythrocyte components without prior deproteination on the Asahipak GS series of HPLC columns, packed with hydrophilic polymer gels, which were developed for the analysis of physiological substances[4,5]. We also reported the retention mechanism to be mainly gel filtration for hydrophilic substances of high molecular weight, such as proteins, polysaccharides and nucleic acids, and adsorption for hydrophobic substances of low molecular weight, such as nucleobases and nucleosides[6]. This paper describes the chromatographic characteristics of amino acids and peptides for an Asahipak GS-320 column.

EXPERIMENTAL

Chromatography was performed with a Hitachi 638-50 high-speed liquid chromatograph, equipped with a Jasco Uvidec-100-IV UV detector operated at 210 nm. Asahipak GS-320 (500 × 7.6 mm I.D.) or GS-320H (250 × 7.6 mm I.D.) columns (Asahi Chemical Industry) were employed. The flow-rate was 1.0–2.0 ml/min and the other chromatographic conditions were varied.

Amino acids were obtained from Kyowa Hakkou Kogyo, peptides from Pep-

0021-9673/85/$03.30

tide Institute or Serva and proteins from Sigma. Other reagents were obtained from Wako. The organic solvents used were of HPLC grade.

The effect of alkali solution on the column performance was determined by measurement of the number of theoretical plates (N) and peak asymmetry (A_s) of the creatinine peaks obtained with 0.1 M sodium phosphate (pH 7.0) containing 0.3 M NaCl as eluent at 1 ml/min and 30°C, before and after the passage of 0.01 M NaOH solution (pH 12.1) containing 0.1 M NaCl at 1 ml/min for 16 h through the GS 320 column (500 × 7.6 mm I.D.).

The resistance of the column to degradation by organic solvents was determined by measurement of the N and A_s of the ethylene glycol peaks using distilled water as the eluent at 1 ml/min and 30°C, before and after the passage of an aqueous organic solution or an organic solvent at 1 ml/min for 2 h through the GS-320 column (500 × 7.6 mm I.D.).

N (4σ) and N (5σ) were calculated by the equations N (4σ) = $16/1.7^2$ $(\bar{V}_R/W_{0.5})^2$ and N (5σ) = 5^2 $(\bar{V}_R/W_{0.044})^2$, where $W_{0.5}$ and $W_{0.044}$ are the width of the band at half-height and 4.4% height of the peak, respectively.

Peak asymmetries were calculated by the equation $A_s = (b/a)^2$, where b is the distance at 4.4% peak height from the tailing end to the perpendicular from the peak maximum to the baseline, and a is the distance from the front end of the peak to the perpendicular.

The protein and peptide recoveries were determined by comparison of the eluted peak areas obtained by passage of isocratic eluent through the GS-320H column (250 × 7.6 mm I.D.) or the GS-320 column (500 × 7.6 mm I.D.) at 1 ml/min and 30°C with those obtained when the same amount (10–25 μg) of each protein or peptide was injected under the same conditions into aproximately 10 m of tightly coiled 0.5 mm I.D. PTFE tubing.

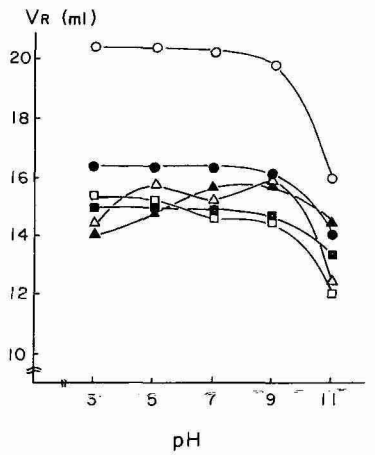

Fig. 1. Influence of pH on elution volume of amino acids. column: Asahipak GS-320 (500 × 7.6 mm I.D.). Sample: ○, phenylalanine; ●, leucine; □, glutamic acid; ■, serine; △, arginine; ▲, histidine, 10 μl (10 μg). Mobile phase: 50 mM sodium phosphate buffer (pH 3.0, 5.0, 7.0, 9.0 and 11.0). Flow-rate: 1 ml/min. Detection: UV at 210 nm. Temperature: 30°C.

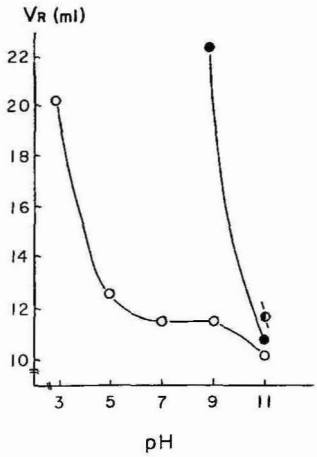

Fig. 2. Influence of pH on elution volume of insulin, insulin A chain and insulin B chain. Sample: ●, insulin; ◑, insulin B chain; ○, insulin A chain. Chromatographic conditions as in Fig. 1.

RESULTS

Influence of pH on retention

The relationship between the eluted volume (V_R) of amino acids and the pH of the eluents on the GS-320 column is shown in Fig. 1. The hydrophobic amino acids, phenylalanine and leucine, were more strongly retained. The elution volume of each amino acid decreased with increasing pH. The basic amino acids, arginine and histidine, were eluted early at both low and high pH.

The effects of eluent pH on the retention of insulin, insulin B chain and insulin A chain are shown in Fig. 2. The insulin and the insulin B chain, which have strong hydrophobic sites, were adsorbed and not eluted at low pH, but were eluted at high pH.

The primary structures of angiotensin I, II and III are shown in Fig. 3. Their early elution at both low and high pH (Fig. 4) may be closely related to their relatively high content of basic amino acids, such as arginine and histidine.

Throughout the investigation of the effect of pH on the eluted volume of amino acids and peptides, with eluent solutions ranging from low to high pH, no degradation of the column or significant changes in the chromatograms were observed.

Table I shows the N and A_s values before and after the passage of alkali solution (pH 12.1). As the results show, alkali solutions had no adverse effect on the column performance.

Angiotensin I	Asp–Arg–Val–Tyr–Ile–His–Pro–Phe–His–Leu
Angiotensin II	Asp–Arg–Val–Tyr–Ile–His–Pro–Phe
Angiotensin III	Arg–Val–Tyr–Ile–His–Pro–Phe

Fig. 3. Primary structures of angiotensin I, II and II.

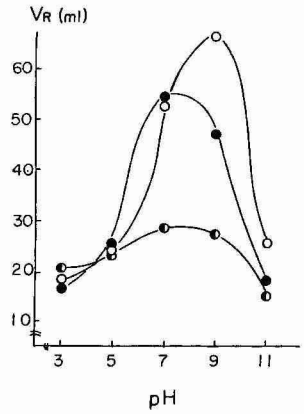

Fig. 4. Influence of pH on elution volume of angiotensin I, II and III. Sample: ●, angiotensin I; ◑, angiotensin II; ○, angiotensin III. Chromatographic conditions as in Fig. 1.

Influence of acetonitrile concentration on retention

The influence of the acetonitrile concentration on retention is shown in Fig. 5. The retention of peptides generally decreased drastically with the addition of acetonitrile to 50 m*M* phosphate buffer (pH 7.0). The insulin B chain, which exhibits high hydrophobicity and was not eluted without acetonitrile, was eluted in approximately 20 min on addition of 5% of acetonitrile to the buffer.

The elution of these peptides approached the polyethylene glycol calibration graph values with high concentrations of acetonitrile. However, for the effective separation of peptides of similar molecular weight, an acetonitrile concentration of several to 20% appears sufficient.

Applicable concentrations of organic solvents

The efficiency (capacity) of the Asahipak GS-320 column was evaluated from changes in N (4σ, 5σ) and A_s of ethylene glycol before and after the use of organic solvents, with the results shown in Table II. No significant change in column performance was observed for most of the solvents, which are indicated by ticks in Table II. Where a decline in performance did occur, with the solvents indicated by crosses in Table II, it appeared to be the result of changes in the packing conformation rather than any chemical change in the gel particles. These results suggest that the column

TABLE I

CHANGE IN COLUMN EFFICIENCY WITH THE USE OF ALKALINE SOLUTION AS ELUENT

Column, Asahipak GS-320 (500 × 7.6 mm I.D.); eluent, 0.1 m*M* sodium phosphate containing 0.3 *M* sodium chloride (pH 7.0); flow-rate, 1 ml/min; sample, creatinine, 20 μl (20μg); detection, UV at 250 nm; temperature, 30°C.

Alkali solution	*Column pressure (kg/cm²)*	*N (4σ)*	*N (5σ)*	A_s
Before	33	19800	15800	1.32
After	34	19800	15800	1.32

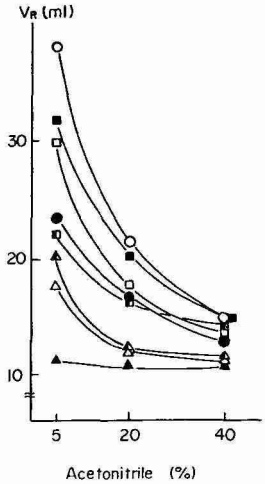

Fig. 5. Effect of acetonitrile concentration on peptide elution volume. Sample: ○, met-enkephalin; ●, leu-enkephalin □, angiotensin I; ◧, angiotensin II; ■, angiotensin III; △, insulin; ▲, insulin B chain; ▲, insulin A chain. Mobile phase: acetonitrile–50 m*M* sodium phosphate buffer (pH 7.0) (5:95, 20:80 and 40:60). Other conditions as in Fig. 1.

efficiency deteriorates when organic solvents that cause gel shrinkage are used, but that it is maintained when organic solvents of relatively high viscosity are used or when an increased column pressure occurs as a result of gel swelling.

With the Asahipak GS-320 column it was thus found possible to use methanol, ethanol, acetonitrile and *n*-propanol, the first two at concentrations of up to 100% and the last two at up to 50% (aqueous solutions). The acetonitrile concentration appropriate for the adsorption chromatography of peptides on this column is 20% or less, and no problem is expected in the practical use of organic solvents, including acetonitrile and tetrahydrofuran, with the column. All of these are commonly used in the analysis of peptides.

Influence of temperature on peptide analysis

Rapid, isocratic separations of α-, β- and γ-endorphin standards were obtained, as shown in Fig. 6. The separations were performed at 30, 40 and 50°C. To reduce the time necessary for analysis, a short column and an eluent flow-rate of 2 ml/min were utilized. Improved chromatograms were obtained at the higher temperatures, owing to decreased peak widths.

Recovery of proteins and peptides

The GS 320 column gave excellent recoveries of proteins and peptides, as indicated by the results in Tables III and IV.

Practical applications

As one practical application, the concurrent isocratic separation of various hydrophilic and hydrophobic dipeptides, such as Arg–Asn and Leu–Tyr, was carried out, as shown in Fig. 7. It was also found possible to separate isomers, such as Trp–Glu and Glu–Trp.

TABLE II

CHANGE IN COLUMN EFFICIENCY WITH THE USE OF ORGANIC SOLVENTS AS ELUENT

Column, Asahipak GS-320 (500 × 7.6 mm I.D.); low-rate, 1-ml/min; temperature, 30°C.

Eluent	*Concentration (%)*	*η (cP)*	*Pressure drop (kg/cm²)*	*Column efficiency*		*Fitness for use*
				Before use	*After use*	
Methanol	50	1.34	63	18900 (N 4σ) 14100 (N 5σ) 1.7 (A_s)	19900 (N 4σ) 14400 (N 5σ) 1.7 (A_s)	V
	100	0.56	24	18900 (N 4σ) 14100 (N 5σ) 1.7 (A_s)	19900 (N 4σ) 14400 (N 5σ) 1.7 (A_s)	V
Ethanol	50	2.02	136	23300 (N 4σ) 17100 (N 5σ) 0.7 (A_s)	23200 (N 4σ) 16200 (N 5σ) 0.7 (A_s)	V
	100	1.00	56	23300 (N 4σ) 17100 (N 5σ) 0.7 (A_s)	23200 (N 4σ) 16200 (N 5σ) 0.7 (A_s)	V
Acetonitrile	50		47	21900 (N 4σ) 12600 (N 5σ) 0.2 (A_s)	21200 (N 4σ) 11500 (N 5σ) 0.3 (A_s)	V
	100	0.33	14	24100 (N 4σ) 17100 (N 5σ) 0.5 (A_s)	24400 (N 4σ) 6700 (N 5σ) 0.1 (A_s)	×
Tetrahydrofuran	100	0.47	22	25300 (N 4σ) 19800 (N 5σ) 0.7 (A_s)	21600 (N 4σ) 11000 (N 5σ) 0.3 (A_s)	×
Acetone	100	0.29	11	21800 (N 4σ) 13800 (N 5σ) 0.4 (A_s)	23700 (N 4σ) 4800 (N 5σ) 0.1 (A_s)	×
n-Propanol	50		104	24600 (N 4σ) 16200 (N 5σ) 1.4 (A_s)	24500 (N 4σ) 18200 (N 5σ) 0.9 (A_s)	V
Distilled water	—	0.80	34	> 16000 (N 4σ) > 1000 (N 5σ) 0.5–3.0 (A_s)	standard value	V

TABLE III

RECOVERY OF PROTEINS

Column, Asahipak GS-320H (250 × 7.6 I.D.); eluent, 0.1 *M* sodium phosphate containing 0.3 *M* sodium chloride (pH 7.0); flow-rate, 1 ml/min; sample, 25 μl (25 μg) standard; detection, UV at 210 nm; temperature, 30°C.

Protein	*Recovery (%)*
Ovalbumin	93
Myoglobin	92
Lysozyme	95
Cytochrome C	86

TABLE IV

RECOVERY OF PEPTIDES

GS-320 column for insulin, insulin A and insulin B and GS-320H column for leu- and met-enkephalin and angiotensin I, II and III; 50 m*M* sodium phosphate (pH 7.0)–methanol (80:20) eluent for insulin, insulin A and insulin B, 50 m*M* sodium phosphate (pH 7.0)–*n*-propanol (80:20) eluent for leu- and met-enkephalin and 50 m*M* sodium phosphate (pH 3.0) for angiotensin I, II and III; flow-rate, 1 ml/min; sample, 10 μl (10 μg); detection, UV at 210 nm; temperature, 30°C.

Peptide	*Recovery (%)*
leu-Enkephalin	82
met-Enkephalin	91
Angiotensin I	97
Angiotensin II	98
Angiotensin III	98
Insulin A	95
Insulin B	94
Insulin	106

Another application was the analysis of RNase F_1 digested with trypsin and chymotrypsin, using 0.1 *M* acetic acid solution as the eluent[7]. The results are shown in Fig. 8. RNase F_1 was digested with trypsin for 14 h at 37°C and then with chymotrypsin for 1 h at 37°C. The faster eluted peak (A) represents trypsin and chymotrypsin and the shoulder peak (B), indicated by the vertical arrow, represents undigested RNase F_1. It was therefore possible to analyse the mixture of peptides and proteins on this column with a single injection and no prior deproteination.

The performance of the column was found to be highly stable even with repeated direct injections of mixed protein solutions, without a guard column. No significant change appeared in the chromatograms of as many as 400 directly injected samples of the above mixed protein solutions. Similarly, no observable change was found in the chromatograms for 300 injections of 20-μl samples of undiluted and otherwise untreated human blood serum with 0.1 *M* sodium phosphate containing 0.3 *M* NaCl as the (pH 7.0).

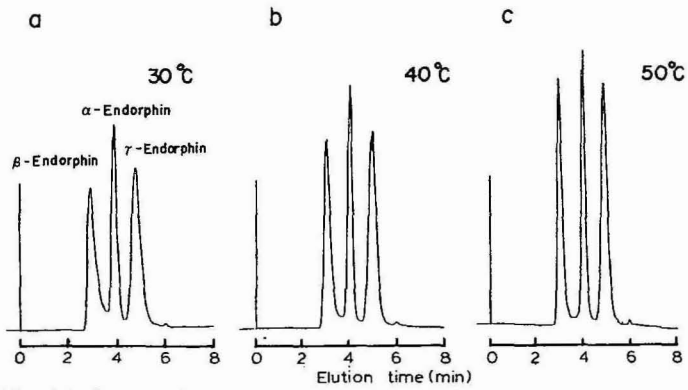

Fig. 6. Influence of temperature on separation of α-, β- and γ-endorphin. Column: Asahipak GS-320H (250 × 7.6 mm I.D.). Sample: mixture of α-, β- and γ-endorphin standards, 5 μl (5 μg) each. Mobile phase: 0.1% trifluoracetic acid–acetonitrile (95:5). Flow-rate: 2 ml/min. Detection: UV at 210 nm. Temperature: (a) 30°C; (b) 40°C; (c) 50°C.

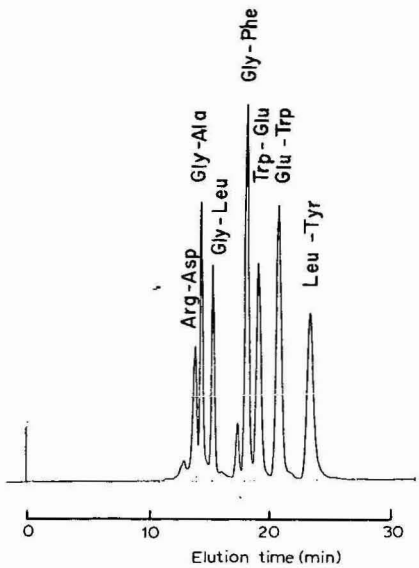

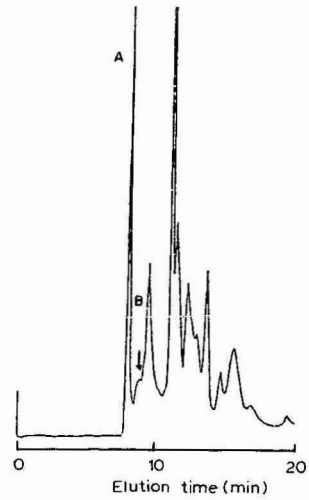

Fig. 7. Separation of a variety of dipeptides. Column: Asahipak GS-320. Sample: mixture of dipeptides, 5 μl (5 μg). Mobile phase: 50 m*M* sodium phosphate buffer (pH 7.0) (isocratic). Flow-rate: 1 ml/min. Detection: UV at 210 nm. Temperature: 30°C.

Fig. 8. Analysis of fractions of RNase F_1 digested by trypsin and chymotrypsin. Column: Asahipak GS-320. Sample: digested fractions of RNase F_1, 10 μl. Mobile phase: 0.1 *M* acetic acid. Flow-rate: 1 ml/min. Detection: UV at 280 nm. Temperature: ambient. (Chromatogram provided by courtesy of Dr. Hiroshi Yoshida).

DISCUSSION

It was found that the Asahipak GS-320 column is capable of the concurrent analysis of various peptides and proteins with molecular weights ranging from 100 to 100000. Because of the hydrophilicity of the gel, originating from its hydroxy groups, the recovery of protein and peptides was high and hydrophobic peptides were eluted with a small addition of organic solvent. In contrast to reversed-phase columns, packed with silica-based gels, the GS-320 column remains effective with alkaline eluents, because it is packed with hydrophilic polymer gel.

When a peptide sample containing proteins was injected into the column, the proteins of high molecular weight were eluted first by gel filtration and the peptides were then separated by adsorption chromatography. It was therefore possible to analyse a mixture of peptides and proteins without prior deproteination, which we refer to as "intra-column deproteination".

Based on these chromatographic characteristics of GS-320, we conclude that it will be effective particularly in the analysis of crude samples, such as digested peptides and extracts of bacteria.

REFERENCES

1 M. T. W. Hearn and B. Grego, *J. Chromatogr.*, 255 (1983) 125–136.
2 H. Wada, K. Makino, T. Takeuchi, H. Hiroyuki and K. Noguchi, *J. Chromatogr.*, 320 (1985) 369–377.
3 K. Noguchi, N. Imai, Y. Yanagihara and M. Kasai, paper presented at the Fourth Annual Conference on Liquid Chromatography, Tokyo, 1983.
4 M. Kasai, N. Itoh, Y. Yanagihara and K. Noguchi, paper presented at the 27th Seminar of The Research Group on Automatic Liquid Chromatography, Kyoto, 1984.
5 K. Yasukawa, M. Kasai, Y. Yanagihara and K. Noguchi, paper presented at the First Mini Seminar (62nd Seminar) on Liquid Chromatography, Tokyo, 1984.
6 K. Yasukawa, M. Kasai, Y. Yanagihara and K. Noguchi, *Nucleic Acids Res.*, 12 (1984) 109–112.
7 J. Hirabayashi and H. Yoshida, *Biochem. Int.*, 7 (1983) 255–262.

Author Index

PUBLICATION SCHEDULE FOR 1985

Journal of Chromatography (incorporating *Chromatographic Reviews*) and *Journal of Chromatography, Biomedical Applications*

MONTH	N 1984	D 1984	J 1985	F	M	A	M	J	J	A	S	O	N	D
Journal of Chromatography	312 314	315 316 317	318/1 318/2 319/1	319/2 319/3 320/1	320/2 321/1 321/2 322/1	322/2 322/3 323/1 323/2	324/1 324/2 325/1	325/2 326 327 328	329/1 329/2 329/3	330/1 330/2 331/1	331/2 332 333/1	333/2		
Chromatographic Reviews		313				334/1				334/2			334/3	
Bibliography Section				335/1		335/2		335/3		335/4		335/5		335/6
Biomedical Applications		336/1 336/2	337/1	337/2 338/1	338/2	339/1	339/2 340 341/1	341/2	342/1	342/2	343/1	343/2	344 345/1	345/2

INFORMATION FOR AUTHORS

(Detailed *Instructions to Authors* were published in Vol. 329, No. 3, pp. 449–452. A free reprint can be obtained by application to the publisher.)

Types of Contributions. The following types of papers are published in the *Journal of Chromatography* and the section on *Biomedical Applications:* Regular research papers (Full-length papers), Short communications and Notes. Short communications are preliminary announcements of important new developments and will, whenever possible, be published with maximum speed. Notes are usually descriptions of short investigations and reflect the same quality of research as Full-length papers, but should preferably not exceed four printed pages. For review articles, see page 2 of cover under Submission of Papers.

Submission. Every paper must be accompanied by a letter from the senior author, stating that he is submitting the paper for publication in the *Journal of Chromatography.* Please do not send a letter signed by the director of the institute or the professor unless he is one of the authors.

Manuscripts. Manuscripts should be typed in double spacing on consecutively numbered pages of uniform size. The manuscript should be preceded by a sheet of manuscript paper carrying the title of the paper and the name and full postal address of the person to whom the proofs are to be sent. Authors of papers in French or German are requested to supply an English translation of the title of the paper. As a rule, papers should be divided into sections, headed by a caption (*e.g.,* Summary, Introduction, Experimental, Results, Discussion, etc.). All illustrations, photographs, tables, etc., should be on separate sheets.

Introduction. Every paper must have a concise introduction mentioning what has been done before on the topic described, and stating clearly what is new in the paper now submitted.

Summary. Full-length papers and Review articles should have a summary of 50–100 words which clearly and briefly indicates what is new, different and significant. In the case of French or German articles an additional summary in English, headed by an English translation of the title, should also be provided. (Short communications and Notes are published without a summary.)

Illustrations. The figures should be submitted in a form suitable for reproduction, drawn in Indian ink on drawing or tracing paper. Each illustration should have a legend, all the *legends* being typed (with double spacing) together on a *separate sheet.* If structures are given in the text, the original drawings should be supplied. Coloured illustrations are reproduced at the author's expense, the cost being determined by the number of pages and by the number of colours needed. The written permission of the author and publisher must be obtained for the use of any figure already published. Its source must be indicated in the legend.

References. References should be numbered in the order in which they are cited in the text, and listed in numerical sequence on a separate sheet at the end of the article. Please check a recent issue for the layout of the reference list. Abbreviations for the titles of journals should follow the system used by *Chemical Abstracts.* Articles not yet published should be given as "in press", "submitted for publication", "in preparation" or "personal communication".

Dispatch. Before sending the manuscript to the Editor please check that the envelope contains three copies of the paper complete with references, legends and figures. One of the sets of figures must be the originals suitable for direct reproduction. Please also ensure that permission to publish has been obtained from your institute.

Proofs. One set of proofs will be sent to the author to be carefully checked for printer's errors. Corrections must be restricted to instances in which the proof is at variance with the manuscript. "Extra corrections" will be inserted at the author's expense.

Reprints. Fifty reprints of Full-length papers, Short communications and Notes will be supplied free of charge. Additional reprints can be ordered by the authors. An order form containing price quotations will be sent to the authors together with the proofs of their article.

Advertisements. Advertisement rates are available from the publisher on request. The Editors of the journal accept no responsibility for the contents of the advertisements.

THEORY, PRACTICE AND APPLICATIONS of

MICROCOLUMN HIGH PERFORMANCE LIQUID CHROMATOGRAPHY

P. Kucera, *Pharmaceutical Research Products Section, Hoffmann-La Roche Inc., Nutley, NJ, USA (editor)*

Journal of Chromatography Library 28

This is the only book currently available that covers the large diverse subject of microcolumn chromatographic techniques in such a way as to satisfy, both the practical and the theoretical needs of analytical chemists and chromatographers.

The distinguished research workers and university professors who have contributed to this important work have adopted a textbook type approach to the discussion of the theoretical aspects of new microcolumn techniques. The practical coverage includes instrumentation, design, columns, detectors, injectors, connecting tubing, gradient elution and special analytical techniques, LC-MS, derivatization, etc. and applications are described using various compounds (e.g. drugs, substances of biological origin, proteins, nucleotides, industrial extracts).

The book represents a vast amount of information collected over a period of many years of intensive work and is an essential acquisition for all those who need to keep up-to-date with the latest developments in microcolumn techniques.

"This book gives us many comprehensive statements of current microcolumn HPLC and is highly recommended to chromatographers as well as analytical chemists," (TrAC).

"The vast amount of information . . . makes it essential for all who must keep abreast of latest developments in microcolumn techniques," (Food Technology in Australia).

1984 xvi, 302 pages. Price: US $ 61.00 / Dutch guilders 165.00 (including postage). ISBN 0-444-42290-0

ELSEVIER SCIENCE PUBLISHERS

P.O. Box 211, 1000 AE Amsterdam, The Netherlands
P.O. Box 1663, Grand Central Station, New York, NY 10163, USA

7332